Microbial Electrolysis Cell-Assisted Anaerobic Digestion for Enhancing Biomethane Recovery from High-strength Wastewater

by

Qi Huang

A thesis submitted in partial fulfillment of the requirements for the degree of

Doctor of Philosophy

in

ENVIRONMENTAL ENGINEERING

Department of Civil and Environmental Engineering

University of Alberta

Abstract

Anaerobic digestion (AD) is a sustainable method for treating high-strength wastewater while concurrently recovering biomethane. Nevertheless, factors such as low temperature and complex organic substrates can limit digestion kinetics, with hydrolysis and methanogenesis as the primary rate-limiting steps. Additionally, inhibitory compounds like sulfate/sulfide and ammonia in some high-strength feedstocks can disrupt methanogenic activity. Microbial electrolysis cell-assisted anaerobic digestion (MEC-AD) is a novel technology to enhance methane recovery. This research primarily focuses on mitigating OLR limitations, overcoming hydrolysis constraints, and alleviating sulfate inhibition in the AD of high-strength wastewater through MEC-AD systems, using source-separated blackwater as representative high-strength wastewater.

Firstly, the research chain started by pushing the organic loading rates (OLRs) of electrochemically assisted anaerobic digestion of vacuum toilet blackwater at ambient temperature. The MEC-AD system sustained a high OLR of 3.03 g COD/L-d, achieving significantly higher methane yield under closed-circuit operation compared to open-circuit operation. Microbial community analysis revealed the enrichment of specific electroactive bacteria and their syntrophic interactions with electrotrophic methanogens.

Secondly, a comprehensive screening of applied voltages (0 - 1.6V) for vacuum toilet blackwater digestion in a MEC-AD reactor at ambient temperature revealed that 1.2 V provided optimal performance, improving chemical oxygen demand (COD) removal, methane yield, and hydrolysis/acidogenesis efficiency. Enrichment of hydrolytic and syntrophic bacteria and an

increase in genes encoding complex organics metabolism were observed.

Thirdly, this thesis also explored a novel MEC-AD scheme incorporating granular activated carbon (GAC) and extended sludge retention time, which mitigated performance deterioration due to increased OLR and temperature drop. GAC addition significantly improved methane yield and hydrolysis, and biomarker analysis highlighted the roles of GAC biofilms and settled sludge in promoting methanogenesis and hydrolysis.

Efforts were made to evaluate the performance of a MEC-AD system under different COD/sulfate ratios. The MEC-AD reactor demonstrated greater resistance to H_2S toxicity, indicating higher specific methanogenic activities. Proposed mechanisms for the superior performance included lower free sulfide concentrations and promoted syntrophic partnerships between sulfate-reducing bacteria (SRB), hydrogenotrophic methanogens, and electroactive bacteria. These insights aid in the development of efficient AD systems for handling sulfate stress.

The final aspect of the thesis assessed the performance of three configurations of MEC-AD systems under sulfate-reducing conditions. The single-chamber MEC-AD reactors exhibited significantly higher methane yield than the control reactor, and conversion to a dual-chamber configuration using an anion exchange membrane (AEM) further increased methane production. In contrast, the MEC-AD reactor with a cation exchange membrane (CEM) experienced a reduction in methane yield due to anolyte acidification.

The results of this thesis have advanced our understanding of MEC-AD systems' potential to enhance the anaerobic digestion of high-strength wastewater, with valuable insights into optimization and performance under various conditions.

Preface

This thesis is an original work conducted by Qi Huang under the supervision of Dr. Yang Liu and Dr. Bipro R. Dhar at the University of Alberta. Qi Huang was responsible for conceptualization, methodology, investigation, formal analysis, data curation, visualization, and writing the original draft. Dr. Yang Liu and Dr. Bipro R. Dhar were responsible for conceptualization, methodology, supervision, review, editing, project administration, resource management, and funding acquisition.

Chapter 2:

A version of this chapter has been published: Huang, Q., Liu, Y., & Dhar, B. R. (2022). A critical review of microbial electrolysis cells coupled with anaerobic digester for enhanced biomethane recovery from high-strength feedstocks. *Critical Reviews in Environmental Science and Technology*, 52(1), 50-89.

https://doi.org/10.1080/10643389.2020.1813065

Chapter 3:

A version of this chapter has been published: Huang, Q., Liu, Y., & Dhar, B. R. (2021). Pushing the organic loading rate in electrochemically assisted anaerobic digestion of blackwater at ambient temperature: insights into microbial community dynamics. *Science of the Total Environment*, 781, 146694.

https://doi.org/10.1016/j.scitotenv.2021.146694

Chapter 4:

A version of this chapter has been published: Huang, Q., Liu, Y., & Dhar, B. R. (2022). A multifaceted screening of applied voltages for electro-assisted anaerobic digestion of blackwater: Significance of temperature, hydrolysis/acidogenesis, electrode corrosion, and energy efficiencies. *Bioresource Technology*, 360, 127533.

https://doi.org/10.1016/j.biortech.2022.127533

Chapter 5:

A version of this chapter has been published: Huang, Q., Liu, Y., & Dhar, B. R. (2023). Boosting resilience of microbial electrolysis cell-assisted anaerobic digestion of blackwater with granular activated carbon amendment. *Bioresource Technology*, 381, 129136.

https://doi.org/10.1016/j.biortech.2023.129136

Chapter 6:

A version of this chapter has been submitted to *Chemical Engineering Journal* as Huang, Q., Liu, Y., & Dhar, B. R. Deciphering the microbial interactions and metabolic shifts at different COD/sulfate ratios in electro-assisted anaerobic digestion.

Chapter 7:

A version of this chapter will be submitted as Huang, Q., Liu, Y., & Dhar, B. R. Electro-assisted anaerobic digestion under sulfate-reducing conditions: impacts of different reactor configurations.

Dedication

To my dear parents: Yongdong & Lingjiao

To all my family and friends

To those whom I love and those who love me

To a more luminous tomorrow

To a cleaner, healthier and greener world

Acknowledgements

For over six years, the University of Alberta has been my haven of enlightenment. Two years were dedicated to my master's degree, and another four for my Ph.D. As I gaze upon the culmination of this relentless effort in the form of a graduation thesis, I am humbled and moved. This moment is not just about the pages filled with research findings; it is about the people and experiences that have shaped my academic odyssey.

First and foremost, I would like to express my deep gratitude and sincere appreciation to my supervisors, Dr. Yang Liu and Dr. Bipro Dhar, for their excellent guidance, dedication, and encouragement throughout my program.

Dr. Liu, a successful female professor, has been an exemplary role model for me through the years. You have been a constant source of inspiration throughout my academic journey. Your achievements, dedication, and resilience have motivated me to strive for excellence in every aspect of my work. Working under your supervision is the treasure of my life.

Dr. Dhar, you have not only been an exceptional mentor in our studies but have also shown genuine concern for our personal well-being. Your patient guidance, constructive criticism, and invaluable support have been instrumental in my growth, both as a student and as an individual. I am fortunate to have had you as my supervisor.

My sincere thanks also go to my Ph.D. candidacy exam committee (Dr. Maricor Arlos, Dr. Dominic Sauvageau, Dr. Evan Davies, and Dr. Wenming Zhang), and PhD defense committee (Dr. Cesar Torres, Dr. Maricor Arlos, Dr. Evan Davies, and Dr. Nicholas Beier) for their time and valuable critical feedback on my thesis work.

I would like to give my sincere thanks to Dr. Lei Zhang and Dr. Yingdi Zhang, who are experts in anaerobic digestion. Thanks for all the experience, knowledge, help, and caring you have offered. I’m grateful to have you as colleagues and friends along my academic journey.

Special thanks to Dr. Basem Zakaria Reda and Sajib Barua, who initiated me into the world of bioelectrochemical systems. I would not forget how you taught me the microbial electrolysis cell operation step by step. Thank you for your patient guidance and generous help to me.

I would like to express many thanks to my colleagues and technicians in the Department of Civil and Environmental Engineering at the University of Alberta: Dr. Huixin Zhang, Dr. Mohamed Meshref, Dr. Seyed Mohammad Mirsoleimani Azizi, Dr. Huijuan Sun, Dr. Bing Guo, Dr. Yun Zhou, Dr. Rui Xu, Dr. Mengjiao Gao, Dr. Qianyi Zhang, Dr. Long Lin, Dr. Anna Patricya Florentino, Dr. Linyu Deng, Dr. Nesma Allam, Yiyang Yuan, Xin Zou, Chenyuan Li, Lu Kong, Carlo Bais, Parisa Niknejad, Nervana Haffiez, Anindya A. Chakrabarty, David Zhao and all my other colleagues, who provided me with immediate help, guidance, and suggestions along the way.

I express my gratitude to the donors of the scholarships (Alberta Graduate Excellence Scholarship, Rick George Graduate Leadership Scholarship in Engineering, Gordon R. Finch Memorial Graduate Scholarship in Environmental Engineering, and Chinese Government Award for Outstanding Self-financed Students Abroad) that I received during my PhD journey.

Thanks for the financial support for this project provided by research grants from the Natural Sciences and Engineering Research Council of Canada (NSERC) Discovery Grants, the Canada Research Chair (CRC) in Future Water Services, and NSERC Industrial Research Chair (IRC) Program in Sustainable Urban Water Development through the support by EPCOR Water Services, EPCOR Drainage Operation, and Alberta Innovates.

Finally, I would like to express my gratitude to my dearest parents and my families for their love, support, and encouragement. Thanks to my close friends Jia Li, Lingjun Meng, Yutong Zhang, Yujue Li, Hui Jin, Yue Huang, Cheng Chen, Yu Wang, Shuai Zhang, and Masong Zhu for their help, caring, and support.

Thank you all, from the depths of my heart, for being a part of this remarkable expedition.

Table of Contents

List of Tables

List of Figures

Abbreviations

AD: anaerobic digestion

MEC: microbial electrolysis cells

MEC-AD: microbial electrolysis cell-assisted anaerobic digestion

BES: bioelectrochemical system

OLR: organic loading rate

HRT: hydraulic retention time

COD: chemical oxygen demand

TCOD: total chemical oxygen demand

SCOD: soluble chemical oxygen demand

GAC: granular activated carbon

SRB: sulfate-reducing bacteria

AEM: anion exchange membrane

CEM: cation exchange membrane

TSS: total suspended solids

VSS: volatile suspended solids

FOG: fats, oils, and grease

TAN: total ammonia nitrogen

FA: free ammonia

FAN: free ammonia nitrogen

VFA: volatile fatty acid

TVFA: total volatile fatty acid

SCVFAs: short-chain volatile fatty acids

F-T: Fischer-Tropsch

UASB: up-flow anaerobic sludge blanket

TOPW: table olive brine processing wastewater

EPS: extracellular polymeric substances

SEOR: soybean edible oil refinery

OFMSW: organic fraction of municipal solid waste

WAS: waste activated sludge

BMP: biochemical methane potential

DIET: direct interspecies electron transfer

SMPRs: specific methane production rates

PCoA: principal coordinate analysis

CSTR: continuous stirred tank

LDA: linear discriminant analysis

LEfSe: the linear discriminant analysis effect size

PICRUSt: phylogenetic investigation of communities by reconstruction of unobserved states

KEGG: Kyoto encyclopedia of genes and genomes

SHE: standard hydrogen electrode

SMA: specific methanogenic activity

ASR: assimilatory sulfate reduction

DSR: dissimilatory sulfate reduction

SAO: syntrophic acetate oxidation

ANOVA: analysis of variance

GC: gas chromatography

IC: ionic chromatography

Chapter 1. Introduction

1.1 Background

The escalating global issues of water scarcity and the excessive demand for fossil fuels have been recognized as significant socio-environmental challenges. These critical areas are intricately linked, necessitating a comprehensive approach, such as implementing a waste-to-energy strategy, to ensure both water security and sustainable energy production (Kothari et al., 2010). Investigating alternative energy solutions has become one of the paramount research areas for the future of global energy systems.

Anaerobic digestion (AD) stands out as a promising technology that generates renewable, methane-rich energy from a variety of waste sources, offering the advantages of low operational costs and minimal sludge production (Barua & Dhar, 2017; Bharathiraja et al., 2018; Zhang et al., 2019). The AD process is driven by a range of microorganisms, primarily proceeding through four key stages: hydrolysis, acidogenesis, acetogenesis, and methanogenesis. High-strength wastewaters, characterized by their substantial organic content, represent exceptional resources for renewable energy. Typically, high-strength wastewater contains significant quantities of chemical oxygen demand (COD), ammonia, total suspended solids (TSS), fats, oils, and grease (FOG), or other organic and inorganic compounds (Mutamim et al., 2012). Anaerobic digestion is widely applied for treating various high-strength wastewaters, including distillery wastewater (Sankaran et al., 2014), slaughterhouse wastewater (Ahmad et al., 2014), dairy wastewater (Charalambous et al., 2020), pulp and paper mill wastewater (Kamali et al., 2016), sewage sludge (Xu et al., 2018b), food waste (Hobbs et al., 2018) and blackwater (Gao et al., 2019b).

In this research, source-separated blackwater was chosen as representative high-strength wastewater due to its inclusion of various inhibitory components that pose challenges to the AD process. There are large variations in blackwater characteristics influenced by different collection systems. Notably, vacuum toilet blackwater contains substantial bacterial biomass and complex

organic compounds, such as humic compounds, carbohydrates, fibers, proteins, and fats, making it less biodegradable (Rose et al., 2015). Due to the high complexity and low biodegradability of the organic content in these high-strength feedstocks, hydrolysis is usually presented as the rate-limiting step (Tsigkou et al., 2022). Besides, the slow growth kinetics of methanogens leads to a low methanogenesis rate, further limiting the AD efficiency (Tsigkou et al., 2022). Consequently, prior blackwater digestion systems have generally exhibited relatively low organic loading rates (OLRs) and reduced methane production rates (Huang et al., 2020b). Moreover, anaerobic treatment has primarily been employed in tropical regions due to its temperature dependence (Zhang et al., 2020c). Previous studies on blackwater digestion have mostly operated at mesophilic or thermophilic temperatures to enhance digestion kinetics, such as hydrolysis and methanogenesis rates (Gao et al., 2019a; Gao et al., 2019b; Zhang et al., 2020a). However, given that blackwater is typically discharged at ambient temperatures, running digesters at higher temperatures would not only increase operational costs but also lead to elevated levels of free ammonia (FA) (Florentino et al., 2019a). Therefore, significant challenges and substantial research gaps persist in the context of anaerobic digestion of blackwater and other high-strength wastewaters at ambient temperatures.

For diluted conventional toilet blackwater, the low COD/sulfate ratio (~10) can also impede the AD of blackwater (Gao et al., 2020a). In anaerobic reactors, sulfate is converted to sulfide by sulfate-reducing bacteria (SRB), leading to two stages of methanogenic inhibition. The first stage involves competition for substrates between SRBs and methanogens, while the second stage results from the decline in the methanogenic population due to the inhibition of cellular functions by soluble sulfides (Chen et al., 2008). Specifically, in the anaerobic treatment of sulfate-containing wastewater, the competition between SRB and methanogens for acetate and H_2, their common primary substrates, can impact treatment efficiency (Chen et al., 2014). Furthermore, research indicates that sulfide production can be toxic to unacclimated methanogens at concentrations as low as 50 mg/L (Parkin et al., 1983), indicating that sulfide toxicity can lead to non-competitive inhibition of methanogenesis and process failure. Therefore, addressing

sulfate/sulfide inhibition is a critical research area to enable high-rate AD processes for high-strength wastewater.

In recent years, there has been a notable increase in research on various microbial electrochemical technologies (Butti et al., 2016; Jadhav et al., 2022). One such technology, microbial electrolysis cell-assisted anaerobic digestion (MEC-AD), has garnered significant attention for its potential to enhance biomethane recovery from diverse organic wastes (Yu et al., 2018b). Typically, electroactive bacteria oxidize organic matter at the anode and transfer electrons and protons to the cathode, where protons combine with electrons to produce hydrogen (Cai et al., 2016). Theoretically, hydrogen production requires an applied voltage of > 0.13 V (Cheng & Logan, 2007). Due to the cathodic hydrogen evolution reaction, hydrogenotrophic methanogenesis on the biocathode's surface has been identified as the dominant methanogenic pathway in MEC-AD systems (Zakaria & Dhar, 2019). Research indicates that hydrogenotrophic methanogens are more resilient to inhibitory factors like high ammonia concentrations, high OLRs, and low temperatures (Florentino et al., 2019b; Gao et al., 2019b; Liu et al., 2016a). This suggests that biocathodes in the MEC-AD system not only catalyze methane production but also promote the growth of hydrogenotrophic methanogens, leading to enhanced digestion performance. Moreover, rapid hydrogen utilization by hydrogenotrophic methanogens maintains a low hydrogen partial pressure, creating thermodynamically favorable conditions for fermentative bacteria to degrade organic compounds (Sasaki et al., 2013; Zhao et al., 2016d). This synergistic relationship between fermentative bacteria and hydrogenotrophic methanogens improves digestion kinetics. Additionally, previous studies have shown that MEC-AD systems can mitigate the decline in digestion efficiency at lower temperatures, as the activity of electroactive bacteria is less reliant on temperature conditions (Feng et al., 2018). Furthermore, MEC-AD systems have demonstrated the ability to counteract the detrimental effects of inhibitory substances, including challenging compounds like phenolic compounds, salts, and ammonia-nitrogen (Cerrillo et al., 2016b; Marone et al., 2016). As a result, MEC-AD holds promise as a technology for enhancing the anaerobic digestion process.

In the early stages of developing MEC-AD systems, research primarily centered around synthetic or low-strength wastewaters (Clauwaert & Verstraete, 2009; Siegert et al., 2015; Zhang et al., 2013a; Zhao et al., 2014). However, recent years have witnessed a growing body of research exploring the potential of MEC-AD systems for the treatment of various high-strength wastewaters, including sewage sludge (Wang et al., 2022; Zakaria & Dhar, 2022), food waste (Choi & Lee, 2019; Park et al., 2018), and livestock waste (Cerrillo et al., 2017; Zou et al., 2021). Yet, there is a notable scarcity of studies evaluating methane recovery from blackwater (Zamalloa et al., 2013). A knowledge gap exists concerning the fundamental microbial mechanisms, optimal operational conditions, and the correlations between reactor configurations, reactor performance, and microbial community dynamics. Therefore, the core emphasis of this thesis is to assess the performance of MEC-AD systems in addressing key limitations in the AD of blackwater, including low OLRs, low hydrolysis efficiency, and sulfate inhibition. Additionally, this thesis aims to contribute to the ongoing optimization of the AD process. The results of this research will not only help to fulfill the current research gaps in blackwater treatment, but also help in guiding future system design, operation, process optimization, and engineering applications for the treatment of various high-strength wastes from both municipal and industrial sectors.

1.2 Research objectives

The primary objective of this research is to mitigate OLR limitations, overcome hydrolysis constraints, and alleviate sulfate inhibition in the AD of high-strength wastewater, by integrating microbial electrolysis cells with AD. Utilizing blackwater as representative high-strength wastewater, this research is devoted to elucidating the underlying mechanisms and microbial factors, as well as refining operational conditions. The ultimate goal is to maximize biomethane recovery and enhance energy efficiency in high-strength wastewater treatment. The specific objectives of this thesis are as follows:

(1) To assess the effectiveness of handling high OLRs: investigate the capacity of the MEC-

AD reactor to handle high OLRs for the anaerobic digestion of vacuum toilet blackwater at ambient temperature. Explore the connections between operational conditions (e.g., OLRs, open/closed circuit), changes in microbial communities, and reactor performance.

(2) To optimize the process for addressing OLR limitation: determine the appropriate applied voltages for electro-assisted anaerobic digestion of vacuum toilet blackwater, considering various factors such as temperature, hydrolysis/acidogenesis efficiencies, electrode corrosion, and energy efficiency.

(3) To assess the effectiveness of overcoming hydrolysis constraints: enhance the resilience and hydrolysis in microbial electrolysis cell-assisted anaerobic digestion of vacuum toilet blackwater by introducing conductive additives and extending sludge retention time.

(4) To assess the effectiveness of alleviating sulfate inhibition: assess the influence of influent COD/sulfate ratios on the anaerobic digestion process and clarify the roles and mechanisms of MEC-AD systems in enhancing methane recovery under varying influent COD/sulfate ratios.

(5) To optimize the process of alleviating sulfate inhibition: examine the impact of different MEC-AD reactor configurations on the anaerobic treatment process in the presence of sulfate-reducing conditions and elucidate the fundamental mechanisms responsible for the observed performance differences.

1.3 Thesis outline

This thesis comprises eight chapters, each serving a distinct purpose. The connections among research gaps, objectives and chapters are shown in Figure 1.1.

Chapter 1: Introduces the thesis by offering an overview of its background, discussing the motivations, scope, and outlining the doctoral research objectives.

Chapter 2: Provides a critical examination of the utilization of MEC-AD systems to enhance biomethane recovery from high-strength feedstocks. It delves into the implications of process parameters, energy efficiencies, and microbial community characteristics, while also shedding light on operational insights and future research requirements.

Chapter 3: Investigates the long-term performance of an MEC-AD reactor for concentrated blackwater digestion at ambient temperature. The study encompasses different OLRs and open/closed circuit conditions. It employs statistical-based microbial community analysis to track dynamic changes and elucidate the roles and interactions of functional microbes throughout the process.

Chapter 4: Evaluates a range of applied voltages for blackwater digestion within MEC-AD systems operating at mesophilic and ambient temperatures. The investigation covers various aspects, including the efficiencies of biochemical steps, microbial community dynamics, functional gene expression, electrode corrosion, and energy efficiency. Bioinformatics analysis is employed to uncover the underlying microbial mechanisms.

Chapter 5: Explores a novel MEC-AD approach incorporating granular activated carbon (GAC) supplementation and extended sludge retention time to enhance anaerobic digestion processes. It assesses hydrolysis and overall digestion efficiencies in response to increased organic loading rates, along with an analysis of microbial succession and dynamics facilitated by MEC-AD and GAC.

Chapter 6: Systematically evaluates the performance of an MEC-AD reactor under varying COD/SO_4^{2-} ratios. It conducts a comprehensive examination of microbial communities, metabolic pathways, and genetic adaptations associated with sulfur metabolism.

Chapter 7: Investigates the performance and microbial dynamics of different MEC-AD reactor configurations under sulfate-reducing conditions. These configurations include a single-

chamber setup, a dual-chamber with an anion exchange membrane (AEM), and a dual-chamber with a cation exchange membrane (CEM), comparing their performance to that of a control reactor.

Chapter 8: Presents the main conclusions derived from the research findings and accomplishments discussed in Chapters 3 to 7. It also provides recommendations for future research directions.

Bibliographies from all chapters are combined and presented at the end.

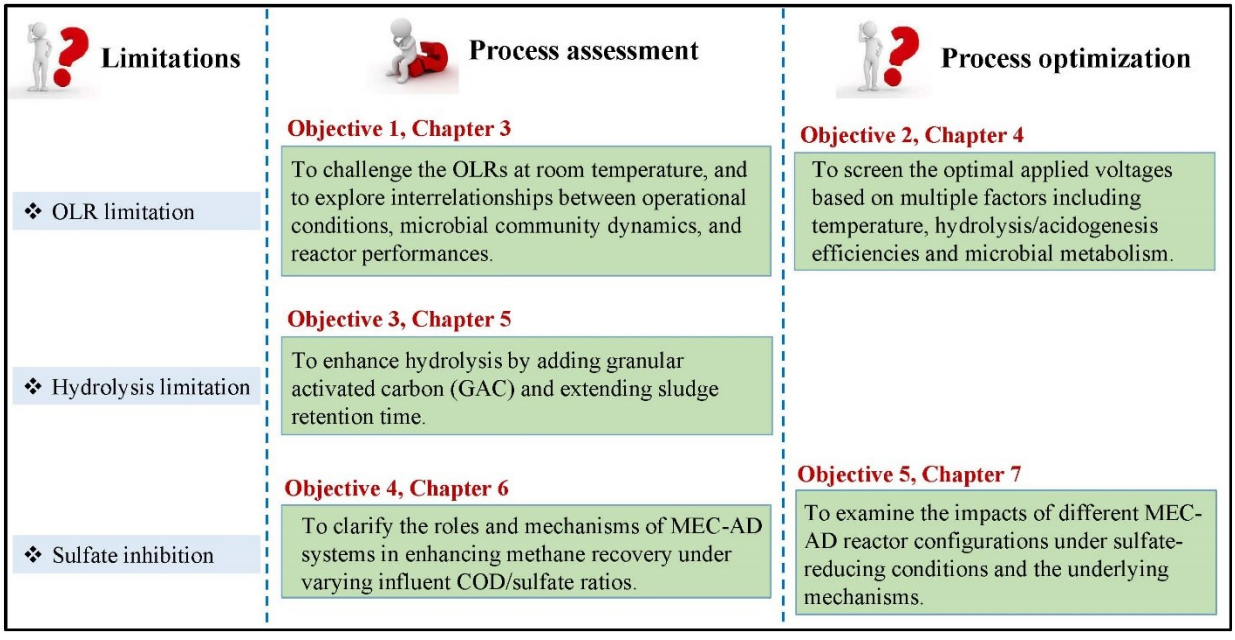

Figure 1.1 Connections among research gaps, objectives, and chapters.

Chapter 2. Literature Review[1]

2.1 Introduction

Biological treatment processes are usually considered as techno-economically feasible options for waste/wastewater treatment due to their relatively low capital and operating costs compared to other treatment technologies (Grady Jr et al., 2011). Aerobic processes are usually used for low- and medium-strength waste/wastewater due to the requirement of high energy consumption for aeration, and excess sludge generation (Chan et al., 2009; Hamza et al., 2016). In contrast, various anaerobic biotechnologies have attracted considerable attention for simultaneous treatment and sustainable bioenergy recovery from high-strength waste/wastewater that are featured by the high concentration of chemical oxygen demand (COD) (Khalid et al., 2011; Lin et al., 2017). Despite being an established method for anaerobic treatment, anaerobic digestion (AD) still faces numerous challenges. The operation of AD could lead to the accumulation of various short-chain volatile fatty acids (SCVFAs) that could cause process instability (Ahring et al., 1995; Duan et al., 2012). Many high-strength waste and wastewater are discharged at low temperatures (< 20ºC), while the methanogenic microbiome is very sensitive to the operating temperature (Chae et al., 2008; De Vrieze et al., 2015; Levén et al., 2007). Usually, mesophilic (25-40ºC) operation is recommended for satisfactory methane yield and stable operation of digesters (El-Mashad et al., 2004; Labatut et al., 2014; Mao et al., 2015). Moreover, the presence of toxic and refractory compounds, such as phenol, sulfides, toluene, and heavy metals in some high-strength feedstocks can disrupt methanogenic activity (Alkalay et al., 1998; Chen et al., 2008; Kawai et al., 2012; Mara & Horan, 2003; Rajagopal et al., 2013; Shahriari et al., 2012; Wang et al., 2011).

In recent years, there has been an increasing number of studies on the application of various microbial electrochemical technologies (Logan & Rabaey, 2012; Wang & Ren, 2013). Notably,

[1] A version of this chapter has been published as: Huang, Q., Liu, Y., & Dhar, B. R. (2022). A critical review of microbial electrolysis cells coupled with anaerobic digester for enhanced biomethane recovery from high-strength feedstocks. *Critical Reviews in Environmental Science and Technology*, 52(1), 50-89.

the combination of microbial electrolysis cells (MECs) and AD (usually referred to as MEC-AD system) has been investigated to improve biomethane recovery from high-strength waste/wastewater generated from various industries and municipal services (e.g., wastewater treatment, landfill operation, etc.) (Cai et al., 2016; Gao et al., 2017; Guo et al., 2013; Mahmoud et al., 2014; Marone et al., 2016; Park et al., 2018; Sasaki et al., 2010; Wang et al., 2017a). These studies demonstrated that MEC-AD systems could overcome the aforementioned challenges associated with conventional digesters (Cerrillo et al., 2016c; Gao et al., 2017; Marone et al., 2016; Park et al., 2018; Yu et al., 2018b; Zhang & Angelidaki, 2014), as detailed below. Although anaerobic technologies are primarily recommended for high-strength feedstocks, some studies demonstrated the effectiveness of MEC-AD for low- and medium-strength wastewater (0.45-1.12 g COD/L) in terms of meeting regulatory limits for discharge (Cheng et al., 2009; Hou et al., 2015; Moreno et al., 2016; Siegert et al., 2015; Villano et al., 2013; Zeppilli et al., 2015).

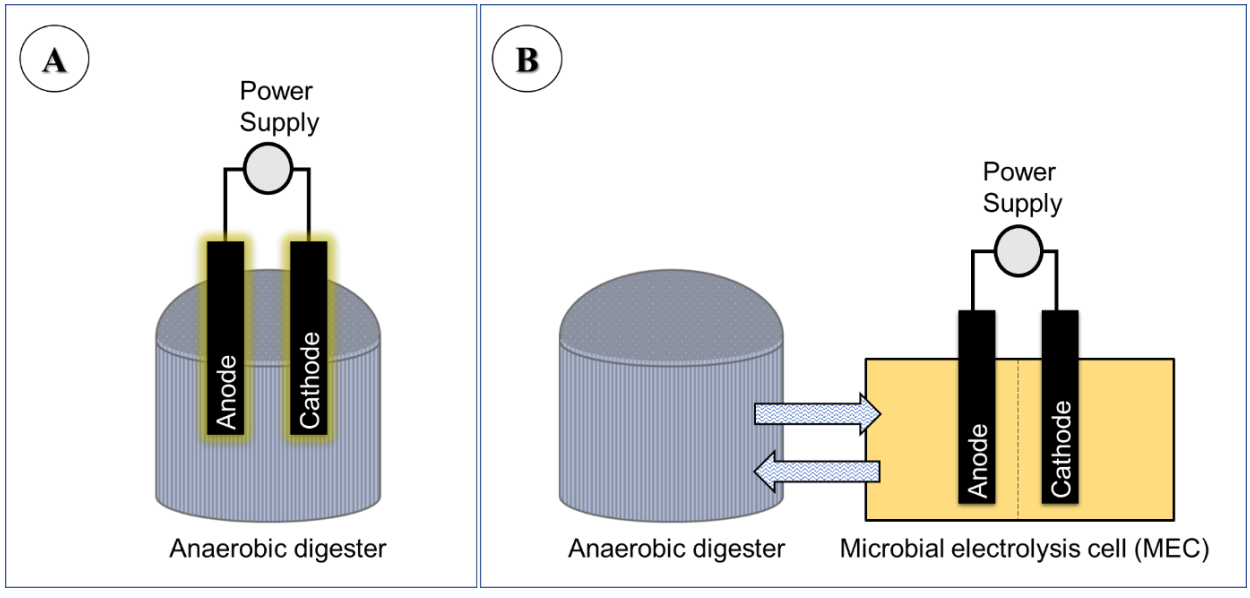

Figure 2.1 MEC-AD configurations: (A) submerged electrodes within a digester, (B) digester hydraulically connected with an external MEC.

As shown in Figure 2.1, MECs have been mostly integrated with conventional digesters under two different schemes: (A) direct retrofitting of electrodes into a conventional digester (Hagos et al., 2018; Sangeetha et al., 2016; Sasaki et al., 2013; Zhen et al., 2015), and (B) circulation of

digester liquid between a conventional digester and a MEC (Cerrillo et al., 2016b; Wang et al., 2017b). In integrated MEC-AD systems, simple organic acids produced by the hydrolysis of complex biopolymers followed by fermentation are oxidized by some specific electroactive bacteria (Lee et al., 2017; Wilson & Kim, 2016). Methane is produced via four pathways (Figure 2.2): (P1) protons (H^+) are first reduced to H_2 gas via a cathodic electrochemical reaction ($2H^+ + 2e^- \rightarrow H_2, E^{0\prime} = -0.41\,V\ vs.\ Standard\ hydrogen\ electrode\ (SHE)$), then H_2 is utilized by hydrogenotrophic methanogens; (P2) some electrotrophic methanogens directly use electrons, protons, and CO_2 to produce CH_4 ($CO_2 + 8H^+ + 8e^- \rightarrow CH_4 + 2H_2O, E^{0\prime} = -0.24\,V\ vs.\ SHE$), which is known as electro-methanogenesis (Cheng et al., 2009; van Eerten-Jansen et al., 2015; Zhen et al., 2015); (P3) syntrophic fermentative bacteria produce H_2 gas which is then utilized by hydrogenotrophic methanogens; and (P4) conventional acetoclastic methanogenesis. The contribution of these two mechanisms associated with the cathode (i.e., P1 and P2) depends on the set cathode potential. For instance, cathode potential of -0.41 V vs. SHE, which is more negative than the cathode potential of -0.24 V vs. SHE needed for the electro-methanogenesis (P2) through direct electron transport, can promote methanogenesis from electrochemically produced H_2 (P1) (van Eerten-Jansen et al., 2015). Due to inferior growth kinetics, acetoclastic methanogens could be outcompeted by anodic electroactive bacteria, which could promote methanogenesis via pathways P1 – P3 (Liu et al., 2016b; Wang et al., 2009). Notably, hydrogenotrophic methanogens, which are less sensitive to low temperature and ammonia inhibition (Enright et al., 2009; Florentino et al., 2019a; Liu et al., 2016a), could be enriched due to increased H_2 production. Thus, MEC-AD systems could provide kinetically and thermodynamically favorable conditions for enhanced methanogenic activity.

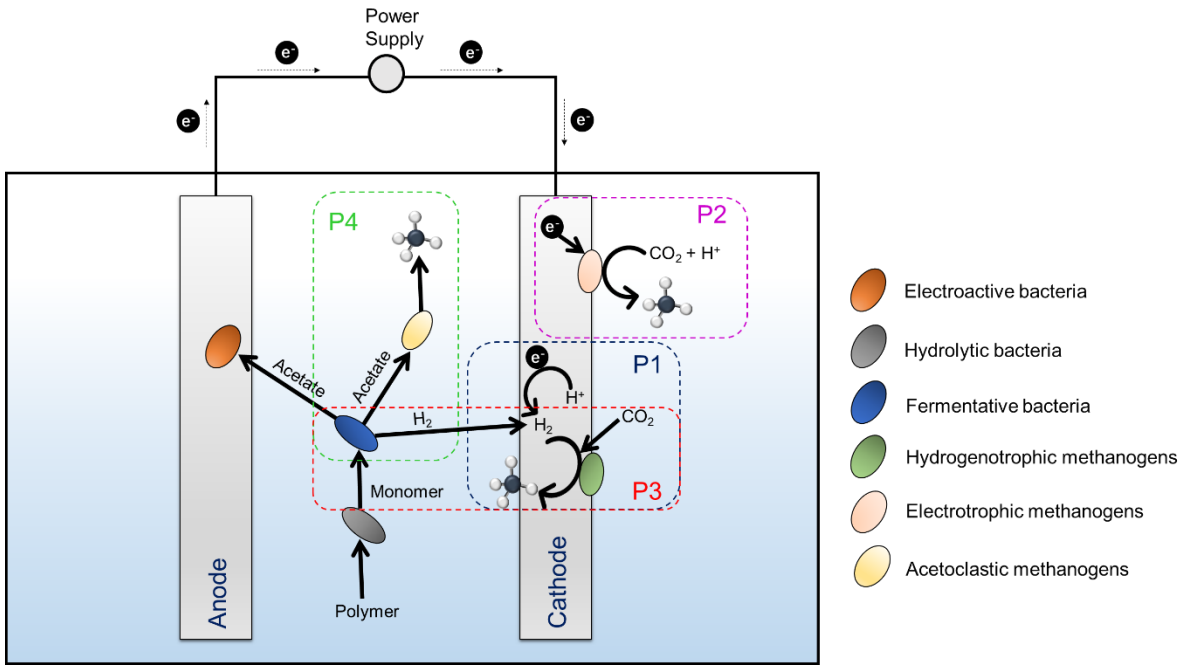

Figure 2.2 Methanogenesis pathways in an integrated MEC-AD system.

Considering acetate as a substrate for anodic electroactive bacteria ($CH_3COOH + 2H_2O \rightarrow 2CO_2 + 8H^+ + 8e^-, E^{0\prime} = -0.28\,V$ vs. SHE), direct electro-methanogenesis (P2) can be spontaneous because the calculated cell voltage is positive ($E_{Cathode} - E_{Anode} = -0.24 - (-0.28) = +0.04\,V$). In constrat, methane production via abiotic H_2 production and subsequent hydrogenotrophic methanogenesis (P1) would require an applied voltage of > 0.13 V ($E_{Cathode} - E_{Anode} = -0.41 - (-0.28) = -0.13\,V$). However, in practice, higher energy input is needed to overcome other energy losses, including electrode overpotential and internal resistances in the system.

Nowadays, both industrial and municipal sectors are facing critical issues towards high strength waste/wastewater treatment and its stringent discharge requirement. The MEC-AD systems could provide an innovative solution to mitigate the aforementioned challenges. In recent years, multiple review articles have appeared on various aspects of MEC-AD systems (Beegle & Borole, 2018; Yu et al., 2018b; Zakaria & Dhar, 2019; Zhen et al., 2017c), while no efforts have been made to critically appraise the literature to provide insights into the application of MEC-AD systems for high-strength feedstocks. Therefore, in this review chapter, our focus is confined to

the application of MEC-AD systems for high-strength waste/wastewater. Particularly, this article presents a critical performance review of MEC-AD systems and summarizes the roles of applied voltage, temperature, organic loading rates (OLRs), and feedstock pretreatment for biomethane recovery from high-strength waste/wastewater. Moreover, implications of energy efficiencies, system optimization, and future research directions with regards to the process scale-up are discussed.

2.2 MEC-AD performance with high-strength feedstocks

An overview of the performance of MEC-AD systems operated with high-strength waste/wastewater is summarized in Table 2.1. The following sub-sections provide a detailed performance analysis of MEC-AD systems and comparison to the conventional digesters highlighted in previous studies.

2.2.1. Sewage Sludge

The MEC-AD systems have been investigated to improve sewage sludge digestibility and methane recovery (Cai et al., 2016; Feng et al., 2015; Gajaraj et al., 2017; Sugnaux et al., 2017; Sun et al., 2015; Xiao et al., 2018; Zhao et al., 2016b; Zhao et al., 2016c), as conventional anaerobic digestion requires extended solids residence times (Dhar et al., 2011; Dhar et al., 2012; Ziganshin et al., 2016). However, differences in sludge solids content in these studies resulted in variations in the COD concentration from 7.8 g/L (Asztalos & Kim, 2015) to 114.2 g/L (Feng et al., 2015) and suspended solids (SS) concentration from 7.4 g/L (Zhen et al., 2014) to 117.9 g/L (Feng et al., 2015). Nonetheless, enhanced methanogenesis was generally reported in MEC-AD systems in comparison with conventional digester (i.e., control). Zhao et al. (2016c) reported an improvement in methane productivity (12.9%) and an improved solids reduction efficiency (17.2%) in a MEC-AD system operated at 0.6V, as compared to the control. Guo et al. (2013) observed marginal enhancement (3 - 6%) in solid removal efficiencies and up to a 13.6-fold improvement in methane production in a sewage sludge-fed MEC-AD system operated at 1.4 -

1.8 V. Promising results were obtained in other MEC-AD studies with sewage sludge (Cai et al., 2016; Feng et al., 2015; Gajaraj et al., 2017; Sugnaux et al., 2017; Sun et al., 2015; Xiao et al., 2018; Zhao et al., 2016b; Zhao et al., 2016c). It was evident that MEC-AD systems could accelerate degradation of proteins and carbohydrates (Asztalos & Kim, 2015; Feng et al., 2015; Guo et al., 2013; Liu et al., 2016b; Xiao et al., 2018; Zhao et al., 2016b), probably due to the high abundance and diversity of functional microbes in biofilms capable of degrading complex substrates (Liu et al., 2016b; Zhao et al., 2016b). For instance, Zhao et al. (2016b) reported enhanced degradation of proteins and carbohydrates in MEC-AD systems along with 11.7-fold improvement in methane production rate compared to the control.

Despite enhancement achieved in terms of methane production, a few studies reported marginal improvement in solids removal efficiencies with MEC-AD systems (Cao & Pawłowski, 2012; Duan et al., 2012; Peces et al., 2013; Takashima & Tanaka, 2014). In contrast, several studies reported that sludge hydrolysis could be enhanced with MECs (Feng et al., 2015; Song et al., 2010; Sugnaux et al., 2017; Zhao et al., 2016e; Zhen et al., 2014). However, the underlying mechanism behind hydrolysis enhancement is still ambiguous. Thus, further research towards a deeper understanding of process parameters on hydrolysis kinetics would be required for promoting MEC-AD systems for sewage sludge management.

2.2.2. Industrial wastewaters

It is widely acknowledged that anaerobic industrial wastewater treatment is facing formidable challenges. Various industrial wastewaters are featured by high COD concentration, low biodegradability, and a large amount of recalcitrant and toxic compounds (Kong et al., 2019). This subsection mainly discussed how MEC-AD systems overcame the challenges to enhance biomethane recovery.

2.2.2.1. Fischer-Tropsch wastewater

The Fischer-Tropsch (F-T) process represents the liquefaction of coal that transforms the CO and

H_2 derived from the coal into crude oil. This process generates wastewater with high concentrations of monohydric alcohols, monocarboxylic acids, ketones, hydrocarbons, and aldehydes, and low pH (3.0 -5.0) (Majone et al., 2010; Nijs & Jacobs, 1981). The typical COD concentration in the F-T process wastewater ranged from 19 to 39 g/L (Majone et al., 2010; Van Zyl et al., 2008; Wang et al., 2017a; Wang et al., 2017c). Up-flow anaerobic sludge blanket (UASB) reactors have been widely employed for the biological treatment of F-T process wastewater. An accumulation of propionate/butyrate was identified as a major limiting factor when UASB reactors operated at high OLRs (11.67 to 20.6 g COD/L-d) (Wang et al., 2017c). As these organic acids can irreversibly acidify the bioreactors, relatively lower OLRs (< 8.75 g COD/L-d) have been recommended for stable operation (Wang et al., 2017c). The control of pH with alkali addition could provide a sensible solution, but it would lead to high O&M costs and elevated salts precipitation (Wang et al., 2017b).

Wang et al. (2017a) investigated the treatability of the F-T process wastewater in a MEC-UASB system with pH control to 7.0. At an applied voltage of 1.5 V, MEC-UASB versus a control USAB exhibited a COD removal efficiency of 86.8 vs. 72.1% and a methanogenesis rate of 2.31 vs. 1.77 m^3 CH_4/m^3-d. Their study suggested that the more reductive microenvironment created by the electric field lowered the oxygen reduction potential and thereby minimized the pH drop, creating a favorable metabolic condition for methanogenesis (Wang et al., 2017a).

The treatability of F-T wastewater was also investigated at the pilot-scale, where the liquid was circulated between a separate UASB (12 m^3) and a MEC (0.8 m^3) (Wang et al., 2017b). The integrated system attained a COD removal efficiency of 93.5% and a methane production rate of 2.01 m^3/m^3-d at an OLR of 18 g COD/L-d. A relatively higher applied voltage of 4 V was required for the pilot-scale MEC in comparison with their previous bench-scale study (Wang et al., 2017a). The requirement of the higher applied voltage is expected due to the increase in the internal resistance after scale-up (Escapa et al., 2015; Kadier et al., 2016b; Sleutels et al., 2012). However, the COD removal efficiencies and methane production rates were fairly comparable among bench-

scale and pilot-scale studies (Wang et al., 2017a; Wang et al., 2017b). The implementation of MEC within the liquid recirculation line seems to be a more manageable approach to integrate MEC with AD. However, integrating MEC within the UASB would minimize the footprint of the overall process. Therefore, it would be interesting to explore the engineering challenges associated with the scale-up of a modular system.

2.2.2.2. Table olive brine processing wastewater

Table olive brine processing wastewater (TOPW) contains high levels of salinity, alkalinity, long-chain fatty acids, and phenolic compounds (Cappelletti et al., 2011; Kopsidas, 1992; Kopsidas, 1994; Niaounakis & Halvadakis, 2004) that can readily inhibit biological treatment (Aggelis et al., 2001; Chen et al., 2008; Rincon-Llorente et al., 2018). Conventional aerobic or anaerobic processes have been found to be ineffective in removing phenolic compounds from TOPW (Aggelis et al., 2001; Hamdi, 1992; Kyriacou et al., 2005). Although COD concentrations in TOPW range from 9.57 to 49.6 g COD/L (Beltran et al., 2008; Niaounakis & Halvadakis, 2004; Paraskeva & Diamadopoulos, 2006; Rincon-Llorente et al., 2018), anaerobic treatment of TOPW succeeded only after dilution to < 3 g COD/L (Beltran et al., 2008; Javier Benitez et al., 2001). In contrast, various physicochemical processes, such as wet air oxidation (Katsoni et al., 2008), ozonation (Beltran-Heredia et al., 2000; Beltrán et al., 1999), electrochemical oxidation (Deligiorgis et al., 2008), and TiO_2 photocatalysis (Chatzisymeon et al., 2008) are effective in removing recalcitrant phenolic compounds from TOPW. However, high capital costs and complex procedures are major barriers to the wide-scale adoption of these techniques. Marone et al. (2016) studied a single-chamber MEC-AD system operated at an anode potential of + 0.24 V vs. SHE. The reactor was able to remove > 80% of the phenolic compounds (e.g., hydroxytyrosol, tyrosol) along with a methane yield of 109 ± 21 NmL CH_4/g $COD_{removed}$. In contrast, the control reactor showed substantially inferior phenol removal (~ 18%) and trivial methane production. A few studies previously reported that phenolic compounds could be efficiently removed (> 85%) by anodic microbial communities in MECs (Friman et al., 2013; Huang et al., 2011; Luo et al., 2009; Song et al., 2014; Zeng et al., 2015). Thus, MEC-AD systems could provide comparable phenol

removal efficiencies that can be achieved with various advanced oxidation processes, while providing biomethane recovery. Nonetheless, a detailed techno-economic analysis to compare these technologies would be required.

2.2.2.3. Methanolic wastewater

UASB systems have been extensively investigated for methane production from methanolic wastewater (Kobayashi et al., 2011; Lu et al., 2015; Lu et al., 2017). When methanol is the major carbon source in wastewater, methanogenesis is accomplished mainly by methylotrophic methanogens (Florencio et al., 1997). Hence, the UASB operation of methanolic wastewater can lead to a less diverse microbial community, poor granulation, and granule wash out (Lu et al., 2015). Providing another carbon source (e.g., acetate) can solve this problem by establishing diverse microbial communities due to the synergy of acetogens and acetoclastic methanogens (Florencio et al., 1997). However, slow-growing acetoclastic methanogens can lead to an accumulation of acetate (Florencio et al., 1996; Lin et al., 2008; Vanwonterghem et al., 2015; Zhen et al., 2017b). Recently, an integrated MEC-UASB system (OLR of 6.65 g COD/L-d) was investigated for methanolic wastewater (Zhen et al., 2017b) that could consistently maintain a 10% higher methane production rate than a control UASB. Their result showed that the enrichment of anodic electroactive bacteria could accelerate acetate utilization (Park et al., 2018; van Eerten-Jansen et al., 2015; Zhang et al., 2013b). Interestingly, this study found that interactions between extracellular polymeric substances (EPS) and $Fe^{2+/3+}$ released from the iron stick anode could promote cell-cell interactions and influenced the morphological characteristics of granular sludge. Microscopic imaging confirmed that the integrated system reinforced the secretion of EPS with a high protein/polysaccharide (PN/PS) ratio of 4.98, which led to the formation of large, intact, firm granules. In contrast, granules established in control UASB were highly dispersed and irregular (PN/PS = 4.06) (Zhen et al., 2017b). Although the release of iron via electrode corrosion seems to have a positive impact on granular sludge formation, corrosion of electrode will be a concern in long-term operation.

2.2.2.4. Soybean edible oil refinery wastewater

The wastewater generated from soybean edible oil refinery (SEOR) contains various recalcitrant compounds, such as free fatty acids, emulsion oil, and soap (Kale et al., 1999; Rajkumar et al., 2010). Conventional treatment scheme for SEOR wastewater includes a membrane bioreactor, floatation, coagulation, and flocculation (Karhu et al., 2014; Pathe et al., 2000; Rajkumar et al., 2010). However, such a process scheme provides lower organics removal at higher costs (Chipasa, 2001). Moreover, pretreatment to separate undesired components such as emulsion oil and grease is required (Yu et al., 2018a). Yu et al. (2017) studied MEC-AD systems with SEOR samples having four different COD concentrations: high (HC, 8.2 g COD/L), medium-high (MHC, 4.2 g COD/L), medium (MC, 2.9 g COD/L), and low (LC, 1.74 g COD/L). The MEC-AD system operated with a high COD concentration (8.2 g COD/L) achieved a maximum COD removal efficiency of 95.8%. The highest methane yield (45.4 ± 1.1 L/kg-COD) and methane production rate (0.133 ± 0.0045 L/L-d) were obtained in the MHC-MEC-AD. Although all MEC-AD groups achieved higher methane yields than the control, HC-MEC-AD showed significantly lower methane yield (7.8 ± 0.26 L/kg-COD) and production rate (0.0544 ± 0.0034 L/L-d) compared to that of MHC-MEC-AD. It was evident that higher concentration of SEOR triggered the inhibition related to pH/VFA, ammonia, long-chain fatty acids, polyphenols, pectins and/or tannins, which can be commonly found in anaerobic digestion of edible-oil processing wastewater (Rashama et al., 2019). MEC-AD systems could provide a promising treatment and methane recovery option for SEOR wastewater. However, efforts are still required to address these shortcomings for high-rate digestion. Besides, foaming, pipe clogging, and electrode fouling could be challenges for long-term digestion of high lipid-based substrates (Rashama et al., 2019). Thus, helpful strategies, including co-digestion, digestate recirculation, and bio-augmentation can be adopted for the process improvement (Rashama et al., 2019).

2.2.3. Food waste

The acidification of bioreactors due to an accumulation of SCVFAs has been identified as a major

challenge in anaerobic digestion of food waste (Banks et al., 2011; Chen et al., 2008; Xu et al., 2018a; Zhang & Jahng, 2012). In contrast, MEC-AD systems could promote the rapid degradation of SCVFAs during food waste anaerobic digestion (Park et al., 2018; Yu et al., 2018b; Zhang et al., 2013b). Park et al. (2018) reported that a MEC-AD system operated at an OLR of 3.0 g COD/L-d could significantly minimize the digester start-up time, as compared to the control. However, at the steady-state, comparable methane production rates and removal efficiencies of COD and solids were achieved from both configurations. In contrast, another study reported that a MEC-AD operating with food waste leachate (63 g COD/L, 37 g VS/L) at a slightly higher OLR of 3.4 g COD/L-d could provide considerably higher methane production than the control at steady-state (Lee et al., 2017). Possibly the impact of MEC addition will be more noticeable when digesters are operated at higher OLRs, as higher OLRs usually lead to an accumulation of SCVFAs (Ahring et al., 1995; Lü et al., 2012). Therefore, MEC performance at higher OLRs of food waste should be further explored to evaluate the feasibility of high-rate food waste digestion with MEC-AD systems.

2.2.4. Artificial garbage slurry

Diversion of the organic fraction of municipal solid waste (OFMSW) from landfills has received significant attention in recent years. Sasaki et al. (2010) examined the performance of a MEC-AD system operated with artificial garbage slurry (122.3 g COD/L, 53.3 g SS/L) as a model OFMSW. At an OLR of 26.9 g COD/L-d, a maximum biogas production rate of 6.6 L/L-d (57% CH_4 content) at a cathode potential of -0.8 V (vs. Ag/AgCl). In contrast, the control reactor operated showed an inferior biogas production rate of 5.3 L/L-d (38.9% CH_4 content). Moreover, a higher methanogenic gene copy number was present on the cathode electrode than on the anode electrode and in the control reactor, which further suggested that the cathodic electrochemical environment had a positive effect on the enrichment of methanogens on its surface. Studies conducted by Sasaki et al. (2010) and Sasaki et al. (2011) achieved very high OLRs (> 30 g COD/L-d) for MEC assisted garbage slurry digestion; however, COD (mostly 40 - 60%) and suspended solids (mostly 30 - 45%) removal efficiencies should be further improved. Besides, artificial garbage slurry was used

in these studies. It's worthwhile to explore the effectiveness of MEC-AD systems for methane recovery from real garbage slurry.

2.2.5. Livestock waste

Livestock waste, such as pig slurry, usually contains a high concentration of ammonia nitrogen that can potentially inhibit methanogenic activity (Chen et al., 2008; Yenigün & Demirel, 2013). It has been widely demonstrated that in dual-chamber MECs, ammonium (NH_4^+) is transported across the cation exchange membrane from the anode to the cathode compartment to maintain electroneutrality in the system (Barua et al., 2018; Barua et al., 2019; Cord-Ruwisch et al., 2011; Dhar & Lee, 2013; Kuntke et al., 2011; Kuntke et al., 2012). Thus, NH_4^+ can be concentrated and recovered in the cathode chamber. Recent studies demonstrated that coupling a dual-chamber MEC and an anaerobic digester could provide in situ recovery of ammonium during anaerobic digestion of livestock waste (Cerrillo et al., 2016b; Cerrillo et al., 2017). Cerrillo et al. (2016b) investigated an integrated system, where a dual-chamber MEC was retrofitted within the recirculation loop of a thermophilic anaerobic digester fed with pig slurry. In phase-1, the operation of digester without MEC at an OLR of 3.02 g COD/L-d, provided a methane production rate of 0.33 L/L-d. After doubling the OLR in phase-2 (6.25 g COD/L-d), the methane production rate decreased by 63% due to ammonia inhibition. Then, the authors introduced a MEC within the recirculation loop. With 50% of feed flow rate recirculation, the integrated system significantly increased methane production to 0.42 L/L-d. As mentioned earlier, retrofitting MEC as a separate unit within the recirculation loop would increase the footprint of the process and operating cost (i.e., heating cost). Therefore, a comprehensive assessment considering the economic benefits of nutrients recovery and enhanced methane recovery would be essential. In general, the MEC-AD system could help mitigate ammonia inhibition through several ways: i) the aforementioned NH_4^+ transport from anode to cathode compartment in dual-chamber MEC-AD systems (Cerrillo et al., 2016b); ii) rapid consumption of H^+ by cathodic hydrogen evolution reaction could reduce the system pH, thus decreasing the free ammonia level; iii) hydrogenotrophic methanogens, which are more tolerant to ammonia inhibition than acetoclastic methanogens (Florentino et al., 2019a),

can be enriched in the MEC-AD systems due to cathodic H_2 production. Moreover, electroactive biofilms were proved to be more tolerant to high ammonia concentrations (Kelly & He, 2014; Seelam et al., 2018).

2.2.6. Leachate

Leachate generated from landfill operations is highly hazardous due to the presence of high levels of recalcitrant organic matters, ammonium-nitrogen, heavy metals, humic compounds, xenobiotic organic compounds, and inorganic salts (Mahmoud et al., 2014). Gao et al. (2017) investigated the performance of a MEC-AD system operated with diluted municipal solid waste incineration leachate (10 g COD/L). Compared to the control, 8.7% higher COD removal efficiencies and 44.3% higher methane production were observed in the MEC-AD system. The MEC-AD demonstrated 15% higher degradation of large refractory macromolecules like humic substances. Of note, humic compounds in leachate have been found to be very difficult to degrade in biological processes (Aeschbacher et al., 2010; Ghernaout et al., 2009; Maurer et al., 2012; Maurer et al., 2010; Satyawali et al., 2007). Although Gao et al. (2017) reported superior degradation of refractory compounds in their MEC, the OLRs used in their study (0.417 - 1.82 g COD/L-d) were comparatively lower than the OLRs typically used in leachate treatment with conventional anaerobic bioreactors. For instance, previous studies used OLRs of 3.273 - 16.2 g COD/L-d in UASB reactors (Castillo et al., 2007; Castrillon et al., 2010; Govahi et al., 2011; Gunay et al., 2008; Peng et al., 2008; Ye et al., 2011), 1.15 - 27.7 g COD/L-d continuous stirred tank reactors (Nayono et al., 2010; Wang & Banks, 2006), and 22.5 - 79 g COD/L-d in expanded granular sludge bed reactors (Liu et al., 2011; Liu et al., 2012; Liu et al., 2010). Hence, further studies are needed to explore the potential application of MEC-AD systems for high-rate leachate treatment.

2.2.7. Blackwater

Blackwater discharged from household toilets contains about 70% of the organic matter in domestic wastewater, while accounting for less than 30% of the volume (Kujawa-Roeleveld & Zeeman, 2006; Moges et al., 2018). This high level of organics makes anaerobic digestion a

technically feasible option for blackwater treatment (Metcalf & Eddy, 2014). Zamalloa et al. (2013) investigated the performance of a dual-chamber MEC integrated with a septic tank for the anaerobic treatment of blackwater (15.5 g COD/L). The biogas production rate in the MEC-septic tank was five times higher than in a control septic tank. The H_2S concentration in the biogas was 2.5 times lower in the MEC-septic tank than the control septic tank. The H_2S removal could be attributed to sulfide oxidation by anodic microbes (Sun et al., 2009). Furthermore, the release of iron into the bulk solution from the continuous corrosion of the anode could enhance the H_2S removal through the precipitation of iron sulfide (Nielsen et al., 2008; Pikaar et al., 2011). Also, the effluent phosphorus concentration was 39% lower for the MEC-septic tank, possibly due to struvite precipitation on the cathode (Cusick & Logan, 2012). However, the study by Zamalloa et al. (2013) was conducted at an OLR of 0.5 g COD/L-d, which is within a lower range of OLRs (0.33 to 4.87 g COD/L-d) previously used in other anaerobic bioreactors for blackwater (De Graaff et al., 2010; Gao et al., 2019b; Kujawa-Roeleveld et al., 2005; Luostarinen & Rintala, 2007; Luostarinen et al., 2007; Moges et al., 2018; Wendland et al., 2007). Thus, future research should focus on high-rate MEC-AD systems to assess the competitiveness of hybrid systems compared to conventional anaerobic bioreactors.

Table 2.1 Overview of operational parameters and performances in integrated MEC-AD systems treating various high-strength waste/wastewater streams.

Wastewater	COD (g/L)	Solids (g/L)	Configuration	Applied voltage (V)	OLR (g COD/L-d)	Temperature (℃)	Performance		Impact on methanogenesis		References
							COD removal (%)	Solids removal (%)	Enhancement on methane production (fold)	Specific methane production rate (L/L-d)	
WAS	15.65	14 (VSS)	Single-chamber MEC (0.7 L)	0.8	-	20	41.2	48.5 (VSS)	1.56	0.0564	Cai et al. (2016)
Sewage sludge	11.75	8.44 (TSS) 5.98 (VSS)	Single-chamber MEC (0.3 L)	1.4-1.8	-	37	-	54.99-55.13 (TSS) 61.22-61.59 (VSS)	11.4-13.6	-	Guo et al. (2013)
WAS	16.98	10.94 (TSS) 7.49 (VSS)	Single-chamber MEC (0.3 L)	0.6-2.3	-	37	39.65-96.65 (SCOD)	20.4-59 (VSS)	1.2-1.79 (0.6-1.8V); 0.34 (2.3V)	-	Xiao et al. (2018)
WAS	15	12.76 (TSS) 9.12 (VSS)	Single-chamber MEC (0.025 L)	0.6	-	20	53.7	42.7 (TSS) 29.6 (VSS)	-	0.23	Sun et al. (2015)

WAS	114.2	117.9 (TSS) 77.2 (VSS)	Single-chamber MEC (2.0)	0.3-0.6	-	35	-	23.3-37.6 (TSS) 29.8-44.0 (VSS)	1.63 (0.3V) 0.65 (0.6V)	-	Feng et al. (2015)
WAS	52.31	104.7 (TSS) 40.67 (VSS)	Single-chamber MEC (0.5L)	0.6	-	37	42.2	8.3 (TSS) 23.0 (VSS)	-	0.384	Zhao et al. (2016b)
WAS	36.69	44.7 (TSS) 29.58 (VSS)	Single-chamber MEC (0.6 L)	0.6	-	35	36.7	38.5 (TSS) 44.4 (VSS)	1.30	0.28	Zhao et al. (2016c)
Sewage sludge	10	-	Single-chamber MEC (1.2 L)	0.3-0.6	-	35	-	-	1.81-1.85	0.02	Gajaraj et al. (2017)
Sludge fermentative liquid	17.51	20.37 (TSS) 14.02 (VSS)	Single-chamber MEC (0.65 L)	0.8	-	20-25	-	48 (VSS)	1.64	0.138	Liu et al. (2016b)
Sewage sludge	74	43.0 (TSS) 37.5 (VSS)	Dual-chamber MEC (2.4L+0.18L)	$E_{working}$= -0.8V	3.6-20.6	55	50-78	38-78 (TSS)	-	1.3-3.57	Sasaki et al. (2013)
Sludge fermentation liquid	13.03	1.60 (TSS) 0.85 (VSS)	Single-chamber MEC (0.038 L)	0.6-1.2	-	25	39.1-51.4 (SCOD)	-	-	0.154 (0.8V)	Linji et al. (2013)

Sewage sludge	36.6	41.6 (TS) 28.8 (VS)	Single-chamber MEC (12 L)	0.3	1.83-7.32	35	38.7-64.0	52.2-70.5 (VS)	-	0.407-1.339	Song et al. (2016)
WAS	-	50.31 (TS) 29.65 (VS)	Single-chamber MEC (1 L)	0.3-1.5	-	35	-	25.6-39.3 (VS)	1.2-1.76 (0.3, 0.6, 1.2, 1.5V) 0.52 (0.9V)	-	Chen et al. (2016)
Sewage sludge	31.7-47.0	43.3-51.0 (VS)	Single-chamber MEC (18 L)	0.3-0.7	1.59-2.35	25	32.6-55.4	31.0-65.9 (VS)	-	0.056-0.37	Feng et al. (2016)
Synthetic medium	10.7	0	Single-chamber MEC (0.18 L)	0.4-1.0	-	30	100	-	1.9-2.3	-	Bo et al. (2014)
Food waste	60.3	52 (TS) 39 (VS)	Single-chamber MEC (25 L)	0.3	3.0	35	76.1	73.2 (VS)	1.03-1.68	0.85	Park et al. (2018)
Food waste leachate	63	37 (VS)	Single-chamber MEC (25 L)	0.3	3.4	35	80.7	70.2 (VS)	2.55	0.93	Lee et al. (2017)
Blackwater	15.5	12 (TS) 8.1 (VS) 8.3 (TSS)	Dual-chamber MEC (20 L + 4.2 L)	2.0	0.49	30	85	90 (TSS)	5	0.038-0.084	Zamalloa et al. (2013)

Artificial garbage slurry	122.3	53.3 (TSS)	Dual-chamber MEC (0.25 L + 0.25 L)	$E_{working}$= 0 – -0.8V	26.9 ($E_{working}$= 0 – -0.8V)	55	32.4-65.1	29.6-46.2 (TSS)	0.83 ($E_{working}$= 0V) 1.1-1.24 ($E_{working}$= -0.3V – -0.8V)	4.46-6.63	Sasaki et al. (2010)
					31.8 ($E_{working}$= -0.6, -0.8V)		58.2-59.1	40.0-44.7 (TSS)	-	7.47-7.61	
Incineration leachate	4.8-21.0	-	Single-chamber MEC (0.5 L)	0.7	0.42-1.83	35	32-94	-	1.25-1.57	-	Gao et al. (2017)
Table olive brine processing wastewater	28.8	84.47 (TS) 15.51 (VS)	Single-chamber MEC (0.7L)	$E_{working}$= +0.2V	-	37	29	-	-	-	Marone et al. (2016)
Soybean edible oil refinery wastewater	1.74-8.2	-	Single-chamber MEC (0.022 L)	1.2	-	35	90-95.8	-	-	0.0126-0.133	Yu et al. (2017)
Methanolic wastewater	13.3	-	MEC amended UASB (0.5L)	0.4-0.6	6.65	35	98.9	-	1.10-1.29	1.50-1.84	Zhen et al. (2017b)
Fischer-Tropsch wastewater	30.3	-	MEC amended UASB (2L)	-	5.05-7.58	34	75.4-80.6	-	-	1.08-1.58	Wang et al. (2016)
Fischer-Tropsch wastewater	28.9-31.2	-	MEC amended UASB (4.8L)	1.5	6.0	34	86.8	-	1.31	2.31	Wang et al. (2017a)

Fischer-Tropsch wastewater	11.42-30.23	-	MEC-UASB coupled system ($0.8m^3$ + 12 m^3)	3.0-4.0	34.26-268.71 (MEC) 2.28-18.14 (UASB)	23 (MEC) 35 (UASB)	72.9-93.5	-	-	0.42-2.01	Wang et al. (2017b)

2.3. Operational conditions

2.3.1. Applied voltage

Applied voltage has been widely investigated as one of the most important operating parameters for MEC-AD systems. As shown in Table 2.1, most of the previous studies with high-strength waste/wastewater used applied voltages in the range of 0.3 - 0.8 V, while reported optimum voltage varied significantly. For instance, Feng et al. (2015) found that methane production increased by 22.4% at 0.3 V, while a higher applied voltage (0.6 V) led to the cathodic accumulation of H_2 gas and alkaline pH (8.8 - 9.2) which caused inhibition of methanogens on the cathode. Zhen et al. (2017b) reported a decline in methanogenic activity when the applied voltage was increased from 0.4 V to 0.6 V in a MEC-AD system fed with methanolic wastewater. In contrast, Chen et al. (2016) found that 0.6 V was optimal for methane production among a wide range of applied voltages (0.3 - 1.5 V). A few studies reported that a voltage of 1.8 V was required to enhance methane production in MEC-AD systems (Guo et al., 2013; Xiao et al., 2018). Relatively high voltage (3.0 - 4.0 V) was required to enhance process stability and methane productivity in a pilot-scale MEC-UASB system treating F-T wastewater (Wang et al., 2017b). The differences in reported optimum voltages could be attributed to the variations in the inoculum, substrate, and system configuration (e.g., electrode material, the distance between electrodes, etc.) (Clauwaert et al., 2008; Fan et al., 2008; Sleutels et al., 2013; Xiao et al., 2018; Zhou et al., 2013). Thus, more attention should be paid on optimum voltage screening for the practical application of MEC-AD systems.

2.3.2. Temperature

As temperature influences microbial kinetics, the operational temperature should have a substantial effect on MEC performance. Although anaerobic digestion can be carried out over different temperature ranges, most of the MEC-AD studies have been conducted at mesophilic (25 - 40°C) or psychrophilic (< 25 °C) conditions (see Table 2.1). The operation of a conventional anaerobic digester at < 25 °C can lead to an accumulation of SCVFAs due to sluggish

methanogenic kinetics (Dhaked et al., 2010; Vanwonterghem et al., 2015). A few studies suggested that methanogenic activity in MEC-AD systems would be less sensitive to temperature changes between mesophilic and psychrophilic conditions because of the enrichment of hydrogenotrophic methanogens commonly reported in MEC-AD studies (Cheng et al., 2009; Li et al., 2016b; Rago et al., 2015; Zhao et al., 2014). Hydrogenotrophic methanogens are relatively more robust than acetoclastic methanogens at low temperature (Enright et al., 2009; Liu et al., 2016a). Liu et al. (2016a) evaluated the performance of a MEC-AD system operated at 10 ℃. The performance of the combined system was compared with multiple control reactors (conventional digester) operated at 10, 15, and 30 ℃. The results showed that MEC-AD operated at 10 ℃ attained much higher methane yield than control reactors at 10 ℃ and 15 ℃, and achieved a methane yield close to the control reactor operated at 30 ℃. Feng et al. (2018) also reported comparable methane production rates from a MEC-AD operated at ambient temperature (25 ℃) and a control digester operated at 35 ℃. These findings suggest that MEC-AD systems could serve as an energy-efficient alternative to promote methane production at ambient and even low temperatures.

2.3.3. HRTs and OLRs

To minimize treatment costs, it is desirable to operate bioreactors at higher OLRs or shorter hydraulic retention times (HRTs). However, at high OLRs, SCVFAs can accumulate in the digester due to an imbalance between hydrolysis/acidogenesis and methanogenesis kinetics (Ahring et al., 1995; Lü et al., 2012). SCVFA accumulation usually leads to a pH drop, followed by process disturbance or digester failure (Ahring et al., 1995; Chen et al., 2008). Most MEC-AD studies have been performed at OLRs of 1.5 to 8 g COD/L-d (Cerrillo et al., 2016a; Feng et al., 2016; Gao et al., 2017; Lee et al., 2017; Park et al., 2018; Song et al., 2016; Wang et al., 2016; Zhen et al., 2017b). Song et al. (2016) investigated the performance of a sewage sludge fed MEC-AD system under different OLRs ranged from 1.44 to 5.76 kg VS/m^3-d at 0.3 V, which was relatively higher than typical OLRs (1.2 - 1.43 kg VS/m^3-d) used in conventional digesters (Bolzonella et al., 2005; Kardos et al., 2011; Peces et al., 2013). In their study, the MEC-AD

system exhibited stable operation at higher OLRs. At an OLR of 1.44 kg VS/m^3-d, the reactor achieved the highest VS removal efficiency (70.5%) and methane content (76.9%) in biogas, which slightly deteriorated with the OLR increase. However, the specific methane production rate consistently increased from 0.407 to 1.339 L/L-d with the increase in OLR. The highest methane yield and energy recovery efficiency were achieved at an OLR of 2.88 kg VS/m^3-d. It is expected that an optimum OLR/HRT would depend on the feedstock characteristics, such as solids content and biodegradability. For instance, under similar operating temperatures, an optimum HRT for easily biodegradable methanolic wastewater (TCOD: 13.3 g/L, no solids) and refractory blackwater (TCOD:15.5 g/L, total solids: 12.0 g/L) was 48 h and 20 - 40 d, respectively (Zamalloa et al., 2013; Zhen et al., 2017b). Thus, HRT/OLR optimization is important in MEC-AD operation.

2.3.4. Pretreatment of feedstock

A recent study by Beegle and Borole (2018) suggested that pretreatment of high-strength feedstocks would be essential to improve energy efficiency and the economic feasibility of MEC-AD systems. In general, pretreatment of high-solids feedstocks has been widely investigated to accelerate the rate-limiting hydrolysis step in conventional anaerobic digestion (Ariunbaatar et al., 2014; Carrère et al., 2010; Li et al., 2012a; Zhen et al., 2017a). In MEC-AD studies, pretreatment of sewage sludge with different methods, such as alkaline pretreatment (Sun et al., 2015; Zhao et al., 2016b), thermal-alkaline pretreatment (Xiao et al., 2018), electrical-alkali pretreatment (Zhen et al., 2014), ultrasonic-fermentation pretreatment (Liu et al., 2016b), ultrasonic-alkaline-fermentation pretreatment (Linji et al., 2013) has been investigated. Although we cannot systematically compare them due to the differences in process conditions and feedstocks, most of these studies suggested that pretreatment of feedstocks can further improve the process performance of MEC-AD systems. For instance, Sun et al. (2015) investigated the effects of alkaline pretreatment of waste activated sludge (WAS) on biomethane generation from a MEC-AD system. The authors found that alkaline pretreatment provided 3-fold higher biomethane production in comparison with raw WAS. Nonetheless, a systematic comparison among different pretreatment methods based on comprehensive techno-economic assessment is required for the

selection of an appropriate pretreatment method.

2.4. Microbial Communities

2.4.1. Microbial spatial structure

Complex microbial interactions are involved in the electro-methanogenesis process. The understanding of the spatial structure of the functional microbiome could help elucidate the roles of different microbes in the MEC-AD systems. Both archaea and bacteria can either present as planktonic cells or form biofilms on anode and cathode. Bacteria are usually dominant in the system despite the location due to higher growth rate, and archaea usually present a higher abundance on cathode than anode and suspension (Cai et al., 2016; Liu et al., 2016b). Only a few studies provided a comprehensive characterization of microbial distribution. However, these studies showed most electroactive bacteria inhabited on the anode instead of cathode and suspension (Liu et al., 2016a; Liu et al., 2016b; Zhao et al., 2016b). In most cases, suspended sludge was dominated by hydrolytic/fermentative bacteria, such as *Cloacamonas*, *Bifidobacterium*, and *Pseudomonas* (Zakaria & Dhar, 2019). For archaeal communities, hydrogenotrophic methanogens were dominant in cathode biofilms and suspension in most cases (Gao et al., 2017; Sasaki et al., 2010; Zakaria & Dhar, 2019). However, limited information was provided in terms of the archaeal community on the anode so far. Interestingly, several previous studies documented that acetoclastic *Methanosaeta* species accounted for the highest proportion of anodic archaeal community (Cai et al., 2016; Zhao et al., 2016c). It was more likely that *Methanosaeta* accept electrons from electroactive bacteria (e.g. *Geobacter*) via direct interspecies electron transfer rather than metabolizing the acetate (Cai et al., 2016).

2.4.2. Bacterial community structures

In several studies, electroactive *Geobacter* species were found to be dominant in MEC-AD systems operated with high-strength feedstocks (Cai et al., 2016; Liu et al., 2016b; Sun et al., 2015; Wang et al., 2017b; Zhao et al., 2016b). The dominance of other known electroactive

Desulfuromondales and *Pseudomonas* species were observed in MEC-AD systems treating F-T wastewater, table olive brine processing wastewater, and incineration leachate (Gao et al., 2017; Marone et al., 2016; Wang et al., 2017a). It must be asserted that most of the electroactive bacteria (e.g., *Geobacter* species) have limited metabolic versatility and cannot directly metabolize complex fermentable organics (Logan, 2009; Lovley et al., 2011). However, *Desulfuromondales* and *Pseudomonas* species are not only electroactive (Boon et al., 2008), but also able to degrade aromatic compounds and other complex hydrocarbons (Fuchs et al., 2011; Gao et al., 2017; Spormann & Widdel, 2000). Nonetheless, various fermentative bacteria play a critical role in the degradation of fermentable organics in MEC-AD systems (Dahiya et al., 2015; Hao & Wang, 2015; Singhania et al., 2013).

A few studies reported enrichment of fermentative bacteria belonging to the class *Clostridia*, which could contribute to faster degradation of complex organics (Chen et al., 2016; Lee et al., 2017; Park et al., 2018; Zhao et al., 2016c). Fermentative bacteria (*Bacteroides*, *Anaerolinea*, *Aminobacterium*, and *Aminomonas*) involved in the degradation of carbohydrates and proteins were also found to be dominant in some studies (Wang et al., 2017b; Zhao et al., 2016b). Moreover, some studies reported enrichment of syntrophic β-oxidizing bacteria, such as *Syntrophomonas* and *Syntrophobacter* (Gao et al., 2017; Wang et al., 2017a; Wang et al., 2017b; Zhao et al., 2016c), that could contribute to the degradation of long-chain fatty acids (Sieber et al., 2010). As discussed later, hydrogenotrophic methanogens were mostly found to be dominant in MEC-AD systems. The rapid hydrogen utilization by hydrogenotrophic methanogens can maintain low H_2 partial pressure and provide thermodynamically favorable conditions for fermentative bacteria (Sasaki et al., 2013; Zhao et al., 2016d). Thus, their syntrophic interactions could enable high-rate conversion of complex feedstocks in MEC-AD systems.

Moreover, some studies showed enrichment of bacteria capable of degrading refractory compounds or surviving under harsh environmental conditions. Notably, the genus of *Anaerolineaceae*, *Longilinea,* and *Ornatilinea* was found in a MEC-AD system fed with F-T

wastewater (Wang et al., 2017b). These bacteria can degrade complex hydrocarbons and phenolic compounds (Feng et al., 2017; Oba et al., 2014). Members of the bacterial phylum *Firmicutes* were found in MEC-AD systems treating pig slurry with high abundance, which could play an important role in maintaining process stability against high ammonia level (Cerrillo et al., 2016a; Cerrillo et al., 2016b; Cerrillo et al., 2017).

2.4.3. Archaeal community structures

Integration of MECs with digesters could increase the presence of fast-growing hydrogenotrophic methanogens, such as *Methanobacterium* (Cai et al., 2016; Gao et al., 2017; Liu et al., 2016b; Sasaki et al., 2010), *Methanocorpusculum* (Sun et al., 2015), *Methanoculleus* (Sasaki et al., 2013). It has been suggested that H_2 produced at the cathode can stimulate the enrichment of hydrogenotrophic methanogens (Cheng et al., 2009; Li et al., 2016b; Rago et al., 2015; Zhao et al., 2014). Moreover, some electroactive bacteria can outcompete acetoclastic methanogens for acetate due to their superior growth kinetics (Liu et al., 2016b; Wang et al., 2009). Hydrogenotrophic methanogens have a higher tolerance to low temperature and ammonia inhibition than acetoclastic methanogens (Enright et al., 2009; Florentino et al., 2019a; Liu et al., 2016a). Thus, the enrichment of hydrogenotrophic methanogens in MEC-AD systems could assist in maintaining system stability under unfavorable metabolic conditions (e.g., high ammonia level) and at ambient or even low temperatures. Moreover, methanogens capable of directly accepting electrons from conductive materials, such as *Methanosaeta* (Cai et al., 2016; Chen et al., 2016; Gajaraj et al., 2017; Wang et al., 2017a; Zhao et al., 2016c), *Methanosarcina* (Lee et al., 2017; Park et al., 2018; Sasaki et al., 2010), and *Methanospirillum* (Bo et al., 2014), were also found to be dominant in some studies. These methanogens can develop a more effective syntrophic partnership with syntrophic fermentative bacteria and alleviate the risk of organic acid accumulation in digesters at high OLRs.

It is expected that various operating conditions and characteristics of feedstocks would play a significant role in shaping microbial communities and thereby influence the performance of

MEC-AD systems. However, to date, only the impact of different applied voltage on microbial communities has been well documented in the literature (Chen et al., 2016; Feng et al., 2016; Feng et al., 2015; Gajaraj et al., 2017). Gajaraj et al. (2017) studied methanogenic communities under applied voltages of 0.3-0.6 V. Compared to control, at applied voltages of 0.3 V and 0.6 V, the relative abundance of hydrogenotrophic *Methanomicrobiales* increased by 10.8-times and 12.0-times, respectively, whereas *Methanobacteriales* population increased by 15.9-times and 17.2-times, respectively. Another study reported that an applied voltage of 0.3 V could enhance the diversity of methanogenic communities while increasing applied voltage to 0.6 V decreased microbial diversity (Feng et al., 2015). Even though it is difficult to compare results from different studies because of the use of different reactor configurations and operating conditions, these results suggested that applied voltage could significantly influence the structure and diversity of methanogenic communities. Thus, for a specific feedstock, systematic investigation of various process parameters, as well as their interactions, should be investigated in the future.

2.5. Significance of process optimization and economic considerations

As documented above, MEC-AD systems demonstrated promising results in terms of enhancing biomethane production from high-strength feedstocks. However, various operating parameters, including applied voltage, OLRs/HRTs, temperature, etc., would significantly influence the process performance. It is still difficult to systematically establish interrelationships between various parameters based on the outcomes from various studies due to the use of different operating conditions. The operation of the MEC-AD systems will require electrical energy input, which will increase operating costs. In this context, evaluation of energy recovery efficiencies would provide a basis for comparison of outcomes from different studies. Therefore, here, we estimated the energy efficiencies from different studies considering electrical energy input (i.e., applied voltage) and improvement in methane production over the control (Feng et al., 2018; Sasaki et al., 2010; Zhao et al., 2016b). Figure 2.3 shows fold change in energy recovery efficiencies in MEC-AD systems relative to the control. The values were calculated based on the

following equation:

$$\text{Change in energy efficiency} = \frac{W_{CH_4\,(MEC-AD)} - W_E}{W_{CH_4\,(AD)}}$$

Where, W_E is the electrical energy input for MEC-AD operation (continuous: kJ/$L_{reactor}$-day; batch: kJ), $W_{CH4\,(MEC\text{-}AD)}$ is the energy recovery as methane from the MEC-AD system (continuous: kJ/$L_{reactor}$-day; batch: kJ), and $W_{CH4(AD)}$ is the energy recovery as methane from the control AD (continuous: kJ/$L_{reactor}$-day; batch: kJ) (Feng et al., 2018; Zhao et al., 2016b). For instance, Sasaki et al. (2010) investigated a 250 mL MEC-AD system operated with garbage slurry at an OLR of 31.8 g COD/L-d. Energy consumption for MEC-AD operation in their study was 0.087 kJ/$L_{reactor}$-day (current: 145 µA; applied voltage: 1.73 V), while energy recovery from the system as biomethane was estimated at 161 kJ/$L_{reactor}$-day. In contrast, the maximum energy recovery of 106 kJ/$L_{reactor}$-day was observed from the control at an OLR of 19.6 g COD/L-d. Thus, overall energy efficiency in their MEC-AD system increased by about 1.5-fold. Moreover, the MEC-AD system could handle higher OLR (31.8 vs. 19.6 g COD/L-d). However, it should be noted that most of the previous studies reviewed did not report the energy recovery efficiencies of their MEC-AD systems. Therefore, the values presented in Figure 2.3, for most cases, are estimated from the information provided in the papers.

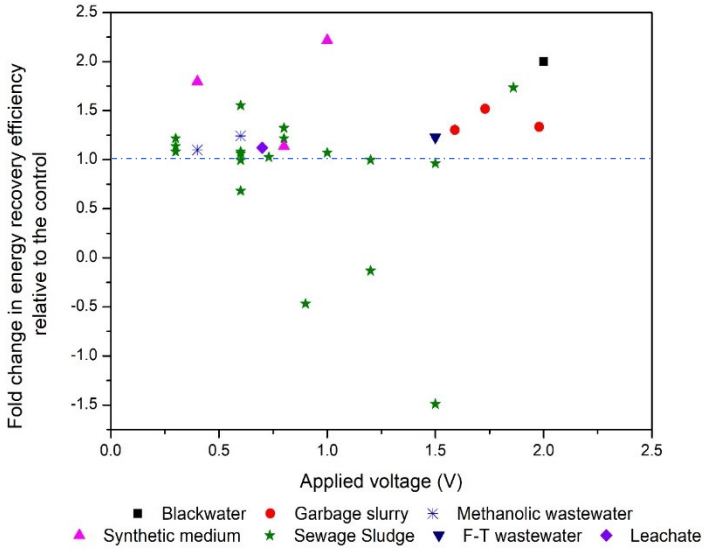

Figure 2.3 Fold change in energy recovery efficiency relative to the control for different high-strength feedstocks at different applied voltages.

As shown in Figure 2.3, several studies showed promising outcomes with an increase in energy recovery efficiencies over the control. In contrast, some studies showed unappealing outcomes (decrease or marginal increase in energy efficiency compared to the control). We showed changes in energy recovery efficiencies for different feedstocks at different applied voltages, while other parameters (OLRs/HRTs, temperature, system configuration, etc.) were also different in these studies. There was a non-linear relationship between energy efficiencies and applied voltage. It was apparent that a MEC-AD system operated a synthetic substrate may also provide a marginal increase in energy efficiency depending on other process parameters (see Figure 2.3). Thus, these results substantiate the importance of systematic optimization of various operating conditions. For a specific feedstock, we need to establish interrelationships between various process parameters and energy efficiencies. In addition to improving energy recovery efficiencies, the capital cost of MEC-AD systems would be another decisive factor in scale-up and practical implementation. Unfortunately, existing literature provides limited information on the capital cost of MEC-AD systems. The capital cost of MEC was estimated at ~€5500/m^3 (Zhang & Angelidaki, 2016). Although many studies emphasized the importance of highly efficient and less expensive electrode materials, construction costs (excluding electrode and membrane costs) represent a major portion of capital investment in this study. Therefore, future research should be directed based on a thorough cost analysis of MEC-AD systems.

2.6. Outlook

In recent years, many researchers have focused on incorporating MECs into anaerobic high-strength waste/wastewater treatment. In addition to enhanced methanogenic activity, MEC-AD systems have shown promising results in terms of organics and solids removal. The total COD concentration in these studies ranged from 8.2 to 122.3 g/L; the removal efficiencies varied from

29% up to 100% (see Figure 2.4). In some studies, solids removal efficiencies also exceeded 60% (see Figure 2.5). As abovementioned, in most of these studies, these performances were higher compared to the control. However, due to differences in other process parameters, no specific trend can be established between initial total COD and solids content and their removal efficiencies.

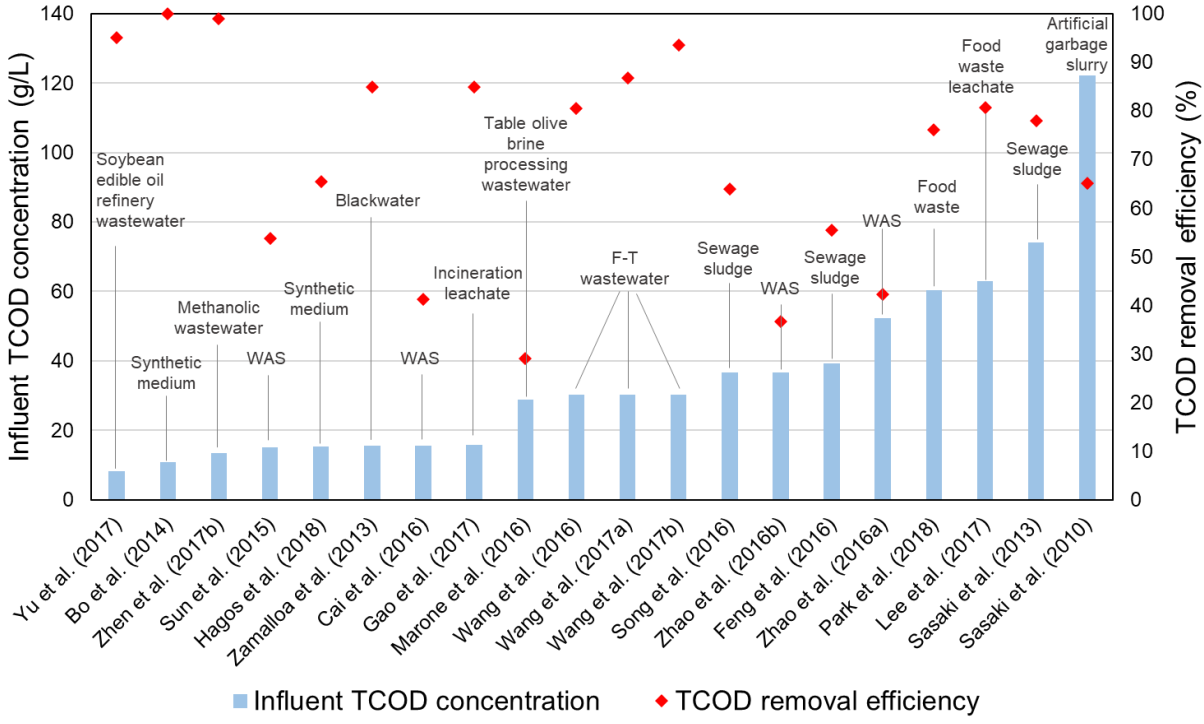

Figure 2.4 Influent TCOD concentrations and TCOD removal efficiencies of different high-strength feedstocks treated by MEC-AD systems.

The optimization of applied voltage has been the primary focus in most of the studies. As evident from this review chapter, the performance of MEC-AD systems can be significantly varied due to the differences in complexity levels of substrates (e.g., solids content, presence of refractory compounds, etc.), organic loading rates, temperature, pH, and so on. These parameters need to be systematically studied as the microbial communities, energy efficiencies, as well as process performance, could be significantly affected by them.

It was obvious that MEC-AD systems could handle high-strength feedstocks having high concentrations of various toxic and refractory compounds (e.g., phenolic compounds, salts, etc.).

However, most of the previous studies only focused on the treatability of waste/wastewater containing such toxic and refractory compounds, while more studies are required to better understand the underlying mechanisms responsible for the better performances of MEC-AD systems. Thus, functional microbes, microbial interactions, metabolic pathways, and functional gene expression in terms of degradation of these compounds require closer investigation. Further, the performance of MEC-ADs depends on multiple electrochemical, physicochemical, and biological factors. The understanding of the interrelationships among these factors through modelling work is critical for making this technology more efficient.

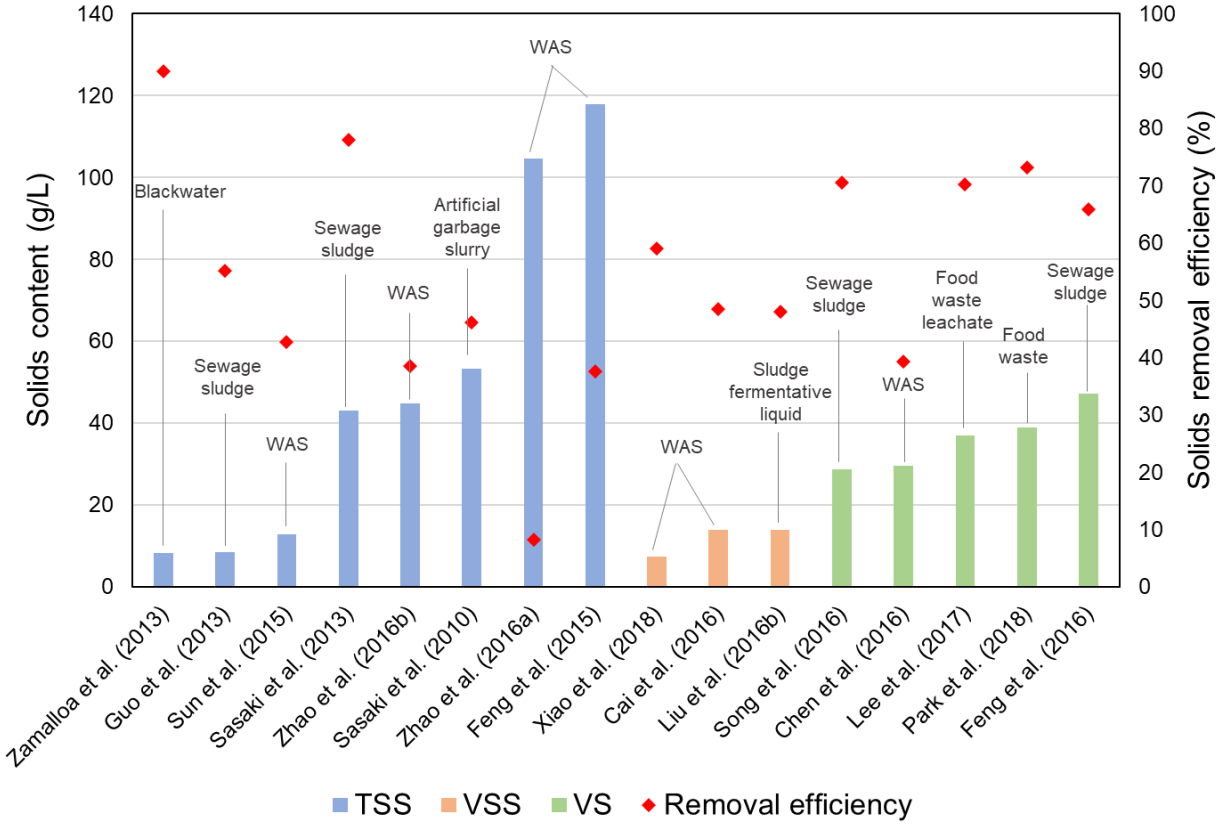

Figure 2.5 Solids content and solids removal efficiencies of different high-strength feedstocks treated by MEC-AD systems.

To date, most of the studies have been conducted at the laboratory scale and primarily focused on the routine evaluation of treatability and methane recovery. Hence, further research should also pay attention to optimization and tailoring of process configuration for scale-up. Instead of

directly inserting electrodes in digester tanks, circulating feedstocks between the digester tank and the anode chamber of MEC appeared to be an easily retrofittable solution for existing AD facilities. In addition to flexibility in construction and operation, the integration of a MEC with a traditional anaerobic digester by a recirculation loop can also buffer the influent acidity (Wang et al., 2017b), and mitigate the inhibition caused by organic and nitrogen overloads (Cerrillo et al., 2016b). Despite the combined MEC-AD reactors achieved satisfactory performance in treating various high-strength feedstocks as discussed above, a recent study also showed the side-stream recirculation between a MEC and a traditional digester had similar performance and methanogenesis pathway (mainly hydrogenotrophic methanogenesis) to a combined MEC-AD system (Park et al., 2020). However, research comparing the performance of these two schemes is still limited, which left open a wide research gap in understanding the detailed mechanism difference and optimizing the operational conditions.

Only a few studies reported long-term operation performance from MEC-AD systems while deteriorating performance might likely be observed as a result of the accumulation of solids on electrodes during long-term operation. Fouling of electrodes can increase mass transfer resistance and decrease system performance (Borole et al., 2011; Li et al., 2016a). Therefore, future studies should consider using computational tools like computational fluid dynamics (CFD) analysis to evaluate flow and mixing conditions for minimizing mass transfer resistance, which can assist in the design of an efficient MEC-AD reactor. The optimization of electrode materials is another important factor for the scale-up of MEC-AD systems. Selecting the electrode material with high catalytic performance and low cost would be the primary consideration. Further, based on the existing material, the conductivity, biocompatibility and electron transfer kinetics of electrodes can be improved through surface modification (Mohan et al., 2018). For instance, nanomaterials can be utilized in electrode surface modification to confer higher surface area, enhanced chemical properties, contact angles and other surface characteristics (Fogel & Limson, 2016; Mohan et al., 2018). Lastly, the electrode structure is another important aspect to consider. Modifying the electrode structure to fit with reactor configuration and avoid being a limiting factor would help

balance the cost and efficiency.

2.7. Conclusions

This review chapter provides an overview of the performance and applicability of MEC-AD systems for enhancing biomethane recovery from various high-strength organic waste and wastewater. MEC-AD systems could considerably mitigate the severe performance decline in conventional anaerobic digesters due to SCVFAs accumulation at higher organic loading rates. Also, MEC-AD systems could alleviate the detrimental effects of various inhibitory constituents, including recalcitrant compounds like phenolic compounds, salts, ammonia-nitrogen. Overall, the integrated process of MEC-AD demonstrated clear advantages and great promises over traditional digesters, including rapid conversion of high-strength feedstocks into biomethane, superior process stability, and better effluent quality. Since most of the studies focused on the optimization of applied voltages, there is still much scope to study various process parameters and fundamental aspects, focusing on further enhancement of energy efficiencies. Also, long-term process stability and scale-up strategies need further investigation.

Chapter 3. Pushing the Organic Loading Rate in Electrochemically Assisted Anaerobic Digestion of Blackwater at Ambient Temperature: Insights into Microbial Community Dynamics[2]

3.1 Introduction

Source-separated blackwater collected from water-conserving toilets (e.g., vacuum toilets) is an ideal feedstock for the anaerobic digestion (AD) due to the small volume (< 30%), high organic proportion (50 - 70%) and high nutrient proportion (~ 80%) in total household wastewater (Moges et al., 2018). However, blackwater contains large amounts of bacterial biomass, complex organics, including carbohydrate, fiber, protein, and fat, resulting in low biodegradability (Rose et al., 2015). Thus, conventional anaerobic digestion of blackwater in previous studies was mostly operated at low organic loading rates (OLRs), ranging from 0.3 to 1.0 g COD/L-d (De Graaff et al., 2010; Gallagher & Sharvelle, 2011; Gallagher & Sharvelle, 2010; Gao et al., 2019a; Tervahauta et al., 2014). Only a few studies reported high-rate blackwater digestion with OLRs > 2 g COD/L-d (Gao et al., 2019b; Huang et al., 2020b; Moges et al., 2018). For instance, our previous study investigated the performance of a carbon fiber-amended anaerobic biofilm reactor on vacuum toilet blackwater treatment at high OLR (3.0 g COD/L-d) and ambient temperature (Huang et al., 2020b). However, the methane yield can only reach up to 27.1% out of 45% biochemical methane potential (BMP). Digestion at mesophilic or thermophilic temperatures can help increase the digestion kinetics. For example, the highest OLR of 4.1 g COD/L-d was achieved in a mesophilic up-flow anaerobic sludge blanket (UASB) treating vacuum toilet blackwater (Gao et al., 2019b). However, blackwater is usually discharged at ambient temperatures. Thus, operating digesters at higher temperatures would not only increase the operating costs but also result in higher free ammonia (FA) levels. Recent studies have reported significant free ammonia inhibition during the

[2] A version of this chapter has been published as: Huang, Q., Liu, Y., & Dhar, B. R. (2021). Pushing the organic loading rate in electrochemically assisted anaerobic digestion of blackwater at ambient temperature: insights into microbial community dynamics. *Science of the Total Environment*, 781, 146694.

anaerobic digestion of vacuum collected blackwater under the mesophilic conditions (35 °C) (Florentino et al., 2019b; Gao et al., 2018). Since blackwater digesters were mostly operated under mesophilic or thermophilic conditions to achieve higher process kinetics (Gao et al., 2019a; Gao et al., 2019b; Zamalloa et al., 2013; Zhang et al., 2020a), high-rate blackwater digestion at ambient temperature is worth great research attention.

In recent years, MEC-AD systems have drawn great attention as an enhanced process for biomethane recovery from various organic wastes (Zakaria & Dhar, 2019). However, there are only a few studies that incorporated MEC-ADs in anaerobic blackwater digestion (Liu et al., 2020; Zamalloa et al., 2013). Zamalloa et al. (2013) investigated blackwater digestion at a low OLR of 0.5 g COD/L-d without any microbial community analysis, which left open a wide research gap in evaluating the high-rate digestion performance and understanding the underlying mechanisms. Besides, most studies on MEC-AD systems treating various feedstocks only reported the changes in the relative abundance of different microbes compared to the control, with a focus on dominant/enriched ones (Cai et al., 2016; Gao et al., 2017; Park et al., 2018; Zhao et al., 2016c). Thus, there is a lack of knowledge regarding the interrelationships of various microbes, the microbial community development during a long-term continuous operation, and the links between operational conditions (e.g., OLRs, open/closed circuit), microbial community dynamics, and reactor performances.

In this study, the long-term performance of a semi-continuous MEC-AD reactor was investigated on concentrated blackwater digestion under ambient temperature. The reactor performance and state variables were investigated at different OLRs ranging from 0.77 to 3.03 g COD/L-d. Moreover, the applied potential was cut off during a stage as a control to compare the open/closed circuit performance, which is one of the novelties of this study. The open-circuit control stage can help directly identify the impacts of applied potential on reactor performance and the microbial community cultivated by the long-term closed-circuit operation. The statistic-based microbial community analysis throughout all operation stages helped accurately ascertain

the dynamic changes and identify the different roles and interactions of functional microbes in the mixed-culture system. The results of this study could help with the elucidation of the underlying microbial driving force and further guide reactor optimization and operation in the future.

3.2 Materials and methods

3.2.1 MEC-AD reactor configuration and inoculation

A single-chamber MEC-AD reactor was fabricated with plexiglass tubes, with a total volume and a working volume of 410 ml and 330 ml, respectively (Figure A.1A in Appendix A). A pair of stainless-steel frames attached with high-density carbon fibers (2293-A, 24A Carbon Fiber, Fibre Glast Development Corp., Ohio, USA) (Figure A.1B in Appendix A), were fixed on the left wall as the anode and right wall as the cathode, respectively. The surface area of each electrode was 39 cm^2, corresponding to a specific surface area of 11.82 m^2/m^3. The carbon fibers were pretreated for 3 days in series before fabrication, following the method previously described in the literature (Dhar et al., 2013). An Ag/AgCl reference electrode (MF-2052, Bioanalytical System Inc., Indiana, USA) was inserted into the reactor with <1 cm distance from the anode electrode. During the experimental operation, anode potential was fixed with a multi-channel potentiostat system (Squidstat Prime, Admiral Instruments, Arizona, USA) at -0.2 V vs. standard hydrogen electrode (SHE), which has been identified as the optimum anode potential for the selection of kinetically efficient electroactive bacteria from mixed culture (Torres et al., 2009). The reactor was equipped with one liquid sampling port and one gas outlet port connected to a gas bag for biogas collection.

The reactor was initially inoculated with i) 30 mL effluent from a dual-chamber MEC that had been fed with 25mM synthetic acetate medium for almost a year; ii) 40 mL anaerobic digester sludge obtained from a lab-scale anaerobic digester with 25 g/L total suspended solids (TSS) and 13 g/L volatile suspended solids (VSS), and iii) 60 mL raw vacuum toilet blackwater (detailed composition provided in Section 2.2). For the enrichment of functional biofilms, the reactor was fed with synthetic blackwater for about 4 months in semi-continuous mode. The detailed

composition and characteristics of the synthetic blackwater were provided in our previous research (Huang et al., 2020b). The OLR was maintained at 1.875 g COD/L-d during the enrichment process. The reactor was purged with nitrogen for 5 min to eliminate oxygen at the beginning of the experiment and incubated at room temperature (20 ± 0.5℃).

3.2.2 Blackwater collection and characterization

As described in our previous study (Huang et al., 2020b), raw blackwater feedstock was collected from the University of Alberta Campus, with an average total COD (TCOD) concentration of ~15 g/L, total ammonia nitrogen (TAN) concentration of ~ 1.0 g/L and pH of 8.6. The blackwater feedstock was stored at 4 ℃ for up to two weeks before further utilization. The physicochemical characteristics of the blackwater were measured immediately after preparation with average concentrations of 15.1 ± 0.6 g/L TCOD, 4.8 ± 0.6 g/L soluble COD (SCOD), 1.04 ± 0.08 g/L TAN, 6.09 ± 0.36 g/L TSS, 5.36 ± 0.16 g/L VSS. Also, we determined the BMP of the collected blackwater with a method described in our previous study (Huang et al., 2020b). The determined BMP of feedstock blackwater was about 45% (see Figure A.2 in Appendix A).

3.2.3 MEC-AD operation

For experiments, the MEC-AD reactor was operated in a semi-continuous mode at 20 ± 0.5℃ as follows: every certain days (the frequent varied in different stages), a predetermined volume of blackwater was discharged and replaced by the same amount of fresh raw blackwater (see Table 3.1). The MEC-AD reactor was continuously mixed by a magnetic stirrer bar, including the effluent discharging and influent feeding processes. To avoid oxygen intrusion into the reactor, the reactor was connected to a nitrogen gas bag through the gas sampling port during the effluent discharging process. The reactor was operated for 419 days in 6 different stages, as detailed in Table 3.1. In Stage 5, the electric circuit was cut off by disconnecting the reactor with the potentiostat, and the reactor was operated under the open circuit condition at OLR of ~3.0 g COD/L-d. In Stage 6, the reactor was reconnected to the potentiostat with anode potential fixed at -0.2V vs. SHE and operated at the same OLR as Stage 4 and 5. Before changing stages, the reactor

was entirely evacuated for the microbial community sampling. The liquid content was centrifuged for 5 mins at 4000 rpm. Then, the supernatant was discarded. 2 mL settled solids were sampled as suspended sludge and the remaining was recycled back to the reactor. Biofilms samples were collected from 10-20 different locations on the surface of electrodes and then mixed samples (~1.5 mL) were used for DNA extraction. After sampling, the reactor was purged with nitrogen gas to create an anaerobic condition.

Table 3.1 Operational parameters and conditions for the MEC-AD reactor treating vacuum toilet blackwater.

	Stage 1	Stage 2	Stage 3	Stage 4	Stage 5	Stage 6
Operation period (day)	0 - 48	49 - 105	106 - 156	157 - 237	238 - 347	348 - 419
OLR (g COD/L-d)	0.77	1.03	1.67	3.03	3.01	2.95
HRT (days)	20	15	9	5	5	5
Duration for each feeding/discharging cycle (days)	4	3	3	2	2	2
Feeding/discharging amount (mL)	66	66	110	132	132	132
Operation condition	Closed circuit	Closed circuit	Closed circuit	Closed circuit	Open circuit	Closed circuit

3.2.4 Analytical methods

Blackwater TCOD and SCOD concentrations were measured using the closed reflux titrimetric method 5220C (standard method). Hach ammonia reagent kits (High Range, 0 – 50 mg nitrogen/L; Hach Co., Loveland, Colorado, USA) were used to measure TAN concentration. For SCOD and TAN analysis, samples were diluted by DI water and filtered using 0.45 μm membrane syringe filters. A B40PCID pH meter (VWR, SympHony) was used to measure the pH. Liquid samples for short-chain volatile fatty acid (SCVFA) measurement were diluted with ultrapure water and filtered with 0.2 μm membrane syringe filters, then measured by a Dionex ICS-2100 ionic chromatography system (Thermo Fisher, Waltham, MA, USA). TSS and VSS were measured

according to the Standard Method described in Federation and Association (2005). A GMH3151 manual pressure meter (Greisinger, Regenstauf, Germany) was used to determine the headspace pressure of serum bottles in the BMP test. A 7890B gas chromatograph (Agilent Technologies, Santa Clara, USA) equipped with a thermal conductivity detector and two columns (i.e. Molsieve 5A 2.44m 2mm for CH_4 and HayeSep N 1.83m 2mm for O_2, N_2, and CO_2) was used to determine the gas composition in the gas bag including O_2, N_2, CO_2, and CH_4.

3.2.5 DNA extraction and sequence analysis

The suspended sludge and biofilm samples from both anode and cathode electrodes were collected at the end of each operation stage. The genomic DNA was extracted from the biomass samples using DNeasy PowerSoil Kit (QIAGEN, Hilden, Germany) following the manufacturer's protocol. After checking the concentration and quality using NanoDrop One (ThermoFisher, Waltham, MA), the DNA samples were stored at − 80 °C until downstream analysis was performed. During the PCR process, 16S rRNA genes were amplified using the universal primer-pair 515F (GTGCCAGCMGCCGCGG) and 806R (GGACTACHVGGGTWTCTAAT). 16S rRNA genes of the representative clones were sequenced by Genome Quebec (Montréal, Canada) on the Illumina MiSeq platform. The DADA2 algorithm (Callahan et al., 2016) in Qiime2 pipelines (Hall & Beiko, 2018) was used to process the raw sequence data by pairing the forward and reverse sequences reads, removing chimeras and low-quality sequences. Taxonomy was assigned using 99% similarity in GreenGenes (version 13_8) reference database (McDonald et al., 2012).

3.2.6 Statistical analysis

Microbial Alpha and Beta diversity and principal coordinate analysis (PCoA) were analyzed at the genus level with the "vegan" package in R (Oksanen et al., 2010). Permutational multivariate analysis of variance was conducted based on distance matrices by Adonis to explain microbial communities with environmental variables using the "vegan" package in R (Oksanen et al., 2010). A *p*-value smaller than 0.05 represents the significant impacts of environmental conditions on microbial communities. Student T-test was performed using Microsoft Excel® software to identify

the performance difference among stages. The statistic analysis and graphing of microbial co-occurrence network were carried out using "psych" (Revelle, 2017) and "igraph" (Csardi & Nepusz, 2006) package in R. A connection (edge) between nodes stands for a strong (Spearman's $\rho > 0.6$) and significant ($p < 0.05$) correlation.

3.2.7 Calculations

Methane production in BMP tests was calculated according to the literature (Gao et al., 2018).

Methane yield (%) was calculated using Equation (1) (Gao et al., 2018):

$$Methane\ yield\ (\%) = \frac{COD_{methane}}{COD_{input}} * 100 \quad (1)$$

where:

$COD_{methane}$: The COD equivalent of produced methane (in mg COD);

COD_{input}: Amount of total COD input (in mg COD).

The free ammonia concentration was calculated using Equation (2) (Gao et al., 2018):

$$FA = 1.214 \times TAN \cdot (1 + \frac{10^{-pH}}{10^{-(0.09018+\frac{2729.92}{T\,(K)})}})^{-1} \quad (2)$$

where:

NH_3: Free ammonia (FA) (in mg L^{-1});

TAN: Total ammonia nitrogen (in mg L^{-1});

T (K): Kelvin temperature.

Electric energy supply (W_E [J/d]) in the MEC-AD system was calculated using Equation (3) (Zhao et al., 2016b):

$$W_E = IE_{AP}\Delta t \quad (3)$$

where I is the average current (A); E_{AP} (V) is the applied voltage; Δt (s) is 86400 seconds per day.

Energy income in the MEC-AD system as methane production was calculated based on Equation (4):

$$W_{close} = \Delta H_S V_{close}/V_m$$

$$W_{open} = \Delta H_S V_{open}/V_m \quad (4)$$

where ΔHs is the energy content of methane based on the heat of combustion (upper heating value) (890.31 × 10^3 J/mol); W_{close} and W_{open} are the energy income from methane production under closed and open circuit conditions (J/ d), respectively; V_{close} and V_{open} are the methane production under closed and open circuit conditions (L/d), respectively; V_m is the molar volume of the gas under room temperature and atmospheric pressure (24.04 L/mol). The energy efficiency was calculated based on the following Equation (5):

$$\text{Change in energy efficiency} = \frac{W_{close} - W_E}{W_{open}} \times 100\% \quad (5)$$

3.3 Results and discussion

3.3.1 System performance

3.3.1.1 Methane production

The steady-state condition of each stage was determined by constant methane yield and TCOD removal with a standard deviation of less than 10% of the average values. Figure 3.1A illustrates the steady-state methane yields during the whole operation period of about 420 days under different operation stages. The highest methane yield of 42.4 ± 2.7% out of 45% BMP was achieved in Stage 1 at OLR of 0.77 g COD/L-d. With the decrease of the HRTs (from 20 to 5 days) and the increase of OLRs (from 0.77 to 3.03 g COD/L-d), the methane yield showed a continuously decreasing trend from Stage 1 to 4 and achieved 32.4 ± 1.7% in Stage 4 at an OLR of 3.03 g COD/L-d. The decreased methane yield with increasing OLR was intensively reported in many previous studies (Gao et al., 2019b; Huang et al., 2020b), mainly due to the washout of methanogens, inhibition brought by organic acid accumulation, and limited substrate uptake capacity of archaeal communities. Interestingly, although the OLR has almost been doubled from Stage 3 to Stage 4 (from 1.67 to 3.03 g COD/L-d), the methane yield only slightly decreased by 2.3%, which indicated the strong methanogenesis capacity of the MEC-AD reactor to withstand the high organic loading rates. In Stage 5, when the applied potential was cut off at a constant

OLR of ~3.0 g COD/L-d, the methane yield decreased significantly from 32.4 ± 1.7% to 24.1 ± 2.3% ($p < 0.01$) with a long unstable period. However, when the reactor was operated again with applied potential in the last stage, the methane yield rebounded to 35.2 ± 2.1%, which further proved the significance of applied potential on methane production improvement. Liu et al. (2016a) demonstrated that MEC-AD operated at 10 ℃ achieved a methane yield close to the control reactor operated at 30 ℃ when using acetate as a model substrate. Because methanogenesis via hydrogenotrophic methanogens and direct interspecies electron transfer (DIET) is less sensitive to low temperatures (Liu et al., 2016a). However, the advantages of MEC-AD at low temperature will be less obvious when treating complex waste streams, since hydrolysis might be the rate-limiting factor. For example, Gao et al. (2019b) showed 44% (out of 48%) methane yield at an OLR of 3.09 g COD/L-d when treating vacuum toilet blackwater in a mesophilic (35 ℃) UASB reactor, which was much higher than 35.2% (out of 45%) achieved in our study at 20 ℃. According to the low SCVFA and soluble COD level in the effluent (discussed below), we can conclude that hydrolysis limited the digestion kinetics.

The peak current density in Stage 1 showed the lowest values (38.82 ± 3.24 A/m^3) as well as the most obvious ups and downs with each feeding cycle (see Figure A.3 in Appendix A). Although the methane yield was the highest in Stage 1, OLR of 0.77 g COD/L-d (HRT of 20 days) was unfavorable for electroactive bacterial activity. It is expected that longer HRTs would stimulate the enrichment of acetoclastic methanogens, which can outcompete electroactive bacteria for acetate (Liu et al., 2016b). The current density increased from 38.82 ± 3.24 (Stage 1) to 67.77 ± 5.32 A/m^3 (Stage 2), when HRT was decreased from 20 to 15 days. However, further decrease in HRTs from 15 to 5 days (Stage 3, 4, and 6), slightly decreased the current density, which could be attributed to the limited availability of hydrolysis/fermentation products for electroactive bacteria. Also, after open circuit operation for more than 100 days, Stage 6 reached comparable current density as Stage 4. However, it took a much longer time (20 - 25 days) to reach a steady peak current in Stage 6, compared to other stages (5 - 15 days), which could be ascribed to the re-enrichment of functional electroactive bacteria.

The specific methane production rates (SMPRs) increased in a stepwise fashion from 117.6 ± 1.9 to 358.5 ± 18.8 mL/L-d with the increase of the OLRs from Stage 1 to 4 (Figure 3.1B). The increase was predictable because the specific substrate utilization rate is proportional to the substrate concentration (within a certain range) according to the Monod equation (Maier & Pepper, 2015). However, a 23.3% decrease in methane production rate (275.1 ± 20.6 mL/L-d) was observed under open-circuit condition (Stage 5) compared to Stage 4 at the same OLR of ~ 3.0 g COD/L-d ($p < 0.01$). After reconnecting to the potentiostat (Stage 6), the methane production rate increased to the comparable level (386.1 ± 18.2 mL/L-d) as Stage 4, indicating a successful system recovery. A recent study investigated a carbon fiber amended anaerobic biofilm reactor for blackwater digestion at the same OLR (3.01 g COD/L-d) and temperature, and achieved an SMPR of 305 ± 14.7 mL/L-d, with great enrichment of electroactive bacteria and electrotrophic archaea capable of DIET (Huang et al., 2020b). However, about 21% higher SMPR was achieved in Stage 6 in this study, indicating power input was an indispensable factor for AD enhancement in the MEC-AD system except for the enrichment of electroactive microbes. During the long unstable period in open-circuit Stage 5, the specific methane production rate showed a continuous decreasing trend until reaching the final steady-state. Some previous studies have demonstrated that intermittent power supply could increase the energy efficiency and organics removal in the MECs while maintaining a stable microbiome (Cho et al., 2019; Zakaria & Dhar, 2021b). Thus, optimizing the closed/open-circuit (or on/off) scheme to increase the economic benefits will be one of the focuses of future studies.

High methane content in biogas was observed throughout the entire operation period (Figure 3.1C). The highest methane content in biogas was achieved in Stage 1 (83.1 ± 0.67%), whereas in open circuit Stage 5, only 74.9 ± 2.32% was reached. After resupplying with power in Stage 6, the methane content increased back to 79.6 ± 1.90% ($p < 0.05$). It has been demonstrated that the MEC-AD system could promote biogas purity by in-situ reduction of CO_2 to CH_4 by dominant hydrogenotrophic methanogens or DIET (Bo et al., 2014; Zakaria & Dhar, 2019). Besides, the pH drop in Stage 5 might also be an influencing factor of biogas content (Feng et al., 2018).

Conventional blackwater digestion systems usually showed lower methane content in biogas, such as 62% in a UASB (Gallagher & Sharvelle, 2010), 66% in a UASB septic tank (Kujawa-Roeleveld et al., 2006), and 70 - 74% in an anaerobic baffled reactor (Moges et al., 2018). Since higher CO_2 content in biogas will contribute to the negative effect on biogas compression, higher methane content achieved in this study would reduce the operating costs when substituting natural gas for electricity and vehicle fuel generation with higher applicability (Bo et al., 2014).

(A)

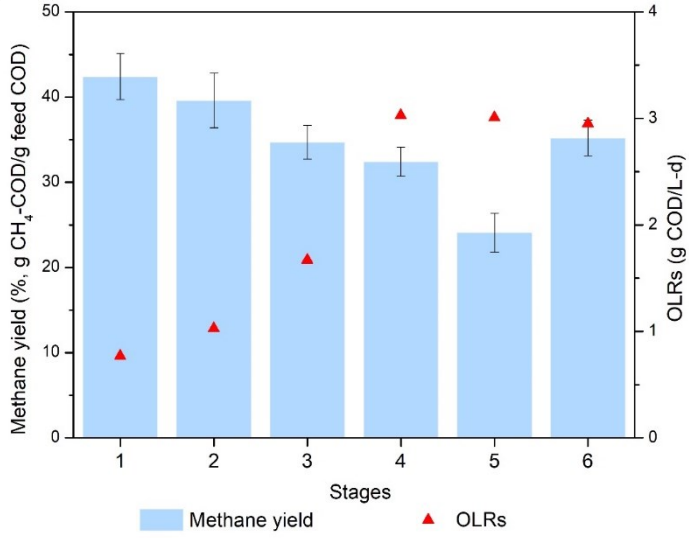

(B)

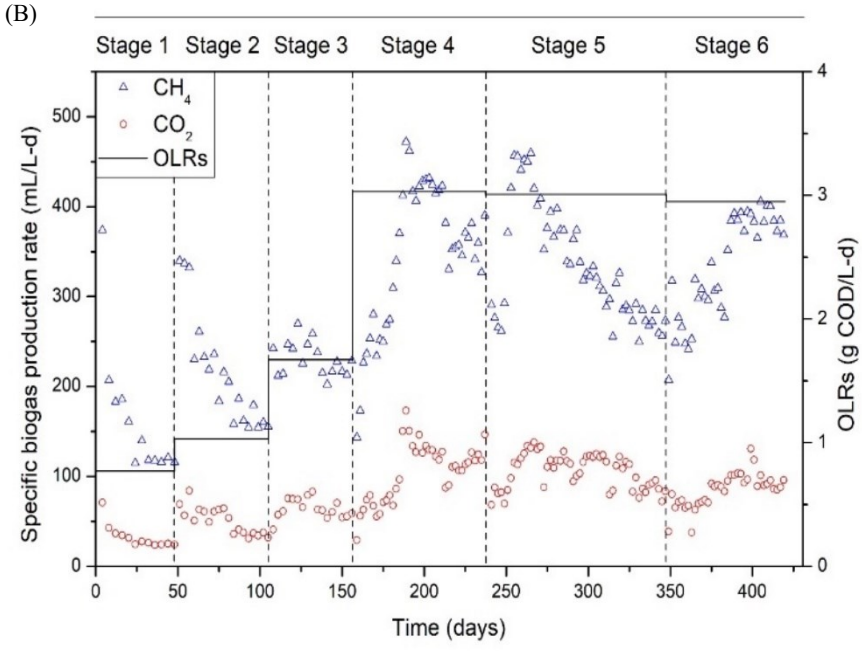

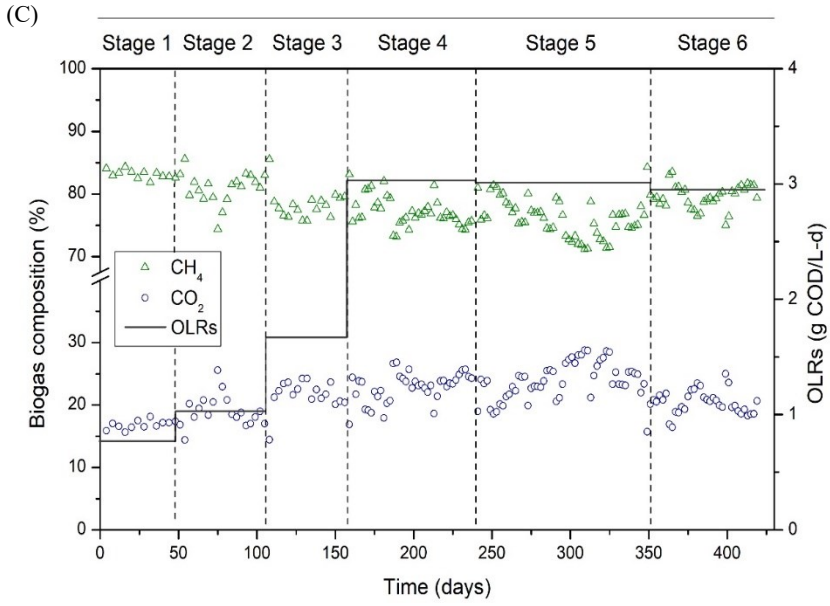

Figure 3.1 (A) Methane yield at steady state of different operation stages; (B) Specific biogas production rates during the entire operation period; (C) Biogas composition during the entire operation period.

3.3.1.2 Organics removal

Figure 3.2A shows the influent and effluent TCOD concentrations and TCOD removal efficiencies under different operating conditions. Based on steady-state results, at the lowest OLR of 0.77 g COD/L-d (20 days HRT) in Stage 1, the average TCOD removal efficiency reached 82.6 ± 0.96%. In most cases, cell synthesis usually utilizes about 10% of TCOD in anaerobic digestion processes (Grady Jr et al., 2011). Thus, according to 42.4% of methane yield, we can estimate ~ 30% of TCOD was accumulated in the reactor, most of which was not biodegradable based on the 45% BMP value. The effluent COD concentration kept increasing from Stage 1 to 4 with the increase in OLRs, while the COD removal efficiency dropped to 47.4 ± 4.4% during steady-state operation (day 180 - 237) of Stage 4. When switched to open circuit condition in Stage 5, the reactor showed the lowest COD removal efficiency of 31.8 ± 2.1%, which was recovered to 42.0 ± 3.2% in Stage 6 after the system was reconnected to the potentiostat. Although the TCOD removal efficiencies were less than 50% in Stage 4 and 6, most TCOD in the effluent was non-biodegradable with low

methane potential, which can be removed by a further aerobic and/or physico-chemical post-treatment. Many studies revealed higher degradation rates of different organics in MEC-AD systems (Gao et al., 2017; Huang et al., 2020a; Zhao et al., 2016e). It has been reported that the electroactive bacteria usually adapted to grow on the low-potential electron acceptor, such as electrode (Zhao et al., 2016e). The enriched electroactive bacteria can utilize a broad type of substrates as electron donors, such as SCVFAs, glucose, and other complex hydrocarbons (Lovley et al., 2011). However, some electroactive bacteria are not capable of degrading complex or refractory compounds alone; thus, syntrophic metabolisms usually play an important role in organics removal (Dhar et al., 2019; Parameswaran et al., 2009). For instance, Sun et al. (2020) indicated the phenol anodic oxidation in their study was mainly attributed to the enhanced syntrophic metabolism among electroactive bacteria and phenol-degrading bacteria. Also, the syntrophic interactions between hydrogenotrophic methanogens and fermentative bacteria can enable high-rate conversion of complex compounds (Huang et al., 2020a).

Similar to the trend of TCOD removal, the highest average TSS (86.2 ± 3.2%) and VSS (84.7 ± 2.8%) removal efficiency were achieved at an OLR of 0.77 g COD/L-d, which gradually decreased to 56.8 ± 1.7% and 52. 2 ± 1.9%, respectively, as OLR increased to 3.03 g COD/L-d in Stage 4 (see Table 3.2). Thus, as expected, lower operating OLRs (i.e., longer HRTs) would be essential for achieving higher suspended solids removal. The lowest TSS and VSS removal efficiency was observed in Stage 5 under open-circuit, while the decrease was marginally lower ($p > 0.05$) as compared to Stage 4 and 6 operated at the same OLR of ~ 3.0 g COD/L-d. Despite the achievements in terms of methane production, a few studies reported marginal improvement in solids removal efficiencies with MEC-AD systems (Park et al., 2018; Zhao et al., 2016a). Contrary to these results, several studies reported enhanced sludge hydrolysis by MEC-AD systems (Feng et al., 2015; Zhao et al., 2016c; Zhao et al., 2016e). However, the underlying mechanisms behind hydrolysis improvement are still ambiguous. Possibly, the rapid removal of hydrolysis products by anodic oxidation could help accelerate the hydrolysis process by mitigating the product inhibition on hydrolytic enzyme release (Kiely et al., 2011; Zhao et al., 2016e).

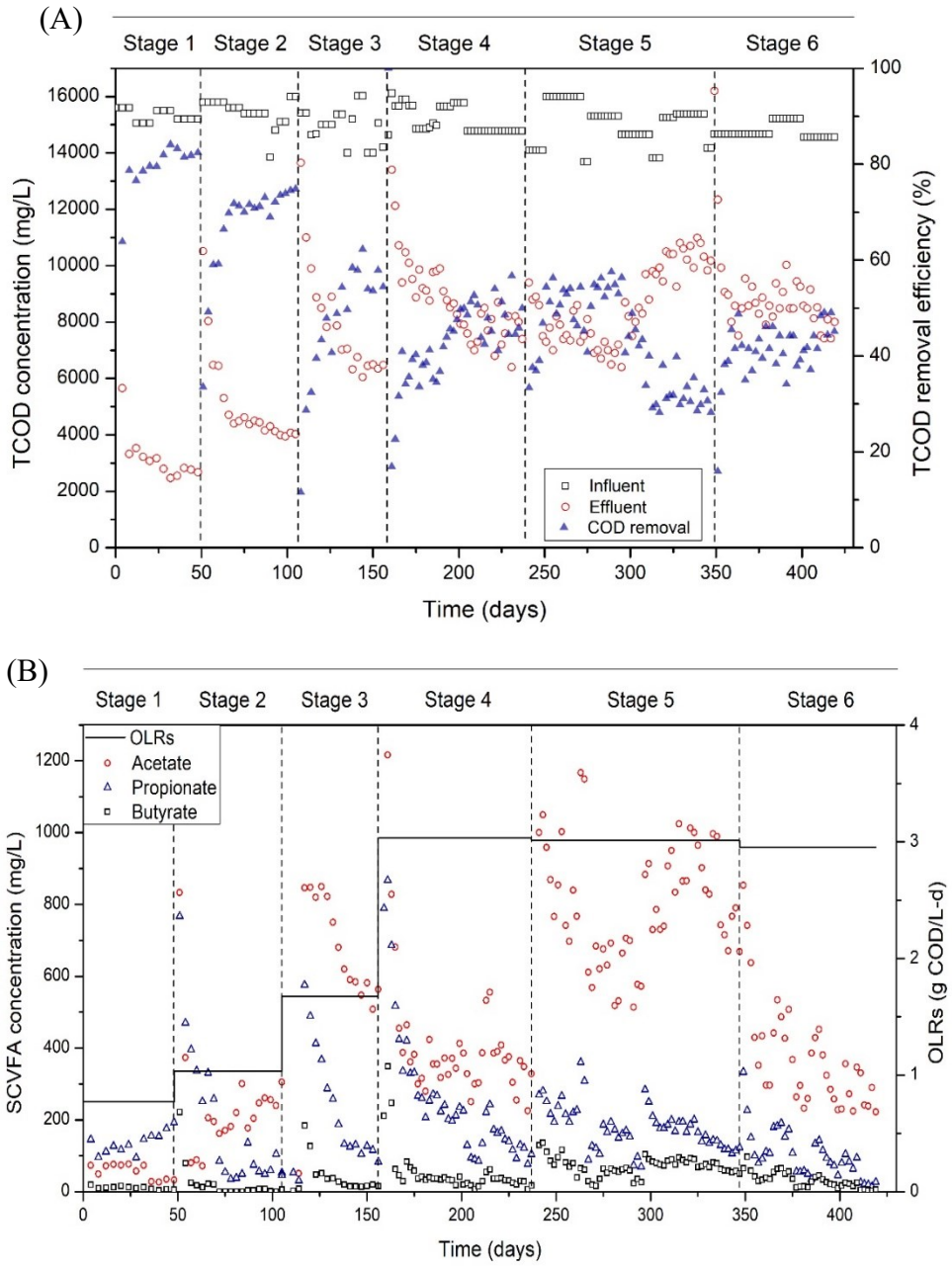

Figure 3.2 (A) The influent and effluent TCOD concentrations and TCOD removal efficiencies during the entire operation period; (B) Changes in SCVFA concentrations during the operation under different OLRs.

Table 3.2 Characteristics for influent and effluent of the MEC-AD reactor treating vacuum toilet blackwater.

	Unit	Influent	Effluent					
			Stage 1	Stage 2	Stage 3	Stage 4	Stage 5	Stage 6
TCOD	mg/L	15074 (± 567)	2655 ± 133	4133 ± 153	6414 ± 196	7733 ± 652	10353 ± 441	8358 ± 624
SCOD	mg/L	4820 (± 606)	1303 ± 120	1820 ± 221	2100 ± 209	2204 ± 389	3208 ± 443	1986 ± 267
TCOD removal efficiency	%		82.6 ± 0.96	72.8 ± 1.83	57.0 ± 2.90	47.4 ± 4.41	31.8 ± 2.1	42.0 ± 3.2
TSS	g/L	6.09 (± 0.36)	0.87 ± 0.18	1.08 ± 0.12	2.52 ± 0.33	2.79 ± 0.26	3.58 ± 0.45	2.98 ± 0.36
TSS removal efficiency	%		86.2 ± 3.2	83.0 ± 1.6	62.2 ± 1.9	56.8 ± 1.7	48.8 ± 2.6	52.6 ± 0.8
VSS	g/L	5.36 (± 0.16)	0.83 ± 0.15	1.14 ± 0.20	2.21 ± 0.28	2.85 ± 0.47	3.39 ± 0.56	2.80 ± 0.36
VSS removal efficiency	%		84.7 ± 2.8	81.7 ± 3.0	57.3 ± 3.3	52. 2 ± 1.9	47.4 ± 2.8	50.9 ± 2.1
Methane yield	%		42.4 ± 2.7	39.6 ± 3.2	34.7 ± 2.0	32.4 ± 1.7	24.1 ± 2.3	35.2 ± 2.1
Specific methane production rate (SMPR)	mL/L-d		117.6 ± 1.9	163.8 ± 1.1	217.1 ± 8.3	358.5 ± 18.8	275.1 ± 20.6	386.1 ± 18.2
Methane content in biogas	%		83.1 ± 0.67	81.8 ± 1.20	78.0 ± 1.47	77.0 ± 2.41	74.9 ± 2.32	79.6 ± 1.90
pH		8.6 (± 0.1)	7.86 ± 0.07	7.60 ± 0.08	7.41 ± 0.06	7.30 ± 0.05	7.12 ± 0.06	7.27 ± 0.05
Acetate	mg/L		30.5 ± 3.2	245.7 ± 39.4	570.7 ± 33.0	372.3 ± 89.3	851.4 ± 115.1	300.6 ± 70.6
Propionate	mg/L		169.8 ± 15.8	69.1 ± 30.0	117.1 ± 16.5	146.0 ± 46.2	146.3 ± 28.6	71.7 ± 39.5
Butyrate	mg/L		5.8 ± 1.4	2.7 ± 1.1	16.4 ± 2.3	32.4 ± 14.0	71.2 ± 13.2	19.0 ± 12.6
TAN	g/L	1.04 (± 0.08)	1.34 ± 0.14	1.33 ± 0.16	1.28 ± 0.21	1.12 ± 0.09	1.18 ± 0.04	1.13 ± 0.07
Free ammonia (FA)	mg/L	171.9	45.3	25.0	15.6	10.7	7.4	10.0

Note: The data were all based on steady-state results of the MEC-AD reactor.

3.3.2 Process state variables (pH, FA, SCVFAs, SCOD)

The highest pH value was observed in Stage 1 due to the readily consumed organic acids at the low organic loading rate. The pH value was sustained within the favorable range for methanogenesis in all stages. Higher NH_4^+-N concentration in the effluent (1.1 - 1.3 g/L) than that in the influent (~ 1.0 g/L in influent) was observed during the digestion process (see Table 3.2), which can be explained by the released ammonia from hydrolysis of blackwater protein content. Slightly decreased TAN and free ammonia concentrations were observed with the increase of OLRs, mainly due to the fraction of the nitrogen assimilated by heterotrophic bacteria for cell synthesis was higher at higher OLRs (Bassin et al., 2016). In addition, the raising OLR caused the increase of organic acid concentration with a pH drop, which also contributed to the free ammonia concentration decrease. Throughout the operational period, no free ammonia inhibition (FA < 50 mg/L) on the methanogenesis process was observed due to the room temperature operation.

The effluent short-chain volatile fatty acids (SCVFAs) are frequently used as an important indicator to assess the process stability and performance of the digestion. The three SCVFAs (i.e. acetate, propionate, butyrate) concentrations in the effluent of the MEC-AD reactor through the whole operational period were monitored (see Table 3.2). During closed-circuit operation (Stage 1 - 4, and 6), the SCVFA concentrations were mostly sustained in a relatively low range (< 400 mg/L) (Figure 3.2B). However, significant increases in the SCVFA concentrations (mainly acetate) were observed during open-circuit operation in Stage 5. The acetate accumulated up to 1000 mg/L, and all SCVFA concentrations almost doubled compared to Stage 4 and 6 under closed-circuit condition. Similarly, the SCOD concentration in Stage 5 increased to 3.2 g /L, which was about 52% higher than that of Stage 4 and 6 at the same OLR of ~ 3.0 g COD/L-d. These results indicated that MEC significantly improved SCVFA utilization via bioelectrochemical pathways. These findings are in agreement with many previous studies, which proved the rapid degradation of SCVFAs in MEC-AD systems (Cai et al., 2016; Feng et al., 2015). For example, Park et al. (2019) investigated the long-term performance of a MEC-AD reactor fed with food waste. In this study, the maximum OLR of AD reactor was 4 g COD/L-d, whereas the methane production was stable

at an OLR as high as 10 g COD/L-d in the MEC-AD, mainly because the MEC-AD could quickly remove the VFAs and reduce H^+ to H_2 to resolve the inhibition and achieve the system stability at high OLRs.

3.3.3 Microbial community analysis

3.3.3.1 Microbial community diversity

The alpha-diversity of archaeal, bacterial, and total communities was analyzed at the genus level (see Figure 3.3A). The Shannon diversity for archaeal communities was much lower than that of the bacterial communities ($p < 0.01$). However, the Shannon index for the total community was not significantly different among different sampling locations ($p > 0.05$), and also did not show large variations among different stages ($p > 0.05$). From stage 2, the Shannon index for the total communities fluctuated among different samples but almost kept stable at about 3.5, similar to that of bacterial communities due to the higher abundance of the bacterial population. All biomass samples from anode, cathode, and suspension had a similar initial Shannon index of about 1.5 for archaeal communities. With the increase in OLRs in different stages, the archaeal diversity in suspended biomass remained stable, while an obvious decreasing trend was observed in anode and cathode samples. The lower archaeal diversity co-occurred with higher methane production at higher OLRs could be attributed to the microbes with higher growth rates selected by the high substrate concentrations, i.e. r-strategists (Gao et al., 2019a). A recent study showed lower bacterial diversity in the anaerobic reactor treating concentrated vacuum toilet blackwater than the reactor treating diluted conventional blackwater (Gao et al., 2019a). The higher stress level selected r-strategists resulted in higher substrate utilization and methane production.

The beta-diversity of total communities was presented by the principal coordinate analysis (PCoA) plot using Bray-Curtis distances among samples (Figure 3.3B). The microbial community difference was much more significant among different stages ($p < 0.01$) than different sampling locations ($p = 0.146$). The anodic microbial communities were similar to the cathodic communities; however, the suspended sludge communities diverged more to the blackwater sample. These

results indicated that the suspended microbial communities were more similar to the communities from the feedstock (i.e., blackwater). Notably, from Stage 1 to 3, the microbial communities shifted towards the consistent direction to the blackwater sample. Nonetheless, a different diverging direction from Stage 1 to 3 but more stable communities were developed in Stage 4 to 6 at the OLR of ~ 3.0 g COD/L-d. Thus, two clusters were formed apart from each other along the PCoA 1 axis, which explained 31.1% of the total sample variance. The results suggested the variation in OLRs could significantly influence the microbial community shifts. Besides, as an open-circuit control stage, Stage 5 showed a more significant difference in bacterial diversity (p = 0.045) than archaeal diversity (p = 0.672) when comparing with those in closed-circuit Stage 4 and 6.

(A)

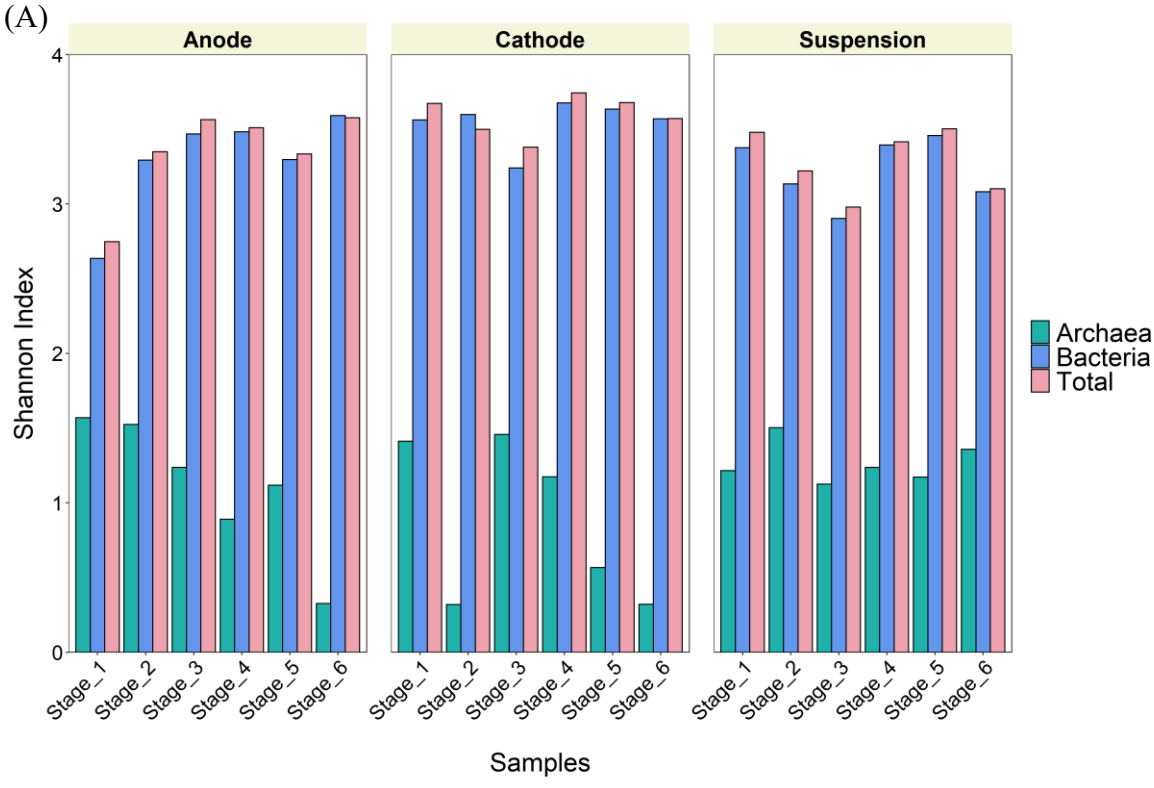

(B)

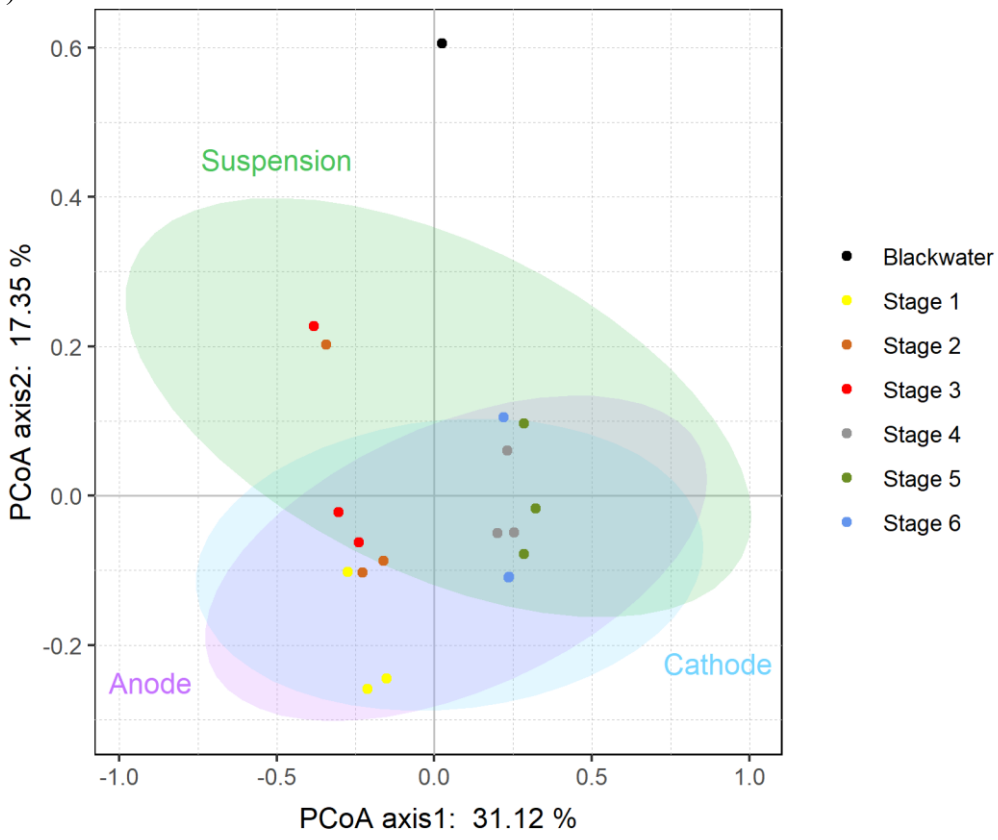

Figure 3.3 (A) Shannon index analyzed at the genus level; (B) Principal coordinate analysis (PCoA) of microbial communities in blackwater and reactor samples. PCoA was computed using Bray-Curtis distance calculated using genus abundance data (ellipse confidence level = 95%).

3.3.3.2 Archaeal structures

Figure 3.4A shows the relative abundance of the archaeal population in the total microbial community for anode, cathode, and suspended biomass, indicating variations in the methanogenic population in different locations. Under different OLRs, the archaeal population was more abundant on the cathode, as compared to anodic and suspended biomass samples. Interestingly, the highest abundance of the archaeal population (17.0%) was found in cathode biofilms in Stage 2, in accordance with the highest current density in Stage 2 (see Figure A.3 in Appendix A), which indicated the syntrophic interaction happening between electroactive bacteria and methanogenic archaea. When the applied potential was stopped in Stage 5, a significant decrease in cathodic

archaeal abundance (3.5%) was observed, which can be attributed to the unfavorable environmental conditions, such as lack of substrate (i.e. H_2). These results indicated that applied potential and/or hydrogen generation on the cathode played a significant role in the enrichment of the methanogenic population on the cathode. In suspension biomass samples, the archaeal abundance showed a decreasing trend with the increase in OLRs or a decrease in HRTs. However, this trend is quite expected, as previous studies suggested that shorter HRTs could lead to the washout of methanogens from continuous stirred tank (CSTR)-type digester (Huang et al., 2020b).

At the genus level, 11 archaeal taxa with abundance > 1% were detected among samples (Figure 3.4B). Comparing samples from different locations, archaeal communities from suspension were more diverse, which mostly contained hydrogenotrophic methanogens but changed significantly subjected to the OLR variance ($p = 0.05$). However, archaeal communities in anodic and cathodic samples showed less significant relevance to the OLR changes ($p > 0.1$). Initially, the anode was predominated by hydrogenotrophic *Methanoculleus* (41.8%) and secondly dominated by acetoclastic *Methanosaeta* (30.4%) in Stage 1. As the OLR increased to 1.03 g COD/L-d in Stage 2, the relative abundance of *Methanosaeta* increased to 40.1% as the most abundant genus. From Stage 3 to 6 at higher OLRs, due to the inferior growth kinetics (Cai et al., 2016), the abundance of *Methanosaeta* decreased to almost undetectable levels, while *Methanosarcina* overwhelmingly dominated with up to 94.1% abundance. In Stage 5 when the applied potential stopped, the abundance of *Methanosarcina* decreased to 61.2%, as compared to Stage 4 (78.5%) and Stage 6 (94.1%) operated under the same OLR. Also, an increase in the abundance of acid-tolerant hydrogenotrophic *Methanobrevibacter* (22.7%) was observed in Stage 5, possibly as a result of pH drop and SCVFA accumulation (Savant & Ranade, 2004).

On cathode, hydrogenotrophic methanogens (e.g. *Methanobacterium* and *Methanogenium*) were dominant from Stage 1 to 4. *Methanobacterium* is one of the most abundant methanogenic genera reported in the MEC-AD systems treating high-strength waste/wastewater in previous studies (Cai et al., 2016; Gao et al., 2017; Liu et al., 2016b; Sasaki et al., 2010). However, the

abundance of *Methanosarcina* significantly increased from 28.5% in Stage 4 to 87.8% in Stage 5 when the applied potential was stopped (i.e., open-circuit). After switching the reactor to closed-circuit operation in Stage 6 with the same OLR, *Methanosarcina* remained dominant with a slight increase in relative abundance. *Methanosarcina* can utilize multiple substrates, like formate, acetate, methanol, and methylamine, as well as hydrogen and carbon dioxide for methane production, even in extreme environments (Park et al., 2018). Also, *Methanosarcina* species are well-known for their ability to conduct interspecies electron transfer via conductive materials or insoluble electron shuttles to accept electrons from certain electroactive bacteria (Gao et al., 2017). The substantial growth of *Methanosacina* population in Stage 5 might be attributed to the significant accumulation of acetate (~ 1000 mg/L), resulting in a switch of the dominant methanogenic pathway to acetoclastic methanogenesis. However, in Stage 6 when acetate was insufficient, the *Methanosacina* species were still dominant in the archaeal community, but the methanogenic pathway might have been switched to hydrogenotrophic methanogenesis or DIET pathway. Some previous studies have demonstrated that applied voltage/potential could stimulate the growth of *Methanosarcina* species, resulting in superior methane production rates (Park et al., 2018; Sasaki et al., 2010). However, the versatile functionalities of *Methanosarcina* make it challenging to identify and quantify the methane production from each pathway, which will be further explored in future studies.

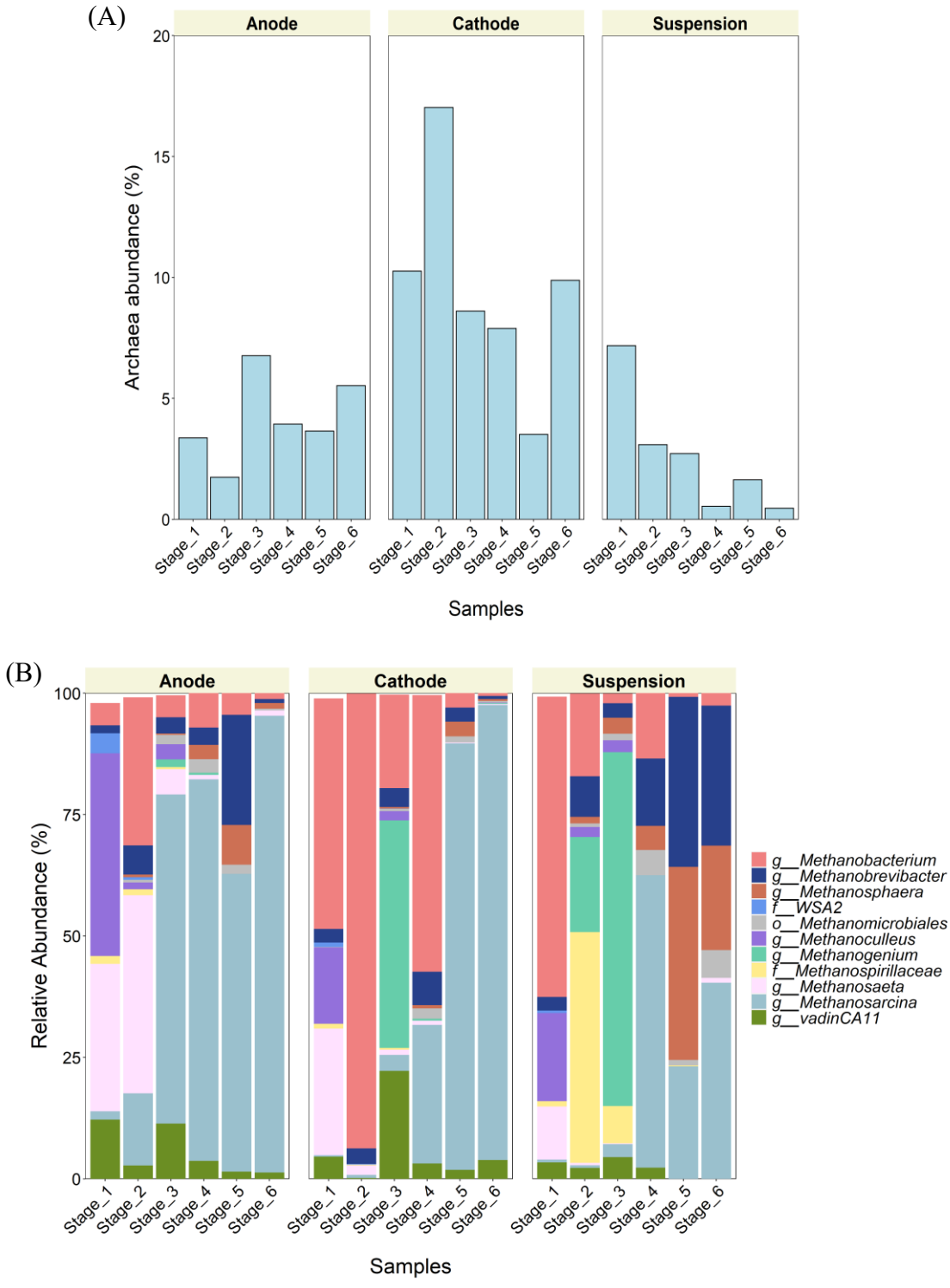

Figure 3.4 (A) Relative abundance of archaea in reactor sludge samples; (B) Relative abundances of archaeal genera with abundance > 1% in the reactor sludge samples. The taxonomic names were as higher level (family: *f_*; order: *o_*) if not identified at genus level.

3.3.3.3 Bacterial structures

The bacterial community was dominated by Firmicutes, Bacteroidetes, and Proteobacteria at the phylum level (see Appendix A Figure A.4) in all samples. For a further assessment, Figure 3.5 illustrates the fold change in relative abundances of 10 most abundant bacterial genera in each sample from reactor sludge and feedstock blackwater. Four groups of genera were classified (Groups A-D in Figure 3.5) based on their fold-changes in relative abundance. Group A clustered the most abundant bacterial genera, which were widely spread in all samples from anode, cathode and suspension, but most of them were absent in blackwater, e.g., *Clostridium*, *Sedimentibacter*, *Syntrophomonas*, *Petrimonas*, *Sphaerochaeta*, an unidentified genus in the order *Bacteroidales*, etc. A recent study demonstrated the syntrophic and electro-active partners of *Petrimonas* and *Methanosarcina* were synergistically enriched in a biochar-supplemented anaerobic digester, resulting in the highly efficient SCVFA degradation (Wang et al., 2020). It was also reported that *Clostridium*, *Sedimentibacter* and *Syntrophomonas* could be electroactive and syntrophic oxidizers that metabolized the substrates to produce acetate, H_2 and CO_2 for H_2-utilizing partners (Huang et al., 2020b; Müller et al., 2016). The extensive enrichment of these genera in this study explained the rapid degradation of SCVFAs with applied potential. Genera in Group B were enriched in Stage 4 to 6 at higher OLRs, and had relatively higher abundance in blackwater than that of Group A, including *Erysipelothrix*, unidentified genera from family *Porphyromonadaceae*, family *Ruminococcaceae* and order *Clostridiales*, etc. Members of *Porphyromonadaceae* are important hydrolytic bacteria capable of the degradation of lignocellulosic biomass (Gao et al., 2019a). Most of these genera in Group B were often detected in high ammonia conditions (Müller et al., 2016). The increased abundance of members in Group B can be attributed to i) the increase of demand for hydrolysis and fermentation of complex organic compounds at higher OLRs, and ii) the increase of sludge community inherited from blackwater.

Genera in Group C, which were all absent in blackwater samples, showed decreasing abundance with the OLR increase and higher abundance in anodic biofilm than cathodic biofilm. Group C contained several important electroactive bacteria, such as *Pseudomonas*, *Arcobacter,*

and *Geobacter*. Notably, *Geobacter* species were often found to be dominant in MEC-AD systems operated with high-strength feedstocks (Cai et al., 2016; Liu et al., 2016b; Zhao et al., 2016b). In this study, *Geobacter* dominated in the anodic bacterial community in Stage 1 with a great abundance of 41.6%; however, with the increase in OLRs, the abundance of *Geobacter* decreased significantly to 0.63% in Stage 4. It must be asserted that most of the electroactive bacteria (e.g., *Geobacter* species) cannot directly metabolize complex fermentable organics due to their limited metabolic versatility (Zhao et al., 2016b). Thus, with the increase of OLR, which introduced more complex organics in the system, fermentative bacteria would play a critical role in the degradation of fermentable organics, resulting in elevated abundance. The bacterial dynamics in Group C offered informative elucidation in how the applied potential affected the anodic performance. For instance, in Stage 5 without applied potential, the abundance of *Geobacter* further decreased to 0.03%, whereas recovered to 1.1% in Stage 6 after switching to closed-circuit operation with the applied potential. Species of *Pseudomonas* are not only electroactive, but also capable of degrading some complex organics including aromatic compounds (Gao et al., 2017). In Stage 5, the abundance of *Pseudomonas* decreased from 0.2% to undetectable level and recovered to 0.2% again in Stage 6. A similar phenomenon was also observed in terms of another electroactive bacteria, *Arcobacter*. These results revealed the crucial role of applied potential in cultivating an electroactive microbiome, which directly affects the system performance. Comparing with other groups, Group C presented the most significant difference in bacterial communities among Stage 5 and other stages (i.e. closed/open circuit). However, consistent with previous studies on microbial electrosynthesis (Rojas et al., 2018), this research revealed the microbial community in the MEC-AD system was resilient and able to recover the electroactivity after a long open circuit period. Lastly, Group D represents the bacterial genera that are predominant in blackwater samples but showed much lower abundance in reactor sludge samples., including *Bifidobacterium*, *Faecalibacterium*, etc., which are mostly present in the intestines and stomach of human bodies (Ramirez-Farias et al., 2008).

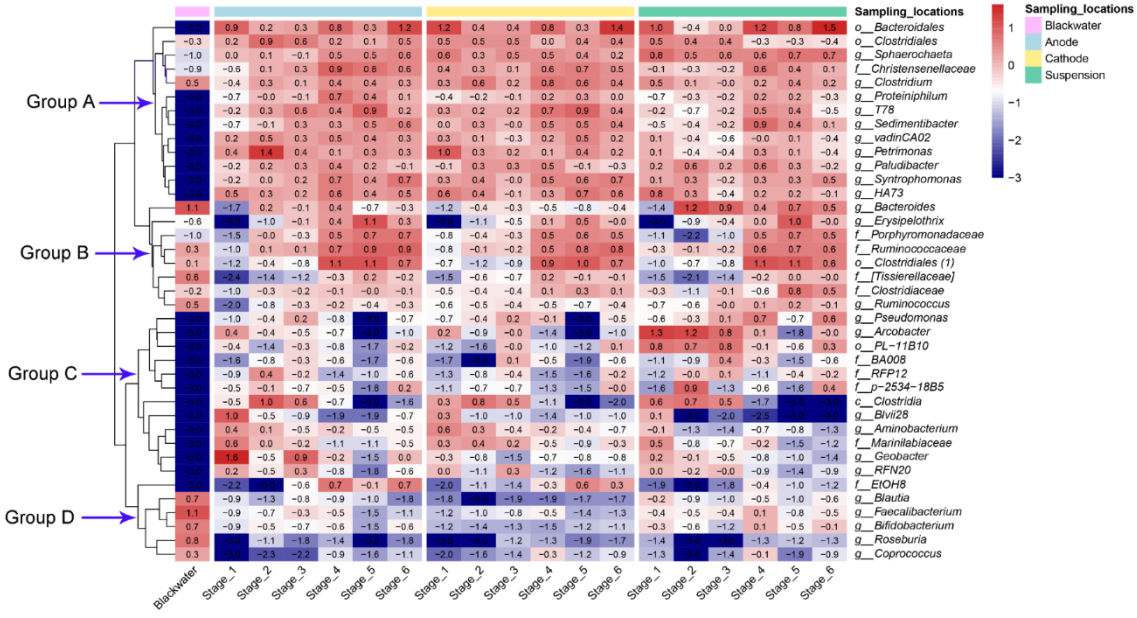

Figure 3.5 Relative abundances of 10 most abundant bacterial genera in each sample from reactor sludge and blackwater. Unidentified genera were named at family (*f*__), order *(o*__) or class level (*c*_). Numbers are log (relative abundances (%)) of genera in each sample. 0.001% was added to absent families to avoid zero denominator.

3.3.3.4 Microbial co-occurrence network

It is widely acknowledged that the degradation of complex organics usually involves mutualistic microbial cooperation (Ju et al., 2014). Meanwhile, competition also happens between microbes that rely on the same substrate for growth. To investigate the potential interactions between important microbial taxa, network analysis was conducted for abundant genera in both archaeal (top 5) and bacterial (top 20) communities on anode and cathode. The resulting biofilm network (Figure 3.6) consisted of 58 edges (correlations) and 20 nodes (genera). A much higher number of strong positive correlations (46) were observed than that of the negative ones (12). The network features a short average path length (2.15) and a high cluster co-efficient (0.63) with a diameter (the longest distance between nodes) of 5 edges, indicating a small-world network (Ju et al., 2014). Details of network topological characteristics were summarized in Appendix A (Table A.1).

Using degree centrality (see Appendix A Table A.1), *Methanosaeta*, *Erysipelothrix*, a genus from order *Bacteroidales*, two genera from family *Christensenellaceae* and *Porphyromonadaceae* were identified as hub microbes in the network. *Christensenellaceae*, which belongs to the *Clostridiales* order, has been frequently shown to degrade cellulose with high anaerobic cellulolytic ability (Zealand et al., 2019). Also, members from order *Bacteroidales*, including *Porphyromonadaceae*, are famous for their superior ability of fiber hydrolysis (Ozbayram et al., 2018). *Erysipelothrix* is a kind of acidogenic bacteria that can further degrade hydrolysis products to SCVFAs (Yuan et al., 2015). Special attention should be given to *Methanosaeta*, the only methanogen among the network hubs. Although lower in abundance (0.5%) than most of the nodes, *Methanosaeta* showed the highest betweenness centrality (the number of the shortest paths that pass through the vertex) of 77.48, indicating a core role in reaching out and connecting the genera that do not directly interact with each other. Whereas, *Methanosarcina*, which was predominant in archaeal communities, only showed a betweenness centrality of 0.55. Thus, consistent with some previous studies (Xu et al., 2018c), the less abundant microbes could also significantly contribute to maintaining the community interactions and functions, which should not be overlooked. These hub microbes were the most influential players in the network that mediate between internal environmental conditions (e.g. substrate availability), colonization and microbial growth, etc. to stabilize the AD process (Xu et al., 2018c).

The most significant negative associations in the network were identified between a genus from order *Bacteroidales* and a genus from order *Clostridiales* (Spearman's $\rho = -0.90$), a genus from family *Ruminococcaceae* (Spearman's $\rho = -0.88$), and a genus from family *Porphyromonadaceae* (Spearman's $\rho = -0.87$). The negative correlations likely resulted from the competition for substrate since these taxa all contain efficient strains for hydrolysis of complex organics (Ozbayram et al., 2018). The network analysis also showed strong positive correlations between some electroactive bacteria and electrotrophic methanogens, such as associations between *Syntrophomonas* and *Methanosarcina* (Spearman's $\rho = 0.74$), *Sedimentibacter* and *Methanosarcina* (Spearman's $\rho = 0.79$), *Petrimonas* and *Methanosaeta* (Spearman's $\rho = 0.76$),

Geobacter and *Methanosaeta* (Spearman's ρ = 0.66). These results further proved the syntrophic interactions happening on the electroactive biofilms. However, as a famous electroactive bacterium in MEC-AD systems, *Geobacter* had a low eigenvector centrality of 0.09, which could be attributed to its limited metabolic versatility. Overall, the co-occurrence microbial network analysis would help design a robust co-culture system by identifying the core microbiome, thus to enhance the system performance.

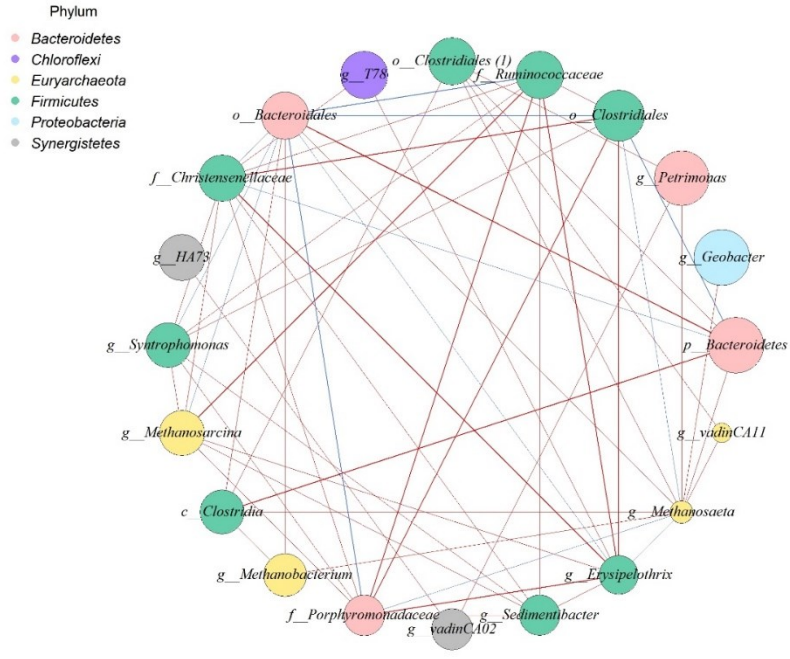

Figure 3.6 Network of co-occurring top 20 bacterial and top 5 archaeal genera by abundance based on correlation analysis for anodic and cathodic biofilm samples. A connection (edge) stands for a strong (Spearman's ρ > 0.6) and significant ($p < 0.05$) correlation. The size of each node is proportional to the mean abundance in the biofilm microbial community. The edges' width is proportional to the strength of the association (Spearman's ρ). Genera were colored by phylum taxonomy. Isolated nodes were removed. Unidentified genera were named at family (*f_*), order (*o_)*, class (*c_*) or phylum (*p_*) level.

3.3.4 Energy efficiency

Energy efficiency in this study was calculated based on the net energy income as methane under closed-circuit conditions (electrical energy consumption was subtracted) and energy income under

the open-circuit condition at the same OLR (see Appendix A Table A.2). The average steady-state current in Stage 6 was about 15.52 mA, and the average applied voltage was about 0.90 V. Thus, the electrical energy consumed per day (W_E) was estimated to be 1206.84 J/d. The methane production rates were 90.78 mL/d and 127.413 mL/d in Stage 5 and Stage 6, respectively. Thus, the energy recovery as methane in the MEC-AD reactor was estimated to be 4718.68 J/d, whereas the energy recovery in Stage 5 under open-circuit was about 3361.81 J/d. Therefore, the MEC-AD system was energy-positive and the energy efficiency was estimated at about 104.5%. In other words, energy consumed by potentiostat has been fully recovered as methane with a 4.5% increase in energy efficiency, which is comparable to some other MEC-AD systems treating raw high-strength waste/wastewater showing 2% to 9% energy efficiency increase (Gajaraj et al., 2017; Huang et al., 2020a; Zhao et al., 2016a; Zhao et al., 2016e). However, some MEC-AD systems applied to synthetic wastewater digestion exhibited significantly higher energy efficiency increment, such as 51.8% for artificial garbage slurry (Sasaki et al., 2010) and 121.6% for synthetic medium (Bo et al., 2014). Based on the knowledge about the MEC-AD systems, it is obvious that they are facing great challenges when handling raw wastewater streams with high levels of complex and particulate organics. Besides, energy loss due to electrode overpotentials and ohmic losses can be critical in bioelectrochemical systems, which can influence energy efficiencies (Kadier et al., 2016a). However, we anticipate further research and innovations will help overcome the impediments to make the MEC-AD system an energy-neutral or energy-positive wastewater treatment option of the future.

3.4 Conclusion

An integrated system of microbial electrolysis cell assisted anaerobic digestion (MEC-AD) operated at ambient temperature could efficiently accelerate methane recovery from vacuum toilet blackwater. High OLR of 3.0 g COD/L-d was achieved in the MEC-AD system with a high methane yield of 35.2% out of 45% estimated from long-term biochemical methane potential test, while only 24.1% was achieved under open-circuit operation. The applied potential did not have

a great impact on the archaeal community shifts but significantly increased the archaeal abundance on the cathode. Several specific electroactive bacteria and some anaerobic fermentative bacteria were enriched by the applied potential. Their syntrophic interactions with H_2 utilizers played an important role in degrading the complex substrates contained in blackwater as well as in supporting their growth, which resulted in the significant enhancement on the methane production efficiencies. Microbial co-occurrence network analysis revealed the critical role of *Methanosaeta* as one of the network hubs with the highest betweenness centrality. The syntrophic interactions between electroactive bacteria and electrotrophic methanogens were further proved by the strong positive correlations. The energy efficiency increased by 4.5%, indicating the MEC-AD system is promising to be developed as a highly efficient and energy-positive wastewater treatment technology.

Chapter 4. A Multifaceted Screening of Applied Voltages for Electro-assisted Anaerobic Digestion of Blackwater: Significance of Temperature, Hydrolysis/Acidogenesis, Electrode Corrosion, and Energy Efficiencies[3]

4.1 Introduction

To further optimize the MEC-AD system for high-rate blackwater digestion at elevated OLRs, the applied voltage emerges as a critical parameter to be considered carefully. The applied voltage appears to enhance electron transfer in the substrate metabolism of electroactive bacteria by anodic oxidation, which can accelerate organics decomposition (Zhao et al., 2016b). Further, the applied voltage can overcome thermodynamic barriers to promote H_2 production for enhanced hydrogenotrophic methanogenesis (Zakaria & Dhar, 2019). However, excessively high applied voltage will inhibit microbial activities and even kill the microbes (Chen et al., 2016). The impacts of applied voltages on the microbial cells involve (Chen et al., 2016): (i) direct impacts on microbial metabolism, including DNA and protein synthesis, and membrane permeability; and (ii) indirect impacts on surrounding cultivation ambient for microbes, such as pH and alkalinity. Thus, it is worth investigating the effects of different applied voltages on AD processes and screening the optimum applied voltages. However, there are only a few studies that evaluated the bioelectrochemical anaerobic digestion of blackwater (Huang et al., 2021; Zamalloa et al., 2013), while the optimum applied voltage has never been reported.

Furthermore, most studies on MEC-AD systems treating high-strength feedstocks only focused on the methanogenesis step (Feng et al., 2016; Huang et al., 2022b; Zhao et al., 2016c). However, hydrolysis is also a crucial rate-limiting AD step, especially for complex feedstocks like blackwater (Choi et al., 2021). As the downstream process of hydrolysis, acidogenesis could not proceed effectively if hydrolysis is limited, further influencing the methanogenesis step. Thus,

[3] A version of this chapter has been published as: Huang, Q., Liu, Y., & Dhar, B. R. (2022). A multifaceted screening of applied voltages for electro-assisted anaerobic digestion of blackwater: Significance of temperature, hydrolysis/acidogenesis, electrode corrosion, and energy efficiencies. *Bioresource Technology*, 360, 127533.

hydrolysis and acidogenesis efficiency should also be considered when screening the optimum voltage. Moreover, other operational aspects, such as operating temperature, and sustainability of electrodes, have often been overlooked while optimizing applied voltages. The microbial activities can be much more accelerated at mesophilic temperatures compared to room temperature, resulting in higher digestion efficiency (Nie et al., 2021). Interestingly, the activity of electroactive bacteria is less sensitive to temperature conditions (Feng et al., 2016), indicating that MEC-AD is a potential energy-efficient alternative to accelerate the AD process under ambient temperatures, and save heating energy. Furthermore, electrode corrosion can occur at high applied voltages, leading to system malfunctions and even failure (Bakar et al., 2019).

Therefore, in this study, different applied voltages were evaluated for blackwater digestion in MEC-AD systems operated under mesophilic and ambient temperatures. A multifaceted screening of applied voltages was carried out by comprehensively evaluating the efficiencies of major biochemical steps, microbial community dynamics, functional gene expression, electrode corrosion, and energy efficiencies. Moreover, bioinformatics analysis was performed to elucidate the underlying microbial driving force and mechanisms to guide future system design and operation.

4.2 Materials and methods

4.2.1 Reactor configuration

Two identical single chamber MEC-AD reactors with 400 mL working volume were fabricated with plexiglass tubes. High-density carbon fibers (2293-A, 24A Carbon Fiber, Fibre Glast Development Corp., Ohio, USA) were fixed on a pair of stainless-steel frames as anodes and cathodes. The carbon fibers were pretreated according to a method described by Dhar et al. (2013). A DC power supply (Model 3645A, Circuit Specialists, Inc., Tempe, AZ) was connected to each reactor to apply specified voltages and realize the directional movements of cations and anions towards the opposite electrodes (Barua et al., 2017). Therefore, highly efficient functional biofilms

could be cultivated at the anode for substrate oxidation and at the cathode for H_2 and CH_4 production. Currents were recorded every 5 mins during the whole operation by Keithley 2700 data acquisition system equipped with a 22-channel M7700 analog input module. One channel was connected in series to the outside electric circuit of each reactor, and the measurements were executed via DCI (direct current measurement) function. The schematic diagram of the system setup was provided in Appendix B Figure B.1A.

4.2.2 Feedstock collection and reactor operation

The collection of raw blackwater was described in a previous study (Huang et al., 2020b). The blackwater was characterized immediately after preparation, and the average physicochemical characteristics were presented in Table 4.1. The reactors were seeded with 40 mL sludge from a full-scale anaerobic digester (37 °C) treating municipal sludge in Alberta, Canada, and 30 mL effluent from a mother MEC reactor that has been operated with acetate medium (25 mM) for > 4 years. The total suspended solids (TSS) and volatile suspended solids (VSS) concentrations in the inoculum mixture were 5.1 g/L and 3.0 g/L, respectively. Two reactors were operated at 20 ± 0.5 °C (R_{20}) and 35.6 ± 0.4 °C (R_{35}), respectively. Heating blankets and Styrofoam were used to wrap R_{35} to provide external heat and prevent heat loss. Most previous studies utilized 0.3 - 2.3 V applied voltages for treating high-strength waste/wastewater by MEC-AD systems, while reported optimum voltages varied significantly from 0.3 to 1.8 V (Huang et al., 2022b). However, higher applied voltages may promote water electrolysis (typically 1.23 - 1.8 V) or cell rupture (Kadier et al., 2016b; Zakaria et al., 2020). Thus, in this study, the long-term (200 days) operation of the reactors was divided into 5 stages with increased applied voltages (0 V, 0.4 V, 0.8 V, 1.2 V, and 1.6 V) in a semi-continuous mode. The hydraulic retention time (HRT) was maintained at 4.5 days, and the average organic loading rate (OLR) was 3.2 ± 0.1 g COD/L-d. The reactors were continuously mixed at 500 rpm by magnetic stirrer bars.

4.2.3 Assessment of hydrolysis and acidogenesis efficiencies

Particulate COD hydrolysis efficiency and acidogenesis efficiency were determined for stages

with 0 - 1.2 V applied voltage at steady-state in 48-hour feeding cycles (the period between consecutive feedings). Initially, liquid samples were collected immediately after feeding fresh blackwater and mixing. The total COD (TCOD) and soluble COD (SCOD) were determined and named as $COD_{T,initial}$ and $COD_{S,initial}$. Then liquid samples and biogas samples were collected at 4 h, 8 h, 16 h, 26 h, 36 h, and 48 h during this feeding cycle. Methane production and SCOD of the effluent were determined at each time point as COD_{CH4} and $COD_{S,effluent}$. The real-time particulate COD hydrolysis efficiency was calculated using Eq. (1) (Gao et al., 2018):

$$\text{Hydrolysis efficiency (\%)} = \frac{COD_{CH4}+COD_{S,effluent}-COD_{S,initial}}{COD_{T,initial}-COD_{S,initial}} \times 100 \quad (1)$$

The final acidogenesis efficiency in terms of total COD input was calculated using Eq. (2) (Gao et al., 2018):

$$\text{Acidogenesis efficiency (\%)} = \frac{COD_{CH4,final}+COD_{VFA,fianl}-COD_{VFA,initial}}{COD_{T,initial}-COD_{VFA,initial}} \times 100 \quad (2)$$

where, $COD_{CH4,final}$ is the methane production at the endpoint as COD (48 h), $COD_{VFA,initial}$ and $COD_{VFA,final}$ are the initial (0 h) and final (48 h) COD of volatile fatty acids (VFA). The cycle tests were performed in triplicates for each stage.

4.2.4 Analytical methods

Concentrations of TCOD, SCOD, TSS, and VSS were determined according to the Standard Methods (APHA, 2005). Hach ammonia reagent kits (High Range, 0 – 50 mg nitrogen/L; Hach Co., Loveland, Colorado, USA) were used to determine total ammonia nitrogen (TAN) concentration. pH was measured by a B40PCID pH meter (VWR, SympHony). The concentrations of various VFAs (including acetate, propionate, and butyrate) were determined by a Dionex ICS-2100 ionic chromatography system (Thermo Fisher, Waltham, MA, USA). A 7890B gas chromatograph (Agilent Technologies, Santa Clara, USA) equipped with two columns (i.e. Molsieve 5A 2.44 m 2 mm for CH_4 and HayeSep N 1.83 m 2 mm for O_2, N_2, and CO_2) and a thermal conductivity detector was used to determine the biogas composition. Dissolved methane concentration in the effluent was measured 3 times per stage in triplicate samples during the steady-state period, following the methods described by (Zhang et al., 2020b). A hand-held

pressure meter (GMH 3510, Regenstauf, Germany) was used to measure the final headspace pressure of the serum bottles.

4.2.5 DNA extraction

At the end of each stage, sludge samples were collected from 10 to 20 different locations on the surface of each electrode. Biomass was not sampled at 1.6 V due to the system failure. The liquid content left in each reactor was centrifuged at 4000 rpm for 5 min. Then, the supernatant was discarded. 2 mL of settled solids were collected as suspended sludge, and the remaining was returned to the reactors. The genomic DNA was extracted from the sludge samples using DNeasy PowerSoil Kit (QIAGEN, Hilden, Germany) following the manufacturer's protocol. NanoDrop One (ThermoFisher, Waltham, MA) was utilized to check the concentration and quality. In the PCR procedure, 16S rRNA genes were amplified using the universal primer-pair 515F and 806R. The thermocycling conditions of PCR consisted of initial denaturation at 95 °C for 3 min followed by 30 cycles of 95 °C for 15s, 55 °C for 30s, 68 °C for 30s, and 1 cycle of 68 °C for 5 min. Then the 16S rRNA genes were sequenced by Genome Quebec (Montréal, Canada) on the Illumina MiSeq platform.

4.2.6 Bioinformatics analysis and statistical analysis

Raw sequence data were processed in Qiime2 pipelines (Hall & Beiko, 2018) for sequence read pairings and removal of low-quality sequences and chimeras. Taxonomy was assigned using 99% similarity in GreenGenes (version 13_8) reference database (McDonald et al., 2012). Microbial Shannon diversity and principal coordinate analysis (PCoA) were analyzed at the genus level through the 'vegan' package in R (Oksanen et al., 2007). Heatmap was produced using the "pheatmap" package in R (Kolde & Kolde, 2015). The linear discriminant analysis (LDA) effect size (LEfSe) method (Segata et al., 2011) was used to investigate the taxonomic biomarkers that contributed to the significant difference between 0 V and 1.2 V applied voltage conditions for R_{20}. The predicted metagenome and functional genes were determined through the Phylogenetic Investigation of Communities by Reconstruction of Unobserved States (PICRUSt) (Langille et al.,

2013). Student t-test was performed using Microsoft Excel®. A p value smaller than 0.05 was considered statistically different.

4.2.7 Calculations

The free ammonia nitrogen (FAN) concentration was calculated according to Gao et al. (2018).

Methane yield (%) was calculated using Eq. (3) (Huang et al., 2021):

$$Methane\ yield\ (\%) = \frac{COD_{methane}}{COD_{input}} * 100 \quad (3)$$

where $COD_{methane}$ is the COD equivalent of produced methane (in mg COD); COD_{input} is the amount of total COD input (in mg COD).

Electric energy supply (W_E [J]) and energy income as methane production (W_{CH4} [J]) in the MEC-AD systems were calculated using equations described by Huang et al. (2021). The heating energy (W_H, kJ) required for raising the reactor temperature was calculated based on Eq. (4) (Qu et al., 2021):

$$W_H = cm(T - T_0) \quad (4)$$

where m is the mass of the liquid (kg); c is the specific heat capacity of the liquid (regarded as water, 4.2 kJ/kg/K); T and T_0 are the final temperature and initial temperature (K), respectively.

The energy efficiency was calculated based on the following Eq. (5):

$$\text{Fold change in energy efficiency } (\%) = \frac{W_{CH4(1)} - W_{Cons(1)}}{W_{CH4\,(2)} - W_{Cons(2)}} \times 100\% \quad (5)$$

where $W_{CH4(1)}$ and $W_{CH4(2)}$ refer to the energy income as methane in different reactors or stages. $W_{Cons(1)}$ and $W_{Cons(2)}$ refer to the total energy consumption (the sum of W_E and W_H).

4.3 Results and discussion

4.3.1 Methane production and organics removal

During the long-term operation (> 200 days), the influent TCOD of blackwater slightly fluctuated

between 13.5 to 14.4 g/L (Figure 4.1A). Steady-state was achieved in each stage, except for the last stage, which showed rapid COD accumulation due to corrosion (discussed later). The effluent TCOD of R_{35} was always lower than R_{20}. R_{20} showed slightly decreased effluent TCOD with elevated applied voltages from 0 V to 0.4 V ($p = 0.167$); however, a significant decrease was found at 0.8 V and 1.2 V ($p < 0.01$). R_{20} showed the highest TCOD removal efficiency at 1.2 V (61.38 ± 2.61%), about 27.0% higher than that of 0 V, while TCOD removal efficiencies in R_{35} narrowly varied (72.10 - 80.08%) under different voltages (Figure 4.1A). However, the highest TSS and VSS removal efficiencies were achieved at 1.2 V in both reactors (see Table 4.1), which indicated the possibility of promoted hydrolysis at 1.2 V.

According to previous studies, the biochemical methane potential (BMP) of vacuum toilet blackwater was around 35 – 60%, with a large proportion of unbiodegradable COD (Gao et al., 2018; Huang et al., 2020b). As shown in Figure 4.1B, methane yield (including dissolved methane) of R_{20} significantly increased by 59.9% at 1.2 V (38.4 ± 0.74%) compared to 0 V (24.01 ± 1.80%) ($p < 0.01$), with specific methane production rate increased from 291.9 to 457.7 mL/L-d (Table 4.1). However, the observed marginal difference between 0 V and 0.4 V was possibly due to the large proportion of ohmic loss (Dhar et al., 2016). The methane yield in R_{35} was almost stable in the first three stages (~ 51%), indicating that the blackwater BMP was almost reached. Thus, the applied voltages could not further increase the BMP of vacuum toilet blackwater at 35 ℃. Instead, methane yield dropped for increasing applied voltage from 0.8 V to 1.2 V, which could be ascribed to the rapid rise of pH to 8.15 ± 0.25, leading to severe ammonia inhibition (FAN ~ 207.07 mg/L). A previous study also reported reduced blackwater digestibility at FAN > 205 mg/L (Gao et al., 2018). The rapid rise of pH could be attributed to anode corrosion similar to the 1.6 V condition and a higher corrosion rate at higher temperatures (Pal et al., 2021).

Dissolved methane was also measured and included in the methane yield calculation (see Appendix B Table B.1). Dissolved methane concentration was higher (~ 75.9 mg CH_4-COD/L) and accounted for a higher proportion of the total methane produced in R_{20} than in R_{35} (~24.8 mg

CH_4-COD/L), due to the higher solubility of methane at lower temperatures (Zhang et al., 2020b). Although the dissolved methane content is trivial in this case (0.31 - 2.10% of total methane produced), developing strategies for its recovery and reuse is essential when considering large-scale applications under ambient temperature. No H_2 was detected from 0 to 1.2V in both reactors due to the rapid H_2 consumption by hydrogenotrophic methanogens. As shown in Table 4.1, the CH_4 content in biogas increased consistently with the increasing applied voltages for both R_{20} (79.31 - 84.95%) and R_{35} (74.43 - 79.52%), along with decreased CO_2 content. Furthermore, enhanced DIET could also result in more CO_2 consumption. Interestingly, R_{20} presented higher CH_4 content and lower CO_2 content than R_{35}, probably because at room temperature, the higher solubility of CO_2 than CH_4 resulted in a larger dissolved CO_2 fraction than dissolved CH_4 fraction (Ramdin et al., 2014).

The current density increased consistently with the increasing applied voltages, from 4.58 to 15.50 A/m^3 in R_{20}, and 7.80 to 26.53 A/m^3 in R_{35} (Table 4.1), while the resistance slightly decreased from 218.6 to 193.5 Ω and from 128.2 to 113.1 Ω in R_{20} and R_{35}, respectively. These results indicated higher oxidation-reduction activity of electroactive biofilms occurred at higher applied voltages and mesophilic temperature, associating well with the higher methane yields and methane contents with increased applied voltages.

For both reactors, 1.6 V led to severe anodic corrosion of the stainless-steel current collectors (see Appendix B Figure B.2), leading to rapid reactor failure. The pH increased to > 9.35, while the optimum pH of AD is 6.8 to 7.2 (Huang et al., 2020b). Excessive electrons released from the corrosion would be transported to the cathode and would be utilized for protons reduction to H_2 (Bakar et al., 2019). Thus, the accumulation of hydroxyl ions led to a significant pH increase. Besides, high H_2 partial pressure would inhibit the fermentation process (Li et al., 2012b). As discussed below in Section 3.4, a supplementary test was conducted with carbon-based current collectors to explore electrode selection options for alleviating corrosion risks.

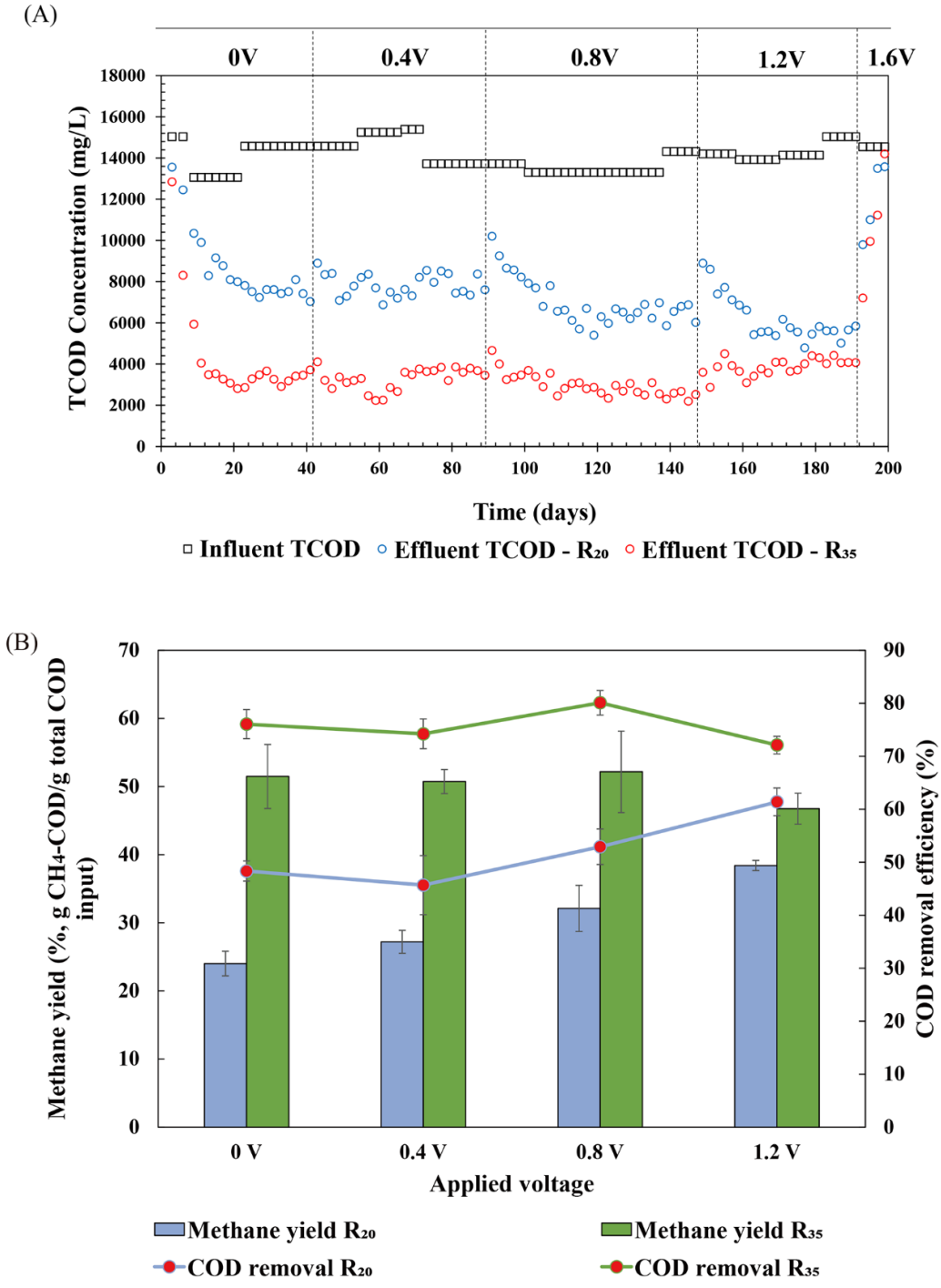

Figure 4.1 (A) The influent and effluent TCOD concentrations at different applied voltages; (B) Average methane yield and COD removal efficiency at different applied voltages based on steady-state results.

4.3.2 Hydrolysis and acidogenesis efficiency

Hydrolysis of macromolecules (e.g., proteins, carbohydrates, lipids) to soluble organics is often considered a rate-limiting step in AD (Choi et al., 2021). Acidogenesis can often be limited by hydrolysis as a downstream process. As shown in Figure 4.2A, R_{35} exhibited substantially higher hydrolysis efficiency than R_{20}, which could be attributed to higher hydrolytic enzyme activity at higher temperatures (Nie et al., 2021). Hydrolysis efficiency marginally increased with the increasing applied voltages from 0 V to 0.8 V in both reactors, while it significantly increased to 35.15 ± 1.23% ($p < 0.01$) at 1.2 V in R_{20}, about 52.0% higher than that of 0 V (23.12 ± 2.25%). A similar trend was also observed for acidogenesis efficiency (Figure 4.2B), as it increased by 44.9% ($p < 0.01$) at 1.2 V compared to 0 V in R_{20}. Some previous studies also reported enhanced hydrolysis/acidogenesis in MEC-AD reactors than in conventional digesters (Wang et al., 2021c; Zhao et al., 2016e). However, the results of this study suggest that such impacts of applied voltages in MEC-AD on hydrolysis/fermentation would be more pronounced at ambient temperature than mesophilic temperature. Wang et al. (2021c) suggested that such observation could be attributed to the higher enrichment of hydrolytic/fermentative bacteria due to applied voltages. As discussed later, compared to 0 V, various applied voltages in MEC-AD systems could lead to higher enrichment of hydrolytic/fermentative bacteria and a higher abundance of functional genes associated with the degradation of various macromolecules. Moreover, as suggested in the literature, the applied voltage can crack microbial cells trapped in the sludge gels, improving sludge flocs disintegration, and releasing biopolymers to the aqueous phase (Kumar et al., 2019).

As shown in Figure 4.2B, R_{20} at 0 V exhibited the highest total VFA (TVFA) concentration containing mainly acetate (> 800 mg/L), suggesting limited methanogenesis capacity. The lowest TVFA concentration in R_{20} was achieved at 0.8 V instead of 1.2 V which showed slightly higher propionate accumulation. The higher applied voltage could increase cathodic H_2 production, leading to higher H_2 partial pressure impeding propionate fermentation (Li et al., 2012b). At 1.2 V, R_{35} showed much higher acetate and propionate accumulation than other conditions. As mentioned earlier, FAN inhibition of methanogens could lead to such a substantial acetate

accumulation. Moreover, propionate fermentation would also be sensitive to acetate concentrations; acetate needs to be consumed by microbial communities in MEC-AD to ensure effective propionate fermentation (Zakaria et al., 2022).

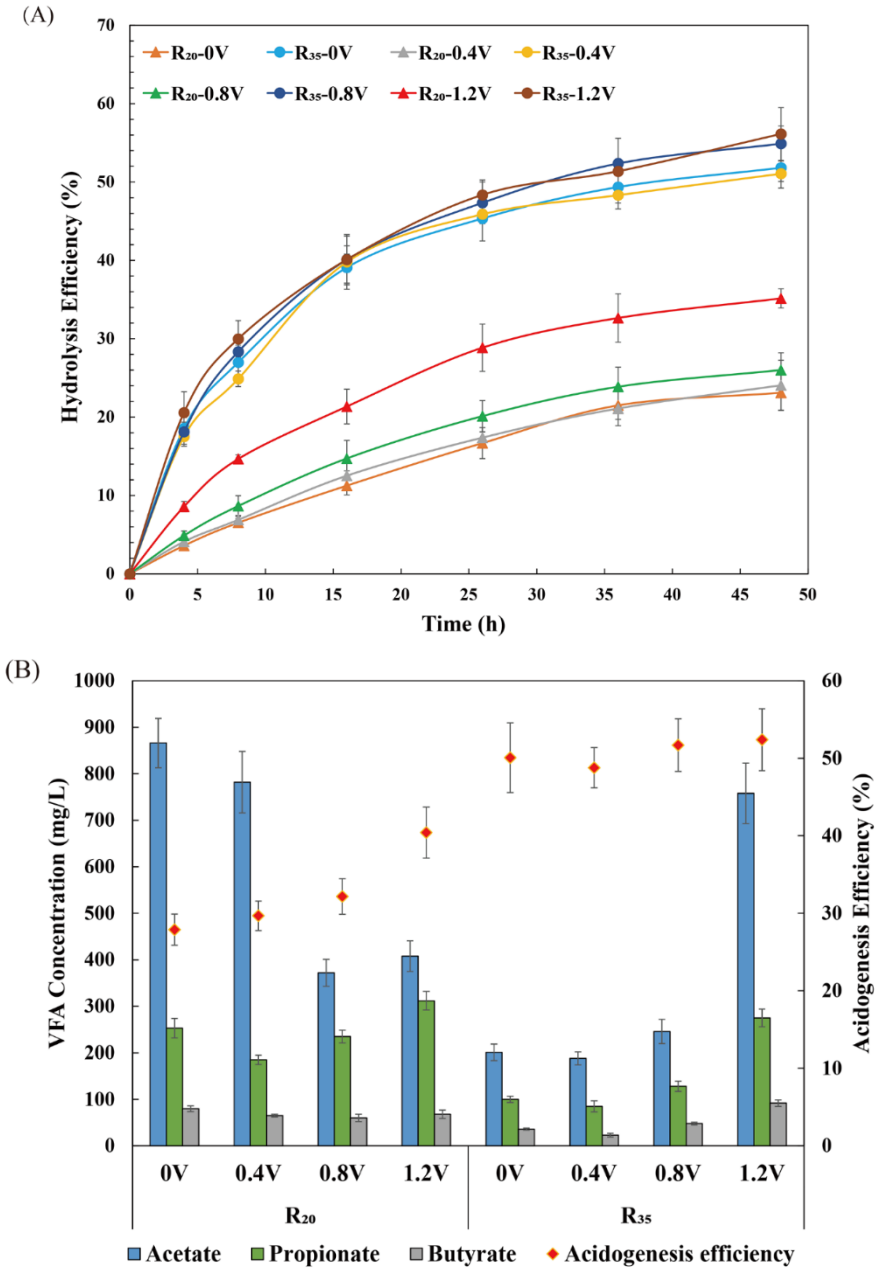

Figure 4.2 (A) The hydrolysis efficiency of particulate COD during the cycle tests; (B) The VFA concentrations in the reactor effluent during the steady-state periods and acidogenesis efficiency generated based on the cycle tests.

Table 4.1 Key parameters of the MEC-AD reactors during the steady-state operation.

	Unit	Influent	R_{20}				R_{35}			
			0V	0.4V	0.8V	1.2V	0V	0.4V	0.8V	1.2V
TCOD	g/L	14.10 ± 0.68	7.53 ± 0.28	7.77 ± 0.51	6.38 ± 0.42	5.56 ± 0.33	3.34 ± 0.32	3.63 ± 0.18	2.69 ± 0.27	4.02 ± 0.25
SCOD	g/L	5.31 ± 0.90	3.10 ± 0.55	2.72 ± 0.19	2.08 ± 0.14	2.16 ± 0.32	1.18 ± 0.39	1.28 ± 0.33	1.50 ± 0.56	2.36 ± 0.34
TCOD removal efficiency	%		48.33 ±1.90	45.68 ± 5.57	52.91 ± 3.35	61.38 ± 2.61	76.05 ± 2.76	74.22 ± 2.81	80.08 ± 2.32	72.10 ± 1.66
TSS	g/L	5.62 ± 0.36	3.02 ± 0.08	3.20 ± 0.20	2.68 ± 0.36	2.45 ± 0.18	0.99 ± 0.12	1.18 ± 0.26	0.87 ± 0.07	0.76 ± 0.13
TSS removal efficiency	%		46.15 ± 2.36	42.98 ± 3.25	51.79 ± 3.13	56.58 ± 2.05	82.40 ± 1.88	79.30 ± 2.31	84.81 ± 3.12	86.88 ± 2.86
VSS	g/L	4.87 ± 0.56	2.65 ± 0.14	2.67 ± 0.04	2.45 ± 0.12	2.08 ± 0.18	0.86 ± 0.08	0.88 ± 0.03	0.65 ± 0.04	0.52 ± 0.04
VSS removal efficiency	%		45.03 ± 2.58	44.86± 1.21	49.50 ± 1.77	57.89 ± 2.35	82.4 ± 1.68	82.1 ± 3.84	86.77 ± 2.36	89.36 ± 2.87
Methane yield	%		24.01 ± 1.80	27.20 ± 1.67	32.1 ± 3.38	38.4 ± 0.74	51.47 ± 6.70	50.72 ± 1.77	52.15 ± 5.98	46.75 ± 2.28
Specific methane production rate	mL/L-d		291.89 ± 21.93	326.31 ± 36.61	361.07 ± 46.03	457.73 ± 26.94	581.44 ± 93.61	598.59 ± 42.14	590.09 ± 72.83	562.22 ± 30.04
CH_4 content in biogas	%		79.31 ± 2.10	78.70 ± 1.34	82.91 ± 1.61	84.95 ± 0.96	74.43 ± 2.24	74.47 ± 1.02	75.62 ± 1.35	79.52 ± 0.89
pH		8.51 ± 0.11	7.33 ± 0.04	7.39 ± 0.15	7.56 ± 0.06	7.46 ± 0.04	7.68 ± 0.03	7.65 ± 0.05	7.36 ± 0.12	8.15 ± 0.25
TVFA	g/L		1.20 ± 0.06	1.032 ± 0.12	0.667 ± 0.09	0.788 ± 0.07	0.337 ± 0.01	0.296 ± 0.05	0.422 ± 0.07	1.125 ± 0.18
FAN	mg/L		9.04	10.55	16.37	8.22	70.44	63.31	35.95	207.07
Current density	A/m^3		-	4.58	9.85	15.50	-	7.80	16.50	26.53

4.3.3 Microbial communities

4.3.3.1 Microbial community diversity

The alpha-diversity of microbial communities was characterized by the Shannon index at the genus level (see Appendix B Figure B.3A). Shannon indices of both anodic and cathodic archaeal communities in both reactors increased with increasing applied voltage from 0 to 0.8 V but decreased at 1.2 V. Thus, lower voltages could promote diverse methanogenic communities, maintaining system stability. Interestingly, with increased applied voltages, R_{20} showed decreased bacterial Shannon indices on both anode and cathode, while R_{35} exhibited opposite trends. These results indicated that at higher substrate stress levels (R_{20}), applied voltages could possibly select and enrich certain microbes with higher substrate utilization rate and growth rate. However, under less substrate stress (R_{35}), the applied voltages could help increase the system stability and robustness via increased diversity (Labatut et al., 2014).

The principal coordinate analysis (PCoA) was performed using Bray-Curtis distances among samples (see Appendix B Figure B.3B) to visualize the microbial community relationships. Two clusters were formed for R_{20} and R_{35} along the PCoA 1 axis, which explained 36.0% of the total sample variance. However, the clusters shared the same diverging direction towards one point from 0 V to 1.2 V conditions. These results indicate that the applied voltages had a significant impact on the microbial community dynamics; and with the same applied voltage, the microbial communities developed under different temperature conditions had high similarities with the long-term electrochemical regulations.

4.3.3.2 Archaeal communities

Figure 4.3 shows the relative abundances of archaeal genera in different samples. The abundance of *Methanosaeta* significantly increased with the increased applied voltages, from 18.2% to 87.7% on the anode in R_{20}, from 16.7% to 75.3% on the cathode in R_{20}, from 53.1% to 80.6% on the anode of R_{35}, and from 55.7% to 65.6% on the cathode of R_{35}. *Methanosaeta* can use acetate exclusively, but is also well-known for the ability to produce methane via DIET (Zhao et al.,

2016c). The vast dominance of *Methanosaeta* in MEC-AD reactors has been found in several studies (Huang et al., 2022b; Liu et al., 2019; Zhao et al., 2016c). It was suggested that *Methanosaeta* would likely be participating in direct electron uptake from a cathode and/or syntrophic electroactive bacteria (Liu et al., 2019; Zhao et al., 2016c).

However, for R_{20} at 0 V, the methanogenic community was predominant by *Methanosarcina* with an abundance of ~76% on both electrodes, whereas the abundance significantly decreased to 5.2% and 4.7% at 1.2 V on anode and cathode, respectively. *Methanosarcina* can utilize diverse substrates, such as H_2/CO_2, acetate, methanol, and formate, for methane production (Chen et al., 2016). Moreover, *Methanosarcina* can also conduct DIET via conductive materials or insoluble electron shuttles (Huang et al., 2022b). A previous study also found enrichment of *Methanosarcina* with increasing OLRs in a MEC-AD reactor operated with vacuum toilet blackwater at room temperature (Huang et al., 2021). It is expected that the changes in applied voltages would alter cathode potential (Su et al., 2016), which can influence the methanogenesis pathways as suggested in the literature (van Eerten-Jansen et al., 2015). Thus, increased applied voltages appeared to be metabolically unfavorable for *Methanosarcina*.

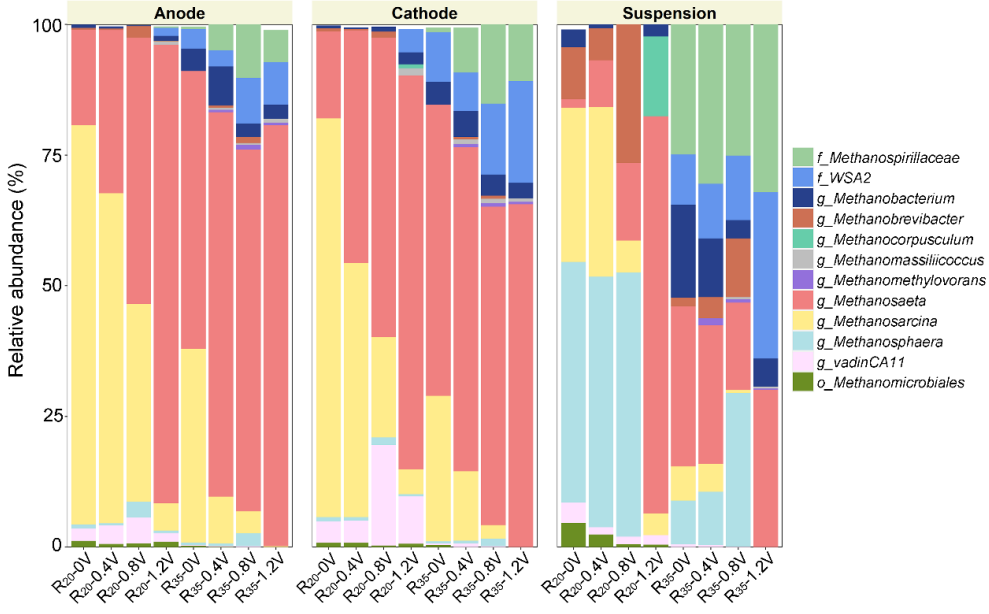

Figure 4.3 Relative abundance of archaeal genera with abundance > 1% in both reactors. The taxonomic names were at a higher level (family: f_; order: o_) if not identified at the genus level.

4.3.3.3 Bacterial communities

Figure 4.4 shows the temporal changes in the relative abundance of the 10 most abundant bacteria from each sample at the genus level. The bacterial genera were classified into 6 groups by the annotation function of the 'pheatmap' package in R (Kolde & Kolde, 2015). Group A mainly contained some thermophilic bacteria genera that were almost absent in R_{20} but showed higher abundance in R_{35} up to 8.1%. In R_{35}, *OPB95* (belonging to *OP8*) was markedly enriched at all sampling locations with increased applied voltages. A recent study suggested a strong positive correlation between *OP8*-related members and *Methanosaeta* in anaerobic digestion (Ma et al., 2017), which was consistent with the increased abundance of *Methanosaeta* in this study. *Simplicispira* also showed increased abundance at higher applied voltages, from almost absent to up to 3.5%. Some previous studies also reported their high abundance in bioelectrochemical systems, and suggested their potential dual roles in organics degradation and extracellular electron transfer (Xin & Qiu, 2021). Similar to Group A, Group B clustered some bacterial genera that were almost absent in R_{35} but showed higher abundance in R_{20}. Also, Group B contained several hydrolytic bacteria and exhibited a higher abundance in suspension than anodic and cathodic biofilms. *Bacteroides* and members from family *Porphyromonadaceae* and *Tissierellaceae* are important fiber or lignocellulosic biomass-degrading bacteria with high ammonia tolerance (Gao et al., 2019a). Notably, in the suspension of R_{20}, the abundance of *Bacteroides* was significantly higher at 1.2 V (10.0%) than 0 V (5.4%). Group C and Group D, microbial populations mainly associated with hydrolysis/fermentation of macromolecules, showed higher abundance in R_{35} than R_{20}. These two groups can be considered the major drivers for higher hydrolysis/fermentation in R_{35}. However, most members in Group C and D exhibited growing abundance in R_{20} with the increased applied voltage. For instance, *Clostridium* and another genus from class *Clostridia*, known for effective cellulose degradation (Hong et al., 2014), showed a significant rise in their abundance in R_{20} from 0 to 1.2 V ($p < 0.05$). Despite the lower abundance, the members in Group C and D in R_{20} showed great potential for enhanced hydrolysis/fermentation with increased applied voltages. Group E and F clustered bacteria populations with higher abundance in R_{20} than

in R_{35}. Notably, the abundance of a genus from order *Bacteroidales* in both reactors increased with the increased applied voltage, especially in R_{20} ($p < 0.01$), from 2.2% to 22.2% on the anode, 4.4% to 47.2% on the cathode, 3.0% to 39.9% in the suspension. *Bacteroidales* are known for their fiber hydrolysis ability (Huang et al., 2020b), which might contribute to the accelerated hydrolysis rates at higher applied voltages. *Sedimentibacter* and *Syntrophomonas* are electroactive syntrophic oxidizers that metabolize the substrates to produce acetate (Yang et al., 2019). They showed a higher positive correlation with applied voltage in R_{20} (Pearson's r> 0.4, $p < 0.01$) than in R_{35}, which indicated the electroactive bacteria might be more sensitive to electrochemical variations at a lower temperature. However, it is also possible that more hydrolytic products resulting from higher hydrolysis rates in R_{20} stimulated their growth.

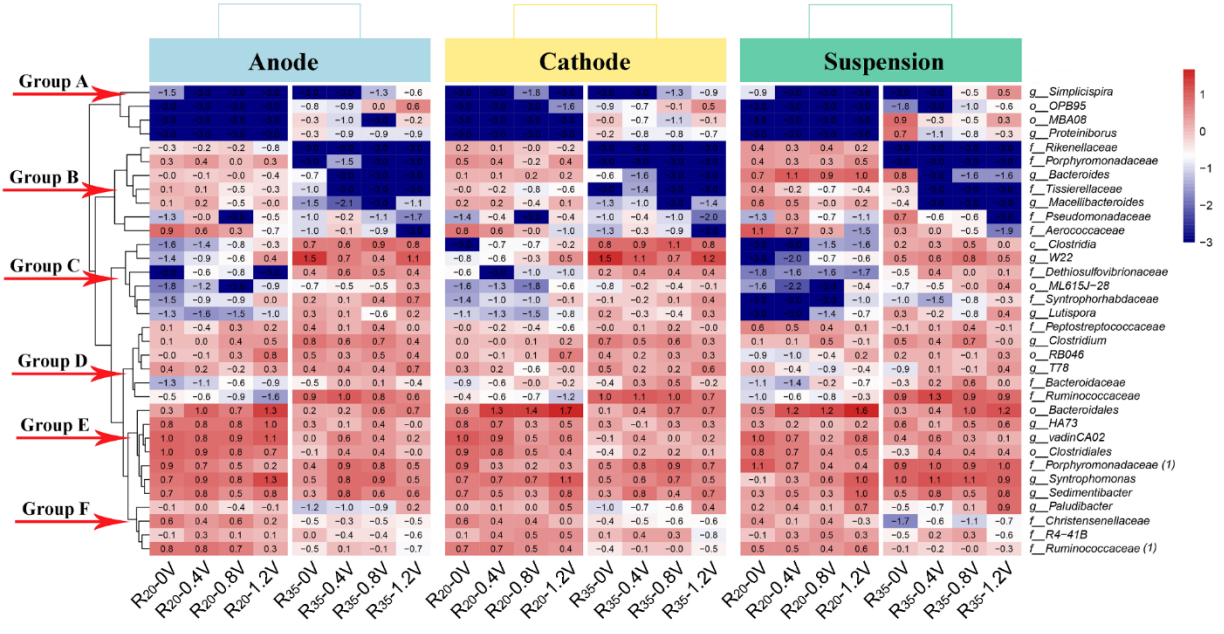

Figure 4.4 Relative abundance of 10 most abundant bacterial general in each sample. Unidentified genera were named at family (*f*_), order (*o*_), or class (*c*_) level. Numbers are log (relative abundance (%)) of genera. 0.001% were added to absent genera to avoid zero denominators.

4.3.3.4 Community differential analysis

The microbial community analysis and interpretation of archaeal and bacterial communities above

focused on the genera with top relative abundances. However, the less abundant microbes could also have significant changes subjected to the applied voltages, which should not be overlooked. To understand the significance of genera variability between 0 V and 1.2 V conditions in R_{20}, LEfSe analysis was performed at a threshold level of LDA score of 5, which identified the community biomarkers (significantly differential taxa). A total of 25 biomarker taxa with LDA score higher than 5 were identified (Figure 4.5A): 18 at 1.2 V and 7 at 0 V. Figure 4.5B depicts the phylogenetic tree of the biomarkers. Noticeably, the biomarker genera at 1.2 V were phylogenetically related and formed a few clusters, implying the significance of the microbial properties and functions they shared. The largest cluster included genus *W22* and genera from phylum *WWE1*, class *Cloacamonae*, order *Cloacamonales*, and family *Cloacamonaceae*. Members in this group can ferment amino acids and propionate to H_2, CO_2 and acetate in a syntrophic partnership with H_2/acetate consumers (Esquivel-Elizondo et al., 2016). *Syntrophomonas* and another genus from *Syntrophomonadaceae* had the highest LDA score, indicating remarkably higher abundance at 1.2 V than 0 V. Other syntrophic bacteria like genera from family *Syntrophorhabdaceae* and order *Syntrophobacterales* were also identified as biomarkers. These syntrophic fatty acid-oxidizing bacteria formed the second-largest cluster, indicating the enhanced methane production from 0 to 1.2 V would probably benefit from their syntrophic partnerships with *Methanosaeta*. The LEfSe analysis also confirmed the importance of electroactive *Arcobacter* as a biomarker that can metabolize acetate to donate electrons for cathodic DIET in partnership with *Methanosaeta*. *Methanosaeta* was identified as a biomarker at 1.2 V, while *Methanosarcina* was a biomarker at 0 V. The LEfSe analysis highlighted the significance of syntrophic bacteria, which can establish partnerships with H_2/acetate users, leading to enhanced system performance.

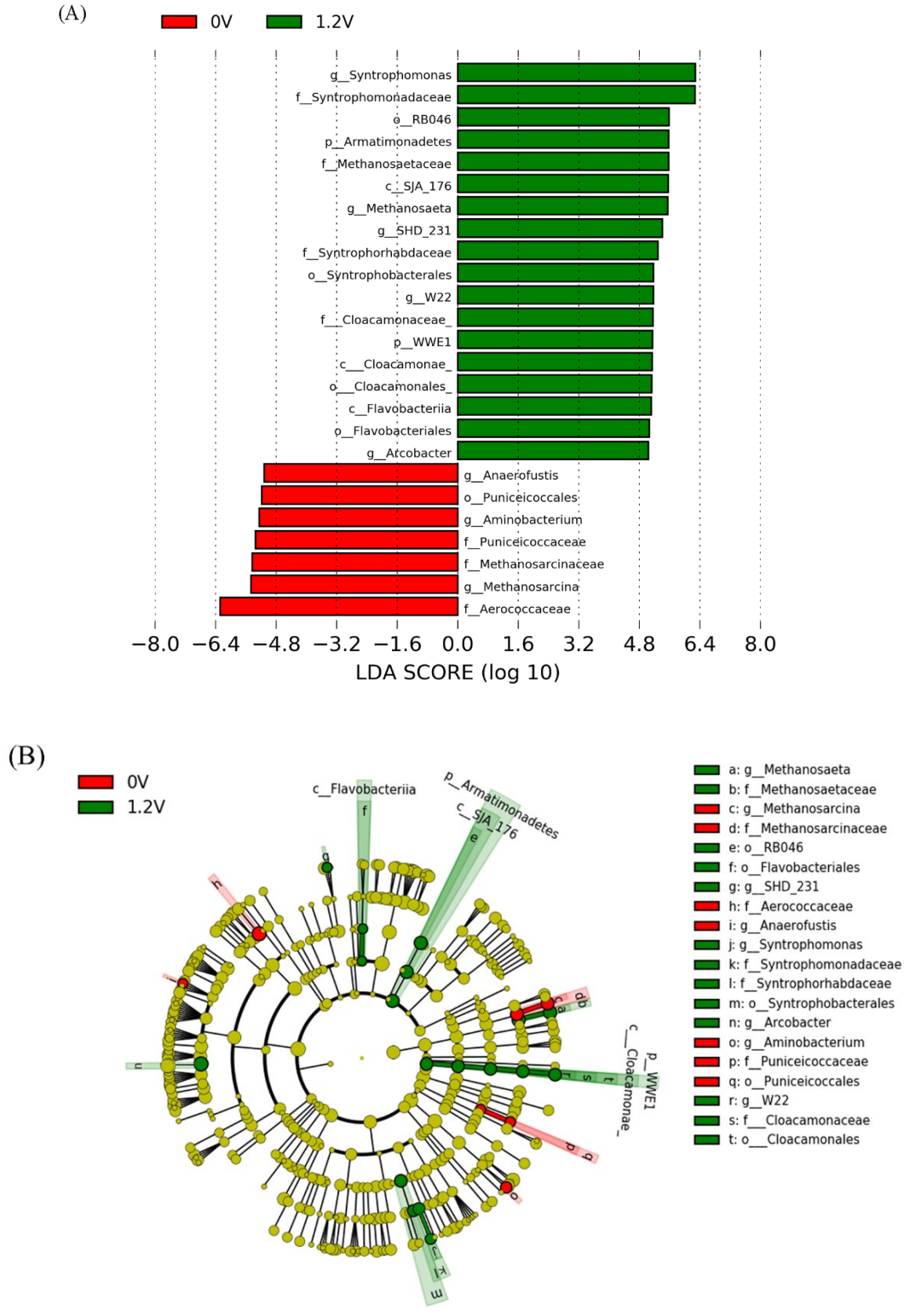

Figure 4.5 LEfSe analysis of microbial communities in R_{20} at 0V and 1.2V. (A) Taxa with LDA score > 5 under both conditions; (B) Phylogenetic distribution of all taxa with LDA score > 5.

4.3.3.5 Prediction of functional genes

A phylogenetic investigation of microbial communities by reconstruction of unobserved states (PICRUSt) was utilized to analyze microbial function in the reactors using the Kyoto Encyclopedia of Genes and Genomes (KEGG) database. As there was no significant difference in the PICRUSt results among samples from anode, cathode and suspension, anodic samples were discussed here (Figure 4.6A).

The major pathways in the MEC-AD reactors treating blackwater involved amino acid, carbohydrate and energy metabolism, translation, replication and repair, and membrane transport. Interestingly, microbes in R_{20} showed a higher prevalence of amino acid metabolism (10.09 - 10.61%) than in R_{35} (9.57 - 10.04%). The highest prevalence of amino acid metabolism in both reactors was observed at 0.8 V instead of 1.2 V. Also, R_{20} at 0.8 V presented the highest prevalence in terms of translation, replication and repair, cellular processes and signaling, metabolism of nucleotide, cofactors, vitamins, and other amino acids. These results indicated microbes at 0.8 V favored cell growth and fermentation of small molecules at room temperature. Meanwhile, it was also implied that higher voltage at 1.2 V might have negative effects on some certain microbes that limit their intracellular processes. However, regarding lipid metabolism, glycan biosynthesis and metabolism, carbohydrate metabolism, and transcription, predicted genes in R_{20} showed overwhelmingly highest prevalence at 1.2 V, compared to all stages in both reactors. For instance, the relative abundance of predicted genes encoding carbohydrate metabolism exhibited an obvious positive correlation with the voltage increase in both reactors. The highest gene abundance was observed in R_{20} at 1.2 V (10.44%), even higher than R_{35} at 1.2 V (10.27%). Also, the highest prevalence of membrane transport was found in R_{20} at 1.2 V. Membrane transport pathways, such as ABC transporters, can utilize the energy of ATP binding and hydrolysis to transport various substrates across the membrane, from smaller to larger molecules, like lipids, amino acids, and nucleotides (Koo et al., 2017). Cellulose and hemicellulose are the major refractory organics in blackwater. The relative abundance of predicted genes encoding enzymes associated with cellulose and hemicellulose hydrolysis (i.e., cellulases and hemicellulases, including endo-1,4-

beta-xylanase, endoglucanase, etc.) was calculated and shown in Figure 4.6B. In R_{20}, the related genes showed slightly higher abundance at 0.8 V (0.127% - 0.131%) than 0 V and 0.4 V (0.110 - 0.118%), while significantly higher abundance was obtained at 1.2 V (0.148 - 0.175%, $p < 0.01$), which was also overwhelmingly higher than that of R_{35} in all stages (0.086 - 0.126%, $p < 0.01$). These findings indicated that the applied voltage, especially 1.2 V, could promote the metabolism of complex organics; however, the enhancement at room temperature could be more prominent than that at mesophilic temperatures. The PICRUSt results correlated well with the enhanced hydrolysis and enriched hydrolytic bacteria with increased applied voltages, resulting in a considerable improvement in methane yields. The prediction of functional genes provided valuable insights into the metabolic dynamics, which could help guide future system optimization.

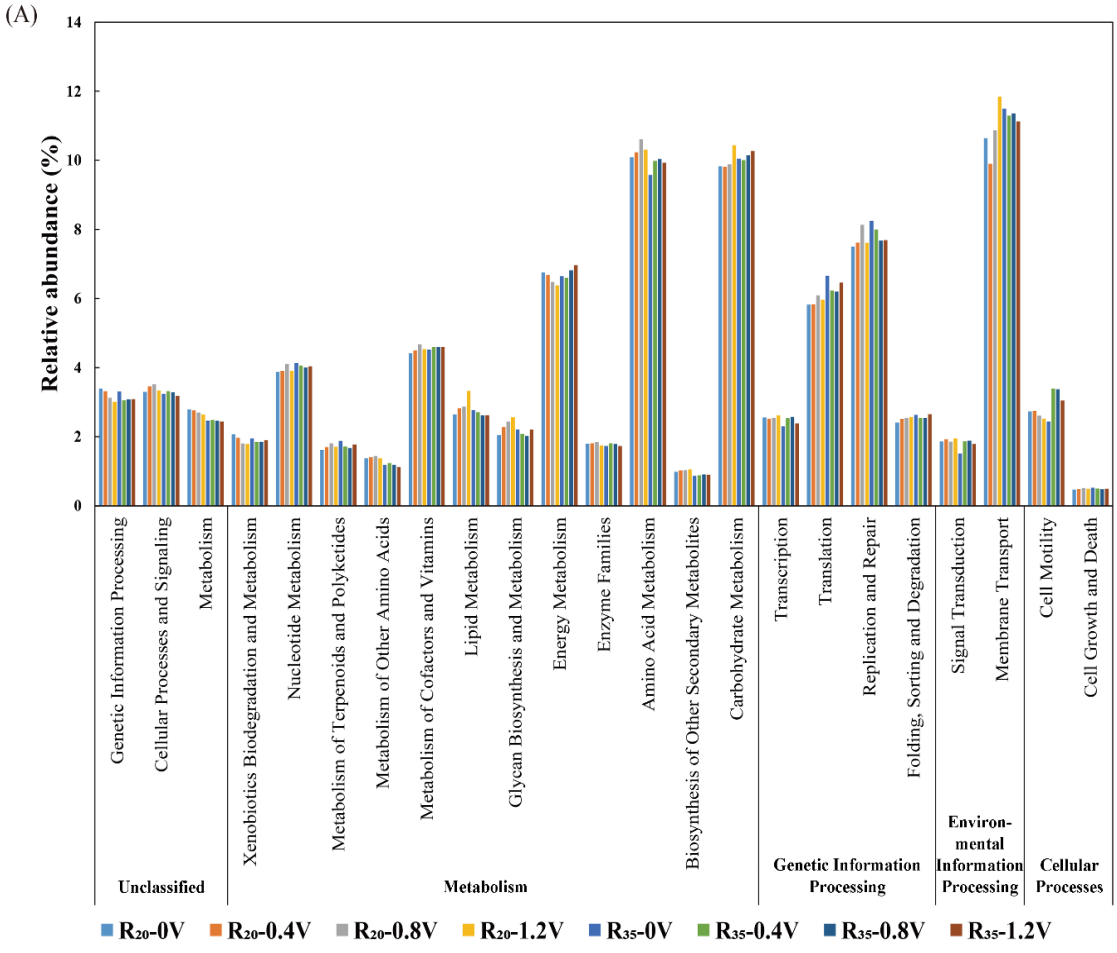

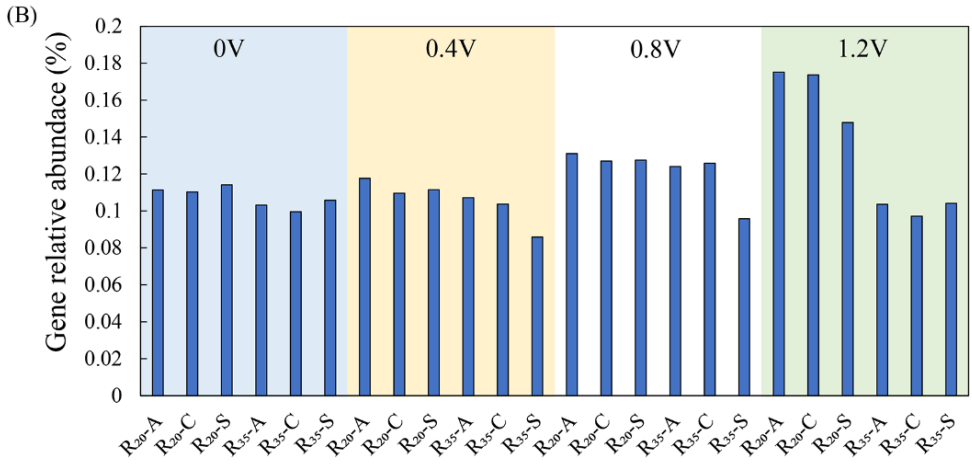

Figure 4.6 (A) Predicted metagenome functions of anodic samples from both reactors at different applied voltages; (B) Relative abundance of genes encoding cellulases and hemicellulases based on PICRUSt predictions. 'A', 'C'and 'S' in the sample names refer to anode, cathode, and suspension, respectively.

4.3.4 Electrode corrosion: significance of electrode selection

As corrosion of stainless-steel current collector was observed for an applied voltage > 1.2 V, a supplementary test of 120 days was conducted at 20 °C by replacing stainless steel current collectors with carbon cloth, but carbon fibers were kept as the main electrode material (see Appendix B Figure B.1B). The applied voltage in the supplementary test was increased from 0 V to up to 2.4 V (see Appendix B Figure B.4). The reactor with carbon cloth current collectors (referred to as R_{20}-CC) showed lower methane yield than R_{20} from 0 to 1.2 V, which could be attributed to the slight variations in feedstock (blackwater) characteristics or differences in conductive materials. However, R_{20}-CC showed a similar increasing trend of methane yield from 24.6% at 0 V to 34.1% at 1.2 V. A higher methane yield of 36.0% was achieved at 1.6 V without any corrosion, which indicated the applied voltage can be further increased for better system performance; however, energy efficiency should be considered when choosing the optimum applied voltage. There was a significant decrease in methane yield at 2.0 V. The pH was in the normal range (7.36), and no hydrogen was detected. Thus, the decreased methane production could be attributed to the excessive applied voltage instead of the impacts of water electrolysis.

The high applied voltage can negatively influence the microbiome due to cell membrane rupture (Chen et al., 2016). Nonetheless, the reactor finally failed at 2.4 V due to the dual negative impacts from excessive voltage and alkaline pH resulting from water electrolysis. These results evidently suggested that the selection of electrodes would be a critical factor influencing optimum applied voltage.

Table 4.2 Energy consumption, generation, and net energy production per liter of blackwater treated in different reactors/stages.

	Electrical energy consumption (kJ/L)	Energy gain as biomethane (kJ/L)	Heating energy consumption (kJ/L)	Net energy gain (kJ/L)
R_{20}-1.2V	7.23	75.19	0	67.96
R_{20}-0V	0	47.00	0	47.00
R_{35}-0.8V	5.13	102.12	65.52	31.47
R_{35}-0V	0	100.79	65.52	35.27
R_{20}-CC-1.2V	6.77	66.77	0	60.01
R_{20}-CC-1.6V	12.91	70.50	0	57.59

4.3.5 Energy efficiency

Energy efficiency is a crucial parameter to consider when selecting optimum applied voltage in MEC-AD systems. For R_{20}, after subtracting the electrical energy consumption, the net energy generation at 1.2 V is 67.96 kJ/L (Table 4.2), while only 47.00 kJ/L of energy was generated at 0 V, resulting in a 45% enhancement of energy efficiency at 1.2 V. R_{35} achieved the highest methane yield at 0.8 V with a considerable heating energy consumption of 65.52 kJ/L, resulting in low net energy production of 31.47 kJ/L. Thus, despite lower methane production, R_{20} at 1.2 V achieved 2.16 times as much energy efficiency as R_{35} at 0.8 V. Interestingly, R_{20} at 0 V provided better energy efficiency that R_{35} at 0.8 V. It should be noted that the heat loss and electrical conversion efficiency to heat energy were neglected in this calculation, which means the net energy

production in R_{35} would be lower in practice than this estimated value. In the supplementary test with a carbon cloth current collector, R_{20}-CC at 1.2 V also showed 4.18% higher energy efficiency than 1.6 V, although methane yield was slightly higher at 1.6 V. These preliminary energy assessments suggest that R_{20} at 1.2 V was the most energy-efficient option for operating MEC-AD with vacuum toilet blackwater digestion.

4.4 Conclusions

The MEC-AD operation with vacuum toilet blackwater at ambient temperature consistently improved COD removal, methane yield, hydrolysis/acidogenesis efficiency and energy efficiency for increasing applied voltage from 0 to 1.2 V, while 1.6 V caused system failure due to anodic corrosion. The improved hydrolysis was demonstrated by some enriched hydrolytic bacteria like *Clostridium*, *Bacteroidales*, etc., as well as the increase of functional genes encoding complex organics metabolism. LEfSe analysis revealed the importance of syntrophic bacteria, and their partnerships with acetate-using bacteria and the dominant archaea *Methanosaeta*. The impacts of applied voltages were more pronounced under ambient temperature than mesophilic temperature.

Chapter 5. Boosting Resilience of Microbial Electrolysis Cell-assisted Anaerobic Digestion of Blackwater with Granular Activated Carbon Amendment[4]

5.1. Introduction

The complex nature and low biodegradability of blackwater present some challenges for treating it at high organic loading rates (OLRs), where hydrolysis is the rate-limiting step (Gao et al., 2019b; Huang et al., 2022c). For instance, a mesophilic up-flow anaerobic sludge blanket (UASB) reactor treating vacuum toilet blackwater achieved superior performance at an OLR of 4.1 g COD/L-d, whereas significant sludge loss and insufficient hydrolysis were observed at an OLR of 4.87 g COD/L-d (Gao et al., 2019b). These previous studies highlighted that it is necessary to employ more advanced engineering approaches, such as pretreatment or the adoption of a new reactor design, to improve hydrolysis or sludge retention and facilitate the digestion of blackwater (Gao et al., 2019b). Moreover, blackwater is discharged at ambient temperature; thus, developing high-rate digesters for ambient temperature is yet to be achieved for blackwater (Huang et al., 2021).

A few studies have demonstrated the effectiveness of MEC-AD systems in promoting blackwater digestion, while the enhancement of the hydrolysis step is yet to be achieved (Huang et al., 2021; Zamalloa et al., 2013). For instance, Huang et al. (2021) reported declining methane yields in a MEC-AD system with raised OLRs from 0.77 to 3.03 g COD/L-d, due to the deterioration in hydrolysis kinetics. In most MEC-AD systems, electrodes with applied voltage/potential are incorporated in continuous stirred tank (CSTR) type digesters (Quashie et al., 2021), leading to an unavoidable occurrence of biomass washout in these arrangements. Thus, developing strategies to prolong sludge retention, prevent biomass washout and retain undigested

[4] A version of this chapter has been published as: Huang, Q., Liu, Y., & Dhar, B. R. (2023). Boosting resilience of microbial electrolysis cell-assisted anaerobic digestion of blackwater with granular activated carbon amendment. *Bioresource Technology*, 381, 129136.

solids for subsequent hydrolysis would be critical for developing high-rate MEC-AD systems.

Recently, amending anaerobic digesters with conductive additives, such as granular activated carbon (GAC), has been widely studied (Zhang et al., 2020b; Zhao et al., 2017). GAC can promote the cell-to-cell electron transfer between electroactive bacteria and electrotrophic archaea, which is a thermodynamically and metabolically favorable pathway known as direct interspecies electron transfer (DIET) (Barua & Dhar, 2017). Meanwhile, a few recent studies reported that GAC could also enhance hydrolysis kinetics in AD (Johnravindar et al., 2020; Peng et al., 2018). Thus, adding GAC in MEC-AD might be a promising strategy to overcome hydrolysis limitations and reinforce microbial activity. So far, only limited studies integrated conductive additives in MEC-AD reactors. LaBarge et al. (2017) improved their MEC-AD performance by supplementing GAC pre-acclimated by methanol/hydrogen, reducing start-up time and increasing methane generation. Vu et al. (2020) reported that other conductive additives, like magnetite addition, could boost biofilm catalytic activity and reduce the solution and charge transfer resistance. However, to date, there have been no reports on incorporating GAC amendments with prolonged sludge retention for the dual purpose of mitigating hydrolysis limitations and promoting methane production in MEC-AD reactors. Furthermore, although conductive materials have the potential to enhance MEC-AD systems, there is currently limited knowledge about how these materials interact with the microbial community in an electroactive environment. Further research is needed to gain insights into this aspect for advancing MEC-AD technologies.

Therefore, this chapter proposes a novel MEC-AD scheme incorporating GAC amendment and extended sludge retention time to enhance AD processes and address the water-energy nexus. Firstly, the hydrolysis and overall digestion efficiencies were evaluated in response to increased organic loading rates. Moreover, the feasibility of successful reactor operation at a lower temperature with more limited hydrolysis capacity was also examined, focusing on temperature sensitivity comparison between the MEC-AD and control reactor. Furthermore, microbial succession and dynamics were analyzed using different bioinformatic methods to

comprehensively evaluate microbial interactions stimulated by MEC-AD and GAC. These insights could guide future development and application of conductive materials amended MEC-AD systems for efficient treatment of various high-strength feedstocks.

5.2 Materials and methods

5.2.1 Bioreactor configuration

A single-chamber MEC-AD reactor was constructed with plexiglass tubes, featuring a total volume of 420 mL and a working volume of 380 mL (see Appendix C Figure C.1). High-density carbon fibers (2293-A, 24A Carbon Fiber, Fibre Glast Development Corp., Ohio, USA) were attached to a pair of stainless-steel frames as electrodes. Then anode and cathode were fixed to the left and right walls of the reactor, respectively. The reactor was equipped with an Ag/AgCl reference electrode (MF-2052, Bioanalytical System Inc., Indiana, USA), which was placed close to the anode electrode (< 1 cm). A potentiostat system (4-channel Squidstat Prime, Admiral Instruments, Tempe, AZ, USA) was used to fix the anode potential at -0.2V vs. standard hydrogen electrode (SHE). An identical reactor was also fabricated with the same electrodes while operated without applied potential as a control reactor. A magnetite stirrer bar was located at the bottom of each reactor for mixing.

5.2.2 Blackwater collection and reactor operation

Vacuum toilet blackwater stock (1 L flushing water/flush) was collected and prepared biweekly according to a protocol reported by Huang et al. (2020b), and stored at 4 ℃ until use. After preparation, the physicochemical characteristics of the blackwater were immediately determined, and the average values were presented in Table 5.1. For the start-up, 40 mL of sludge obtained from a full-scale anaerobic digester (operated at 37 °C) treating municipal sludge in a wastewater treatment plant (Edmonton, AB, Canada), and 30 mL of effluent from a mature MEC reactor, which had been running on acetate medium (25 mM) for over 6 years, were used to inoculate the reactors. The total suspended solids (TSS) and volatile suspended solids (VSS) concentrations of

the inoculum mixture were 8.2 g/L and 6.1 g/L, respectively.

The experiments were carried out over a period of approximately 250 days, comprising four different stages. In Stage 1, both reactors were operated semi-continuously at 35 ± 0.5 ℃ and an OLR of 3.0 (± 0.0) g COD/L-d with vacuum toilet blackwater. In Stage 2, the OLR was raised to 4.5 (± 0.1) g COD/L-d. For Stage 3 and Stage 4, the OLRs were maintained similar to Stage 2 at 4.5 (± 0.2) g COD/L-d, but the mixing was stopped, and GAC (4 – 12 mesh, Sigma-Aldrich, St. Louis, USA) was added to both reactors at a concentration of 25 g/L. The GAC and settled solids formed GAC-sludge aggregates, which could not be discharged with the effluent. The reactors were operated at 35 ± 0.5 ℃ in Stage 3, the same as in previous stages, while the operating temperature decreased to 20 ± 0.5 ℃ in Stage 4. Detailed operating conditions are shown in Table 5.1. Effluent dissolved methane concentrations were measured 3 times per stage in triplicate at steady-state using the methods outlined by Zhang et al. (2020b).

5.2.3 Characterization of sludge stability and specific methanogenic activity

At the end of Stage 3&4, the accumulated sludge of the reactors was collected from different locations and mixed. The sludge COD, TSS, and VSS were measured before conducting batch tests to assess the stability (i.e., undigested fraction) and specific methanogenic activity (SMA) of the sludge. To determine the amount of biodegradable COD in the sludge, which could potentially be converted to methane, batch tests were carried out using freshly collected samples of the accumulated sludge to evaluate the sludge stability, following a previous study (Gao et al., 2019b). The tests were conducted in triplicate and presented in g CH_4-COD/g sludge COD with the average values and standard deviations. Higher values indicate a greater fraction of biodegradable COD accumulated in the settled sludge, i.e., higher sludge instability.

Batch assays were performed to measure the specific methanogenic activity (SMA), which represents the maximum specific methane production rates that the sludge can perform through either acetoclastic or hydrogenotrophic pathway. 3 mL of settled sludge from the bottom of the reactor was sampled and mixed with 12 mL deionized water for SMA tests on H_2 + CO_2 gas, or

12 mL of sodium acetate resulting in the final substrate concentration of 2 g COD/L for SMA tests on acetate. The mixed sludge and substrate (or DI water) were added to serum bottles with a volume of 38 mL. N_2 gas or H_2 + CO_2 gas (molar ratio 4:1) was used for flushing the bottles for SMA tests on acetate and H_2 + CO_2 gas, respectively. The bottles were then sealed with rubber stoppers and aluminum caps, and incubated in a shaking incubator (120 rpm; under the dark condition) at 35 ℃ for Stage 3 and 20 ℃ for Stage 4. Blank controls were also set up with no substrate added/flushed to determine the methane production from sludge.

5.2.4 Analytical methods

The total COD (TCOD), soluble COD (SCOD), TSS and VSS of samples were measured according to the standard methods (APHA, 2005). A B40PCID pH meter (VWR, SympHony) was used to determine the pH. The concentrations of volatile fatty acids (VFAs) were measured after filtering with 0.2 μm membrane syringe filters by ionic chromatography (IC) system (DIONEX ICS-2100, Thermo Fisher, USA). Biogas composition was determined using a gas chromatograph (Huang et al., 2021). The headspace pressure of serum bottoms in batch tests was measured by a GMH3151 manual pressure meter (Greisinger, Regenstauf, Germany).

5.2.5 DNA extraction

At the end of each stage, electrode-attached biofilm samples and settled sludge samples were collected from around 15 different locations on the electrode surface and settled sludge, respectively. Suspended sludge samples were collected by centrifuging the effluent at 4000 rpm for 5 mins and discharging the supernatant. GAC granules were separated from the settled sludge and directly used in the DNA extraction process for GAC biofilm microbial community analysis. The genomic DNA was extracted using DNeasy PowerSoil Kit (QIAGEN, Hilden, Germany) following the manufacturer's protocol. NanoDrop One (ThermoFisher, Waltham, MA) was used to check the DNA concentration and quality. The extracted DNA was stored at -80 ℃ before downstream sequencing. 16S rRNA gene was sequenced by Illumina Miseq with universal primer-pair 515F/806R at the Research and Testing Laboratory (Lubbock, TX, USA).

5.2.6 Bioinformatics and statistical analyses

The raw sequencing data were processed using the Qiime2 pipeline (Hall & Beiko, 2018) for read pairings after being filtered and denoised by the DADA2 algorithm (Callahan et al., 2016). Taxonomy was assigned using 99% similarity in Silva 138 SSU reference database (Quast et al., 2012). Principal coordinate analysis (PCoA) was carried out at the genus level through the 'vegan' package in R (Oksanen et al., 2007). The linear discriminant analysis (LDA) effect size (LEfSe) method (Segata et al., 2011) was used to determine the taxonomic biomarkers among suspended sludge, GAC biofilms and settled sludge. Co-occurrence network analysis was carried out using R "igraph" (Csardi & Nepusz, 2006) and "psych" packages (Revelle, 2017). The Spearman's correlations at $\rho > 0.6$ and $p < 0.05$ were used for network construction. The functional genes annotation was determined using the Phylogenetic Investigation of Communities by Reconstruction of Unobserved States (PICRUSt) (Langille et al., 2013), and the Kyoto Encyclopedia of Genes and Genomes (KEGG) reference database (Kanehisa et al., 2012). Single-factor analysis of variance (ANOVA) was performed through Microsoft Excel®. A p-value < 0.05 was considered statistically different.

5.2.7 Calculations

Methane yield was estimated using Eq. (1) (Huang et al., 2021):

$$\text{Methane yield (\%)} = \frac{COD_{CH4}}{COD_{input}} * 100 \quad (1)$$

where COD_{CH4} represents the COD equivalent of produced methane (in mg COD); COD_{input} represents the amount of total COD input (in mg COD).

The hydrolysis efficiency calculation was based on the whole stage (~ 60 days) instead of average values of different feeding cycles due to the impact of accumulated solids, using Eq. (2) (Huang et al., 2022c):

$$\text{Hydrolysis efficiency (\%)} = \frac{\sum(COD_{CH4}+COD_{S,eff}-COD_{S,inf})}{\sum(COD_{T,inf}-COD_{S,inf})} \times 100 \quad (2)$$

where $COD_{T,inf}$ and $COD_{S,inf}$ are the total COD and soluble COD from the influent,

respectively (in mg COD); $COD_{S,eff}$ is the soluble COD from the effluent (in mg COD).

Energy efficiencies were calculated using equations detailed in Huang et al. (2021).

5.3 Results and discussions

5.3.1 Methane production

The biochemical methane potential (BMP) of blackwater represents the anaerobically biodegradable fraction (%) of the total COD, which can be affected by the human diet, flushing system, and seed sludge, etc. (Gao et al., 2018; Gao et al., 2020b). The typical BMP values reported in previous studies were around ~ 45% (Huang et al., 2021). As shown in Figure 5.1A, in Stage 1 at OLR 3.0 g COD/L-d, both MEC-AD and control reactors showed superior methane yield of 42.7 ± 1.2% and 40.8 ± 1.8%, respectively, approaching the 45% BMP value. However, when the OLR was increased to 4.5 g COD/L-d in Stage 2, the methane yield significantly decreased ($p < 0.05$) to 34.4 ± 0.8% and 28.2 ± 1.4% in MEC-AD and control reactors, respectively. As discussed later, the significantly higher effluent particulate COD concentrations indicated the limited hydrolysis capacity at a higher OLR.

After introducing the GAC and stopping the mixing in Stage 3, the unhydrolyzed suspended solids were settled to the reactor bottom and formed GAC-sludge aggregates for subsequent hydrolysis. While both prolonged sludge retention and GAC addition could possibly contribute to improved hydrolysis, the exact mechanisms underlying the enhancement of hydrolysis by GAC addition remain unclear (Johnravindar et al., 2020; Peng et al., 2018). This combined strategy significantly increased the overall hydrolysis efficiency from 31.11% to 37.15% in the MEC-AD reactor and from 29.09% to 35.92% in the control reactor (Table 5.1), resulting in a remarkable increase ($p < 0.05$) in methane yield to 38.3 ± 1.0% and 32.3 ± 1.5% in the MEC-AD and control reactors, respectively. However, the MEC-AD reactor still showed an 18.4% higher methane yield compared to the control. Considering the similar hydrolysis efficiencies of the two reactors, it's obvious that hydrolysis was not the only limiting factor for the control reactor. Upon reducing the

operating temperature to 20 ℃ in Stage 4, a decline in methane yield was noted in both reactors, which was anticipated due to the temperature sensitivity of the biochemical reaction kinetics. However, a more pronounced decrease in methane yield was observed in control, with yield plummeting to as low as 23.7 ± 0.4%. This observation indicated the constrained influence of conductive materials alone. In contrast, the combined impact of applied potential and conductive materials contributed to the considerable improvement in methane yield. In a previous study by Huang et al. (2021), the highest methane yield achieved in a MEC-AD reactor treating blackwater was only 35.2 ± 2.1% at a much lower OLR of 3.0 g COD/L-d and 20 ℃. Therefore, the current study's finding of a methane yield of 33.2 ± 0.3% at an OLR of 4.5 g COD/L-d and 20 ℃ in the MEC-AD reactor represents a significant advancement.

Moreover, electrical energy consumption by the MEC-AD reactor was fully recovered as methane from Stage 2 to 4, with energy efficiency increased by 17.9% to 38.3% compared to the control reactor. Furthermore, an elevated methane content in biogas (Table 5.1) was observed in the MEC-AD reactor (78.2 - 82.9%) compared to the control (72.4 - 79.3%). Meanwhile, the improved methane purity in Stage 3 and 4 in both reactors can be attributed to the formation of GAC-sludge aggregates, which facilitated a partial shift in the methanogenesis pathway from acetoclastic methanogenesis to DIET, and effectively reduced CO_2 content (discussed later).

5.3.2 Organics removal

The performances of the reactors were compared based on TCOD removal efficiency (Figure 5.1B), effluent VFA concentrations (Figure 5.1C), TSS and VSS removal efficiency, and hydrolysis efficiency along with the effluent properties (Table 5.1). The influent quality was maintained at a stable level of 14.9 ± 0.5 g COD/L throughout the study. During Stage 1, both reactors exhibited similar TCOD removal efficiencies of ~ 65%. However, upon increasing the OLR in Stage 2, the TCOD removal efficiencies decreased to 53.0 ± 3.8% and 45.4 ± 3.3% in the MEC-AD and control reactors, respectively, with a considerable amount of particulate COD present in the effluent (4.8 vs. 5.3 g/L). After prolonging the sludge retention via GAC addition

as well as operation under non-mixing conditions in Stage 3, the TCOD removal efficiencies improved to 75.0 ± 4.2% and 68.6 ± 4.7% in the MEC-AD and control reactors, respectively. In Stage 4, with a decrease in temperature, the effluent TCOD levels were maintained at a similar level to that in Stage 3. However, a remarkable reduction in overall hydrolysis efficiency was observed (31.3% vs. 28.4%), leading to a higher level of unhydrolyzed particulate COD in the settled sludge. Notably, throughout the operation, the effluent from the MEC-AD reactor demonstrated 10.9% to 28.0% lower SCOD than that from the control reactor, indicating a higher methanogenic activity with applied potential.

As illustrated in Figure 5.1C, the MEC-AD reactor consistently exhibited lower levels of total VFAs throughout the study. The higher VFA utilization, particularly acetate, could be ascribed to facilitated anodic oxidation by enriched electroactive bacteria (Zakaria & Dhar, 2021a; Zhao et al., 2021). Higher VFA levels were observed in Stage 3 and 4 due to higher overall hydrolysis efficiencies, where severe VFA accumulation was observed in the control reactor, with total VFA concentrations reaching as high as 1410 ± 132 mg/L. In contrast, the acetate (500.6 mg/L) and total VFA (723.7 mg/L) concentrations in the MEC-AD reactor were approximately half of those in the control reactor. GAC has been intensively studied as a potential means of facilitating VFA oxidation by maintaining a lower H_2 partial pressure through its syntrophic partnership with hydrogenotrophic methanogens (Johnravindar et al., 2020; Zhang et al., 2020b). However, the results of this study indicated that combining applied potential and conductive materials could degrade VFAs more efficiently than GAC alone.

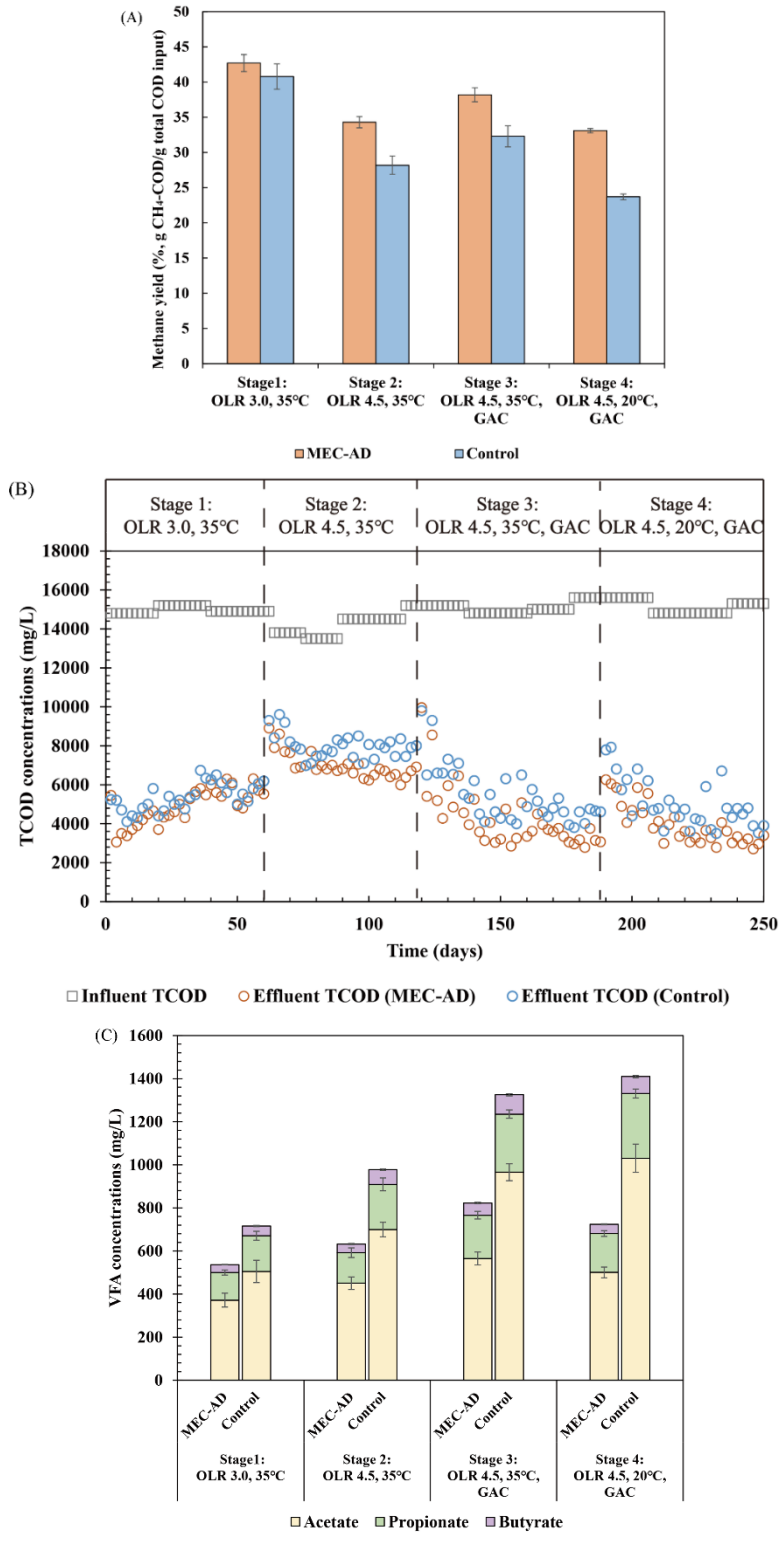

Figure 5.1 (A) Average methane yield based on steady-stage results; (B) Influent and effluent TCOD concentrations during the operating period; (C) Effluent VFA concentrations based on steady-stage results.

Table 5.1 Influent/effluent properties and key parameters of the reactors during the steady-state operation.

	Unit	Influent	MEC-AD				Control			
			Stage 1: OLR 3.0, 35°C	Stage 2: OLR 4.5, 35°C	Stage 3: OLR 4.5, 35°C, GAC[1]	Stage 4: OLR 4.5, 20°C, GAC[1]	Stage 1: OLR 3.0, 35°C	Stage 2: OLR 4.5, 35°C	Stage 3: OLR 4.5, 35°C, GAC[1]	Stage 4: OLR 4.5, 20°C, GAC[1]
TCOD	g/L	14.9 ± 0.5	5.4 ± 0.6	6.7 ± 0.4	3.6 ± 0.6	3.3 ± 0.4	5.7 ± 0.6	7.8 ± 0.4	4.8 ± 0.7	4.5 ± 0.8
SCOD	g/L	3.3 ± 0.2	1.8 ± 0.1	1.9 ± 0.1	2.4 ± 0.2	2.3 ± 0.2	2.0 ± 0.1	2.5 ± 0.1	3.0 ± 0.3	3.2 ± 0.4
PCOD	g/L	11.5 ± 0.4	3.6 ± 0.5	4.8 ± 0.3	1.2 ± 0.4	1.1 ± 0.2	3.7 ± 0.4	5.3 ± 0.4	1.7 ± 0.4	1.3 ± 0.6
TCOD removal efficiency	%		64.1 ± 4.0	53.0 ± 3.8	75.0 ± 4.2	77.7 ± 3.1	62.0 ± 3.8	45.4 ± 3.3	68.6 ± 4.7	70.7 ± 5.1
TSS	g/L	7.2 ± 0.6	2.2 ± 0.4	3.1 ± 0.3	0.7 ± 0.1	0.7 ± 0.1	2.3 ± 0.2	3.3 ± 0.3	1.1 ± 0.1	0.8 ± 0.1
TSS removal efficiency	%		68.9 ± 2.6	56.8 ± 3.3	90.6 ± 1.4	90.9 ± 1.2	67.3 ± 2.9	53.9 ± 3.2	85.7 ± 1.8	88.9 ± 2.0
VSS	g/L	6.6 ± 0.5	2.1 ± 0.2	2.8 ± 0.2	0.7 ± 0.1	0.6 ± 0.1	2.1 ± 0.3	2.9 ± 0.4	1.0 ± 0.1	0.7 ± 0.1
VSS removal efficiency	%		68.1 ± 1.9	57.8 ± 2.6	90.1 ± 1.6	91.2 ± 2.0	68.1 ± 3.5	55.9 ± 3.7	85.5 ± 1.7	89.1 ± 1.9
Methane yield	%		42.7 ± 1.2	34.4 ± 0.8	38.3 ± 1.0	33.2 ± 0.3	40.8 ± 1.8	28.2 ± 1.4	32.3 ± 1.5	23.7 ± 0.4
Methane content in biogas	%		78.2 ± 0.5	79.9 ± 0.4	82.6 ± 1.0	82.9 ± 1.3	72.4 ± 0.7	73.5 ± 0.7	78.4 ± 1.4	79.3 ± 0.8
pH		8.58 ± 0.10	7.48 ± 0.18	7.37 ± 0.09	7.29 ± 0.10	7.33 ± 0.09	7.42 ± 0.16	7.34 ± 0.11	7.27 ± 0.08	7.24 ± 0.06
TVFA	g/L		0.54 ± 0.06	0.63 ± 0.09	0.82 ± 0.10	0.72 ± 0.09	0.72 ± 0.11	0.98 ± 0.10	1.33 ± 0.09	1.41 ± 0.13
Hydrolysis efficiency	%		41.70	31.11	37.15	31.32	41.30	29.09	35.92	28.36

[1]Operated without any mixing

5.3.3 Sludge properties

In Stage 3, the settled sludge had high VSS concentrations for both MEC-AD (28.5 ± 0.6 g/L) and control (24.3 ± 0.3 g/L) reactors, which were comparable to or higher than the typically reported VSS concentration range (9.1 – 25.9 g/L) of UASB sludge beds for blackwater treatment (Zhang et al., 2021a; Zhang et al., 2022a). Such an observation could result from longer sludge retention due to GAC addition as well as operation under non-mixing conditions. The high biomass retention is expected to enhance the excretion of hydrolase enzymes, thereby further promoting hydrolysis efficiency (Zhang et al., 2021a). The overall hydrolysis efficiencies in Stage 3 with prolonged solids retention time at 35 ℃ ranged from 35.9% to 37.2%, which were higher than the hydrolysis efficiency (29.5 ± 5.2% - 33.2 ± 5.0%) previously reported by Gao et al. (2019b) at lower OLRs ranging from 0.28 to 4.07 g COD/L-d and 35 ℃. In comparison, this study significantly improved hydrolysis efficiency by retaining the solids in the reactor and forming dense GAC-sludge aggregates.

Sludge methanogenic activity is widely recognized as a crucial parameter in evaluating reactor behavior. The results of SMA (acetate) and SMA (H_2 + CO_2) for settled sludge in Stage 3 and 4 were illustrated in Figure 5.2. Hydrogenotrophic methanogenesis was identified as the ascendancy pathway by consistently and significantly higher SMA (H_2 + CO_2) than SMA (acetate). The MEC-AD reactor achieved significantly higher (32.5 – 53.9%, $p < 0.05$) SMA (H_2 + CO_2) values than that of the control, while SMA (acetate) remained similar between the two reactors. Interestingly, hydrogenotrophic methanogens became more active and competitive at a lower temperature, demonstrated by a raised SMA (H_2 + CO_2)/SMA (acetate) ratio from 1.51 - 2.51 in Stage 3 to 2.36 - 3.04 in Stage 4. The sensitivity of acetoclastic methanogens to low temperatures may contribute to this observation (Traversi et al., 2014).

The sludge stability value expresses the undigested fraction of biodegradable substrates in sludge (Gao et al., 2020b). In this study, the settled sludge stability of the MEC-AD reactor increased from 0.20 ± 0.02 g CH_4-COD/g sludge COD (Stage 3) to 0.25 ± 0.03 g CH_4-COD/g

sludge COD (Stage 4) due to decreased digestion efficiency at a lower temperature. Considerably higher sludge stability values were observed in the control reactor (see Figure 5.2), indicating lower levels of organics degradation. Although non-mixing conditions may potentially restrict mass transfer, the advantages of long sludge retention could possibly outweigh the associated drawbacks. Firstly, longer sludge retention can promote the enrichment of slow-growing microorganisms, better suited to degrade complex organics and improve system performance (Jegatheesan et al., 2016). Moreover, longer sludge retention leading to biomass accumulation can enhance the treatment capacity and overall resilience of the system (Vergine et al., 2021). Additionally, Bose et al. (2021) reported GAC-amended batch digester achieved the highest methane production without any mixing compared to intermittent or continuous mixing conditions, due to higher enrichment/retention of active microbes on conductive materials, resulting in more stabilized microbial communities. Furthermore, considering the substantial energy consumption by mixing, which accounts for around 14 - 54% of the total energy demand (Bose et al., 2021), the implementation of non-mixing AD operation can be regarded as an energy-efficient and sustainable strategy. In summary, although lack of mixing may create obstacles for mass transfer, the potential benefits of biomass retention should not be overlooked when designing and optimizing anaerobic treatment systems.

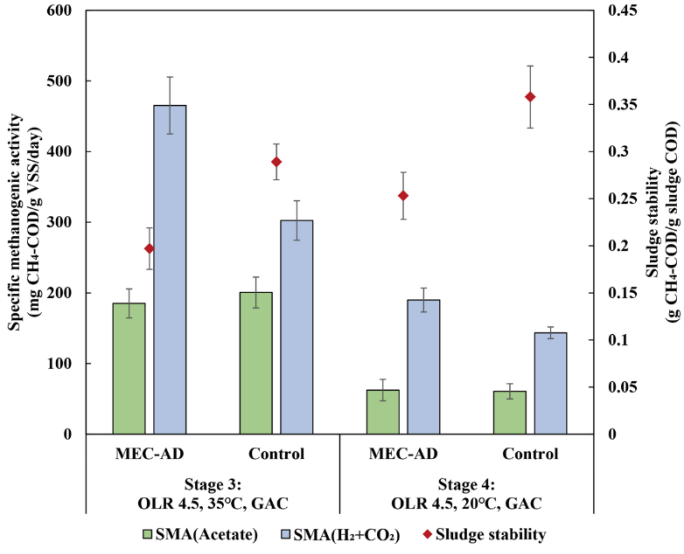

Figure 5.2 Specific methanogenic activity and sludge stability of the sludge settled/accumulated in the bottom of the reactor in Stage 3 and 4.

5.3.4 Microbial community

5.3.4.1 Microbial community diversity

The principal coordinate analysis (PCoA) was carried out using Bray-Curtis distances among samples to analyze the microbial community relationships. Three clusters were formed for samples of Stage 2 – 4 along the PCoA 1 axis, which explained 35.28% of the total sample variance (Figure 5.3). Samples in Stage 2 formed a loosely clustered group, indicating substantial differences in microbial communities across different locations and reactors. However, the addition of GAC and formation of GAC-sludge aggregates in Stage 3 resulted in more closely clustered samples, suggesting the microbial community in MEC-AD and control reactor shared more similarities. Therefore, GAC-sludge aggregates played a critical role in bridging the gap between the microbial communities of the two reactors by creating a more favorable environment for microbial activity. Furthermore, samples in Stage 4 formed the most compact cluster, potentially due to a higher substrate stress level at 20 ℃, which could select microbes with higher growth rates and substrate utilization rates, namely r-strategists (Huang et al., 2021).

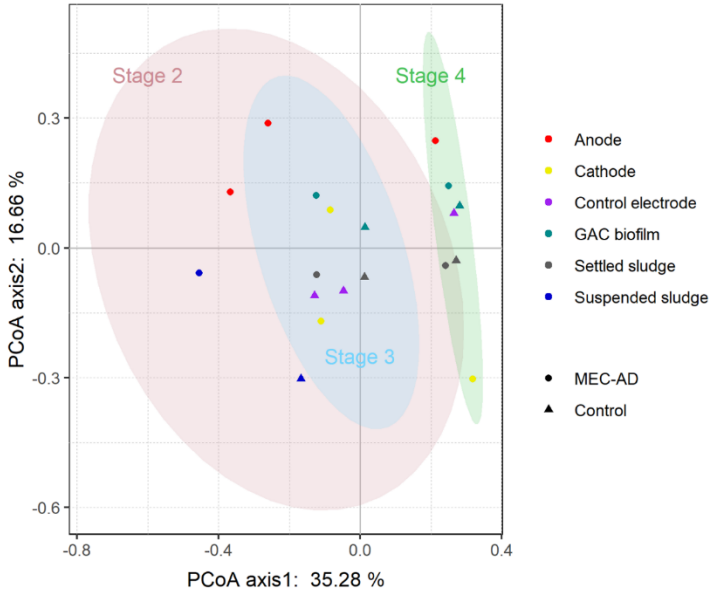

Figure 5.3 Principal coordinate analysis (PCoA) of microbial communities. PCoA was computed using Bray-Curtis distance calculated using genus abundance data (ellipse confidence level = 95%).

5.3.4.2 Archaeal communities

As presented in Figure 5.4A, the anode harbored a more diverse archaeal community, with the predominant methanogens shifting from *Methanoculleus* (33.2%) in Stage 2 to *Methanosaeta* (41.3%) in Stage 4. The enrichment of *Methanosaeta* on the anode from Stage 3 might be attributed to higher acetate concentrations resulting from the enhanced hydrolysis followed by facilitated fermentation. Hydrogenotrophic *Methanobacterium* overwhelmingly dominated the cathode electrode in the MEC-AD (60.9 - 75.6%), control reactor electrode (45.1 - 70.2%), and settled sludge (45.2 – 67.2%). The GAC biofilms in the control reactor also showed the predominance of *Methanobacterium* (65.5 – 68.5%); however, *Methanosaeta* dominated the GAC biofilms in the MEC-AD reactor (43.3 – 58.8%). Notably, both *Methanobacterium* and *Methanosaeta* are well-known electrotrophic methanogens capable of conducting the DIET pathway and are widely enriched in MEC-AD reactors (Huang et al., 2022b; Zhao et al., 2021; Zhao et al., 2016c) and reactors amended with conductive materials (Zhang et al., 2020b; Zhang et al., 2021b; Zhao et al., 2017). Therefore, these results indicated that applied potential could select and shift the electrotrophic archaeal community on conductive materials. Additionally, the abundance of *Methanosaeta* decreased by 26.3% in the GAC biofilms in the MEC-AD reactor from Stage 3 to 4, probably due to its temperature sensitivity (Traversi et al., 2014).

5.3.4.3 Bacterial communities

Figure 5.4B illustrates the dynamics of the relative abundance of the top 10 most abundant bacterial genera in each sample. *Lentimicrobium* was the most widely spread genus, with relative abundance exceeding 10% (and up to 63.9%) in most samples. *Lentimicrobium* is strictly fermentative, producing VFAs, ethanol, H_2 and CO_2 from complex organics (Zhang et al., 2017). Particularly, *Lentimicrobium* exhibited a higher abundance in the GAC-sludge aggregates during Stage 3 compared to Stage 4, presumably due to the hydrolysis limitation in Stage 4. *Geobacter*, a well-known electroactive bacteria genus, was significantly enriched on the anode in Stage 2 and 3, with relative abundance reaching up to 15.0%, but declined to 0.6% in Stage 4. Due to their

limited metabolic versatility, most electroactive bacteria (e.g., *Geobacter*) cannot directly degrade complex fermentable organics (Zhao et al., 2016b). Consequently, with the accumulation of particulate substrates in Stage 4, hydrolytic and fermentative bacteria would play a more prominent role than electroactive bacteria.

Interestingly, on GAC biofilms, *Geobacter* was only detectable in the MEC-AD reactor, with an abundance of 0.1 - 0.3%, suggesting an electrochemically active environment could enhance the impact of conductive materials on enriching electroactive bacteria. Similar results were also observed in terms of *Pseudomonas*, *Thermovirga*, *Sedimentibacter*, *Syntrophobacter*, *Syntrophorhabdus*, *Syntrophomonas*, and a genus from the family *Syntrophomonadaceae*. These microbes are considered key players in accelerating the degradation of organic acids by syntrophic interactions with hydrogenotrophic methanogens in reactors supplemented by conductive materials (Xu et al., 2018d; Zhang et al., 2020b; Zhang et al., 2021b). However, these bacteria genera showed significantly lower abundance (or even undetectable) in the GAC-sludge aggregates in the control reactor than that in the MEC-AD reactor, which further proved the significant positive impact of applied potential on the function of conductive materials.

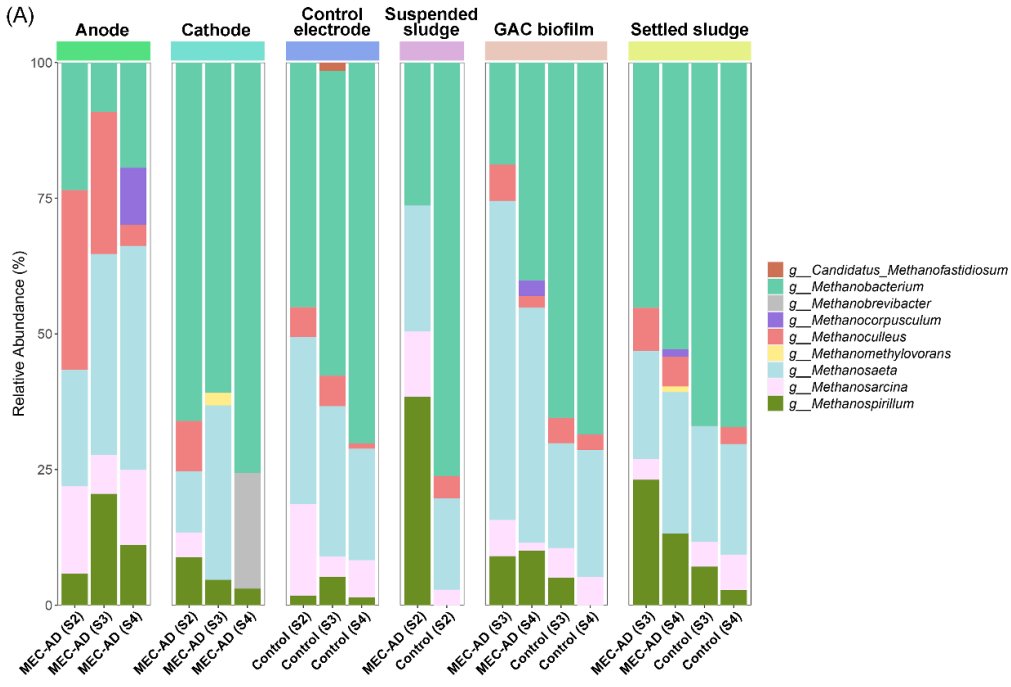

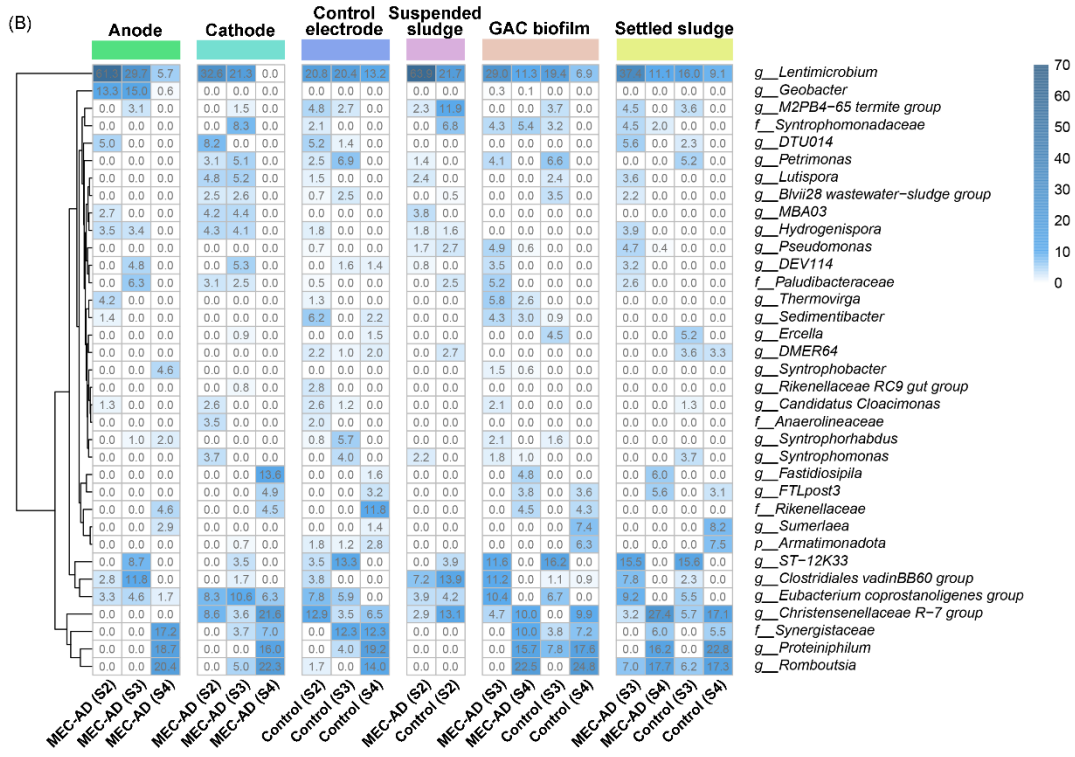

Figure 5.4 (A) Relative abundances of archaeal genera with abundance >1% in each sample; (B) Relative abundances of 10 most abundant bacterial genera in each sample. Unidentified genera were named at family (*f__*), or phylum level (*p_*). Numbers are relative abundances (%) of genera. 'S2' - 'S4' represents 'Stage 2' - 'Stage 4'.

5.3.4.4 Community differential analysis

To obtain deeper insights into the potential ecological roles of GAC biofilms and settled sludge, as well as their different functions from suspended sludge, LEfSe analysis was performed to identify biomarkers among the three groups. As shown in Figure 5.5A, the analysis revealed 25 microbial taxa with significant differences in their relative abundance (LDA score > 2) between suspended sludge (15 taxa), GAC biofilms (8 taxa), and settled sludge (2 taxa). Not surprisingly, suspended sludge contained a high fraction of bacteria (LDA score 5.20), whereas GAC biofilms significantly enriched archaea (LDA score 5.23). The microbial taxa enriched in suspended sludge primarily originated from the human gut microbiome, including the genus *Clostridia vadinBB60 group* with its family and order, genus *M2PB4-65 termite group* and its family, genus *Eubacterium*

coprostanoligenes group and its family (Kaiyrlykyzy et al., 2022). These taxa mainly belong to phylum Firmicutes and formed the largest cluster in the cladogram plot (Figure 5.5B). On the other hand, the enriched microbial taxa on GAC biofilms mainly included potentially DIET-active methanogens, including genus *Methanosaeta* and its family, and order *Methanosarcinales* (Barua & Dhar, 2017). They all belong to the class *Methanomicrobia* and phylum Euryarchaeota, which formed the second largest cluster as depicted in Figure 5.5B. Phylum Desulfobacterota was also identified as a biomarker on GAC biofilms, which includes several important syntrohic or electroactive bacteria, e.g., *Syntrophorhabdus*, *Syntrophobacter*, and *Geobacter*. The biomarkers in settled sludge included the family *Rikenellaceae* and class *Bacilli*, which contain efficient strains for the hydrolysis of complex organics (Kim et al., 2022; Yadav et al., 2016). Therefore, the LEfSe analysis revealed the important roles of GAC biofilms and settled sludge in promoting superior syntrophic methanogenesis and hydrolysis, respectively. In contrast, the suspended sludge was mostly inherited from feedstock blackwater.

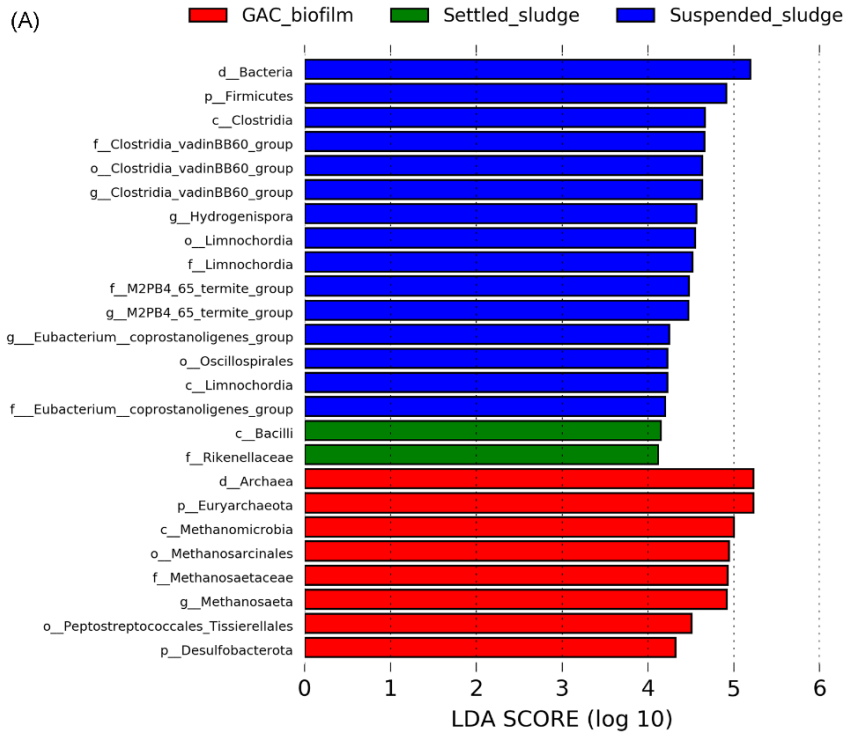

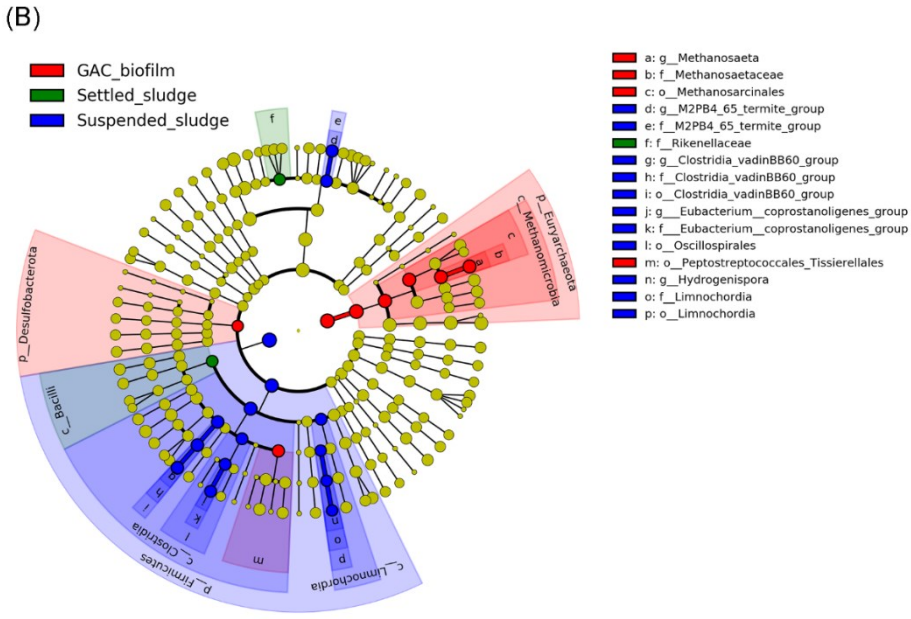

Figure 5.5 LEfSe analysis of microbial communities in GAC biofilms, settled sludge and suspended sludge. (A) Taxa with LDA score > 2; (B) Phylogenetic distribution of all taxa with LDA score > 2.

5.3.4.5 Co-occurrence network analysis

Although GAC biofilms and settled sludge were investigated separately in the above microbial community analysis, they functioned as a whole as GAC-sludge aggregates. Given the intricate nature of microbiome structure and function, focusing exclusively on the temporal abundance changes in specific microbes may provide limited insights into the microbial interactions within GAC-sludge aggregates as a functional unit. Therefore, the co-occurrence network analysis was performed for the total microbial community of GAC-sludge aggregates in the MEC-AD and the control reactor separately (see Appendix C Figure C.2). By utilizing the significant correlations among genera (Spearman's correlation coefficient $\rho > 0.6$, $p < 0.05$), two co-occurrence networks were constructed based on the clustering pattern of the two groups. The complexity of the network and the presence of strong interactions among microbes are reflected by the clustering coefficient. The GAC-sludge aggregates network in the MEC-AD reactor showed a much higher clustering

coefficient of 0.87 (see Appendix C Table C.1) than that of the control reactor (0.78), indicating strong microbial interactions. According to a previous study, a higher clustering coefficient is indicative of a more dynamic and active community (Guo et al., 2022). The network of the MEC-AD reactor also showed a lower average path length than that of the control reactor (1.17 vs. 1.27), suggesting more compact network properties and stronger microbial interactions, correlated with higher hydrolysis and methanogenesis efficiency. Of note, the average path lengths of these two networks were lower than those of 5 networks constructed for 12 anaerobic digesters treating blackwater (2.63 – 7.52) (Guo et al., 2022), indicating GAC-sludge aggregates functioned as a cohesive entity.

5.3.4.6 Functional shift of microbial communities

As evident from the microbial community results, hydrogenotrophic methanogens dominated in both reactors throughout the operation, and correlated well with higher SMA (H_2 + CO_2) than SMA (acetate). In such a system where hydrogenotrophic methanogenesis dominates, acetate degradation often occurs through the combination of the syntrophic acetate oxidation (SAO) process and hydrogenotrophic methanogenesis, converting acetate to H_2 + CO_2 first followed by methane production (Gao et al., 2020b). However, information on the SAO community has not been well-developed yet. In this study, 16S rRNA data were used to predict the *fhs* gene, which is an important indicator of the SAO community encoding a key enzyme of the Wood–Ljungdahl pathway (Müller et al., 2013). As shown in Figure 5.6, sludge in the MEC-AD reactor showed an overall higher *fhs* gene abundance than that in the control reactor. Interestingly, after introducing GAC into the reactors in Stage 3, the relative abundance of the *fhs* gene significantly increased on the MEC-AD reactor anode (from 0.012% to 0.032%) and control reactor electrode (0.010% to 0.029%). This observation indicated the GAC addition to reactors could help enrich the SAO community on the electrodes. Given the applied potential in the MEC-AD reactor could promote the proliferation of syntrophic acid-oxidizing bacteria (e.g., *Syntrophobacter*, *Syntrophorhabdus*, *Syntrophomonas*) on GAC-sludge aggregates as described earlier, it may be inferred that there exists a mutually reinforcing relationship between conductive materials and an electrochemically

active environment. Upon reaching Stage 4, where the temperature was lowered to 20 ℃, the abundance of *fhs* genes on the electrodes declined to a level comparable to that of Stage 2. However, the *fhs* gene abundance in the settled sludge significantly increased to 0.029% and 0.013% in MEC-AD and control reactor, respectively. The reduced abundance on the electrodes could be attributed to the decreased fermentation products diffused from settled sludge to electrode biofilms. Meanwhile, the competitive advantage of the SAO community over *Methanosaeta* at a lower temperature could contribute to the increased *fhs* gene abundance in the settled sludge (Traversi et al., 2014). These results underscored that the collaboration of conductive additives and applied potential effectively facilitated the DIET-related or hydrogenotrophic methanogenesis pathway by strengthening microbial syntrophic interactions, thereby enhancing system performance.

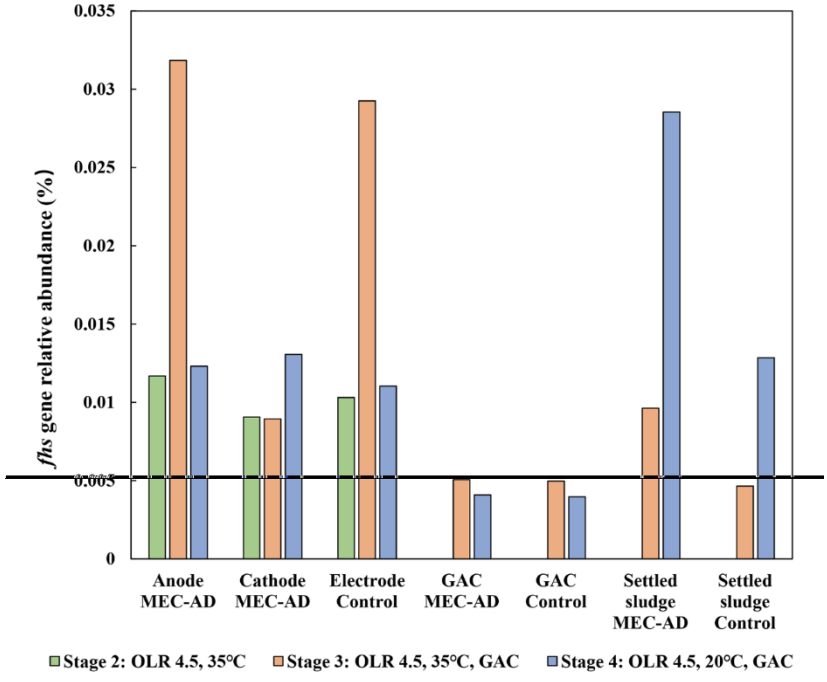

Figure 5.6 Relative abundance of *fhs* gene based on metagenome prediction.

5.3.5 Future perspectives

The economic viability of the proposed MEC-AD system was also evaluated from a financial perspective. Considering the revenue price of biomethane ($0.54/m^3) and purchasing price of

electricity consumed ($0.16/kWh) (Li et al., 2020), the net revenue of treating 1 m^3 of vacuum toilet blackwater at ambient temperature with GAC amendment is $0.97/$m^3$ in MEC-AD reactor and $0.71/$m^3$ in control reactor. Considering the significant energy requirements of conventional aerobic domestic wastewater treatment schemes (McCarty et al., 2011), the proposed MEC-AD system exhibits considerable economic potential.

However, despite the significant progress made in fundamental understanding, process development, and economic feasibility assessment of MEC-AD systems based on bench-scale results, numerous challenges still need to be addressed for successful scale-up. High capital costs, high internal resistances, and ohmic losses pose significant obstacles to large-scale applications. Additionally, controlling working electrode potential is not a practical approach for large-scale reactors due to the heterogeneous distribution of applied potential within a large electrode (Zakaria & Dhar, 2019). Therefore, a significant effort will be required in terms of various aspects, such as electrode materials, surface area, surface chemistry, and spacing, for the successful commercialization of MEC-AD technology.

Furthermore, although satisfactory results were achieved in terms of hydrolysis and methanogenesis efficiencies, the effluent quality failed to meet the discharge standards due to the presence of nutrients and some refractory residues, necessitating post-treatment. It is advisable to devote future research to nutrient recovery from digestion residues (Maroušek et al., 2020). Of note, the production of fertilizer or biochar from digestate would further contribute to water and economic sustainability (Maroušek et al., 2023).

5.4 Conclusions

This study showed the GAC addition with longer sludge retention was an effective approach to counter the performance deterioration caused by OLR increase and temperature drop, resulting in significant improvements in hydrolysis and methane yield. The GAC-sludge aggregates greatly enriched DIET-related methanogens and various hydrolytic bacteria. A mutually reinforcing

relationship between GAC and an electrochemically active environment was identified, which effectively enriched the necessary syntrophic acetate/acid-oxidizing bacteria, resulting in a highly resilient microbiome. These valuable findings could guide future research on conductive materials amended MEC-AD systems for efficient treatment of various types of high-strength feedstocks.

Chapter 6. Deciphering the Microbial Interactions and Metabolic Shifts at Different COD/sulfate Ratios in Electro-assisted Anaerobic Digestion[5]

6.1 Introduction

Various organic waste streams have been used as feedstocks in AD, among which many high-strength wastewaters from industries, such as food processing, mining, and pharmacy, often exhibit elevated sulfate (SO_4^{2-}) levels (Yuan et al., 2020). Unfortunately, high SO_4^{2-} concentrations can lead to severe inhibition of AD efficiencies (Chen et al., 2008). The presence of SO_4^{2-} in the substrate can promote the proliferation of sulfate-reducing bacteria (SRB), which can reduce sulfate to sulfide (Muyzer & Stams, 2008). Under sulfate-depleted conditions, SRB and methanogens complement each other for organic degradation. However, under sulfate-rich conditions, SRB can outcompete methanogens for common substrates, including acetate and H_2, as their substrate metabolism processes are thermodynamically more favorable (Gao et al., 2020a). For example, the standard Gibbs free energy for acetate utilization by SRB ($CH_3COO^- + SO_4^{2-} \rightarrow 2HCO_3^- + HS^-$; $\Delta G^{0'}$ = -47.6 kJ/reaction) is lower than that for acetoclastic methanogenesis ($CH_3COO^- + H_2O \rightarrow CH_4 + HCO_3^-$; $\Delta G^{0'}$ = -31.0 kJ/reaction). Moreover, SRB grow faster and have a higher affinity for substrate than methanogens (lower K_s and higher μ_{max}), enabling SRB to maintain competitive advantages (Yuan et al., 2020). Despite substrate competition, the produced sulfides during sulfate reduction are toxic to anaerobic microbes in AD, especially methanogens (Zhang et al., 2022c). Free H_2S, the most toxic sulfide species, can diffuse into the cell membrane, decrosslink the polypeptide chain and denature proteins (Wu et al., 2018). Although certain methods, such as alkaline addition, metal ion precipitation, SRB inhibition, etc., can help decrease the sulfide levels, high operational costs hinder their application in long-term and large-scale operations (Jung et al., 2022).

Microbial electrolysis cell-assisted anaerobic digestion (MEC-AD) is a novel biotechnology,

[5] A version of this chapter has been submitted to *Chemical Engineering Journal*.

capable of enhancing methane production and system resilience (Huang et al., 2022b). Several studies have been conducted towards bioelectrochemical sulfate reduction, focusing on electrochemical aspects, sulfate removal efficiency and the fate of sulfate (Gacitúa et al., 2018; Huang et al., 2022a; Shi et al., 2023). For instance, Huang et al. (2022a) observed higher SO_4^{2-} removal and S^0 recovery in the single-chamber bioelectrochemical system (BES) than that in the dual-chamber BES. Gacitúa et al. (2018) investigated the effects of applied potential and inoculum type on bioelectrochemical sulfate reduction. However, to the best of the authors' knowledge, only two studies have been conducted to explore the potential of MEC-AD systems in treating sulfate-rich wastewater, with a primary focus on methane production (Yuan et al., 2020; Yuan et al., 2022). These studies reported that the MEC-AD reactor could create weak alkaline environments to significantly decrease the free H_2S levels (pKa 7.0), thus enhancing methane production under sulfate-rich conditions (Yuan et al., 2020; Yuan et al., 2022).

Influent COD/SO_4^{2-} ratio was widely reported as a key parameter influencing the relationships between SRB and methanogens, thereby influencing the reactor performance (Gao et al., 2020a; Lu et al., 2016). A previous study documented a 49% reduction in methane yield from antibiotic biowaste when the COD/SO_4^{2-} ratio decreased to ≤ 1.5 (Qiang et al., 2018). Hulshoff et al. (2001) reported that system failure for methane recovery occurred at a COD/SO_4^{2-} ratio of < 10. Li et al. (2015b) reported that high methane generation and COD removal could be maintained at a COD/SO_4^{2-} ratio of 8, but a ratio of 1.5 inhibited methanogenesis. However, no study has been performed on investigating the performance of MEC-AD systems under different COD/SO_4^{2-} ratios. Moreover, an in-depth analysis of microbial communities and their metabolic pathways is required to understand the potential interactions between different microbial groups in a complex mixed-cultured system.

In light of these research gaps, the goal of this study is to systematically assess the performance of a MEC-AD reactor at different COD/SO_4^{2-} ratios. A comprehensive investigation was performed into the microbial communities, metabolic pathways, and genetic adaptations

involved in sulfur metabolism. This study aims to provide deep insights into developing more robust electro-assisted anaerobic bioreactors under sulfate-rich conditions.

6.2 Materials and methods

6.2.1 Bioreactor setup and operation

A single chamber MEC-AD reactor was fabricated using plexiglass tubes, with a total volume of 420 mL and a working volume of 380 mL. The anode electrode was composed of high-density carbon fibers (2293-A, 24A Carbon Fiber, Fibre Glass Development Corp., Ohio, USA) affixed to a stainless-steel frame, while the cathode electrode consisted of a stainless-steel mesh (304, McMaster-CARR, USA). Prior to usage, the carbon fibers underwent a pretreatment process as documented by Dhar et al. (2013). An Ag/AgCl reference electrode (MF-2052, Bioanalytical System Inc., Indiana, USA), was inserted into the reactor at a close distance (~ 1 cm) to the anode electrode. The anode potential was fixed at -0.2V vs. standard hydrogen electrode (SHE) using a potentiostat system (Squidstat Prime, Admiral Instruments, Tempe, AZ, USA). A control reactor, identical in structure and equipped with the same electrodes, was also fabricated but operated without an applied potential. The reactors were continuously mixed using magnetic stirrers throughout the operation.

In the beginning, each reactor was inoculated with a mixture comprising 30 mL of sludge from a full-scale anaerobic digester operated with municipal sludge, and 30 mL of effluent from a well-established MEC reactor operated with 25 mM acetate medium. The reactors were fed with synthetic glucose medium (2048 ± 56 mg COD/L) with composition as following: glucose 1.87 g/L, $NaHCO_3$ 2 g/L, $NaH_2PO_4 \cdot H_2O$ 0.15 g/L, NH_4Cl 0.36 g/L, $MgCl_2 \cdot 6H_2O$ 0.02 g/L, K_2HPO_4 0.03 g/L, and 1 ml/L of a trace element solution. The detailed composition of the trace element solution was previously documented by Dhar et al. (2013). The reactors were operated in a semi-continuous mode at room temperature (20.0 ± 0.5 °C), maintaining an organic loading rate (OLR) of 1 g COD/L-d and a hydraulic retention time (HRT) of 2 days. The long-term (200 days)

performance of the reactors was investigated at varying COD/SO_4^{2-} ratios, which were 0 (Stage 1, no SO_4^{2-}), 20 (Stage 2, 100 mg/L SO_4^{2-}), 10 (Stage 3, 200 mg/L SO_4^{2-}), 5 (Stage 3, 400 mg/L SO_4^{2-}), 1 (Stage 3, 2000 mg/L SO_4^{2-}). The sulfate source was provided by Na_2SO_4. At the end of Stage 5, the MEC-AD reactor was operated under open circuit conditions for 5 HRTs to evaluate the potential of electrochemical sulfide oxidation.

6.2.2 Specific methanogenic activity (SMA)

After the completion of each stage, sludge samples were taken from the biofilms on the anode, cathode, and electrodes in the control reactor. Batch assays were performed in duplicate to determine the specific methanogenic activity (SMA) of the sludge, which signifies the maximum achievable rate of biomethane generation through hydrogenotrophic or acetoclastic methanogenesis. The tests were performed in 38 mL serum bottles following the method documented by Huang et al. (2023). To determine SMA on H_2 + CO_2, 1 mL sludge and 14 mL deionized water were added into the serum bottles, which were then flushed with H_2 + CO_2 gas (molar ratio 4:1). To determine SMA on acetate, 1 mL sludge and 14 mL sodium acetate medium were added into the serum bottles with a final COD concentration of 1 g/L. The bottles were then flushed with N_2 gas. All serum bottles were sealed immediately after gas flushing and were incubated in a dark incubator at 120 rpm and 20 ℃.

6.2.3 Analytical methods

The concentrations of total COD (TCOD), soluble COD (SCOD) and volatile suspended solids (VSS) were determined following the standard methods (APHA, 2005). Hach sulfide reagent sets (5 to 800 μg/L S^{2-}, methylene blue method; Hach Co., Loveland, Colorado, USA) were used to measure total sulfide concentrations. The sulfate concentrations were measured using Hach sulfate reagent powder pillows (2 – 70 mg/L SO_4^{2-}, Hach Method 8051; Hach Co., Loveland, Colorado, USA). The volatile fatty acids (VFAs) concentrations were determined by ionic chromatography (IC) system (DIONEX ICS-2100, Thermo Fisher, USA). The biogas composition in the gas bag was determined using a 7890B gas chromatograph (Agilent Technologies, Santa Clara, USA).

The gas pressure of serum bottles was determined by a pressure meter (GMH3151, Greisinger, Regenstauf, Germany). The solution pH was measured with a B40PCID pH meter (VWR, SympHony). The gaseous H_2S concentration was measured using an Acrulog H_2S gas monitor (0-2000 ppm; Acrulog, Clontarf, Australia). At the steady-state period of each stage, the dissolved methane concentrations within the reactors were measured 4 times per stage in triplicate, following the methods outlined by Zhang et al. (2020b).

6.2.4 DNA extraction, sequencing, and bioinformatics analysis

At the end of each stage, biofilms were sampled from around 15 different locations on each electrode. The genomic DNA extraction was performed using DNeasy PowerSoil Kit (QIAGEN, Hilden, Germany) according to the manufacturer's protocol. NanoDrop One (ThermoFisher, Waltham, MA) was utilized to determine DNA concentration and quality, followed by DNA storage at -80 ℃ until further sequencing. The Illumina Miseq platform was employed for 16S rRNA gene sequencing using universal primer-pair 515F/806R at the Research and Testing Laboratory (Lubbock, TX, USA). The processing of raw sequencing data was conducted through the Qiime2 pipeline (Hall & Beiko, 2018). After using the DADA2 algorithm to eliminate chimeras and low-quality sequences (Callahan et al., 2016), taxonomy was assigned using Silva 138 SSU reference database with a 99% similarity threshold (Yilmaz et al., 2014). Phylogenetic Investigation of Communities by Reconstruction of Unobserved States (PICRUSt) (Langille et al., 2013) was utilized to predict the functional genes from 16S rRNA data. The metabolic functional shifts of the microbial community in response to different COD/SO_4^{2-} ratios have been performed using the predicted metagenomes and the Kyoto Encyclopedia of Genes and Genomes (KEGG) reference database (Kanehisa et al., 2012). A single-factor analysis of variance (ANOVA) was conducted utilizing Microsoft Excel®. Statistical significance was determined if a *p*-value was below 0.05.

6.2.5 Calculations

Methane yield was calculated using Eq. (1) (Huang et al., 2021):

$$\text{Methane yield (\%)} = \frac{COD_{CH4}}{COD_{input}} * 100 \quad (1)$$

where COD_{CH4} refers to the COD equivalent of generated methane (mg); COD_{input} represents the total COD input (mg).

Unionized H_2S concentration was calculated based on the measured total sulfide concentration using Eq. (2) (Yuan et al., 2020):

$$\text{Unionized } H_2S = \frac{Total\ sulfide}{(1+\frac{K_1}{10^{-pH}})} \quad (2)$$

where K_1 is the first ionization constant of H_2S at 20 ℃, which can be calculated based on the first ionization constant of H_2S (9.1×10^{-8}) at 25 ℃ and Van't Hoff Equation, considering the temperature dependence of equilibrium constant (Sawyer et al., 2003).

6.3 Results and discussion

6.3.1 SO_4^{2-} reduction and sulfur balance

The effluent sulfate concentrations are presented in Table 6.1. Overall, both reactors demonstrated high sulfate removal efficiencies (> 99%) through Stage 1 to Stage 4, with effluent sulfate concentrations consistently < 3.0 mg/L. Nonetheless, when the COD/SO_4^{2-} ratio reduced to 1 in Stage 5, a substantial quantity of sulfate remained unreduced and was consequently discharged with the effluent. The measured effluent sulfate concentrations in Stage 5 were 1237.1 ± 43.3 mg/L in the MEC-AD reactor and 1271.4 ± 39.8 mg/L in the control reactor.

The sulfur mass balance and unionized H_2S concentrations in each stage are illustrated in Figure 6.1. Given the minimal addition of metal elements to the substrate medium (Section 2.1), the sulfur content in the form of insoluble metal sulfide was negligible. Thus, sulfur is primarily presented in four forms: SO_4^{2-}, ionized HS^-, unionized H_2S, and gaseous H_2S, among which unionized H_2S is the most toxic species. The proportion of gaseous H_2S slightly varied across different stages and reactors, ranging from 2.9 – 4.2%. The proportion of unionized H_2S in the total sulfide is contingent upon the pH of the solution (pKa 7.0). As shown in Table 6.1, the pH of

the MEC-AD reactor consistently declined from Stage 1 (7.28 ± 0.03) to Stage 4 (7.10 ± 0.02), potentially attributed to the organic acid accumulation. However, the pH rebounded to 7.22 ± 0.02 in Stage 5, which could be related to the alkalinity (HCO_3^-) generation during the sulfate reduction process (Lu et al., 2016). The pH in the control reactor presented a similar trend. Overall, the MEC-AD reactor had a higher pH than the control reactor in each stage ($p < 0.05$), which can be attributed to the rapid oxidation of organic acids at the anode and proton (H^+) reduction along with alkali (OH^-) generation at the cathode (Yuan et al., 2020). Therefore, although comparable sulfate reduction and total sulfide generation (Table 6.1) were observed in the two reactors from Stage 1 to 4, the MEC-AD reactor exhibited relatively lower unionized H_2S proportion (35.2 – 42.6%) and concentration (11.7 – 56.8 mg/L) than the control reactor (37.9 – 45.6%; 12.6 – 58.3 mg/L). Yuan et al. (2020) also reported MEC-AD systems could create weak alkaline conditions, reducing the concentration of unionized H_2S and mitigating H_2S inhibition under sulfate-rich conditions. In Stage 5, the unionized H_2S proportion significantly decreased to 10.1 ± 0.8% in the MEC-AD and 12.3 ± 0.9% in the control reactor, while effluent sulfate proportions increased to over 60%. However, due to the substantial increment in sulfur input, the unionized H_2S concentration significantly increased to 67.3 ± 2.1 and 81.7 ± 1.6 mg/L, respectively.

Interestingly, a more pronounced discrepancy in the sulfur balance (89.9%) between total sulfur measured and total sulfur input was observed in Stage 5 in the MEC-AD reactor, in comparison to other stages (> 95%, $p < 0.05$). This observation suggested the existence of alternate sulfur sinks in the MEC-AD reactor under low COD/SO_4^{2-} ratios. For instance, the missing sulfide might undergo electrochemical oxidation to other forms of sulfur, since this phenomenon was not observed in the control reactor.

To investigate the fate of the missing sulfides, targeted experiments were performed by stopping the potentiostat and operating the MEC-AD reactor under open circuit conditions for 5 HRTs. As anticipated, the total sulfide concentration increased significantly from 169.0 ± 23.0 to 229.6 ± 29.8 mg/L ($p < 0.05$) after switching to open circuit conditions. Subsequently, the sulfur

balance percentage was increased to 98.3 ± 1.9%, which was the highest among all stages. Previous studies documented that sulfide oxidation can generate over 30 different sulfur species, subject to specific reaction conditions and redox potentials (Ateya et al., 2003; Pikaar et al., 2011). Specifically, under standard conditions, sulfide can be oxidized to element sulfur (S^0) at potentials exceeding -0.274 V vs. SHE, while elevating the potential beyond this point enables further oxidation of S^0 to more oxidized sulfur species, such as sulfite (SO_3^{2-}) and sulfate (SO_4^{2-}) (Rabaey et al., 2006). In this study, the anode potential of -0.2V vs. SHE met the minimum requirements for sulfide oxidation. However, in addition to redox potential, sulfide level is also a critical parameter determining the progress of the sulfide oxidation reactions ($HS^- + H^+ \rightarrow S^0 + H^+ + 2e^-$; $\Delta G^{0'}$ = -51.5 kJ), which explains higher sulfide oxidation observed in Stage 5. Thermodynamic calculations indicated that the threshold of electrogenic oxidation of sulfide at -0.2V vs. SHE was around 3.2×10^{-3} mol of sulfide (Zhao et al., 2020). However, the necessary anode potential and sulfide level for sulfide oxidation could only be roughly estimated since the reactions are not dictated by thermodynamics alone (Rabaey et al., 2006; Zhao et al., 2020). Furthermore, because of the heterogeneous deposition of the element sulfur in the reactor and the potential presence of other oxidized sulfur species, an accurate sulfur mass balance is challenging to establish. Future research is required to establish more rigorous electrochemical limits and achieve a comprehensive understanding of the sulfur cycle in bioelectrochemical systems.

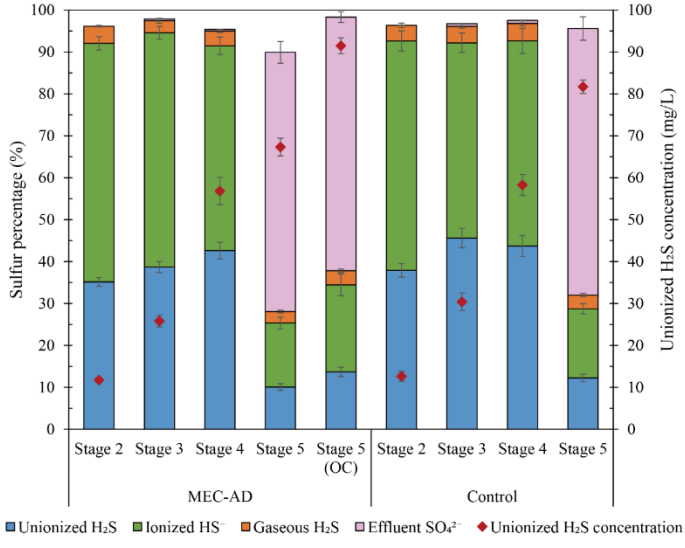

Figure 6.1 Sulfur balance and unionized H_2S concentration. 'OC' represents 'open circuit'.

Table 6.1 Methane production and effluent qualities of the reactors during steady-state period.

	Unit	Control					MEC-AD				
		Stage 1	Stage 2	Stage 3	Stage 4	Stage 5	Stage 1	Stage 2	Stage 3	Stage 4	Stage 5
Methane yield (dissolved)	%	4.4 ± 0.6	4.6 ± 0.8	4.2 ± 0.4	3.8 ± 0.7	3.7 ± 0.5	4.7 ± 0.6	4.5 ± 0.5	4.3 ± 0.6	4.4 ± 0.8	3.9 ±0.4
Methane yield (gas)	%	65.2 ± 2.3	60.2 ± 1.4	48.1 ± 3.9	48.5 ± 3.3	29.1 ± 2.2	74.0 ± 2.4	75.0 ± 1.6	63.0 ± 1.2	60.3 ± 2.1	52.4 ± 2.0
pH		7.24 ± 0.04	7.20 ± 0.03	7.05 ± 0.02	7.09 ± 0.02	7.17 ± 0.03	7.28 ± 0.03	7.25 ± 0.03	7.20 ± 0.02	7.10 ± 0.02	7.22 ± 0.02
Sulfate	mg/L	0.0 ± 0.0	0.0 ± 0.0	1.2 ± 0.1	2.8 ± 0.3	1271.4 ± 39.8	0.0 ± 0.0	0.0 ± 0.0	0.8 ± 0.1	1.6 ± 0.1	1237.1 ± 43.3
Total sulfide	mg/L	0.0 ± 0.0	30.9 ± 3.8	61.4 ± 5.0	123.5 ± 13.3	191.7 ± 23.0	0.0 ± 0.0	30.7 ± 4.2	63.1 ± 5.2	121.9 ± 9.2	169.0 ± 14.7
Total VFAs	mg/L	243.1 ± 12.3	219.3 ± 13.3	399.4 ± 20.4	371.3 ± 16.8	480 ± 26.6	77.5 ± 3.5	64.6 ± 4.5	154.9 ± 8.0	163.5 ± 10.0	143.9 ± 8.7

6.3.2 Methane production

The methane yield (%) in terms of total COD input is shown in Table 6.1. For low-strength feedstocks, the dissolved methane is an essential part of total methane production, due to higher methane solubility at lower temperatures (Huang et al., 2022c). The dissolved methane concentration in the reactors ranged from 74.6 to 93.9 mg CH_4-COD/L, accounting for 3.7 – 4.7% of the total COD input. The MEC-AD reactor achieved a total methane yield of 78.7 ± 2.3% in Stage 1 (Figure 6.3C), which slightly increased to 79.5 ± 2.8% in Stage 2 ($p > 0.05$). However, starting from Stage 3, the methane yield in the MEC-AD reactor consistently declined with the reduced COD/SO_4^{2-} ratio, ultimately dropping to 56.2 ± 2.0% in Stage 5. In comparison, the control reactor exhibited significantly lower methane yield than the MEC-AD reactor in each stage ($p < 0.05$), with a more substantial decrease from 69.6 ± 3.6% in Stage 1 to 32.8 ± 1.5% in Stage 5.

Determining the specific biological activities of core microbial consortia, particularly methanogens, is crucial for monitoring AD performance and microbial community development. In this study, SMA was evaluated for biofilms on each electrode in both reactors (Figure 6.2). The anode sludge exhibited the highest SMA (acetate), while the cathode sludge demonstrated overwhelmingly highest SMA (H_2 + CO_2). Overall, both reactors showed a decreasing trend in SMA (acetate) and SMA (H_2 + CO_2) with reduced COD/SO_4^{2-} ratios. However, there was an exception where the anode sludge showed an increase ($p < 0.05$) in SMA (acetate) from 134.7 ± 6.7 (Stage 1) to 144.5 ± 8.0 mg COD/g VSS/d (Stage 2), whilst the cathode sludge exhibited a significant increase ($p < 0.05$) in SMA (H_2 + CO_2) from 87.4 ± 2.9 (Stage 1) to 97.8 ± 4.2 mg COD/g VSS/d (Stage 3). In this study, glucose was first fermented into ethanol and VFAs, which could be further utilized by SRB, leading to the production of acetate and H_2 (Lu et al., 2016). Therefore, the acetate- and hydrogen-utilizing methanogens could benefit from the proliferation of SRB in the presence of low sulfate concentrations. These syntrophic partnerships between SRB and methanogens explained the SMA increase in the MEC-AD reactor during Stage 2 and 3. The increase in SMA (H_2 + CO_2) but decrease in SMA (acetate) during Stage 3 also suggested the

superior robustness of hydrogenotrophic methanogens compared to acetoclastic methanogens under sulfide toxicity, which aligns with the findings of Zhang et al. (2022c). For sludge from the control reactor, the consistent decrease in both SMA (acetate) and SMA (H_2 + CO_2) could be attributed to competition between SRB and methanogens for substrates, as well as the inhibitory effects of sulfide toxicity.

Previous studies have reported significant discrepancies regarding the threshold for inhibitory concentrations of unionized free H_2S. The reported half-maximal inhibitory concentrations (IC_{50}) of free H_2S widely ranged from 50 – 380 mg H_2S-S/L (Hu et al., 2015; Yamaguchi et al., 1999). Notably, despite the higher concentration of free H_2S observed in the MEC-AD reactor during Stage 5 (67.3 ± 2.1 mg/L) compared to the control reactor during Stage 4 (58.3 ± 2.5 mg/L), the MEC-AD reactor exhibited higher methane yield and SMA. These results implicated that the superior performance of the MEC-AD reactor could not only be attributed to higher pH and lower sulfide concentrations in the system, but more importantly, higher tolerance of microbiome to sulfide toxicity.

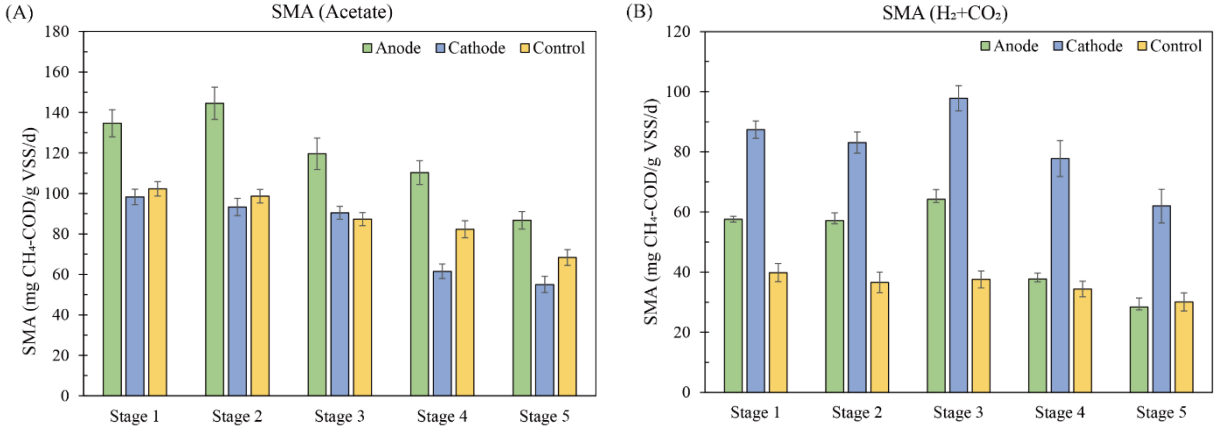

Figure 6.2 Specific methanogenic activity (SMA) of sludge from different electrodes across different stages. (A) SMA (Acetate); (B) SMA (H_2 + CO_2).

6.3.3 COD removal and balance

The temporal changes of effluent TCOD and SCOD in the reactors are depicted in Figure 6.3A. Throughout the operation, the MEC-AD reactor consistently maintained significantly ($p < 0.05$)

lower effluent SCOD levels (120.0 ± 21.2 mg/L – 303.0 ± 13.8 mg/L) compared to the control reactor (377.8 ± 21.7 mg/L – 660.5 ± 34.0 mg/L). However, substantial disparities between TCOD and SCOD were observed in both reactors during Stage 4 and 5. For instance, in Stage 5, the effluent SCOD was observed at 211.2 ± 13.1 in the MEC-AD and 660.5 ± 34.0 mg/L in the control reactor, while the effluent TCOD increased to 504.1 ± 30.9 and 898.7 ± 66.5 mg/L, respectively. The presence of particulate COD in the effluent can be attributed to biomass washout caused by long-term operation or the existence of toxic or inhibitory substances, such as free H_2S (Luis Campos et al., 2001).

As illustrated in Figure 6.3B, the control reactor exhibited considerably higher total VFA concentrations (219.3 - 480.0 mg/L) compared to the MEC-AD reactor (64.6 - 163.5 mg/L). In the MEC-AD reactor, a remarkable decrease in propionate concentrations from ~50 mg/L (Stage 1 & 2) to ~20 mg/L (Stage 3 - 5) was observed, along with an increase in acetate concentrations. Such a pattern was most likely attributed to the activity of incomplete oxidizing SRB, which have a high affinity for propionate (Kiyuna et al., 2017). Moreover, the thermodynamics of propionate oxidation reactions mediated by SRB ($C_3H_5O_2^- + 0.75SO_4^{2-} \rightarrow 0.75HS^- + HCO_3^- + 0.25H^+ + CH_3COO^-$; $\Delta G^{0'} = -37.7$ kJ/mol) are more favorable than reactions carried out by syntrophic acetogens ($C_3H_5O_2^- + 2H_2O \rightarrow CH_3COO^- + 3H_2 + CO_2$; $\Delta G^{0'} = +76.2$ kJ/mol) (Kiyuna et al., 2017). In the control reactor, a slight gradual decrease in the propionate concentration was also observed from Stage 1 (89.8 ± 4.3 mg/L) to Stage 5 (65.5 ± 6.3 mg/L), with a dramatical increase in acetate concentrations starting from Stage 3. This observation could probably be attributed to the inhibited acetoclastic methanogens and the lack of hydrogenotrophic methanogens (discussed in Section 3.4.2), which could scavenge H_2 and acetate and thermodynamically drive propionate oxidation reactions.

Qualitative analysis of the electron flow is critical in evaluating the competition between methanogens and SRB. Figure 6.3C shows the substrate electron distribution (based on SCOD) in the reactors. As mentioned earlier, the majority of the COD was transformed into methane

throughout all stages in the MEC-AD reactor (56.2 – 79.5%), while methane yield in the control reactor was much lower (32.8 – 64.8%), with a large proportion of COD discharged with the effluent (18.9 – 33.0%). The COD consumed by sulfate reduction was comparable between the reactors and increased up to ~25% with the reduced COD/SO_4^{2-} ratios. A consistent increase in electron flow to SRB accompanied by a decrease in electron flow to methanogens was observed in both reactors, indicating intense substrate competition. However, SRB did not outcompete methanogens in either reactor, as evidenced by < 50% electron flow to SRB throughout the operation. Nonetheless, previous studies stated that the predominant electron consumers switched from methanogens to SRB at low COD/SO_4^{2-} ratios. For instance, Wu et al. (2018) reported that the electron flow to SRB increased to 70.5% at a COD/SO_4^{2-} ratio of 1.0 in a digester operated with ethanol and acetate for a long term. Jeong et al. (2009) found that SRB suppressed methanogens in terms of electron utilization at a COD/SO_4^{2-} ratio of 5 during anaerobic sludge degradation. Lu et al. (2016) documented that SRB began to outcompete methanogens for starch when the COD/SO_4^{2-} ratio dropped below 2. In contrast, other studies also reported that methanogens kept predominant in terms of electron consumption even at low COD/SO_4^{2-} ratios (Hu et al., 2015; O'Reilly & Colleran, 2006). It is worth noting that the complex and variable relationships between methanogens and SRB may depend not solely on COD/SO_4^{2-} ratios but also on multiple factors, such as HRT, pH gradient, inoculum, substrate types, the site where methanogenesis/sulfidogenesis occurs, and the diffusion and transportation of substrates and sulfur compounds (Lu et al., 2016). Furthermore, the conductive carbon fiber electrode used in both reactors could also contribute to the superior electron flow to methanogens, since direct interspecies electron transfer (DIET) mediated by conductive materials could enhance the activities of methanogens and reduce electron capture for sulfate reduction (Li et al., 2017; Zhang et al., 2022c).

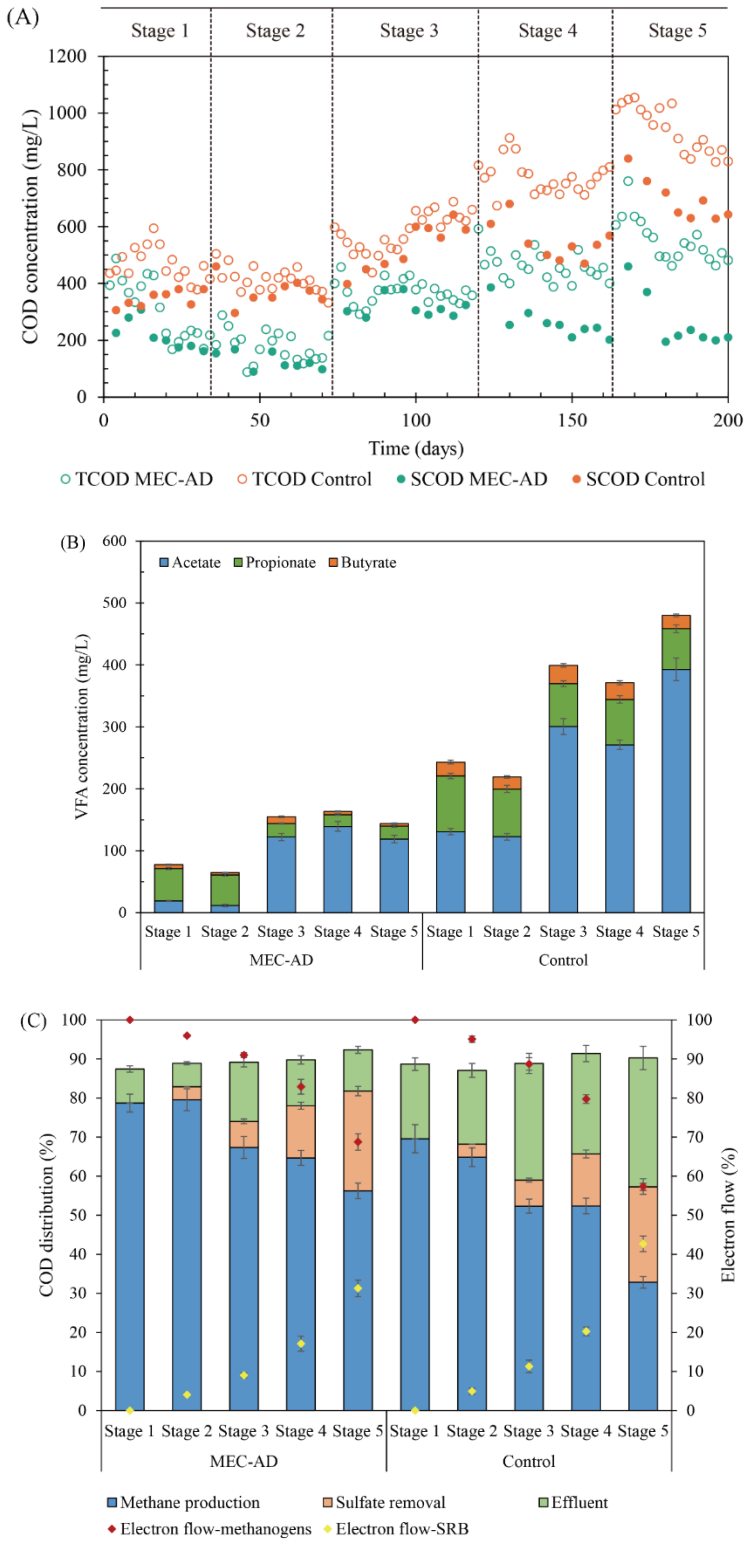

Figure 6.3 (A) TCOD and SCOD concentrations in the effluent during long-term operation; (B) VFA concentrations in the effluent; (C) Distribution of initial COD and electron flows to SRB and methanogens.

6.3.4 Microbial community

6.3.4.1 Bacterial communities

Figure 6.4 depicts the dynamic changes in the relative abundance of the top 10 most prevalent bacteria genera within each sample, among which three incomplete oxidizing SRB genera (i.e., *Desulfomicrobium*, *Desulfovibrio*, *Desulfobulbus*) were observed. No complete oxidizing SRB, which degrades acetate to CO_2 (Muyzer & Stams, 2008), was detected in this study. Previous studies reported that only a limited number of SRB species belong to complete oxidizers, including *Desulfotomaculum* and *Desulfobacter*, which are typically outcompeted by incomplete oxidizers in terms of specific growth rate when excessive sulfate is present (Zeng et al., 2019). Consistent growth patterns of *Desulfomicrobium* were observed on electrodes in both reactors, displaying an increasing trend from Stage 1 (0.4 – 0.7%) to Stage 3 (1.4 – 2.7%), followed by a subsequent decrease to ~ 0.5% in Stage 5. Likewise, the abundance of *Desulfovibrio* in sludge samples from all electrodes kept increasing, reaching its peak in Stage 4, and subsequently decreasing in Stage 5. *Desulfomicrobium* and *Desulfovibrio* can incompletely oxidize organic carbon to acetate, utilizing sulfate as the electron acceptor (Lu et al., 2017). Under sulfate limited conditions, many *Desulfovibrio* and *Desulfomicrobium* species can also ferment pyruvate, lactate and ethanol to form acetate, CO_2 and H_2 as products, but only when H_2 is efficiently removed by hydrogenotrophic methanogens (Muyzer & Stams, 2008). These syntrophic relationships between SRB and methanogens are supported by the enhanced SMA (both acetate and $H_2 + CO_2$) in Stage 2 and 3. Notably, the effluent sulfate concentration is very low (< 3.0 mg/L) from Stage 1 to 4, which may trigger the metabolic function shift from sulfate reduction to fermentation for *Desulfomicrobium* and *Desulfovibrio*. *Desulfobulbus*, the most abundant SRB genus detected, exhibited its highest abundance (3.0 – 5.0%) in Stages 2 and 3 across all samples. *Desulfobulbus* is crucial for the rapid degradation of propionate to acetate through the pyruvate and propanoate metabolic pathway (Zeng et al., 2019), which aligns with the low propionate levels observed in the reactors. The enrichment of different SRB genera in different stages indicated variations in their sulfide tolerance levels. The decrease in their abundance in Stage 5 indicated that they were

all inhibited at a COD/SO_4^{2-} of 1. It is important to note that sulfide can also inhibit the sulfidogenic activity of SRB. However, similar to methanogens, the reported sensitivity of SRB to sulfide toxicity is contradictory and depends on multiple factors (Lopes et al., 2007).

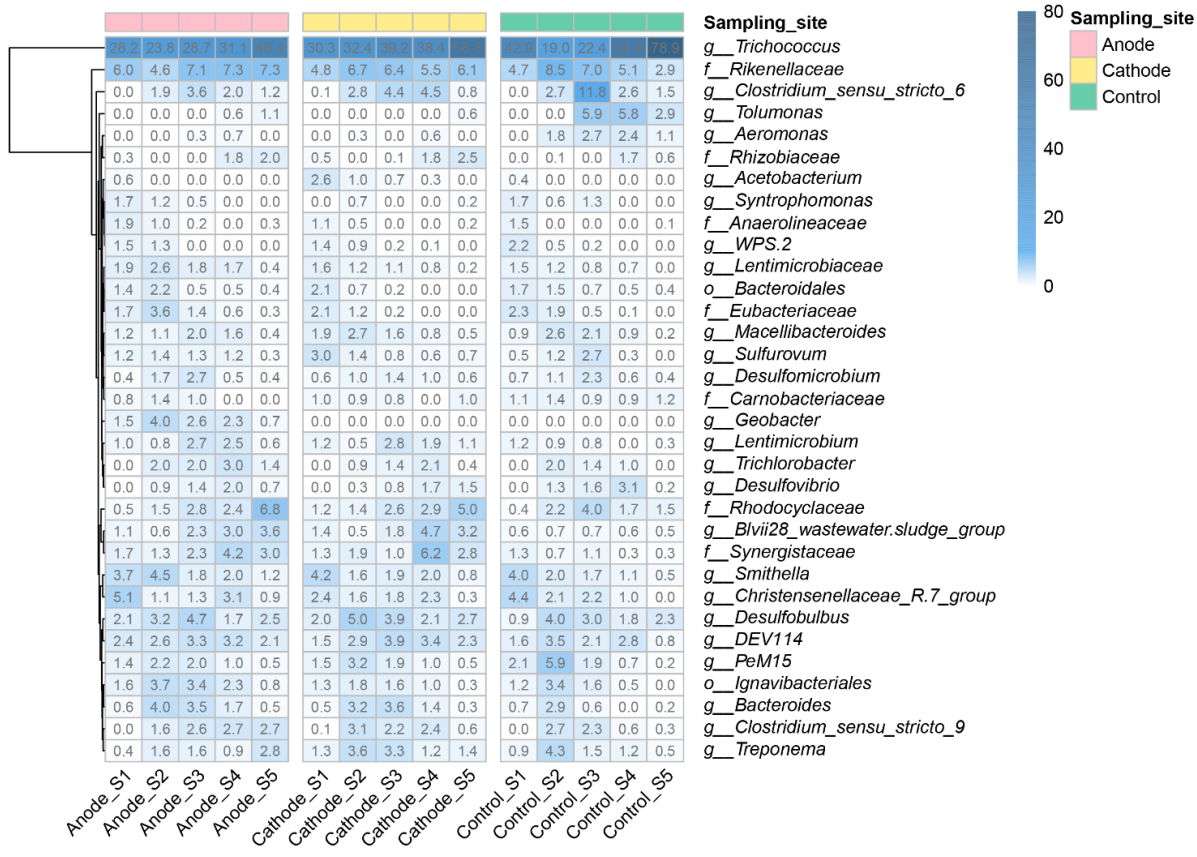

Figure 6.4 Relative abundances of 10 most abundant bacterial genera in each sample. Unidentified genera were named at family (*f__*), or order (*o_*) level. Numbers are relative abundances (%) of genera. 'S2' - 'S5' represents 'Stage 2' - 'Stage 5'.

Geobacter, an important electroactive bacterium, has garnered significant research interest in MEC-AD systems (Logan et al., 2019). In this study, *Geobacter* was only detected on the anode in the MEC-AD reactor. The sulfate addition in Stage 2, with a relatively high COD/SO_4^{2-} ratio of 20, significantly stimulated the growth of *Geobacter*, resulting in an abundance increase from 1.5% in Stage 1 to 4.0% in Stage 2. As discussed earlier, the acetate generation during sulfate reduction could contribute to the growth of *Geobacter*. However, as the COD/SO_4^{2-} ratios further reduced, the abundance of *Geobacter* started to decline, but still maintained > 2.3%, until a substantial

decrease in Stage 5 (0.7%). This decreasing trend is expected for several reasons. Firstly, SRB can compete with electroactive bacteria for substrate and space on the anode; Secondly, by serving as an electron acceptor, sulfate competes with the anode for the reducing equivalents present in organics, thus diverting electrons away from the electroactive bacteria (Zhao et al., 2020); Further, sulfide toxicity can also contribute to the decrease.

A significant abundance decrease of certain acetogens, such as *Acetobacterium*, *Syntrophomonas* and *Smithella,* was observed with the decreased COD/SO_4^{2-} ratios, even reaching undetectable levels. These acetogens play a vital role in syntrophic VFA oxidation (Li et al., 2023), but they were outcompeted by SRB in both reactors. Muyzer and Stams (2008) also documented that sulfate reducers were the predominant acetogenic bacteria under sulfate-rich conditions. The abundance of some fermentative bacteria, such as *Clostridium_sensu_stricto_9*, *Bacteroides*, *DEV114*, *PeM15*, *Treponema*, and a genus from the order *Ignavibacteriales*, sharply decreased from Stage 3 in the control reactor, probably due to sulfide inhibition. Their relatively higher abundance in the MEC-AD reactor suggested the electro-cultivated microbes may possess higher sulfide tolerance levels. *Trichococcus*, the most abundant genus across all samples, is capable of fermenting glucose and producing ethanol, lactate, formate, and acetate (Zhang et al., 2022c). Its remarkable increase from Stage 1 to Stage 5 indicated its high tolerance to sulfide toxicity. However, the overwhelming dominance of *Trichococcus* in the control reactor, reaching up to 78.9%, simplified the microbial community and may result in low resilience and system instability.

6.3.4.2 Archaeal communities

The temporal dynamics of archaeal relative abundance at both domain and genus levels are depicted in Figure 6.5A and Figure 6.5B, respectively. Overall, the archaeal abundance presented a declining trend primarily attributed to sulfide toxicity, with the highest abundance observed on the cathode in each stage. Different from the control reactor, the MEC-AD reactor displayed a significant increase in archaeal abundance during Stage 3, reaching 6.0% and 9.3% on the anode and cathode, respectively. This observation could be attributed to the establishment of a solid

syntrophic relationship between SRB and methanogens, as discussed earlier.

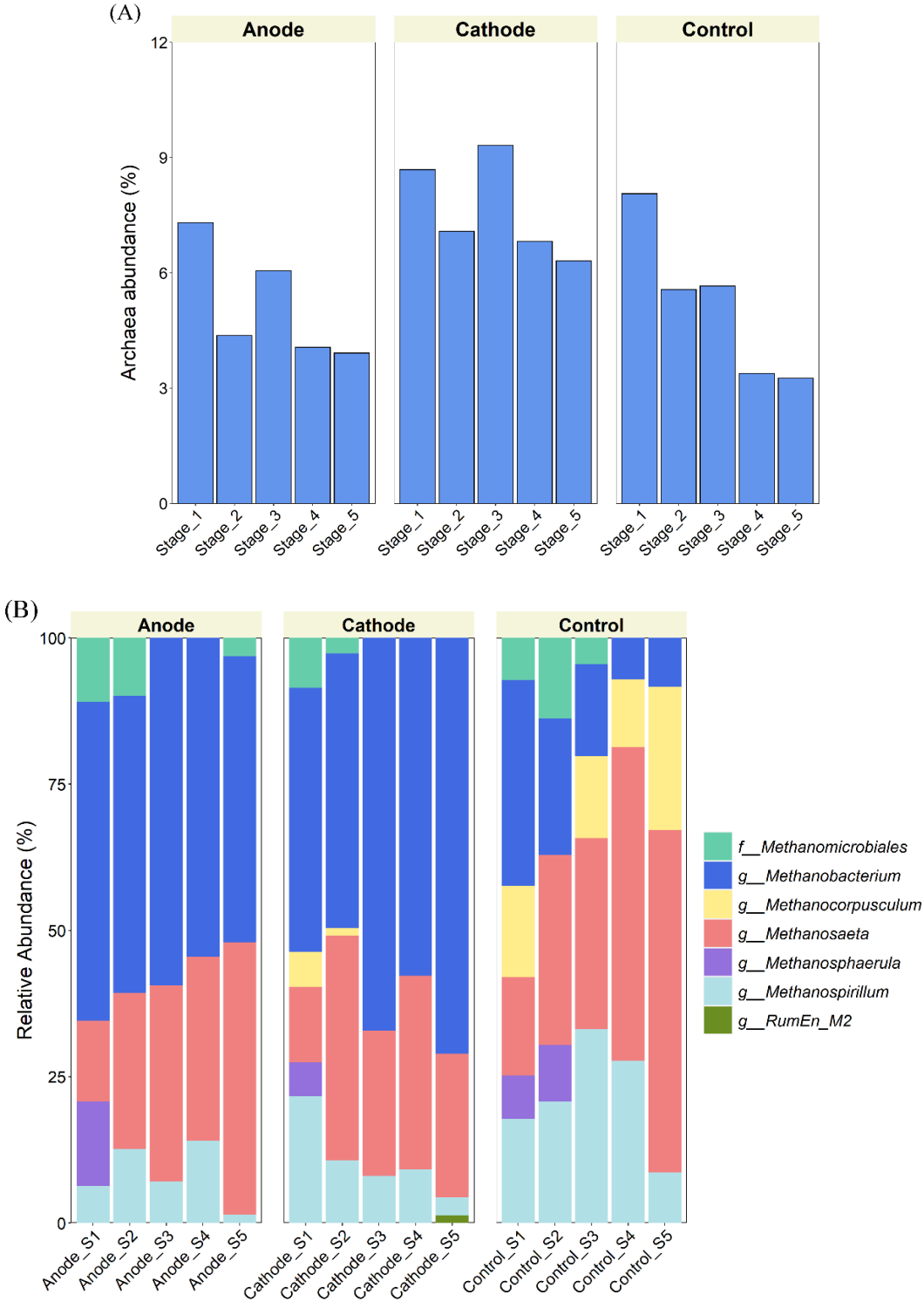

Figure 6.5 (A) Archaea abundance in each sample; (B) Relative abundances of archaeal genera in each sample. The unidentified genus was named at family (*f__*) level.

Across all COD/SO_4^{2-} ratios, hydrogenotrophic *Methanobacterium* was found to be predominant on both anode and cathode in the MEC-AD reactor. The dominance of *Methanobacterium* in MEC-AD systems has been widely reported, owing to its electrotrophic nature and higher potential for H_2 generation in such systems (Cai et al., 2016; Huang et al., 2022b). The abundance of *Methanobacterium* slightly fluctuated on the anode, while the abundance of acetoclastic *Methanosaeta* remarkably increased from 13.8% in Stage 1 to 46.5% in Stage 5. Similarly, a considerable increase in *Methanosaeta* abundance was observed in the control reactor, rising from 16.8% in Stage 1 to 58.5% in Stage 5. These observations could be ascribed to the promoted acetogenic process mediated by SRB, as well as the absence of competition between *Methanosaeta* and complete oxidizing SRB. In contrast, on the cathode, a substantial increase in the abundance of *Methanobacterium* was observed from Stage 2 (46.9%) to Stage 3 (67.2%), further reaching 71.1% in Stage 5. This enrichment can be attributed to the proliferation of incomplete oxidizing SRB (i.e., *Desulfobulbus*, *Desulfovibrio* and *Desulfomicrobium*) during these stages, which may promote H_2 production under sulfate-limited conditions, thus stimulating the growth of *Methanobacterium* through syntrophic interactions.

6.3.4.3 Metabolic function shifts

To obtain insights into the influence of difference COD/SO_4^{2-} ratios on sulfur metabolic functions in the reactors, functional genes involved in the sulfur cycle were analyzed via PICRUSt based on the KEGG database. Figure 6.6A presents the assimilatory and dissimilatory sulfate reduction pathways, along with related functional genes. During the assimilatory sulfate reduction (ASR) process, reduced sulfur is utilized for synthesizing essential sulfur-containing biomolecules; whereas during the dissimilatory sulfate reduction (DSR) process, sulfate is reduced to sulfide, providing energy for bacterial activities (Rückert, 2016). During DSR, H_2S is generated in considerably higher amounts as a byproduct instead of serving as a precursor (Rückert, 2016).

In the selected sulfur metabolism process, sulfate is initially taken up from extracellular environments into the cells, regulated by genes such as *cysP* (encoding sulfate/thiosulfate

transport system substrate-binding protein), *cysA* (encoding sulfate-transporting ATPase), and *cysUW* (encoding sulfate/thiosulfate transport system permease protein). As shown in Figure 6.6B, the abundance of these genes initially increased from Stage 1 to 3, and then significantly decreased during Stage 4 and 5 in the control reactor. In contrast, a consistent increase in gene abundance was observed on the anode with reduced COD/SO_4^{2-} ratios. These observations suggested that the sulfate reduction process was severely hindered at the initial transportation step under high sulfate/sulfide stress in the control reactor.

The ASR pathway involves four phases: sulfate to ammonium persulfate (APS) through sulfate adenylyltransferase (*cysN*, *cysD*, *sat*, *cysNC*), APS to PAPS (3′-phosphoadenosine 5′ - phosphosulfate) via sulfate adenylyltransferase (*cysNC*) or adenylylsulfate kinase (*cysC*), PAPS to sulfite by phosphoadenosine phosphosulfate reductase (*cysH*), followed by sulfite to sulfide via sulfite reductase (*sir*, *cysI, cysJ*) (Koprivova & Kopriva, 2014). A significant increase in the abundance of gene *cysN*, c*ysC, cysD*, *cysNC*, and *cysH* to 0.03 - 0.04% was observed in Stage 3 for samples from the control reactor. Similarly, enrichment of these genes was also observed on the anode in Stage 3. These results indicated that a COD/SO_4^{2-} ratio of 10 favored substantial growth of SRB with a large biosynthesis of sulfur-containing biomolecules.

The DSR pathway follows the same conversion pattern (sulfate → APS → sulfite → sulfide), but involves different genes (Figure 6.6A). Notably, during Stage 3, there was a remarkable decrease in the abundance of genes regulating adenylylsulfate reductase (*aprB*) as well as dissimilatory sulfite reductase (*dsrA*, *dsrB*) in biofilms from both anode and control reactor electrode. The decrease in DSR-related gene abundance corresponded well with the increase in ASR-related gene abundance, further demonstrating the pathway shift from DSR to ASR in Stage 3. However, the DSR-related gene abundance recovered in Stage 4, together with the decrease in ASR-related gene abundance, indicating that a COD/SO_4^{2-} ratio of 5 could not further support the growth of SRB. The pathway shift from DSR to ASR was observed on the cathode in Stage 2 rather than Stage 3, indicating that the establishment of the SRB community can occur earlier via

syntrophic growth with hydrogenotrophic methanogens. Interestingly, in the MEC-AD reactor, most of the functional genes experienced a relatively smaller decrease in Stage 5 compared to the control reactor, suggesting that enhanced SRB activities were maintained under sulfide toxicity.

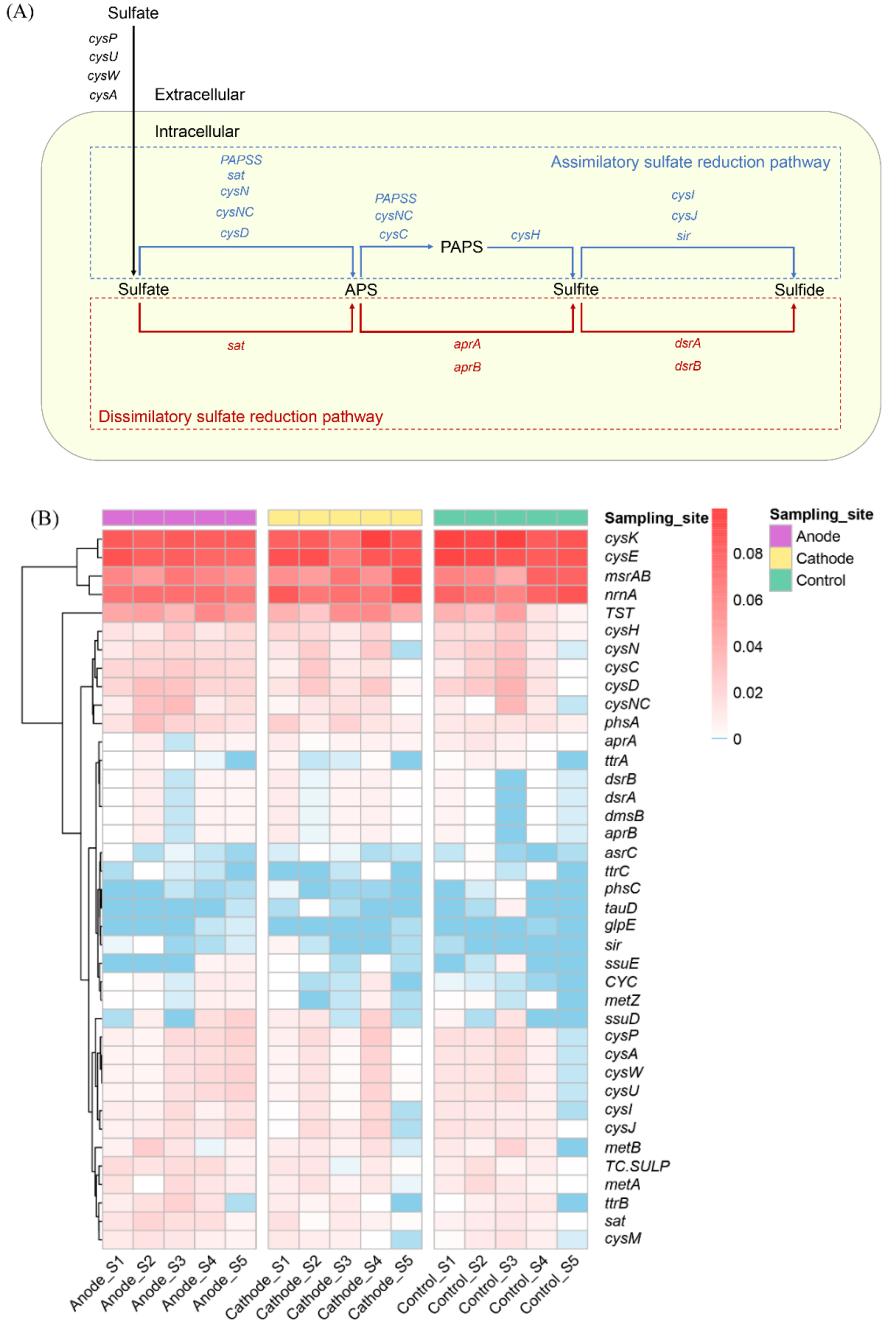

Figure 6.6 (A) Assimilatory and dissimilatory sulfate reduction pathways; (B) The dynamic changes of the abundance of functional genes in the sulfur cycle. Undetected genes are not shown in this figure.

6.3.5 Proposed mechanisms

The current results demonstrated that the MEC-AD reactor could retain higher methanogenic activity under low COD/SO_4^{2-} ratios than traditional anaerobic digesters. To better understand the complex relationships (e.g., competition and syntrophy) among SRB and other anaerobic microbes, reactions carried out by different microbial groups and their Gibbs free energy (ΔG) were provided in Table 6.2 (Dyksma et al., 2020; Hu et al., 2015; Muyzer & Stams, 2008). Here, we propose that the impacts of sulfide stress on the MEC-AD reactor were mitigated through the following mechanisms (Figure 6.7):

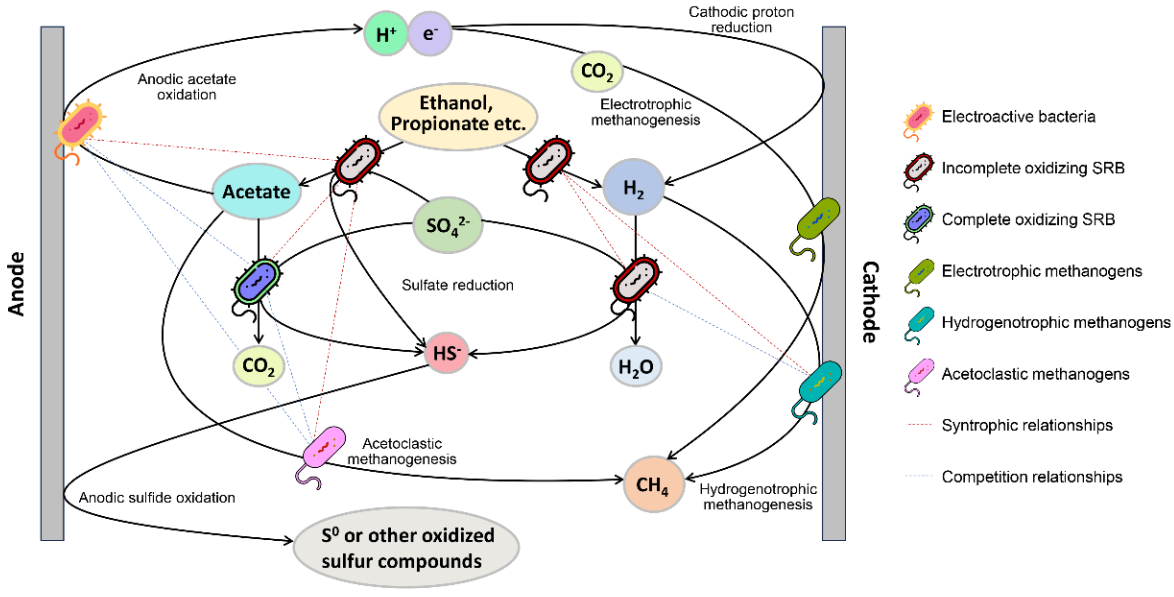

Figure 6.7 The proposed sulfate reduction pathways and microbial interactions in the MEC-AD reactor.

(i) Due to the electrochemical H_2 generation at the cathode, a large number of hydrogenotrophic methanogens were enriched in the MEC-AD reactor. Once sulfate is rapidly consumed (Stage 1 to 4), the enriched SRB can potentially shift their metabolic function towards organic fermentation, leading to the production of acetate and H_2. The promoted H_2 production further stimulated the activities and growth of hydrogenotrophic methanogens, which presented a

strong syntrophic partnership. Notably, hydrogenotrophic methanogens and SRB exhibited similar thermodynamic affinity to H_2 (Reaction (1) and (9)). Nevertheless, for the control reactor, due to the limited presence of hydrogenotrophic methanogens, the H_2-utilizing SRB had a competitive advantage, diverting electrons away from methane production.

(ii) According to Reactions (3) – (8), the incomplete oxidizing SRB can more efficiently ferment ethanol, propionate, butyrate, etc., than acetogens, producing acetate as products. The large amount of acetate production by SRB and inhibited acetoclastic methanogens resulted in the acetate accumulation in the control reactor at low COD/SO_4^{2-} ratios. Although complete oxidizing SRB were not detected in this study, they possess great advantages in competing for acetate with acetoclastic methanogens and syntrophic acetate oxidizing bacteria (Reaction (2), (10) and (11)). It is worth noting that the syntrophic acetate oxidation (Reaction (11)) is not thermodynamically favorable, whereas thermodynamic barriers can be overcome via power input in the MEC-AD systems. The acetate could be rapidly oxidized by electroactive bacteria on the anode (Zakaria et al., 2022). Meanwhile, the generated oxidation products (i.e., CO_2, H^+, e^-) could be efficiently used for hydrogenotrophic or electrotrophic methanogenesis on the cathode, which are less sensitive to sulfide toxicity (Zhang et al., 2022c).

(iii) The rapid removal of organics acids by SRB and electroactive bacteria, along with cathodic H^+ reduction, contributed to the relatively higher pH in the MEC-AD reactor, resulting in lower free H_2S levels compared to the control reactor.

(iv) Anodic oxidation of sulfide into S^0 or other oxidized sulfur compounds can be an important contributor to lower the toxic sulfide levels.

Understanding the mechanisms underlying this enhanced tolerance provides valuable insights into developing strategies for managing sulfide toxicity in anaerobic bioprocesses. The significance of the MEC-AD reactor's ability to mitigate sulfide inhibition and its higher sulfide tolerance levels extends beyond fundamental research, offering great opportunities for advancing

both future scientific investigations and engineering applications in the field of anaerobic bioprocesses.

Table 6.2 Major biochemical reactions in the reactors.

Microbes	Substrate	Reaction	$\Delta G^{0'}$ (kJ/reaction)	No.
SRB	H_2	$4H_2 + SO_4^{2-} + H^+ \rightarrow HS^- + 4H_2O$	–151.9	(1)
	Acetate	$Acetate^- + SO_4^{2-} \rightarrow 2HCO_3^- + HS^-$	–47.6	(2)
	Propionate	$Propionate^- + 0.75SO_4^{2-} \rightarrow Acetate^- + HCO_3^- + 0.75HS^- + 0.25H^+$	–37.7	(3)
	Butyrate	$Butyrate^- + 0.5SO_4^{2-} \rightarrow 2Acetate^- + 0.5HS^- + 0.5H^+$	–27.8	(4)
	Ethanol	$2Ethanol + SO_4^{2-} \rightarrow 2Acetate^- + HS^- + 2H_2O + H^+$	–132.7	(5)
Acetogens	Propionate	$Propionate^- + 3H_2O \rightarrow Acetate^- + HCO_3^- + H^+ + 3H_2$	+76.1	(6)
	Butyrate	$Butyrate^- + 2H_2O \rightarrow 2Acetate^- + H^+ + 2H_2$	+48.3	(7)
	Ethanol	$Ethanol + H_2O \rightarrow Acetate^- + H^+ + 2H_2$	+9.6	(8)
Methanogens	H_2	$4H_2 + HCO_3^- + H^+ \rightarrow CH_4 + 3H_2O$	–135.6	(9)
	Acetate	$Acetate^- + H_2O \rightarrow CH_4 + HCO_3^-$	–31.0	(10)
Syntrophic acetate oxidizing bacteria	Acetate	$Acetate^- + 4H_2O \rightarrow 2HCO_3^- + 4H_2 + H^+$	+104.6	(11)

6.3.6 Future perspectives

This study demonstrated lower free H_2S levels and superior resistance to H_2S toxicity in the MEC-AD reactor compared to the control reactor. The analysis of microbial communities and metabolic functions revealed that enriching electroactive bacteria and hydrogenotrophic methanogens within the MEC-AD reactor may foster stronger syntrophic relationships with SRB, resulting in high metabolic activities and methanogenic capacities maintained under high sulfate stress. Overall, MEC-ADs show significant advantages over traditional sulfide control technologies in AD (Table

6.3). Nevertheless, despite these foundational insights gained in this study, the effective implementation of MEC-AD systems would demand additional research and system modifications, as highlighted below:

- One notable challenge is the potential deposition and accumulation of S^0 or some metal sulfides on the electrodes over the period, potentially blocking the electrode surface and affecting the electron-transfer efficiencies. Specialized techniques, such as Energy Dispersive Spectrometry (EDS), would be useful for more detailed monitoring and analysis. Optimizing the design of electrode materials or incorporating anti-fouling coatings could effectively mitigate sulfur deposition and ensure sustained electron transfer efficiency (Kousar et al., 2021).
- Although sulfide inhibition in the MEC-AD reactor was alleviated compared to the control reactor, a notable decline in performance was still evident under intensified sulfate stress. To effectively manage sulfide toxicity, it is essential to optimize operational parameters such as pH, temperature, HRT, and applied voltages/potentials, aiming to create conditions conducive to the activity of functional microbial groups while concurrently minimizing the inhibitory impact of sulfide.

Table 6.3 Comparisons of MEC-AD systems with conventional in-situ sulfide toxicity control technologies in AD.

Technologies	Mechanisms	Advantages	Disadvantages	References
Metal sulfide precipitation	Reaction of ions with dissolved sulfide forms poorly soluble precipitates	Process simplicity; Low toxicity	Continuous chemical supply needed; Rise in salinity	(Kiilerich et al., 2017)
Chemical oxidation	Oxidation of sulfides by chemical oxidants	Process simplicity	Continuous chemical supply needed; Harmful effects on methanogens; Non-specific oxidation of organics	(Jung et al., 2022)
Adsorption	Formation of weak attractive forces (van der Waals forces) or chemical bonds between the adsorbent and adsorbate	Low-cost; Process simplicity	Restricted adsorption capacity; Non-specific adsorption of organics or ions; Periodic replacement or regeneration needed	(Ahmad et al., 2021)
Microaeration	Injecting a small amount of air or oxygen to provide electron acceptor	Enhanced hydrolysis; Possible S^0 recovery	Energy consumption; Risk of explosion; Reduced biogas purity	(Krayzelova et al., 2015)
Suppression of sulfidogenesis	Preventing sulfide generation by inhibiting the activity of SRB	Reduced H_2S formation; Mitigated competition between SRB and methanogens	Risk of harming beneficial microorganisms; By-products formation	(Jung et al., 2022)
MEC-AD	Reducing sulfide levels by elevating pH and anodic sulfide oxidation; Promoting syntrophic partnerships between SRB and other microbial groups (e.g., hydrogenotrophic methanogens and electroactive bacteria)	Possible S^0 recovery; Chemical-free and cost-effective; High energy efficiency; Improved microbial resistance to H_2S toxicity	Passivation of electrode surfaces by S^0; Regeneration of sulfide from S^0	This study

6.4 Conclusion

Under reduced COD/SO_4^{2-} ratios from 20 to 1, the MEC-AD reactor demonstrated superior performance in comparison to the control reactor, exhibiting enhanced methane production, COD removal, and specific methanogenic activity. Despite similar sulfate reduction efficiencies between the reactors, the MEC-AD reactor maintained lower sulfide concentrations due to its relatively higher pH and the occurrence of anodic sulfide oxidation. Low COD/SO_4^{2-} ratios not only intensified sulfide inhibition on methanogens and the competition between SRB and methanogens, but also hindered the activities of SRB, suggesting by the decreased abundance of SRB community and functional genes in the sulfur cycle. Competition and cooperation between SRB and other microbial groups can coexist in both reactors. However, the enrichment of electroactive bacteria and hydrogenotrophic methanogens within the MEC-AD reactor may foster stronger syntrophic relationships with SRB, resulting in a high methanogenic capacity maintained under high sulfate stress. These advancements pave the way for the development of more robust and sustainable designs of anaerobic digesters that can effectively handle sulfide-rich feedstocks and ensure stable operation.

Chapter 7. Electro-assisted Anaerobic Digestion under Sulfate-reducing Conditions: Impacts of Different Reactor Configurations[6]

7.1 Introduction

Previous research has examined the use of microbial electrolysis cell (MEC) reactors for sulfate removal, but often without incorporating them into AD processes (Luo et al., 2014; Wang et al., 2017d; Wang et al., 2017e). For instance, Luo et al. (2014) investigated the effects of different cathode potentials and feeding modes on an autotrophic biocathode designed for sulfate removal. Limited attention has been given to the performance of MEC-AD systems under sulfate-reducing conditions, with a specific focus on methane production. The findings in Chapter 6 indicate that MEC-AD reactors can mitigate sulfate inhibition by anodic sulfide oxidation, establishing mildly alkaline conditions, and promoting syntrophic partnerships between SRB and other microbial groups. However, further process optimization is required to maximize these benefits and ensure sustained effectiveness in addressing sulfate inhibition.

The configuration of the MEC-AD reactor, a critical factor influencing its performance, is determined by the presence or absence of a membrane module, resulting in two categories: single-chamber and dual-chamber MEC-AD systems. Single-chamber MEC-AD systems, lacking a membrane, exhibit reduced internal resistance, facilitate efficient material exchange between the anode and cathode chambers, and enhance biogas production efficiency (Wang et al., 2021b). In dual-chamber MEC-AD systems, ion exchange membranes assume a crucial role, acting as a pivotal interface that separates the anode and cathode chambers while permitting ion transport, thereby favoring biogas purification (Wang et al., 2021a). However, as far as the authors are aware, no prior study has systematically investigated the impacts of different reactor configurations on sulfate fate and MEC-AD efficiencies. Furthermore, a comprehensive microbial community analysis is currently lacking to underscore the microbial driving forces and potential

[6] A version of this chapter will be submitted for journal publication.

interrelationships within these complex mixed-culture systems.

In light of these research gaps, this study marks the first investigation of various MEC-AD reactor configurations operating under sulfate-reducing conditions. This investigation encompasses MEC-AD reactors with single-chamber, dual-chamber with an anion exchange membrane (AEM), and dual-chamber with a cation exchange membrane (CEM), with a performance comparison to a control reactor. A comprehensive investigation was conducted into the sulfur species distribution, methane yield, COD distribution, specific methanogenic activities, and microbial dynamics. The primary objective of this study is to provide critical insights into comprehending the inhibitory mechanisms induced by sulfate and to formulate strategies for their mitigation. This knowledge is essential for optimizing advanced MEC-AD systems for the treatment of sulfate-rich wastewater.

7.2 Materials and methods

7.2.1 Reactor setup and operation

Two single-chamber MEC-AD reactors were constructed with plexiglass tubes, featuring a total volume of 420 mL, with 365 mL as their operational capacity. The anode electrode, composed of high-density carbon fibers (2293-A, 24A Carbon Fiber, Fibre Glass Development Corp., Ohio, USA), was affixed to a stainless-steel frame, while the cathode electrode was constructed using a combination of stainless-steel mesh (304, McMaster-CARR, USA) and carbon fibers. Prior to use, the carbon fibers underwent a pretreatment process outlined by Dhar et al. (2013). An Ag/AgCl reference electrode (MF-2052, Bioanalytical System Inc., Indiana, USA) was placed in close proximity (~ 1 cm) to the anode electrode within the reactor. The anode potential was consistently maintained at -0.2V relative to the standard hydrogen electrode (SHE) through the use of a potentiostat system (Squidstat Prime, Admiral Instruments, Tempe, AZ, USA). Additionally, an identical control reactor with the same structure and electrode configuration was fabricated, but it operated without an applied potential. Magnetic stirrers were employed for continuous mixing of

the reactors throughout their operation.

Initially, all three reactors received an inoculation of 55 mL of sludge from a full-scale anaerobic digester that processed municipal sludge, along with 55 mL of effluent from a well-established MEC reactor that utilized a 25 mM acetate medium. For the enrichment process, these reactors were supplied with a synthetic glucose medium (3056 ± 108 mg COD/L) composed of the following: glucose 2.81 g/L, $NaHCO_3$ 3.43 g/L, $NaH_2PO_4 \cdot H_2O$ 0.15 g/L, NH_4Cl 0.36 g/L, $MgCl_2 \cdot 6H_2O$ 0.02 g/L, K_2HPO_4 0.03 g/L, and 1 ml/L of a trace element solution, the detailed composition of which was previously reported by Dhar et al. (2013). The reactors were operated under semi-continuous conditions at room temperature (20.0 ± 0.5 °C), maintaining an organic loading rate (OLR) of 1.5 g COD/L-d and a hydraulic retention time (HRT) of 2 days.

When the three reactors achieved steady states in terms of methane production, COD removal, and current density (if applicable), sulfate was introduced by adding Na_2SO_4 to a concentration of 300 mg/L ($COD/SO_4^{2-} = 10$). Figure 7.1 illustrates the flowchart of different reactor configurations and experimental scheme during the operation stages. In Stage 1 of the operation, two MEC reactors retained their single-chamber configuration. In Stage 2, ion-exchange membranes with a projected area of 38.5 cm^2 were introduced between the anode and cathode electrodes, transforming the single-chamber MEC-AD reactors into dual-chamber reactors, while no modification was made on the control reactor. In one MEC-AD reactor, referred to as MEC-AD1, the anode and cathode chambers were separated by an AEM (AMI-7001, Membranes International Inc., Ringwood, New Jersey, USA). In the other MEC-AD reactor, designated as MEC-AD2, the chambers were divided by a CEM (CMI-7000, Membranes International Inc., Ringwood, New Jersey, USA). The working volume of the cathodic chambers was 200 mL. These cathode chambers received a buffer solution comprising $NaHCO_3$ 5.0 g/L, NH_4Cl 0.87 g/L, K_2HPO_4 0.03 g/L, $Na_2HPO_4 \cdot 7H_2O$ 10.0 g/L, $NaH_2PO_4 \cdot H_2O$ 2.0 g/L, $MgCl_2 \cdot 6H_2O$ 0.416 g/L, and 1 ml/L of the aforementioned trace element solution, with $NaHCO_3$ serving as the source of CO_2. Magnetic stirrers were employed to ensure thorough mixing of the catholyte during operation.

The anode chamber was supplied with the previously mentioned glucose medium. The HRT of 2 days was consistently maintained for both the anolyte and catholyte. Given the utilization of a dual-chamber design in this study, the reported current density was based on the membrane's projected area, in accordance with Barua et al. (2018).

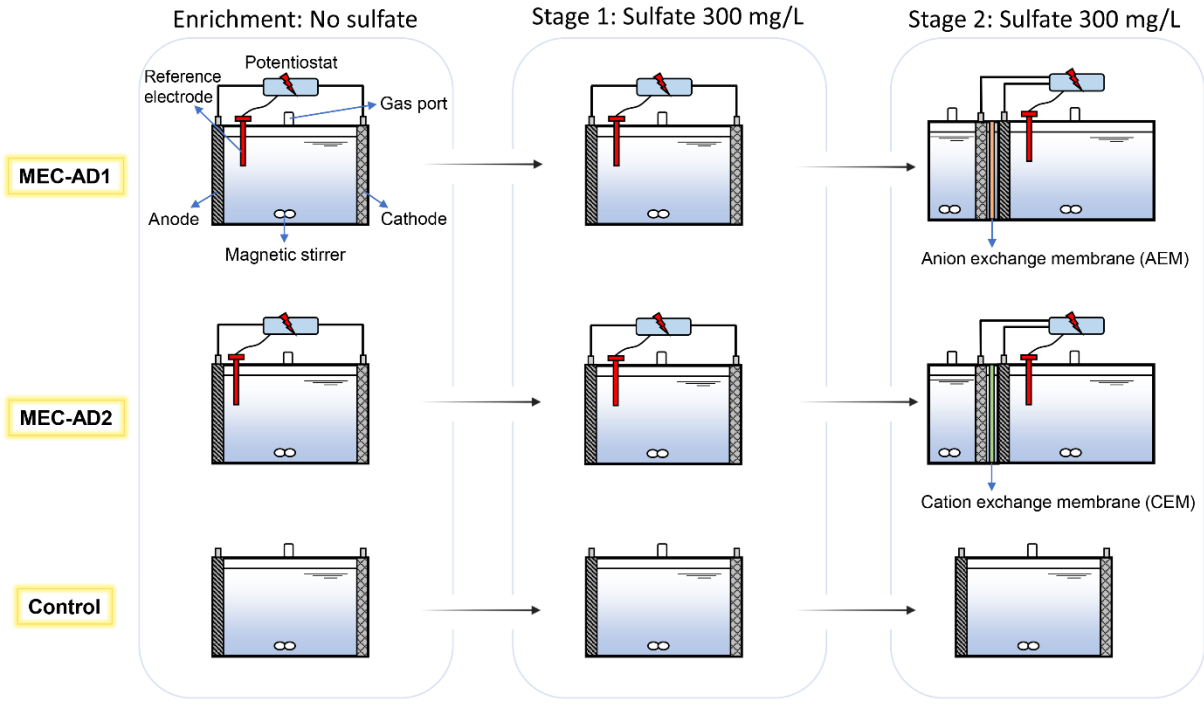

Figure 7.1 Flowchart of different reactor configurations and experimental scheme during the operation stages.

7.2.2 Specific methanogenic activity (SMA)

At the end of Stage 1 and 2, 2.5 mL of biofilm samples were collected from each electrode, including the anodes and cathodes of the MEC-AD reactors, as well as the electrodes in the control reactor. The volatile suspended solids (VSS) concentrations of the biofilm sludge were determined after sampling. Duplicate batch assays were carried out to assess the specific methanogenic activity (SMA) of the sludge. SMA serves as an indicator of the maximum achievable rate of biomethane production, either through hydrogenotrophic or acetoclastic methanogenesis. These tests were conducted in 38 mL serum bottles, following the methodology outlined in Huang et al.

(2023). For SMA determination on H_2 + CO_2, 0.5 mL of sludge and 14.5 mL of deionized water were introduced into the serum bottles, which were then purged with H_2 + CO_2 gas (in a molar ratio of 4:1). In the case of SMA using acetate, 0.5 mL of sludge and 14.5 mL of sodium acetate medium were added to the serum bottles, resulting in a final COD concentration of 1 g/L. Subsequently, the bottles were purged with N_2 gas. Following gas flushing, all serum bottles were promptly sealed and placed in a dark incubator operating at 120 rpm and 20 ℃.

7.2.3 Analytical methods

The concentrations of total chemical oxygen demand (COD) and VSS were determined in accordance with standard methods (APHA, 2005). Total sulfide concentrations were quantified using Hach sulfide reagent sets (5 - 800 μg/L S^{2-}; Hach Co., Loveland, Colorado, USA) through the methylene blue method. The measurement of sulfate concentrations was carried out using Hach sulfate reagent powder pillows (2 - 70 mg/L SO_4^{2-}; Hach Co., Loveland, Colorado, USA) following Hach Method 8051. Volatile fatty acids (VFAs) concentrations were determined via an ionic chromatography (IC) system (DIONEX ICS-2100, Thermo Fisher, USA). For the analysis of biogas composition within the gas bags, a 7890B gas chromatograph (Agilent Technologies, Santa Clara, USA) was employed. The gas pressure in the serum bottles was ascertained using a pressure meter (GMH3151, Greisinger, Regenstauf, Germany). Solution pH measurements were conducted with a B40PCID pH meter (VWR, SympHony). A H_2S gas monitor (0 - 2000 ppm; Acrulog, Clontarf, Australia) was used to quantify the gaseous H_2S concentration. During the steady-state phase of each stage, the dissolved methane concentrations in the reactors were measured five times per stage in duplicate, following the methodologies detailed by Zhang et al. (2020b).

7.2.4 DNA extraction, sequencing, and bioinformatics analysis

Upon completing Stage 1 and Stage 2, biofilm samples were collected from approximately 20 distinct locations on each electrode of the three reactors. Genomic DNA extraction was carried out using the DNeasy PowerSoil Kit (QIAGEN, Hilden, Germany), following the manufacturer's

guidelines. Subsequently, NanoDrop One (ThermoFisher, Waltham, MA) was employed to assess DNA concentration and quality, with the DNA stored at -80 ℃ until it was ready for sequencing. For 16S rRNA gene sequencing, the Illumina Miseq platform was employed, utilizing the universal primer-pair 515F/806R at the Research and Testing Laboratory (Lubbock, TX, USA). Raw sequencing data underwent processing through the Qiime2 pipeline (Hall & Beiko, 2018). After implementing the DADA2 algorithm to eliminate chimeric sequences and sequences of low quality (Callahan et al., 2016), taxonomy assignments were carried out using the Greengenes2 reference database with a 99% similarity threshold (McDonald et al., 2023). Microbial alpha and beta diversity were assessed at the genus level using the "vegan" package in R (Oksanen et al., 2010). Student's t-test was performed, utilizing Microsoft Excel®, to ascertain statistical significance, with a p-value considered significant if it fell below 0.05.

7.2.5 Calculations

Methane yield was determined using Eq. (1) (Huang et al., 2021):

$$\text{Methane yield (\%)} = \frac{COD_{CH4}}{COD_{input}} * 100 \quad (1)$$

where COD_{CH4} stands for the COD equivalent of generated methane (mg); COD_{input} refers to the total COD input (mg).

The concentration of unionized H_2S was computed based on the measured total sulfide concentration using Eq. (2) (Yuan et al., 2020):

$$\text{Unionized } H_2S = \frac{Total\ sulfide}{(1+\frac{K_1}{10^{-pH}})} \quad (2)$$

where K_1 denotes the first ionization constant of H_2S at 20 ℃. It can be determined by considering the first ionization constant of H_2S (9.1×10^{-8}) at 25 ℃ and applying the Van't Hoff Equation which alters the equilibrium constant according to the temperature dependency (Sawyer et al., 2003).

7.3 Results and discussion

7.3.1 SO_4^{2-} reduction and sulfur balance

Overall, all three reactors successfully achieved complete sulfate removal in both operational stages. Sulfate was only detected in the cathode chamber of the MEC-AD1 reactor with a very low concentration of 1.44 ± 0.09 mg/L, which only accounted for 0.26% of the total sulfur input. The sulfur mass balance is depicted in Figure 7.2, illustrating that sulfur primarily exists in four distinct forms: SO_4^{2-}, ionized HS^-, unionized H_2S, and gaseous H_2S. Among these forms, unionized H_2S stands out as the most toxic species. Notably, the total gaseous H_2S constituted a consistent 4.1% to 5.0% within all three reactors across the operational stages. Gaseous H_2S was also detected in the cathode chambers, but only at minimal levels, representing approximately 0.16% and 0.01% in the MEC-AD1 and MEC-AD2 reactors, respectively.

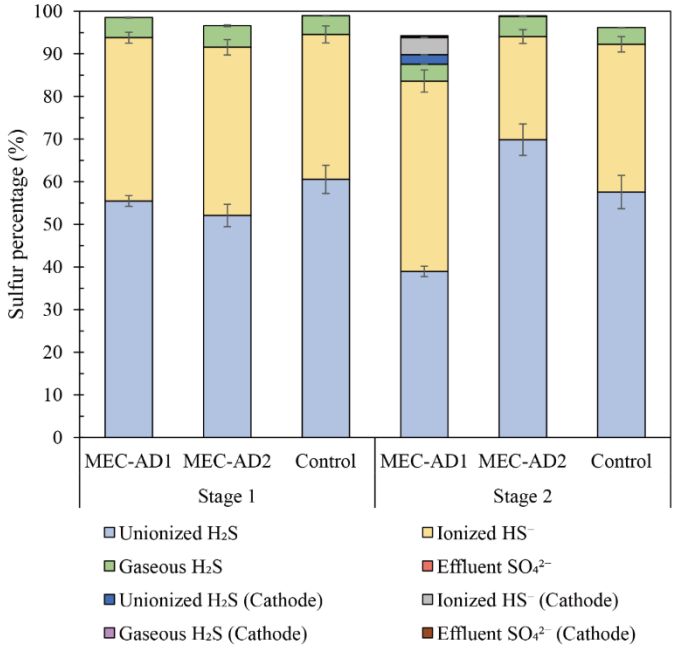

Figure 7.2 Sulfur balance in the reactors under different operating stages.

During Stage 1, due to the rapid oxidation of organic acids at the anode and the concurrent reduction of protons (H^+) along with the generation of alkali (OH^-) at the cathode, the parallel

MEC-AD reactors showed slightly higher pH (6.88 - 6.92) than the control reactor (6.79 ± 0.06). It's noteworthy that the proportion of unionized H_2S in the total sulfide content depends on the pH of the solution (pKa 7.0). Consequently, even though similar total sulfide concentrations were observed in the liquid phase across all three reactors, ranging from 94.6 ± 6.0 to 97.7 ± 8.1 mg/L (Table 7.1), the control reactor displayed relatively higher percentages of unionized H_2S (60.6 ± 3.3%) and concentrations (62.6 ± 5.9 mg/L) compared to the MEC-AD reactors (52.1% - 55.1%; 53.8 - 57.3 mg/L). In Stage 2, with the introduction of AEM that separated the anodes and cathodes of the MEC-AD1 reactor into two chambers, a noticeable increase in pH was observed in the anode chamber (7.10 ± 0.10), while the cathode chamber exhibited a slightly higher pH of 7.30 ± 0.08. In contrast, the MEC-AD2 reactor with a CEM displayed a significant ($p < 0.05$) reduction in pH within the anode chamber (6.58 ± 0.05), while the cathode chamber featured a more alkaline pH of 7.56 ± 0.12. As a result, the MEC-AD1 reactor with an AEM exhibited significantly lower percentages of unionized H_2S (34.2 ± 1.2% in the anode chamber and 2.2 ± 0.03% in the cathode chamber) when compared to the MEC-AD2 and the control reactor. The presence of an AEM allowed for the diffusion of anions through the membrane, including sulfate. While anions typically move from the cathode to the anode chamber to maintain electroneutrality, in this case, differences in ion concentrations on either side of the AEM drove the transfer of sulfate from the anode to the cathode. Hence, sulfur species in the cathode chamber constitute 6.6% of the total sulfur input in the MEC-AD1 reactor with an AEM, whereas only 0.06% of sulfur was detected in the cathode chamber of the MEC-AD2 reactor with a CEM.

7.3.2 Methane production and COD balance

As shown in Table 7.1, during the initial enrichment phase without sulfate supplementation in the substrate, both parallel MEC-AD reactors demonstrated a high COD removal efficiency ranging from 91.8% to 92.1%, while the control reactor showed a comparatively lower COD removal efficiency of 82.2 ± 2.6%. Following the introduction of sulfate in Stage 1, the reactors maintained consistent COD removal efficiencies similar to those observed in the enrichment stage. Notably, the MEC-AD reactors consistently exhibited a 10% higher COD removal efficiency compared to

the control reactor (Figure 7.3A). However, during Stage 2, a significantly higher COD removal efficiency ($p < 0.05$) was observed in the MEC-AD1 reactor (93.7 ± 0.8%) in contrast to the MEC-AD2 reactor (77.2 ± 2.3%) and the control reactor (82.9 ± 1.1%).

Figure 7.3B provides a visual representation of the VFA concentrations in the effluent from each compartment of the three reactors in both stages. In the enrichment stage, the MEC-AD reactors maintained a low total VFA (TVFA) concentration of approximately ~ 50 mg/L (Table 7.1). However, with the introduction of sulfate in Stage 1, the TVFA concentrations increased to approximately ~ 110 mg/L in the MEC-AD reactors and ~ 320 mg/L in the control reactor, with acetate being the predominant VFA component. This observation can be attributed to sulfide inhibition on anaerobic microbes, particularly acetoclastic methanogens (Zhang et al., 2022c). In Stage 2, a remarkable reduction ($p < 0.05$) in TVFA concentration was observed in the MEC-AD1 reactor, reaching 54.7 ± 3.0 mg/L in the anode chamber and 15.2 ± 0.8 mg/L in the cathode chamber. In contrast, there was a notable increase ($p < 0.05$) in TVFA concentration in the anode chamber of the MEC-AD2 reactor, accumulating to 457.0 ± 14.9 mg/L, while the TVFA level in the cathode chamber reached 97.3 ± 6.2 mg/L. The presence of VFAs in the cathode chamber could be attributed to the diffusion of these simple acids from the anode to the cathode, driven by a substantial concentration gradient (Dhar & Lee, 2013). Additionally, it's worth noting that homo-acetogens have the capability to grow on gaseous substrates like $H_2/CO_2/CO$, and as a result, they produce acetic acid as the principal product of their metabolic processes (Karekar et al., 2022).

Figure 7.3C depicts the substrate electron distribution based on COD within the reactors. Given the complete reduction of sulfate in all reactors, the COD consumed for sulfate removal remained consistent at approximately 6.7% throughout the operational period. Notably, methane production served as the primary COD sink in all three reactors. Compared to the enrichment stage without sulfate addition (Table 7.1), the methane yield in the MEC-AD reactors decreased from ~ 79% to ~ 75%, while the control reactor's methane yield declined from 70.7% to 64.4%. The reduction in methane yield can be attributed to the competition between SRB and methanogens

for substrate along with the sulfide toxicity on the microbes. However, in Stage 2, the MEC-AD1 reactor with an AEM demonstrated a significant increase ($p < 0.05$) in methane yield, reaching 80.6 ± 1.8%. Notably, a portion of this methane (11.9 ± 0.9%) was generated in the cathodic chamber (Table 7.1). Conversely, the MEC-AD2 reactor with a CEM exhibited deteriorated performance, resulting in an increased discharge of COD in the effluent (22.8 ± 2.3%) and a reduction in COD conversion to methane yield (63.2 ± 4.2%). Minimal methane generation occurred in the cathode chamber, accounting for around 1.3 ± 0.06% of the total COD input. Overall, the electron flow to methanogens, relative to SRB, was consistently maintained at over 90% in all three reactors across the operation stages, while the highest value of 92.4% was achieved by the MEC-AD1 reactor in Stage 2.

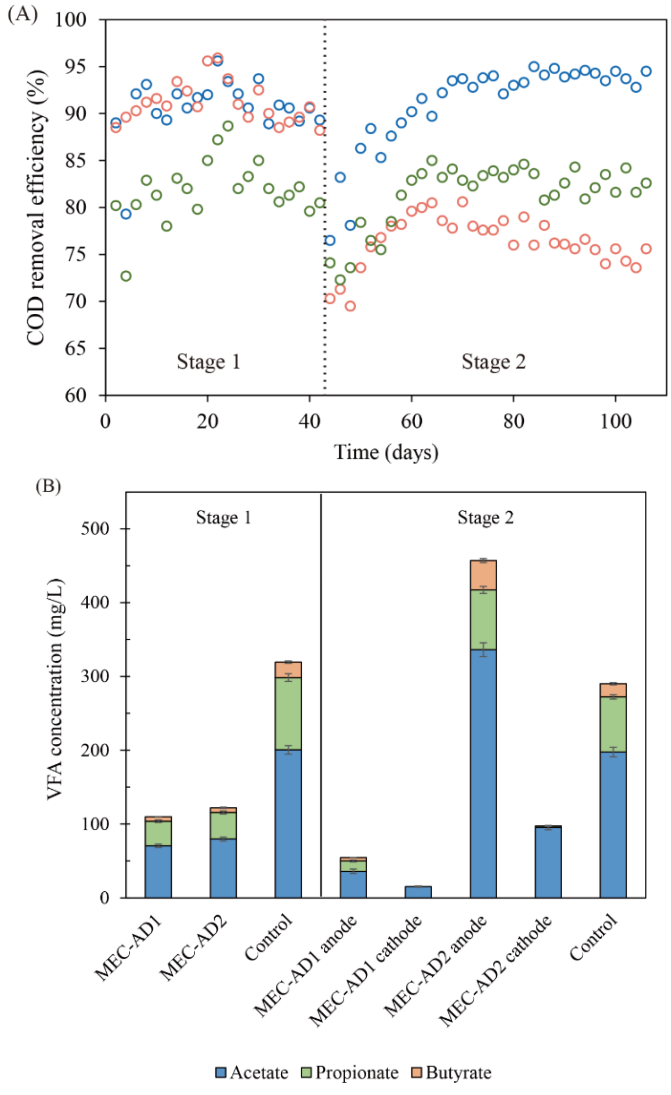

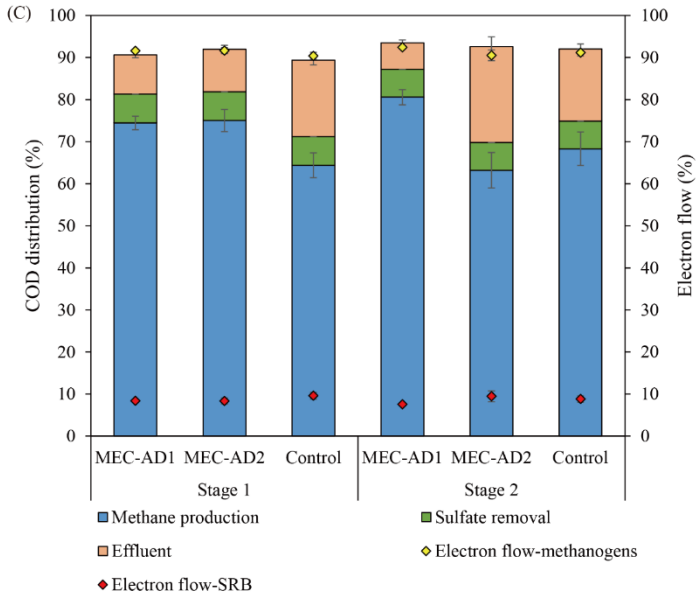

Figure 7.3 (A) COD removal efficiency of the reactors during the long-term operation; (B) VFA concentrations in the effluent of each reactor compartment; (C) Distribution of COD input after treatment and electron flow to SRB and methanogens.

A reduced current density (Table 7.1) was observed as the MEC-AD reactors transitioned from the enrichment stage (8.3 ± 0.6 A/m^2) to operational Stage 1 (7.4 ± 0.5 A/m^2) upon the introduction of sulfate. Several factors contribute to this decrease: firstly, competition occurred between SRB and electroactive bacteria for substrate and space on the anode; secondly, as an electron acceptor, sulfate contends with the anode for the available reducing equivalents within organic matter, consequently redirecting electrons away from the electroactive bacteria (Zhao et al., 2020). The increased current density observed in the MEC-AD1 reactor in Stage 2, reaching 9.0 ± 0.7 A/m^2, indicates heightened bioelectrochemical activities and microbial syntrophic interactions under reduced sulfide inhibition. However, the significant decrease in current density to 4.1 ± 0.5 A/m^2 in the MEC-AD2 reactor during Stage 2 suggested greater resistance and lower reaction efficiency. Previous studies have highlighted various advantages of AEMs over CEMs, including the effective control of pH gradients across the membrane (Kim et al., 2007), lower ion transport resistance (Sleutels et al., 2009), and reduced biofouling risks due to cation precipitation on the cathode surface (Mo et al., 2009).

7.3.3 Specific methanogenic activities (SMA)

The specific biological activities of key microbial groups, particularly methanogens, constitute critical parameters for evaluating AD performance and deciphering the microbial driving forces. Figure 7.4A and Figure 7.4B illustrate the SMA (acetate) and SMA (H_2 + CO_2), respectively, of biofilms on the electrodes in all three reactors. During Stage 1, the biofilms on the anodes and cathodes of the MEC-AD reactors exhibited comparable SMA (acetate) levels around 200 mg CH_4-COD/g VSS-d. In contrast, the control reactor displayed a notably lower ($p < 0.05$) SMA (acetate) at 160.6 ± 9.6 mg CH_4-COD/g VSS-d. However, in Stage 2, the availability of acetate in the cathode chamber was limited, resulting in remarkably low SMA (acetate) values ranging from 13.6 to 27.2 mg CH_4-COD/g VSS-d for the cathodic biofilms in both MEC-AD1 and MEC-AD2 reactors. Contrasting outcomes were observed in terms of SMA (acetate) for the biofilms on the anodes of the MEC-AD1 and MEC-AD2 reactors in Stage 2. Specifically, the SMA (acetate) significantly increased to 255.9 ± 10.0 mg CH_4-COD/g VSS-d in the MEC-AD1 reactor, whereas it decreased to 166.9 ± 8.9 mg CH_4-COD/g VSS-d in the MEC-AD2 reactor. Similar trends were observed concerning SMA (H_2 + CO_2). In Stage 1, the cathodic microbes in the MEC-AD reactors exhibited the highest SMA (H_2 + CO_2) levels, approximately 123 mg CH_4-COD/g VSS-d on average. However, notable variations emerged during Stage 2. The cathodic biofilms in the MEC-AD1 reactor displayed an augmented SMA (H_2 + CO_2) of 137.2 ± 12.2 mg CH_4-COD/g VSS-d, whereas a significant ($p < 0.05$) decrease in cathodic SMA (H_2 + CO_2) to 77.0 ± 6.3 mg CH_4-COD/g VSS-d was noted in the MEC-AD2 reactor. This observation could be attributed to reduced electron transfer efficiency and the homoacetogenesis activities in the MEC-AD2 reactor, which will be discussed in the following section. Furthermore, owing to the constrained diffusion of H_2 from cathode to anode in the dual-chamber configuration compared to the single-chamber configuration, the SMA (H_2 + CO_2) exhibited a decline in anodic biofilms for both MEC-AD reactors in Stage 2.

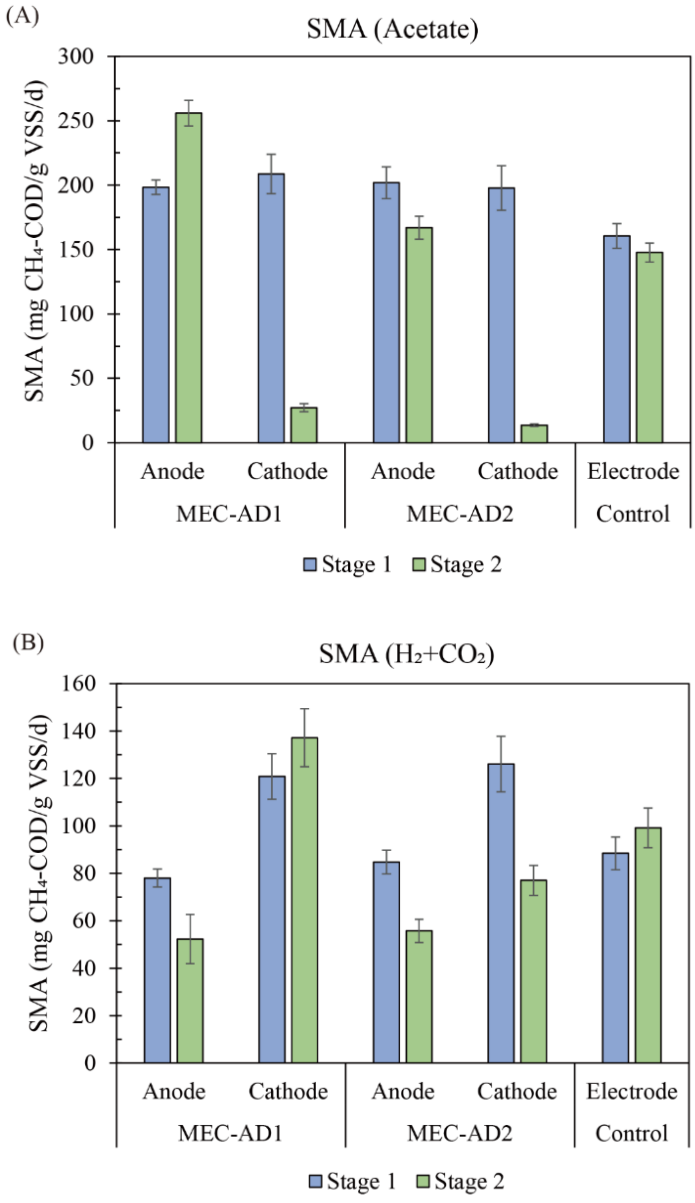

Figure 7.4 Specific methanogenic activity (SMA) of biofilm sludge from each electrode collected during different stages. (A) SMA (Acetate); (B) SMA (H_2 + CO_2).

Table 7.1 Major performance parameters of the reactors during the steady-state period of enrichment and operation stages.

		Enrichment (no sulfate)			Stage 1			Stage 2		
	Unit	MEC-AD1	MEC-AD2	Control	MEC-AD1	MEC-AD2	Control	MEC-AD1	MEC-AD2	Control
COD removal	%	92.1 ± 1.6	91.8 ± 2.0	80.2 ± 2.6	90.7 ± 1.4	89.9 ± 1.3	81.8 ± 1.5	93.7 ± 0.8	77.2 ± 2.3	82.9 ± 1.1
Methane yield	%	79.0 ± 3.6	79.6 ± 2.8	70.7 ± 3.5	74.5 ± 4.9	75.0 ± 5.0	64.4 ± 4.5	68.7 ± 2.3[a] 11.9 ± 0.9[b]	61.9 ± 2.0[a] 1.3 ± 0.06[b]	68.3 ± 2.6
pH		6.96 ± 0.08	6.92 ± 0.07	6.87 ± 0.05	6.88 ± 0.06	6.94 ± 0.05	6.79 ± 0.06	7.10 ± 0.10[a] 7.30 ± 0.08[b]	6.58 ± 0.05[a] 7.56 ± 0.12[b]	6.82 ± 0.09
Total sulfide	mg/L	-	-	-	96.9 ± 7.8	94.6 ± 6.0	97.7 ± 8.1	86.4 ± 5.2[a] 6.4 ± 0.9[b]	97.2 ± 7.6[a] 0.065 ± 0.01[b]	95.3 ± 6.9
Unionized H_2S concentration	mg/L	-	-	-	57.3 ± 4.0	53.8 ± 4.7	62.6 ± 5.9	40.3 ± 3.6[a] 2.28 ± 0.3[b]	72.2 ± 3.9[a] 0.02 ± 0.0[b]	59.5 ± 3.7
Total VFAs	mg/L	57.7 ± 3.9	49.8 ± 4.0	200.7 ± 12.0	109.7 ± 6.2	122 ± 5.0	319.4 ± 9.7	54.7 ± 3.0[a] 15.2 ± 0.8[b]	457.0 ± 14.9[a] 97.3 ± 6.2[b]	290.1 ± 7.2
Peak current density	A/m^2	8.3 ± 0.6	8.7 ± 0.8	-	7.4 ± 0.5	7.6 ± 0.6	-	9.0 ± 0.7	4.1 ± 0.5	-

[a] anode chamber
[b] cathode chamber

7.3.4 Microbial community

7.3.4.1 Microbial diversity

Table 7.2 presents the alpha diversity indices of the microbial community on each electrode in all three reactors based on genus level. Chao1 index, which characterizes microbial richness, reached over 120 for both anodic and cathodic communities in the MEC-AD reactors in Stage 1, whereas a lower value of 87 was observed in the control reactor. Similarly, the Shannon and Simpson indices, which reflect the diversity of microbial communities, as well as the Pielou index (evenness), also exhibited higher values in the MEC-AD reactors in comparison to the control reactor. This observation aligns with previous studies (Wang et al., 2021c; Zhao et al., 2022), which reported greater microbial richness and diversity in MEC-AD reactors compared to control reactors. It underscores the notion that applying an electrical potential can stimulate the enrichment of core microbial populations within electrode biofilms, consequently enhancing microbial community diversity and richness, thereby contributing to the increased stability of the AD process. In Stage 2, there was a substantial increase in all alpha diversity indices within the cathodic communities in both MEC-AD reactors. In contrast, significant decreases in these indices were observed in the control reactor and the anodic community of the MEC-AD2 reactor. These fluctuations can be attributed to variations in sulfide toxicity. The limited diffusion of sulfate to the cathode chambers of MEC-AD1 and MEC-AD2 resulted in substantially lower sulfide levels. This, in turn, led to an augmentation in microbial richness, diversity, and evenness. However, the increased levels of free H_2S, resulting from reduced pH in the anode chamber of the MEC-AD2 reactor and long-term exposure to sulfide of the control reactor, selectively enriched microbial populations with a high tolerance to sulfide toxicity. Consequently, the microbial communities within these compartments exhibited lower alpha diversity indices.

The beta-diversity of the total microbial communities was elucidated through Principal Coordinate Analysis (PCoA) employing Bray-Curtis distances at the genus level (Figure 7.5). The PCoA analysis revealed the formation of two distinct clusters corresponding to the two operational

stages, exhibiting spatial separation along the PCoA 1 axis, which explained 76.28% of the overall sample variance. During Stage 1, the parallel operation of MEC-AD1 and MEC-AD2 led to remarkably close proximity between their microbial communities, particularly within the anodic communities, which exhibited an overlap. Due to similar cultivation environments with buffer solution and low organic content, the cathodic communities in two MEC-AD reactors diverged in the same direction from Stage 1 to 2, still maintaining a close distance. However, significantly high similarities between the anodic community in the MEC-AD2 reactor and that of the control reactor were observed in Stage 2. This finding indicated declined efficiencies of the bioelectrochemical reactions and a reduced regulatory effect of the applied potential on the anodic microbes in the MEC-AD2 reactor. This result aligns with the deteriorated performance and decreased current density in the MEC-AD2 reactor during Stage 2.

Table 7.2 Microbial alpha diversity indices of the microbial community on each electrode in all three reactors based on genus level. 'A' and 'C' refer to the anode and cathode, respectively. 'S1' and 'S2' represent Stage 1 and Stage 2, respectively. Values in 'MEC-AD_A_S1' and 'MEC-AD_C _S1'stand for the average archaea abundance on the anodes and cathodes of the two parallel MEC-AD reactors, respectively.

	Chao1	Shannon	Simpson	Pielou
MEC-AD_A_S1	124	3.92	0.85	0.56
MEC-AD_C_S1	121	4.03	0.87	0.58
Control_S1	87	3.13	0.76	0.49
MEC-AD1_A_S2	122	4.09	0.86	0.59
MEC-AD1_C_S2	196	4.97	0.93	0.65
MEC-AD2_A_S2	91	1.65	0.35	0.25
MEC-AD2_C_S2	182	5.17	0.93	0.69
Control_S2	64	1.13	0.23	0.19

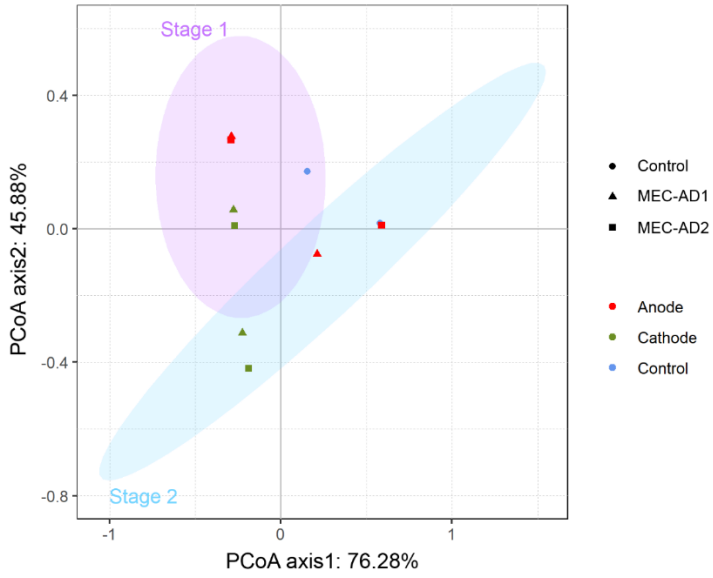

Figure 7.5 Principal coordinate analysis (PCoA) of microbial communities of biofilm samples on each electrode. PCoA was computed using Bray-Curtis distance based on genus level (ellipse confidence level = 95%).

7.3.4.2 Archaeal communities

The temporal dynamics of archaeal relative abundance, at both the domain and genus levels, are presented in Figure 7.6A and Figure 7.6B, respectively. Notably, the control reactor consistently exhibited the lowest archaeal abundance (3.2 - 5.0%). The archaeal abundance remained relatively stable on the anodes of both MEC-AD reactors, ranging from 8.6% to 10.0%. In contrast, a significant increase in archaeal abundance was observed on the cathodes from Stage 1 to Stage 2, rising from 9.9% to 32.2% (MEC-AD1) and 27.7% (MEC-AD2). The extremely low levels of organic matter present in the catholyte resulted in a decrease in the abundance of heterotrophic fermentative bacteria, which consequently facilitated an increase in archaeal abundance.

As shown in Figure 7.6B, acetoclastic *Methanosaeta*, hydrogenotrophic *Methanobacterium* and *Methanospirillum* are three predominant archaea genera across all samples, collectively constituting over 96% of the archaeal community. Among these genera, *Methanosaeta* and *Methanobacterium* were frequently reported as the dominant methanogens in the MEC-AD

system since they are well-recognized electrotrophic methanogens capable of performing the DET and/or direct interspecies electron transfer (DIET) pathways (Huang et al., 2023; Huang et al., 2022b; Zhao et al., 2021). In particular, *Methanosaeta* overwhelmingly dominates the anodic communities in MEC-AD reactors, with an abundance ranging from 74.2% to 79.5%, and also exhibits substantial prevalence in the control reactor communities, ranging from 78.9% to 82.6% across operational stages. During Stage 1, the cathodic communities within MEC-AD reactors notably demonstrated a higher abundance of *Methanobacterium* (34.9%) in comparison to the anodic communities (18.9%) and electrodes of the control reactor (12.3%). Upon introducing different ion exchange membranes in Stage 2, a significant increase in the abundance of *Methanobacterium* was observed in the MEC-AD1 reactor, reaching 76.4%, while a substantial decrease to 15.1% was noted in the MEC-AD2 reactor. These findings signify divergent fates for protons within the two MEC-AD reactors. Specifically, the protons in the MEC-AD1 cathode chamber were more likely to undergo reduction to form H_2 or participate in the DET pathway, ultimately contributing to methane production. In contrast, in the MEC-AD2 cathode chamber, most protons that travelled to the cathode were probably converted into acetate by homoacetogens. This distinction underscores the complex interplay of microbial activities and electron transfer mechanisms within the two reactor configurations.

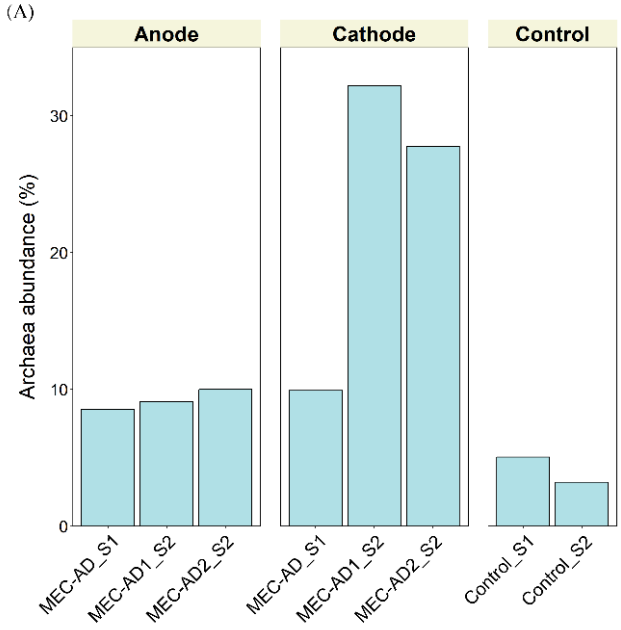

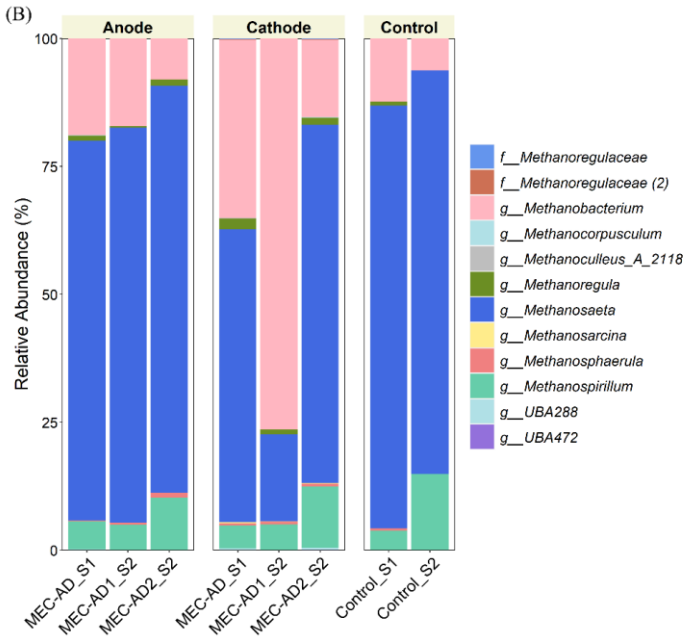

Figure 7.6 (A) Archaea abundance on each electrode; (B) Relative abundances of archaeal genera on each electrode. The unidentified genus was named at family (*f__*) level. 'S1' and 'S2' represent Stage 1 and Stage 2, respectively. Values in 'MEC-AD _S1' stand for the average archaea abundance on the anodes or cathodes of the two parallel MEC-AD reactors, respectively.

7.3.4.3 Bacterial communities

Figure 7.7 illustrates the temporal changes in the relative abundance of bacterial genera with abundance > 1% within at least one biofilm sample. In both stages, two fermentative bacteria, *Trichococcus* and *Lactococcus_A_343306*, were identified as the most predominant genera in the compartments holding glucose medium. *Trichococcus* is known for its ability to ferment glucose into formate, acetate, lactate, and ethanol (Zhang et al., 2022c). *Lactococcus* is a typical lactic acid bacterial group, capable of rapidly fermenting proteins and sugars to lactic acid (McAteer et al., 2020). In Stage 1, the anode and cathode of single-chamber MEC-AD reactors displayed similar dominance of *Lactococcus*, constituting 47.6% and 45.7%, respectively. However, in Stage 2, *Trichococcus* took precedence on the anodes, accounting for 36.6% and 82.0% in the MEC-AD1 and MEC-AD2 reactors, respectively. In the control reactor, *Trichococcus* was predominant in Stage 1 (43.8%) and its dominance further increased to 88.8% in Stage 2. The enrichment of

Trichococcus on control reactor electrodes and the anode of the MEC-AD1 reactor indicated its remarkable tolerance to long-term exposure to sulfide or high sulfide levels. The lower levels of free H_2S in the anode chamber of the MEC-AD1 reactor compared to the MEC-AD2 reactor in Stage 2 (Table 7.1) align with the corresponding lower abundance of *Trichococcus*, further supporting this hypothesis. However, the overwhelming dominance of a single genus simplified the microbial community, potentially leading to system instability and reduced resilience. Therefore, in conjunction with the alpha diversity indices (Table 7.2), it can be inferred that the MEC-AD1 reactor equipped with an AEM could promote microbial diversity under sulfate/sulfide stress. This, in turn, could directly contribute to a more robust and stable system, possibly through functional redundancy and/or niche complementation (Shade et al., 2012).

As an important electroactive bacterium in bioelectrochemical systems, *Geobacter* was only detected on the anodes within two MEC-AD reactors. From Stage 1 to 2, the abundance of *Geobacter* remarkably increased from 0.5% to 2.4% in the MEC-AD1 reactor, but slightly reduced to 0.4% in the MEC-AD2 reactor. Similarly, several other prevalent electroactive bacteria exhibited substantial enrichment on the anode of the MEC-AD1 reactor in Stage 2 with abundance ranging from 4.4% to 8.6%, such as *Anaeromusa* (Liu et al., 2023), *Aeromonas* (Zhang et al., 2022b), and a genus from family *Enterobacteriaceae_A* (Zakaria & Dhar, 2020). These findings align with the observed higher current density (Table 7.1) and methane yield in the MEC-AD1 reactor in Stage 2 compared to both Stage 1 and the MEC-AD2 reactor, indicating a more robust syntrophic relationship established between the electroactive bacteria and methanogens.

The cathodic biofilms of the MEC-AD reactors in Stage 2 were dominated by *Clostridium* and *Acetobacterium*, both of which contain efficient strains for homoacetogenesis (Karekar et al., 2022). These homoacetogens exhibit the capacity to autotrophically grow on gaseous compounds, employing the acetyl-CoA pathway to assimilate CO_2 while utilizing H_2 to synthesize acetate (Ye et al., 2014). The higher abundance of these genera on the cathode of the MEC-AD2 reactor, as compared to the MEC-AD1 reactor, correlates well with the lower methane yield and higher

acetate concentration in the MEC-AD2 cathode chamber.

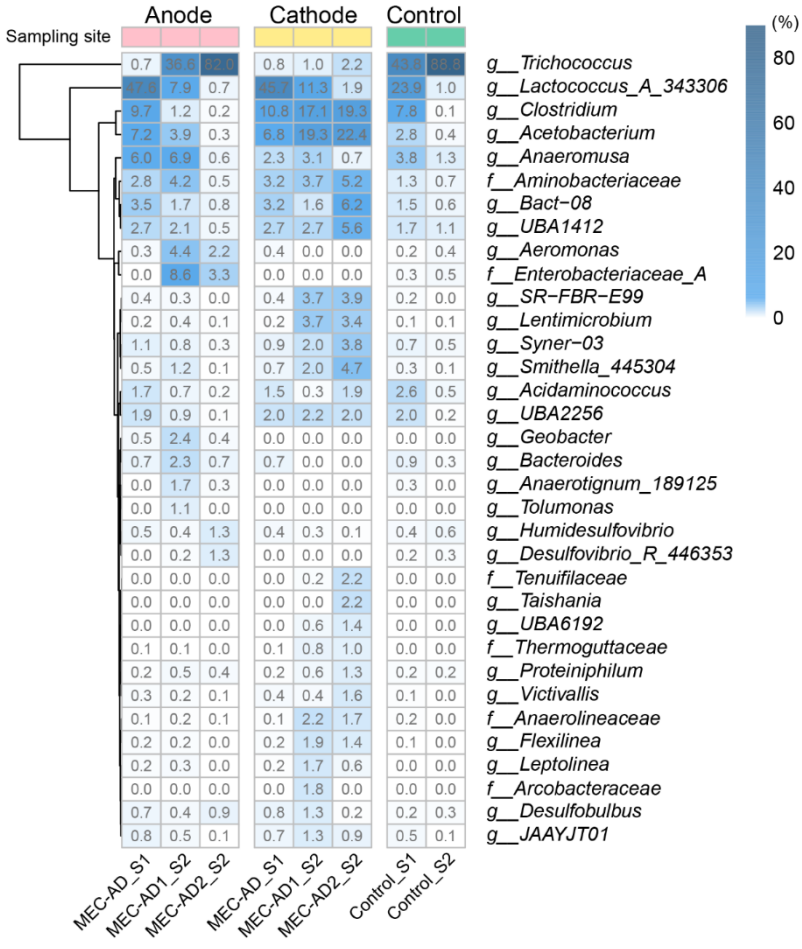

Figure 7.7 Relative abundances of bacterial genera with >1% abundance in at least one sludge sample. Unidentified genera were named at family (*f__*). Numbers are relative abundances (%) of genera. 'S1' and 'S2' represent Stage 1 and Stage 2, respectively. Values in 'MEC-AD_S1' stand for the average bacteria abundance on the anodes or cathodes of the two parallel MEC-AD reactors, respectively.

The most prevalent SRB genera in the reactors were identified as *Humidesulfovibrio*, *Desulfovibrio_R_446353*, and *Desulfobulbus*, which have the capacity to partially oxidize organic carbon, leading to the production of acetate while utilizing sulfate as the electron acceptor (Lu et al., 2017). The anode of the MEC-AD1 reactor consistently exhibited a lower presence of SRB genera compared to the MEC-AD2 reactor. Hence, in conjunction with the elevated prevalence of

electroactive bacteria, these findings suggest that SRB are less competitive for substrates when compared to the electroactive bacteria inhabiting the MEC-AD1 anode chamber. However, due to the diffusion of sulfate from the anode to the cathode chamber in the MEC-AD1 reactor via an AEM, the cathodic biofilm of the MEC-AD1 reactor exhibited significantly higher SRB abundance (1.6%) in contrast to the cathode of the MEC-AD2 reactor (0.3%).

7.3.5 Mechanisms and significance of MEC-AD configurations

In this study, distinct performance differences were observed when employing an AEM and a CEM in MEC-AD reactors treating sulfate-rich feedstock. Here, elucidation of the underlying mechanisms is provided based on the performance parameters mentioned above.

For the MEC-AD1 reactor, equipped with an AEM, the membrane's positive charge selectively transports counter-ions (anions). Typically, OH^- ions are transferred from the cathode to the anode chamber to maintain electroneutrality. Notably, prior studies have indicated that negatively charged chemical buffers, such as bicarbonate (HCO_3^-) and various orthophosphate anions (HPO_4^{2-} and $H_2PO_4^-$), can permeate AEMs (Cheng & Logan, 2007; Kim et al., 2007; Logan et al., 2008). In this study, high buffer concentrations ($Na_2HPO_4 \cdot 7H_2O$ 10.0 g/L, $NaH_2PO_4 \cdot H_2O$ 2.0 g/L, $NaHCO_3$ 5.0g/L) were introduced into the catholyte to ensure cathodic pH stability. The increase in pH observed in the MEC-AD1 reactor during Stage 2 (7.10 ± 0.10), compared to its performance in the single-chamber operation in Stage 1 (6.88 ± 0.06), indicated that phosphate and bicarbonate ions were effectively transported from the cathode to the anode chamber. This transport mitigated the pH decrease in the anode chamber, while ensuring a balanced charge in both chambers. The ability of phosphate groups to facilitate proton transfer and serve as pH buffers proved advantageous for the AEMs compared to CEMs. The increase in pH significantly reduced the proportion of free H_2S, thereby alleviating sulfide inhibition on anaerobic microbes, especially methanogens. In addition, the concentration gradient facilitated the transport of sulfate from the anode to the cathode chamber, lowering sulfate levels in the anode chamber. Under sulfate-limited conditions, SRB can ferment organic compounds like ethanol, lactate, and pyruvate to produce

acetate, CO_2, and H_2 in syntrophy with methanogens (Muyzer & Stams, 2008). In the cathode chamber, where H_2 was produced and hydrogenotrophic methanogens were enriched, the impact of SRB on methanogenesis was less pronounced, because hydrogenotrophic methanogens exhibit greater resilience to sulfate stress and sulfide toxicity than acetoclastic methanogens (Zhang et al., 2022c).

In contrast, the MEC-AD2 reactor equipped with a CEM exhibited inferior performance in Stage 2. It has been previously documented that cations (e.g., Na+, Mg^{2+}, K^+, Ca^{2+}, NH_4^+, and others), which are typically present at concentrations three to four orders of magnitude higher than protons, are primarily transported as positive charges from the anode to the cathode across CEMs to maintain charge neutrality (Dhar & Lee, 2013; Kim et al., 2007). The transport of these cations, instead of protons, can result in increased pH in a cathode chamber, acidification of an anode chamber, and internal energy loss (Dhar & Lee, 2013; Kim et al., 2007). Because of the pH decrease in the anode chamber, the free H_2S concentration significantly increased from 57.3 to 72.2 mg/L, exacerbating sulfide inhibition. In this study, a substantial pH gradient between the anode and cathode chambers (6.58 vs. 7.56) was observed in the MEC-AD2 reactor in Stage 2, possibly resulting in substantial potential losses.

Interestingly, in Stage 2 of the MEC-AD2 reactor's cathode chamber, only 1.3% of methane yield (equivalent to ~14.2 mg COD) was detected, while a considerable amount of total TVFA amounting to 97.3 mg/L (equivalent to ~21.5 mg COD) was observed. It was documented that homoacetogenesis ($2CO_2/HCO_3^- + 8H^+ + 8e^- \rightarrow CH_3COO^- + H_2O$) only occurs when methanogenesis is inhibited (Parameswaran et al., 2010). However, some studies have reported that H_2 generation can lead to the co-occurrence of homoacetogenesis and methanogenesis in the cathode chamber (Liu et al., 2016b; Zeppilli et al., 2016). Similar to this study, Zeppilli et al. (2016) observed higher acetate accumulation in the cathode chamber of the MEC-AD reactor with a PEM (over 2500 mg/L) compared to the MEC-AD reactor with an AEM (lower than 350 mg/L). Zeppilli et al. (2016) attributed the differences in acetate concentrations to the membrane types, as AEMs

allow for greater acetate diffusion from the cathode to the anode compared to CEMs. However, in this study, the higher abundance of homoacetogens (i.e., *Clostridium* and *Acetobacterium*) and the lower abundance of methanogens detected in the cathodic biofilms of the MEC-AD2 reactor compared to the MEC-AD1 reactor suggest that other factors may contribute to the higher cathodic acetate concentrations in the MEC-AD2 reactor. For instance, the local pH on cathodic biofilms may be very alkaline for methanogens as they are sensitive to environmental conditions. However, Katakojwala et al. (2022) reported that maximum VFA yield was achieved at an alkaline pH (8.5) compared to pH 6.5 and 7.5 when employing homoacetogenic chemolithoautotrophs. Therefore, the high local pH on the cathode may inhibit methanogens but favor homoacetogenesis.

Understanding the underlying mechanisms responsible for the superior performance of the MEC-AD reactor equipped with an AEM provides valuable insights into the efficient treatment of sulfate-rich wastewater in combination with cathodic CO_2 fixation. The findings from this study hold significant potential for advancing both scientific investigations and practical applications of MEC-AD systems for mitigating inhibitory effects on AD.

7.4 Conclusion

Different configurations of MEC-AD reactors were investigated for anaerobic digestion of sulfate-rich wastewater. Single-chamber configured MEC-ADs outcompeted the control reactor. Owing to anodic pH increase, diversified microbial communities and enrichment of electroactive bacteria and hydrogenotrophic methanogens, the MEC-AD1 reactor employing an AEM demonstrated the most superior performance, featuring reduced free H_2S concentrations and enhanced methane yield. However, the MEC-AD2 reactor with a CEM exhibited deteriorated performance mainly due to the substantially decreased anodic pH, which intensified the sulfide inhibition. This study offers valuable insights into simultaneous sulfate reduction and CO_2 fixation by MEC-ADs with an AEM configuration.

Chapter 8. Conclusions and Recommendations

8.1 Conclusions

This doctoral thesis delves into both the fundamental and practical aspects of advancing microbial electrolysis cell-assisted anaerobic digestion (MEC-AD) to enhance biomethane recovery from high-strength wastewater. Through targeted efforts to address process constraints, including challenges with low hydrolysis efficiency, slow methanogenesis rates, and sulfate/sulfide inhibition, an effective high-rate treatment strategy was successfully demonstrated, resulting in impressive organic removal efficiency and methane generation. The key findings and conclusions are summarized as follows:

Overcoming sluggish digestion kinetics at ambient temperature

- Source-separated blackwater, a typical high-strength wastewater stream from the municipal sector, has been treated within a MEC-AD reactor at ambient temperature (Chapter 3). The OLR was incrementally increased from 0.77 g COD/L-d and ultimately reached 3.03 g COD/L-d, demonstrating the MEC-AD system's capacity to sustain a high OLR at ambient temperature. Notably, the closed-circuit operation resulted in a substantial methane yield of 35.2%, which significantly exceeded 24.1% achieved under open-circuit conditions. This observation highlights the MEC-AD system's effectiveness in expediting methane recovery from complex organic compounds present in blackwater. The applied potential led to the enrichment of specific electroactive and fermentative bacteria, whose synergistic interactions with H_2 utilizers played a pivotal role in the degradation of the intricate substrates found in blackwater. Furthermore, the existence of syntrophic interactions between electroactive bacteria and electrotrophic methanogens was confirmed by strong positive correlations in the microbial co-occurrence network analysis.

- Building upon the findings in Chapter 3, which demonstrated enhanced methane

production and increased OLRs through MEC-AD systems, Chapter 4 conducted a comprehensive screening of optimal applied voltages. The operation of MEC-AD with vacuum toilet blackwater at ambient temperature consistently improved various parameters, such as COD removal, methane yield, hydrolysis/acidogenesis efficiency, and energy efficiency, as the applied voltage was increased from 0 to 1.2 V. The hydrolysis improvement was achieved, with the enrichment of hydrolytic bacteria like *Clostridium* and *Bacteroidales*, along with an increase in functional genes related to the metabolism of complex organic compounds. Further analysis using LEfSe highlighted the significance of syntrophic bacteria and their collaborations with acetate-utilizing bacteria and the dominant archaea *Methanosaeta*. Importantly, the impact of applied voltages was more pronounced at ambient temperatures compared to mesophilic temperatures, underscoring the high efficiency and energy-saving potential of MEC-AD technology for psychrophilic anaerobic digestion processes.

- While Chapters 3 and 4 highlighted the improved efficiencies in hydrolysis and methanogenesis achieved by MEC-AD systems, Chapter 5 delved into the investigation of whether reactor amendment (i.e., GAC addition) and operational scheme modification (i.e., extended sludge retention) could further enhance system performance. The results revealed that these strategies effectively mitigated the performance deterioration associated with increased OLRs and reduced temperature, leading to significant improvements in hydrolysis and methane yield. The introduction of GAC-sludge aggregates notably enriched DIET-related methanogens and various hydrolytic bacteria. A mutually reinforcing relationship between GAC and an electrochemically active environment was uncovered, which facilitated the enrichment of essential syntrophic acetate/acid-oxidizing bacteria, resulting in the establishment of a highly resilient microbiome.

Mitigating sulfide inhibition and competition between SRB and methanogens

- High sulfate levels in wastewater can be a significant inhibitory factor in anaerobic digestion operation, particularly for feedstocks with low COD/SO_4^{2-} ratios. In Chapter 6, the

performance of a MEC-AD reactor was systematically assessed at reduced COD/SO_4^{2-} ratios ranging from 20 to 1. The MEC-AD reactor consistently outperformed the control reactor, demonstrating improved methane production, COD removal, and specific methanogenic activity. The underlying mechanisms for the superior performance of the MEC-AD reactor were proposed: (1) The MEC-AD reactor maintained lower sulfide concentrations, primarily due to its relatively higher pH and the occurrence of anodic sulfide oxidation, and (2) The enrichment of electroactive bacteria and hydrogenotrophic methanogens within the MEC-AD reactor appeared to foster stronger syntrophic relationships with sulfate-reducing bacteria (SRB), resulting in a high methanogenic capacity sustained even under high sulfate stress.

- After uncovering the mechanisms for AD enhancement under sulfate-rich conditions through MEC-AD systems in Chapter 6, Chapter 7 delved into an investigation of the performance of MEC-AD systems with different configurations. Notably, single-chamber MEC-AD configurations outperformed the control reactor. Among these, the MEC-AD reactor employing an anion exchange membrane (AEM) exhibited the most remarkable performance, characterized by effectively maintaining anodic pH, establishing diverse microbial communities, and enriching electroactive bacteria and hydrogenotrophic methanogens. This configuration led to reduced free H_2S concentrations and enhanced methane yield. Conversely, the MEC-AD reactor with a cation exchange membrane (CEM) experienced a decline in performance primarily due to a significant decrease in anodic pH, exacerbating sulfide inhibition.

In conclusion, these results can help overcome the challenges in the treatment of blackwater and sulfate-rich wastewater, including guiding future system design, operation, process optimization, and engineering applications for the treatment of various high-strength wastes from both municipal and industrial sectors. The success of this research will guide solutions that can gradually displace current practices and greatly benefit sustainable future water/energy management.

8.2 Recommendations

Despite the proven feasibility and associated advantages, the practical implementation of the MEC-AD system has been limited to date. Addressing existing constraints and further improving the system's sustainability necessitates additional research and necessary modifications:

- For the investigation of fundamental aspects of sulfate-rich wastewater treatment using MEC-AD systems, synthetic wastewater was employed to mitigate potential disruptions inherent in complex raw wastewater. This approach allowed for clearer insights into system mechanisms. However, conducting studies on the treatment of real raw sulfate-rich wastewater is necessary to gain a more comprehensive understanding relevant to real-world applications.

- The present research advanced our understanding of microbial community development and functional pathways through 16S rRNA sequencing and PICRUSt prediction. However, these methods have limitations in terms of accuracy and resolution. In contrast, metagenomics offers a more comprehensive approach, allowing for the exploration of the functional potential of microbial communities by identifying and characterizing the entire set of genes present. This method provides a heightened resolution for microbial diversity, including strain-level differences. Moreover, metatranscriptomics is invaluable for revealing active genes within a community, offering insights into gene expression patterns and facilitating the connection between potential functions and actual activities. Concurrently, proteomics plays a crucial role in identifying and quantifying proteins produced by the microbial community. This enables the correlation of gene expression with the synthesis of actual proteins, providing a more dynamic understanding of microbial activities. Therefore, to enhance applications like bioaugmentation with functional microorganisms or enzymes for improved biogas production and pollutant removal, conducting metagenome, metatranscriptomics, and proteomic analyses is recommended to validate the metabolic pathways of core microorganisms.

- The current research was conducted in bench-scale MEC-AD reactors, while further

research is necessary to provide more insights into the feasibility of the technology for engineering practice. Conducting scale-up studies is of paramount importance to assess the practicality and efficiency of implementing MEC-AD systems on a larger, more representative scale. Thus, scale-up studies are required to help bridge the gap between laboratory findings and real-world applications, offering critical data on system scalability, operational stability, and economic viability.

- The effluent resulting from blackwater digestion within MEC-AD systems comprises various components, including pathogens, micropollutants, nutrients, and residual organic matter, which do not meet discharge standards and consequently require post-treatment. Further efforts are required to simultaneously recover bioenergy and nutrients, by incorporating struvite or calcium phosphate precipitation in the MEC-AD systems. Pathogens and micropollutants, such as pharmaceuticals, hormones, and bacteria with antibiotic-resistant genes, pose significant challenges for the recycling and reusing treated wastewater. Future studies are recommended to explore electrochemical oxidation for effective micropollutants' removal in the MEC-AD systems.

Overall, combining microbial electrolysis cells with anaerobic digestion opens up novel prospects for resource recovery from high-strength wastewater. Rapid advancements in microbial and engineered technologies hold the potential to enhance our understanding of the MEC-AD technology, augment its efficiency, address its limitations, and broaden its scope of application. Going forward, gaining a deeper understanding of anaerobic microbes and implementing bioreactor modifications are imperative steps for addressing constraints and further enhancing the sustainability of this technology.

Bibliography

Aeschbacher, M., Sander, M., Schwarzenbach, R.P. 2010. Novel electrochemical approach to assess the redox properties of humic substances. *Environ Sci Technol*, **44**(1), 87-93.

Aggelis, G., Gavala, H.N., Lyberatos, G. 2001. SE—Structures and Environment: Combined and Separate Aerobic and Anaerobic Biotreatment of Green Olive Debittering Wastewater. *Journal of agricultural engineering research*, **80**(3), 283-292.

Ahmad, M.I., Ejaz, O., Ali, A., Durrani, M.A.Q.J., Khan, I.A. 2014. Anaerobic digestion of waste from a slaughterhouse. *Journal of Environmental Chemical Engineering*, **2**(3), 1317-1320.

Ahmad, W., Sethupathi, S., Kanadasan, G., Lau, L.C., Kanthasamy, R. 2021. A review on the removal of hydrogen sulfide from biogas by adsorption using sorbents derived from waste. *Reviews in Chemical Engineering*, **37**(3), 407-431.

Ahring, B.K., Sandberg, M., Angelidaki, I. 1995. Volatile fatty acids as indicators of process imbalance in anaerobic digestors. *Applied microbiology and biotechnology*, **43**(3), 559-565.

Alkalay, D., Guerrero, L., Lema, J., Mendez, R., Chamy, R. 1998. Anaerobic treatment of municipal sanitary landfill leachates: the problem of refractory and toxic components. *World journal of microbiology and Biotechnology*, **14**(3), 309-320.

APHA. 2005. APHA standard methods for the examination of water and wastewater. *Standard methods for the examination of water & wastewater. Washington, DC: American Public Health Association*.

Ariesyady, H.D., Ito, T., Okabe, S. 2007. Functional bacterial and archaeal community structures of major trophic groups in a full-scale anaerobic sludge digester. *Water research*, **41**(7), 1554-1568.

Ariunbaatar, J., Panico, A., Esposito, G., Pirozzi, F., Lens, P.N. 2014. Pretreatment methods to enhance anaerobic digestion of organic solid waste. *Applied energy*, **123**, 143-156.

Asztalos, J.R., Kim, Y. 2015. Enhanced digestion of waste activated sludge using microbial electrolysis cells at ambient temperature. *Water Res*, **87**, 503-12.

Ateya, B., AlKharafi, F., Al-Azab, A. 2003. Electrodeposition of sulfur from sulfide contaminated brines. *Electrochemical and Solid-State Letters*, **6**(9), C137.

Bakar, M.H.A., Daud, W.R.W., Hong, K.B., Jahim, J.M. 2019. Can electrochemically active biofilm protect stainless steel used as electrodes in bioelectrochemical systems in a similar way as galvanic corrosion protection? *International journal of hydrogen energy*, **44**(58), 30512-30523.

Banks, C.J., Chesshire, M., Heaven, S., Arnold, R. 2011. Anaerobic digestion of source-segregated domestic food waste: performance assessment by mass and energy balance. *Bioresour Technol*, **102**(2), 612-20.

Barua, S., Dhar, B.R. 2017. Advances towards understanding and engineering direct interspecies electron transfer in anaerobic digestion. *Bioresource technology*, **244**, 698-707.

Barua, S., Zakaria, B.S., Al-Mamun, A., Dhar, B.R. 2018. Anodic Performance in Microbial Electrolysis Cells in Response to Ammonia Nitrogen. *Journal of Environmental Engineering and Science*, 1-28.

Barua, S., Zakaria, B.S., Chung, T., Hai, F.I., Haile, T., Al-Mamun, A., Dhar, B.R. 2019. Microbial electrolysis followed by chemical precipitation for effective nutrients recovery from digested sludge centrate in WWTPs. *Chemical Engineering Journal*, **361**, 256-265.

Barua, V.B., Raju, V.W., Lippold, S., Kalamdhad, A.S. 2017. Electrohydrolysis pretreatment of water hyacinth for enhanced hydrolysis. *Bioresource technology*, **238**, 733-737.

Bassin, J., Dias, I., Cao, S., Senra, E., Laranjeira, Y., Dezotti, M. 2016. Effect of increasing organic loading rates on the performance of moving-bed biofilm reactors filled with different support media: Assessing the activity of suspended and attached biomass fractions. *Process Safety and Environmental Protection*, **100**, 131-141.

Beegle, J.R., Borole, A.P. 2018. Energy production from waste: Evaluation of anaerobic digestion and bioelectrochemical systems based on energy efficiency and economic factors. *Renewable and Sustainable Energy Reviews*, **96**, 343-351.

Beltran-Heredia, J., Torregrosa, J., Dominguez, J.R., Garcia, J. 2000. Aerobic biological treatment

of black table olive washing wastewaters: effect of an ozonation stage. *Process Biochemistry*, **35**(10), 1183-1190.

Beltrán, F.J., García-Araya, J.F., Frades, J., Álvarez, P., Gimeno, O. 1999. Effects of single and combined ozonation with hydrogen peroxide or UV radiation on the chemical degradation and biodegradability of debittering table olive industrial wastewaters. *Water Research*, **33**(3), 723-732.

Beltran, J., Gonzalez, T., Garcia, J. 2008. Kinetics of the biodegradation of green table olive wastewaters by aerobic and anaerobic treatments. *J Hazard Mater*, **154**(1-3), 839-45.

Bharathiraja, B., Sudharsana, T., Jayamuthunagai, J., Praveenkumar, R., Chozhavendhan, S., Iyyappan, J. 2018. Biogas production–A review on composition, fuel properties, feed stock and principles of anaerobic digestion. *Renewable and sustainable Energy reviews*, **90**(April), 570-582.

Bo, T., Zhu, X., Zhang, L., Tao, Y., He, X., Li, D., Yan, Z. 2014. A new upgraded biogas production process: Coupling microbial electrolysis cell and anaerobic digestion in single-chamber, barrel-shape stainless steel reactor. *Electrochemistry Communications*, **45**, 67-70.

Bolzonella, D., Pavan, P., Battistoni, P., Cecchi, F. 2005. Mesophilic anaerobic digestion of waste activated sludge: influence of the solid retention time in the wastewater treatment process. *Process biochemistry*, **40**(3-4), 1453-1460.

Boon, N., De Maeyer, K., Höfte, M., Rabaey, K., Verstraete, W. 2008. Use of Pseudomonas species producing phenazine-based metabolites in the anodes of microbial fuel cells to improve electricity generation. *Applied microbiology and biotechnology*, **80**(6), 985-993.

Borole, A.P., Reguera, G., Ringeisen, B., Wang, Z.-W., Feng, Y., Kim, B.H. 2011. Electroactive biofilms: Current status and future research needs. *Energy & Environmental Science*, **4**(12).

Bose, R.S., Chowdhury, B., Zakaria, B.S., Tiwari, M.K., Dhar, B.R. 2021. Significance of different mixing conditions on performance and microbial communities in anaerobic digester amended with granular and powdered activated carbon. *Bioresource Technology*, **341**, 125768.

Butti, S.K., Velvizhi, G., Sulonen, M.L., Haavisto, J.M., Koroglu, E.O., Cetinkaya, A.Y., Singh, S., Arya, D., Modestra, J.A., Krishna, K.V. 2016. Microbial electrochemical technologies with the perspective of harnessing bioenergy: maneuvering towards upscaling. *Renewable and Sustainable Energy Reviews*, **53**, 462-476.

Cai, W., Liu, W., Yang, C., Wang, L., Liang, B., Thangavel, S., Guo, Z., Wang, A. 2016. Biocathodic Methanogenic Community in an Integrated Anaerobic Digestion and Microbial Electrolysis System for Enhancement of Methane Production from Waste Sludge. *ACS Sustainable Chemistry & Engineering*, **4**(9), 4913-4921.

Callahan, B.J., McMurdie, P.J., Rosen, M.J., Han, A.W., Johnson, A.J.A., Holmes, S.P. 2016. DADA2: high-resolution sample inference from Illumina amplicon data. *Nature methods*, **13**(7), 581.

Cao, Y., Pawłowski, A. 2012. Sewage sludge-to-energy approaches based on anaerobic digestion and pyrolysis: Brief overview and energy efficiency assessment. *Renewable and Sustainable Energy Reviews*, **16**(3), 1657-1665.

Cappelletti, G., Nicoletti, G., Russo, C. 2011. Wastewater from table olive industries. in: *Waste Water-Evaluation and Management*, InTech.

Carrère, H., Dumas, C., Battimelli, A., Batstone, D., Delgenès, J., Steyer, J., Ferrer, I. 2010. Pretreatment methods to improve sludge anaerobic degradability: a review. *Journal of hazardous materials*, **183**(1-3), 1-15.

Castillo, E., Vergara, M., Moreno, Y. 2007. Landfill leachate treatment using a rotating biological contactor and an upward-flow anaerobic sludge bed reactor. *Waste Manag*, **27**(5), 720-6.

Castrillon, L., Fernandez-Nava, Y., Ulmanu, M., Anger, I., Maranon, E. 2010. Physico-chemical and biological treatment of MSW landfill leachate. *Waste Manag*, **30**(2), 228-35.

Cerrillo, M., Oliveras, J., Vinas, M., Bonmati, A. 2016a. Comparative assessment of raw and digested pig slurry treatment in bioelectrochemical systems. *Bioelectrochemistry*, **110**, 69-78.

Cerrillo, M., Vinas, M., Bonmati, A. 2016b. Overcoming organic and nitrogen overload in

thermophilic anaerobic digestion of pig slurry by coupling a microbial electrolysis cell. *Bioresour Technol*, **216**, 362-72.

Cerrillo, M., Vinas, M., Bonmati, A. 2016c. Removal of volatile fatty acids and ammonia recovery from unstable anaerobic digesters with a microbial electrolysis cell. *Bioresour Technol*, **219**, 348-356.

Cerrillo, M., Vinas, M., Bonmati, A. 2017. Unravelling the active microbial community in a thermophilic anaerobic digester-microbial electrolysis cell coupled system under different conditions. *Water Res*, **110**, 192-201.

Chae, K., Jang, A., Yim, S., Kim, I.S. 2008. The effects of digestion temperature and temperature shock on the biogas yields from the mesophilic anaerobic digestion of swine manure. *Bioresource technology*, **99**(1), 1-6.

Chan, Y.J., Chong, M.F., Law, C.L., Hassell, D. 2009. A review on anaerobic–aerobic treatment of industrial and municipal wastewater. *Chemical Engineering Journal*, **155**(1-2), 1-18.

Charalambous, P., Shin, J., Shin, S.G., Vyrides, I. 2020. Anaerobic digestion of industrial dairy wastewater and cheese whey: performance of internal circulation bioreactor and laboratory batch test at pH 5-6. *Renewable Energy*, **147**, 1-10.

Chatzisymeon, E., Stypas, E., Bousios, S., Xekoukoulotakis, N.P., Mantzavinos, D. 2008. Photocatalytic treatment of black table olive processing wastewater. *J Hazard Mater*, **154**(1-3), 1090-7.

Chen, J.L., Ortiz, R., Steele, T.W., Stuckey, D.C. 2014. Toxicants inhibiting anaerobic digestion: a review. *Biotechnology advances*, **32**(8), 1523-1534.

Chen, Y., Cheng, J.J., Creamer, K.S. 2008. Inhibition of anaerobic digestion process: a review. *Bioresour Technol*, **99**(10), 4044-64.

Chen, Y., Yu, B., Yin, C., Zhang, C., Dai, X., Yuan, H., Zhu, N. 2016. Biostimulation by direct voltage to enhance anaerobic digestion of waste activated sludge. *RSC Advances*, **6**(2), 1581-1588.

Cheng, S., Logan, B.E. 2007. Sustainable and efficient biohydrogen production via

electrohydrogenesis. *Proc Natl Acad Sci U S A*, **104**(47), 18871-3.

Cheng, S., Xing, D., Call, D.F., Logan, B.E. 2009. Direct biological conversion of electrical current into methane by electromethanogenesis. *Environmental science & technology*, **43**(10), 3953-3958.

Chipasa, K. 2001. Limits of physicochemical treatment of wastewater in the vegetable oil refining industry. *Polish Journal of Environmental Studies*, **10**(3), 141-147.

Cho, S.-K., Lee, M.-E., Lee, W., Ahn, Y. 2019. Improved hydrogen recovery in microbial electrolysis cells using intermittent energy input. *International Journal of Hydrogen Energy*, **44**(4), 2253-2257.

Choi, G., Kim, H., Lee, C. 2021. Long-term monitoring of a thermal hydrolysis-anaerobic co-digestion plant treating high-strength organic wastes: Process performance and microbial community dynamics. *Bioresource Technology*, **319**, 124138.

Choi, J.-M., Lee, C.-Y. 2019. Bioelectrochemical enhancement of methane production in anaerobic digestion of food waste. *International Journal of Hydrogen Energy*, **44**(4), 2081-2090.

Clauwaert, P., Aelterman, P., De Schamphelaire, L., Carballa, M., Rabaey, K., Verstraete, W. 2008. Minimizing losses in bio-electrochemical systems: the road to applications. *Applied microbiology and biotechnology*, **79**(6), 901-913.

Clauwaert, P., Verstraete, W. 2009. Methanogenesis in membraneless microbial electrolysis cells. *Applied microbiology and biotechnology*, **82**, 829-836.

Cord-Ruwisch, R., Law, Y., Cheng, K.Y. 2011. Ammonium as a sustainable proton shuttle in bioelectrochemical systems. *Bioresource technology*, **102**(20), 9691-9696.

Csardi, G., Nepusz, T. 2006. The igraph software package for complex network research. *InterJournal, complex systems*, **1695**(5), 1-9.

Cusick, R.D., Logan, B.E. 2012. Phosphate recovery as struvite within a single chamber microbial electrolysis cell. *Bioresour Technol*, **107**, 110-5.

Dahiya, S., Sarkar, O., Swamy, Y., Mohan, S.V. 2015. Acidogenic fermentation of food waste for

volatile fatty acid production with co-generation of biohydrogen. *Bioresource technology*, **182**, 103-113.

De Graaff, M.S., Temmink, H., Zeeman, G., Buisman, C.J.N. 2010. Anaerobic Treatment of Concentrated Black Water in a UASB Reactor at a Short HRT. *Water*, **2**(1), 101-119.

De Vrieze, J., Saunders, A.M., He, Y., Fang, J., Nielsen, P.H., Verstraete, W., Boon, N. 2015. Ammonia and temperature determine potential clustering in the anaerobic digestion microbiome. *Water research*, **75**, 312-323.

Deligiorgis, A., Xekoukoulotakis, N.P., Diamadopoulos, E., Mantzavinos, D. 2008. Electrochemical oxidation of table olive processing wastewater over boron-doped diamond electrodes: treatment optimization by factorial design. *Water Res*, **42**(4-5), 1229-37.

Dhaked, R.K., Singh, P., Singh, L. 2010. Biomethanation under psychrophilic conditions. *Waste Manag*, **30**(12), 2490-6.

Dhar, B.R., Elbeshbishy, E., Hafez, H., Nakhla, G., Ray, M.B. 2011. Thermo-oxidative pretreatment of municipal waste activated sludge for volatile sulfur compounds removal and enhanced anaerobic digestion. *Chemical engineering journal*, **174**(1), 166-174.

Dhar, B.R., Gao, Y., Yeo, H., Lee, H.S. 2013. Separation of competitive microorganisms using anaerobic membrane bioreactors as pretreatment to microbial electrochemical cells. *Bioresour Technol*, **148**, 208-14.

Dhar, B.R., Lee, H.-S. 2013. Membranes for bioelectrochemical systems: challenges and research advances. *Environmental technology*, **34**(13-14), 1751-1764.

Dhar, B.R., Nakhla, G., Ray, M.B. 2012. Techno-economic evaluation of ultrasound and thermal pretreatments for enhanced anaerobic digestion of municipal waste activated sludge. *Waste management*, **32**(3), 542-549.

Dhar, B.R., Park, J.-H., Park, H.-D., Lee, H.-S. 2019. Hydrogen-based syntrophy in an electrically conductive biofilm anode. *Chemical Engineering Journal*, **359**, 208-216.

Dhar, B.R., Ryu, H., Santo Domingo, J.W., Lee, H.-S. 2016. Ohmic resistance affects microbial

community and electrochemical kinetics in a multi-anode microbial electrochemical cell. *Journal of Power Sources*, **331**, 315-321.

Duan, N., Dong, B., Wu, B., Dai, X. 2012. High-solid anaerobic digestion of sewage sludge under mesophilic conditions: feasibility study. *Bioresource technology*, **104**, 150-156.

Dyksma, S., Jansen, L., Gallert, C. 2020. Syntrophic acetate oxidation replaces acetoclastic methanogenesis during thermophilic digestion of biowaste. *Microbiome*, **8**(1), 105.

El-Mashad, H.M., Zeeman, G., Van Loon, W.K., Bot, G.P., Lettinga, G. 2004. Effect of temperature and temperature fluctuation on thermophilic anaerobic digestion of cattle manure. *Bioresource technology*, **95**(2), 191-201.

Enright, A.-M., McGrath, V., Gill, D., Collins, G., O'Flaherty, V. 2009. Effect of seed sludge and operation conditions on performance and archaeal community structure of low-temperature anaerobic solvent-degrading bioreactors. *Systematic and applied microbiology*, **32**(1), 65-79.

Escapa, A., San-Martin, M.I., Mateos, R., Moran, A. 2015. Scaling-up of membraneless microbial electrolysis cells (MECs) for domestic wastewater treatment: Bottlenecks and limitations. *Bioresour Technol*, **180**, 72-8.

Esquivel-Elizondo, S., Parameswaran, P., Delgado, A.G., Maldonado, J., Rittmann, B.E., Krajmalnik-Brown, R. 2016. Archaea and bacteria acclimate to high total ammonia in a methanogenic reactor treating swine waste. *Archaea*, **2016**.

Fan, Y., Sharbrough, E., Liu, H. 2008. Quantification of the internal resistance distribution of microbial fuel cells. *Environmental science & technology*, **42**(21), 8101-8107.

Federation, W.E., Association, A.P.H. 2005. Standard methods for the examination of water and wastewater. *American Public Health Association (APHA): Washington, DC, USA*.

Feng, H., Wang, Y., Zhang, X., Shen, D., Li, N., Chen, W., Huang, B., Liang, Y., Zhou, Y. 2017. Degradation of p-fluoronitrobenzene in biological and bioelectrochemical systems: differences in kinetics, pathways, and microbial community evolutions. *Chemical Engineering Journal*, **314**, 232-239.

Feng, Q., Song, Y.-C., Kim, D.-H., Kim, M.-S., Kim, D.-H. 2018. Influence of the temperature and hydraulic retention time in bioelectrochemical anaerobic digestion of sewage sludge. *International Journal of Hydrogen Energy*.

Feng, Q., Song, Y.C., Bae, B.U. 2016. Influence of applied voltage on the performance of bioelectrochemical anaerobic digestion of sewage sludge and planktonic microbial communities at ambient temperature. *Bioresour Technol*, **220**, 500-508.

Feng, Y., Zhang, Y., Chen, S., Quan, X. 2015. Enhanced production of methane from waste activated sludge by the combination of high-solid anaerobic digestion and microbial electrolysis cell with iron–graphite electrode. *Chemical Engineering Journal*, **259**, 787-794.

Florencio, L., Field, J., Lettinga, G. 1997. High-rate anaerobic treatment of alcoholic wastewaters. *Brazilian Journal of Chemical Engineering*, **14**(4).

Florencio, L., Field, J., Van Langerak, A., Lettinga, G. 1996. pH-stability in anaerobic bioreactors treating methanolic wastewaters. *Water Science and Technology*, **33**(3), 177-184.

Florentino, A.P., Sharaf, A., Zhang, L., Liu, Y. 2019a. Overcoming ammonia inhibition in anaerobic blackwater treatment with granular activated carbon: the role of electroactive microorganisms. *Environmental Science: Water Research & Technology*, **5**(2), 383-396.

Florentino, A.P., Xu, R., Zhang, L., Liu, Y. 2019b. Anaerobic digestion of blackwater assisted by granular activated carbon: From digestion inhibition to methanogenesis enhancement. *Chemosphere*.

Fogel, R., Limson, J. 2016. Applications of nanomaterials in microbial fuel cells. in: *Nanomaterials for Fuel Cell Catalysis*, Springer, pp. 551-575.

Friman, H., Schechter, A., Ioffe, Y., Nitzan, Y., Cahan, R. 2013. Current production in a microbial fuel cell using a pure culture of C upriavidus basilensis growing in acetate or phenol as a carbon source. *Microbial biotechnology*, **6**(4), 425-434.

Fuchs, G., Boll, M., Heider, J. 2011. Microbial degradation of aromatic compounds—from one strategy to four. *Nature Reviews Microbiology*, **9**(11), 803.

Gacitúa, M.A., Muñoz, E., González, B. 2018. Bioelectrochemical sulphate reduction on batch reactors: Effect of inoculum-type and applied potential on sulphate consumption and pH. *Bioelectrochemistry*, **119**, 26-32.

Gajaraj, S., Huang, Y., Zheng, P., Hu, Z. 2017. Methane production improvement and associated methanogenic assemblages in bioelectrochemically assisted anaerobic digestion. *Biochemical Engineering Journal*, **117**, 105-112.

Gallagher, N., Sharvelle, S. 2011. Demonstration of anaerobic digestion of black water for methane capture and use in an office building. *Water Practice and Technology*, **6**(1).

Gallagher, N.T., Sharvelle, S.E. 2010. Decentralized anaerobic blackwater management: a sustainable development technology concept for urban water management. *Proceedings of the World Environmental and Water Resources Congress 2010, Providence, Rhode Island, USA, 16-20 May, 2010*. American Society of Civil Engineers (ASCE). pp. 4118-4128.

Gao, M., Guo, B., Zhang, L., Zhang, Y., Liu, Y. 2019a. Microbial community dynamics in anaerobic digesters treating conventional and vacuum toilet flushed blackwater. *Water research*, **160**, 249-258.

Gao, M., Guo, B., Zhang, L., Zhang, Y., Yu, N., Liu, Y. 2020a. Biomethane recovery from source-diverted household blackwater: Impacts from feed sulfate. *Process Safety and Environmental Protection*, **136**, 28-38.

Gao, M., Zhang, L., Florentino, A.P., Liu, Y. 2018. Performance of anaerobic treatment of blackwater collected from different toilet flushing systems: Can we achieve both energy recovery and water conservation? *J Hazard Mater*, **365**, 44-52.

Gao, M., Zhang, L., Guo, B., Zhang, Y., Liu, Y. 2019b. Enhancing biomethane recovery from source-diverted blackwater through hydrogenotrophic methanogenesis dominant pathway. *Chemical Engineering Journal*, **378**, 122258.

Gao, M., Zhang, L., Liu, Y. 2020b. High-loading food waste and blackwater anaerobic co-digestion: Maximizing bioenergy recovery. *Chemical Engineering Journal*, 124911.

Gao, Y., Sun, D., Dang, Y., Lei, Y., Ji, J., Lv, T., Bian, R., Xiao, Z., Yan, L., Holmes, D.E. 2017. Enhancing biomethanogenic treatment of fresh incineration leachate using single chambered microbial electrolysis cells. *Bioresour Technol*, **231**, 129-137.

Ghernaout, D., Ghernaout, B., Saiba, A., Boucherit, A., Kellil, A. 2009. Removal of humic acids by continuous electromagnetic treatment followed by electrocoagulation in batch using aluminium electrodes. *Desalination*, **239**(1-3), 295-308.

Govahi, S., Karimi-Jashni, A., Derakhshan, M. 2011. Treatability of landfill leachate by combined upflow anaerobic sludge blanket reactor and aerated lagoon. *International Journal of Environmental Science and Technology*, **9**(1), 145-151.

Grady Jr, C.L., Daigger, G.T., Love, N.G., Filipe, C.D. 2011. *Biological wastewater treatment*. CRC press.

Gunay, A., Karadag, D., Tosun, I., Ozturk, M. 2008. Combining Anerobic Degradation and Chemical Precipitation for the Treatment of High Strength, Strong Nitrogenous Landfill Leachate. *CLEAN - Soil, Air, Water*, **36**(10-11), 887-892.

Guo, B., Zhang, L., Sun, H., Gao, M., Yu, N., Zhang, Q., Mou, A., Liu, Y. 2022. Microbial co-occurrence network topological properties link with reactor parameters and reveal importance of low-abundance genera. *npj Biofilms and Microbiomes*, **8**(1), 3.

Guo, X., Liu, J., Xiao, B. 2013. Bioelectrochemical enhancement of hydrogen and methane production from the anaerobic digestion of sewage sludge in single-chamber membrane-free microbial electrolysis cells. *International Journal of Hydrogen Energy*, **38**(3), 1342-1347.

Hagos, K., Liu, C., Lu, X. 2018. Effect of endogenous hydrogen utilization on improved methane production in an integrated microbial electrolysis cell and anaerobic digestion: Employing catalyzed stainless steel mesh cathode. *Chinese Journal of Chemical Engineering*, **26**(3), 574-582.

Hall, M., Beiko, R.G. 2018. 16S rRNA gene analysis with QIIME2. in: *Microbiome Analysis*, Springer, pp. 113-129.

Hamdi, M. 1992. Toxicity and biodegradability of olive mill wastewaters in batch anaerobic digestion. *Applied Biochemistry and Biotechnology*, **37**(2), 155-163.

Hamza, R.A., Iorhemen, O.T., Tay, J.H. 2016. Advances in biological systems for the treatment of high-strength wastewater. *Journal of Water Process Engineering*, **10**, 128-142.

Hao, J., Wang, H. 2015. Volatile fatty acids productions by mesophilic and thermophilic sludge fermentation: biological responses to fermentation temperature. *Bioresource technology*, **175**, 367-373.

Hobbs, S.R., Landis, A.E., Rittmann, B.E., Young, M.N., Parameswaran, P. 2018. Enhancing anaerobic digestion of food waste through biochemical methane potential assays at different substrate: inoculum ratios. *Waste Manag*, **71**, 612-617.

Hong, W., Zhang, J., Feng, Y., Mohr, G., Lambowitz, A.M., Cui, G.-Z., Liu, Y.-J., Cui, Q. 2014. The contribution of cellulosomal scaffoldins to cellulose hydrolysis by Clostridium thermocellum analyzed by using thermotargetrons. *Biotechnology for biofuels*, **7**(1), 1-17.

Hou, Y., Zhang, R., Luo, H., Liu, G., Kim, Y., Yu, S., Zeng, J. 2015. Microbial electrolysis cell with spiral wound electrode for wastewater treatment and methane production. *Process Biochemistry*, **50**(7), 1103-1109.

Hu, Y., Jing, Z., Sudo, Y., Niu, Q., Du, J., Wu, J., Li, Y.-Y. 2015. Effect of influent COD/SO42− ratios on UASB treatment of a synthetic sulfate-containing wastewater. *Chemosphere*, **130**, 24-33.

Huang, D.-Y., Zhou, S.-G., Chen, Q., Zhao, B., Yuan, Y., Zhuang, L. 2011. Enhanced anaerobic degradation of organic pollutants in a soil microbial fuel cell. *Chemical Engineering Journal*, **172**(2-3), 647-653.

Huang, J., Zeng, C., Luo, H., Bai, J., Liu, G., Zhang, R. 2022a. Enhanced sulfur recovery and sulfate reduction using single-chamber bioelectrochemical system. *Science of The Total Environment*, **823**, 153789.

Huang, Q., Liu, Y., Dhar, B.R. 2023. Boosting resilience of microbial electrolysis cell-assisted anaerobic digestion of blackwater with granular activated carbon amendment. *Bioresource*

Technology, **381**, 129136.

Huang, Q., Liu, Y., Dhar, B.R. 2020a. A critical review of microbial electrolysis cells coupled with anaerobic digester for enhanced biomethane recovery from high-strength feedstocks. *Critical Reviews in Environmental Science and Technology*, 1-40.

Huang, Q., Liu, Y., Dhar, B.R. 2022b. A critical review of microbial electrolysis cells coupled with anaerobic digester for enhanced biomethane recovery from high-strength feedstocks. *Critical Reviews in Environmental Science and Technology*, **52**(1), 50-89.

Huang, Q., Liu, Y., Dhar, B.R. 2022c. A multifaceted screening of applied voltages for electro-assisted anaerobic digestion of blackwater: Significance of temperature, hydrolysis/acidogenesis, electrode corrosion, and energy efficiencies. *Bioresource Technology*, **360**, 127533.

Huang, Q., Liu, Y., Dhar, B.R. 2021. Pushing the organic loading rate in electrochemically assisted anaerobic digestion of Blackwater at ambient temperature: Insights into microbial community dynamics. *Science of The Total Environment*, 146694.

Huang, Q., Zakaria, B.S., Zhang, Y., Zhang, L., Liu, Y., Dhar, B.R. 2020b. A high-rate anaerobic biofilm reactor for biomethane recovery from source-separated blackwater at ambient temperature. *Water Environment Research*.

Hulshoff, L., Lens, P., Weijma, J., Stams, A. 2001. New developments in reactor and process technology for sulfate reduction. *Water Science and Technology*, **44**(8), 67-76.

Jadhav, D.A., Park, S.-G., Pandit, S., Yang, E., Abdelkareem, M.A., Jang, J.-K., Chae, K.-J. 2022. Scalability of microbial electrochemical technologies: Applications and challenges. *Bioresource Technology*, **345**, 126498.

Javier Benitez, F., Acero, J.L., Gonzalez, T., Garcia, J. 2001. Organic matter removal from wastewaters of the black olive industry by chemical and biological procedures. *Process Biochemistry*, **37**(3), 257-265.

Jegatheesan, V., Pramanik, B.K., Chen, J., Navaratna, D., Chang, C.-Y., Shu, L. 2016. Treatment of textile wastewater with membrane bioreactor: a critical review. *Bioresource technology*,

204, 202-212.

Jeong, T.-Y., Chung, H.-K., Yeom, S.H., Choi, S.S. 2009. Analysis of methane production inhibition for treatment of sewage sludge containing sulfate using an anaerobic continuous degradation process. *Korean journal of chemical engineering*, **26**, 1319-1322.

Johnravindar, D., Liang, B., Fu, R., Luo, G., Meruvu, H., Yang, S., Yuan, B., Fei, Q. 2020. Supplementing granular activated carbon for enhanced methane production in anaerobic co-digestion of post-consumer substrates. *Biomass and bioenergy*, **136**, 105543.

Ju, F., Xia, Y., Guo, F., Wang, Z., Zhang, T. 2014. Taxonomic relatedness shapes bacterial assembly in activated sludge of globally distributed wastewater treatment plants. *Environmental Microbiology*, **16**(8), 2421-2432.

Jung, H., Kim, D., Choi, H., Lee, C. 2022. A review of technologies for in-situ sulfide control in anaerobic digestion. *Renewable and Sustainable Energy Reviews*, **157**, 112068.

Kadier, A., Kalil, M.S., Abdeshahian, P., Chandrasekhar, K., Mohamed, A., Azman, N.F., Logroño, W., Simayi, Y., Hamid, A.A. 2016a. Recent advances and emerging challenges in microbial electrolysis cells (MECs) for microbial production of hydrogen and value-added chemicals. *Renewable and Sustainable Energy Reviews*, **61**, 501-525.

Kadier, A., Simayi, Y., Abdeshahian, P., Azman, N.F., Chandrasekhar, K., Kalil, M.S. 2016b. A comprehensive review of microbial electrolysis cells (MEC) reactor designs and configurations for sustainable hydrogen gas production. *Alexandria Engineering Journal*, **55**(1), 427-443.

Kaiyrlykyzy, A., Kozhakhmetov, S., Babenko, D., Zholdasbekova, G., Alzhanova, D., Olzhayev, F., Baibulatova, A., Kushugulova, A.R., Askarova, S. 2022. Study of gut microbiota alterations in Alzheimer's dementia patients from Kazakhstan. *Scientific Reports*, **12**(1), 15115.

Kale, V., Katikaneni, S., Cheryan, M. 1999. Deacidifying rice bran oil by solvent extraction and membrane technology. *Journal of the American Oil Chemists' Society*, **76**(6), 723-727.

Kamali, M., Gameiro, T., Costa, M.E.V., Capela, I. 2016. Anaerobic digestion of pulp and paper

mill wastes–An overview of the developments and improvement opportunities. *Chemical Engineering Journal*, **298**, 162-182.

Kanehisa, M., Goto, S., Sato, Y., Furumichi, M., Tanabe, M. 2012. KEGG for integration and interpretation of large-scale molecular data sets. *Nucleic acids research*, **40**(D1), D109-D114.

Kardos, L., Juhasz, A., Palko, G., Olah, J., Barkacs, K., Zaray, G. 2011. Comparing of mesophilic and thermophilic anaerobic fermented sewage sludge based on chemical and biochemical tests. *Applied Ecology and Environmental Research*, **9**(3), 293-302.

Karekar, S., Stefanini, R., Ahring, B. 2022. Homo-acetogens: Their metabolism and competitive relationship with hydrogenotrophic methanogens. *Microorganisms*, **10**(2), 397.

Karhu, M., Leiviskä, T., Tanskanen, J. 2014. Enhanced DAF in breaking up oil-in-water emulsions. *Separation and Purification Technology*, **122**, 231-241.

Katakojwala, R., Tharak, A., Sarkar, O., Mohan, S.V. 2022. Design and evaluation of gas fermentation systems for CO2 reduction to C2 and C4 fatty acids: Non-genetic metabolic regulation with pressure, pH and reaction time. *Bioresource Technology*, **351**, 126937.

Katsoni, A., Frontistis, Z., Xekoukoulotakis, N.P., Diamadopoulos, E., Mantzavinos, D. 2008. Wet air oxidation of table olive processing wastewater: determination of key operating parameters by factorial design. *Water Res*, **42**(14), 3591-600.

Kawai, M., Kishi, M., Hamersley, M., Nagao, N., Hermana, J., Toda, T. 2012. Biodegradability and methane productivity during anaerobic co-digestion of refractory leachate. *International biodeterioration & biodegradation*, **72**, 46-51.

Kelly, P.T., He, Z. 2014. Nutrients removal and recovery in bioelectrochemical systems: a review. *Bioresource technology*, **153**, 351-360.

Khalid, A., Arshad, M., Anjum, M., Mahmood, T., Dawson, L. 2011. The anaerobic digestion of solid organic waste. *Waste management*, **31**(8), 1737-1744.

Kiely, P.D., Regan, J.M., Logan, B.E. 2011. The electric picnic: synergistic requirements for exoelectrogenic microbial communities. *Current opinion in biotechnology*, **22**(3), 378-385.

Kiilerich, B., Van de Ven, W., Nielsen, A.H., Vollertsen, J. 2017. Sulfide precipitation in wastewater at short timescales. *Water*, **9**(9), 670.

Kim, J.R., Cheng, S., Oh, S.-E., Logan, B.E. 2007. Power generation using different cation, anion, and ultrafiltration membranes in microbial fuel cells. *Environmental science & technology*, **41**(3), 1004-1009.

Kim, S.I., Aghasa, A., Choi, S., Hong, S., Park, T., Hwang, S. 2022. Variations in Lipid Accumulation and Methanogenic Predominance in Full-Scale Anerobic Digestors Treating Food Waste Leachate. *Waste and Biomass Valorization*, 1-12.

Kiyuna, L.S.M., Fuess, L.T., Zaiat, M. 2017. Unraveling the influence of the COD/sulfate ratio on organic matter removal and methane production from the biodigestion of sugarcane vinasse. *Bioresource Technology*, **232**, 103-112.

Kobayashi, T., Yan, F., Takahashi, S., Li, Y.Y. 2011. Effect of starch addition on the biological conversion and microbial community in a methanol-fed UASB reactor during long-term continuous operation. *Bioresour Technol*, **102**(17), 7713-9.

Kolde, R., Kolde, M.R. 2015. Package 'pheatmap'. *R package*, **1**(7), 790.

Kong, Z., Li, L., Xue, Y., Yang, M., Li, Y.-Y. 2019. Challenges and prospects for the anaerobic treatment of chemical-industrial organic wastewater: a review. *Journal of cleaner production*, **231**, 913-927.

Koo, H., Hakim, J.A., Morrow, C.D., Eipers, P.G., Davila, A., Andersen, D.T., Bej, A.K. 2017. Comparison of two bioinformatics tools used to characterize the microbial diversity and predictive functional attributes of microbial mats from Lake Obersee, Antarctica. *Journal of microbiological methods*, **140**, 15-22.

Koprivova, A., Kopriva, S. 2014. Molecular mechanisms of regulation of sulfate assimilation: first steps on a long road. *Frontiers in plant science*, **5**, 589.

Kopsidas, G. 1992. Wastewater from the preparation of table olives. *Water Research*, **26**(5), 629-631.

Kopsidas, G. 1994. Wastewater from the table olive industry. *Water Research*, **28**(1), 201-205.

Kothari, R., Tyagi, V., Pathak, A. 2010. Waste-to-energy: A way from renewable energy sources to sustainable development. *Renewable and Sustainable Energy Reviews*, **14**(9), 3164-3170.

Kousar, A., Peltola, E., Laurila, T. 2021. Nanostructured geometries strongly affect fouling of carbon electrodes. *ACS omega*, **6**(40), 26391-26403.

Krayzelova, L., Bartacek, J., Díaz, I., Jeison, D., Volcke, E.I., Jenicek, P. 2015. Microaeration for hydrogen sulfide removal during anaerobic treatment: a review. *Reviews in Environmental Science and Bio/Technology*, **14**, 703-725.

Kujawa-Roeleveld, K., Elmitwalli, T., Zeeman, G. 2006. Enhanced primary treatment of concentrated black water and kitchen residues within DESAR concept using two types of anaerobic digesters. *Water Science and Technology*, **53**(9), 159-168.

Kujawa-Roeleveld, K., Fernandes, T., Wiryawan, Y., Tawfik, A., Visser, M., Zeeman, G. 2005. Performance of UASB septic tank for treatment of concentrated black water within DESAR concept. *Water Science and Technology*, **52**(1-2), 307-313.

Kujawa-Roeleveld, K., Zeeman, G. 2006. Anaerobic treatment in decentralised and source-separation-based sanitation concepts. *Reviews in Environmental Science and Bio/Technology*, **5**(1), 115-139.

Kumar, A.N., Bandarapu, A.K., Mohan, S.V. 2019. Microbial electro-hydrolysis of sewage sludge for acidogenic production of biohydrogen and volatile fatty acids along with struvite. *Chemical Engineering Journal*, **374**, 1264-1274.

Kuntke, P., Geleji, M., Bruning, H., Zeeman, G., Hamelers, H., Buisman, C. 2011. Effects of ammonium concentration and charge exchange on ammonium recovery from high strength wastewater using a microbial fuel cell. *Bioresource technology*, **102**(6), 4376-4382.

Kuntke, P., Śmiech, K., Bruning, H., Zeeman, G., Saakes, M., Sleutels, T., Hamelers, H., Buisman, C. 2012. Ammonium recovery and energy production from urine by a microbial fuel cell. *Water research*, **46**(8), 2627-2636.

Kyriacou, A., Lasaridi, K., Kotsou, M., Balis, C., Pilidis, G. 2005. Combined bioremediation and

advanced oxidation of green table olive processing wastewater. *Process Biochemistry*, **40**(3-4), 1401-1408.

LaBarge, N., Yilmazel, Y.D., Hong, P.-Y., Logan, B.E. 2017. Effect of pre-acclimation of granular activated carbon on microbial electrolysis cell startup and performance. *Bioelectrochemistry*, **113**, 20-25.

Labatut, R.A., Angenent, L.T., Scott, N.R. 2014. Conventional mesophilic vs. thermophilic anaerobic digestion: a trade-off between performance and stability? *Water research*, **53**, 249-258.

Langille, M.G., Zaneveld, J., Caporaso, J.G., McDonald, D., Knights, D., Reyes, J.A., Clemente, J.C., Burkepile, D.E., Thurber, R.L.V., Knight, R. 2013. Predictive functional profiling of microbial communities using 16S rRNA marker gene sequences. *Nature biotechnology*, **31**(9), 814-821.

Lee, B., Park, J.G., Shin, W.B., Tian, D.J., Jun, H.B. 2017. Microbial communities change in an anaerobic digestion after application of microbial electrolysis cells. *Bioresour Technol*, **234**, 273-280.

Levén, L., Eriksson, A.R., Schnürer, A. 2007. Effect of process temperature on bacterial and archaeal communities in two methanogenic bioreactors treating organic household waste. *FEMS microbiology ecology*, **59**(3), 683-693.

Li, B., Zhang, C., Jin, C., Wu, J., Li, P. 2023. Intermediate Accumulation and Process Stability for Facultative and Obligate Anaerobic Treatment of Leachate from Waste Transfer Stations. *Fermentation*, **9**(5), 465.

Li, D., Liu, J., Qu, Y., Wang, H., Feng, Y. 2016a. Analysis of the effect of biofouling distribution on electricity output in microbial fuel cells. *Rsc Advances*, **6**(33), 27494-27500.

Li, H., Li, C., Liu, W., Zou, S. 2012a. Optimized alkaline pretreatment of sludge before anaerobic digestion. *Bioresource Technology*, **123**, 189-194.

Li, J., Ban, Q., Zhang, L., Jha, A.K. 2012b. Syntrophic propionate degradation in anaerobic digestion: a review. *International Journal of Agriculture and Biology*, **14**(5).

Li, J., Rui, J., Yao, M., Zhang, S., Yan, X., Wang, Y., Yan, Z., Li, X. 2015a. Substrate type and free ammonia determine bacterial community structure in full-scale mesophilic anaerobic digesters treating cattle or swine manure. *Frontiers in microbiology*, **6**, 1337.

Li, W., Niu, Q., Zhang, H., Tian, Z., Zhang, Y., Gao, Y., Li, Y.-Y., Nishimura, O., Yang, M. 2015b. UASB treatment of chemical synthesis-based pharmaceutical wastewater containing rich organic sulfur compounds and sulfate and associated microbial characteristics. *Chemical Engineering Journal*, **260**, 55-63.

Li, Y., Han, Y., Zhang, Y., Luo, W., Li, G. 2020. Anaerobic digestion of different agricultural wastes: A techno-economic assessment. *Bioresource Technology*, **315**, 123836.

Li, Y., Zhang, Y., Liu, Y., Zhao, Z., Zhao, Z., Liu, S., Zhao, H., Quan, X. 2016b. Enhancement of anaerobic methanogenesis at a short hydraulic retention time via bioelectrochemical enrichment of hydrogenotrophic methanogens. *Bioresour Technol*, **218**, 505-11.

Li, Y., Zhang, Y., Yang, Y., Quan, X., Zhao, Z. 2017. Potentially direct interspecies electron transfer of methanogenesis for syntrophic metabolism under sulfate reducing conditions with stainless steel. *Bioresource technology*, **234**, 303-309.

Lin, C.-Y., Lay, C.-H., Chen, C.-C. 2017. High-strength wastewater treatment using anaerobic processes. in: *Current Developments in Biotechnology and Bioengineering*, Elsevier, pp. 321-357.

Lin, Y., He, Y., Meng, Z., Yang, S. 2008. Anaerobic treatment of wastewater containing methanol in upflow anaerobic sludge bed (UASB) reactor. *Frontiers of Environmental Science & Engineering in China*, **2**(2), 241-246.

Linji, X., Wenzong, L., Yining, W., Aijie, W., Shuai, L., Wei, J. 2013. Optimizing external voltage for enhanced energy recovery from sludge fermentation liquid in microbial electrolysis cell. *International Journal of Hydrogen Energy*, **38**(35), 15801-15806.

Liu, C., Sun, D., Zhao, Z., Dang, Y., Holmes, D.E. 2019. Methanothrix enhances biogas upgrading in microbial electrolysis cell via direct electron transfer. *Bioresource technology*, **291**, 121877.

Liu, D., Zhang, L., Chen, S., Buisman, C., Ter Heijne, A. 2016a. Bioelectrochemical enhancement of methane production in low temperature anaerobic digestion at 10 degrees C. *Water Res*, **99**, 281-287.

Liu, H., Lv, Y., Xu, S., Chen, Z., Lichtfouse, E. 2020. Configuration and rapid start-up of a novel combined microbial electrolytic process treating fecal sewage. *Science of the Total Environment*, **705**, 135986.

Liu, J., Hu, J., Zhong, J., Luo, J., Zhao, A., Liu, F., Hong, R., Qian, G., Xu, Z.P. 2011. The effect of calcium on the treatment of fresh leachate in an expanded granular sludge bed bioreactor. *Bioresour Technol*, **102**(9), 5466-72.

Liu, J., Luo, J., Zhou, J., Liu, Q., Qian, G., Xu, Z.P. 2012. Inhibitory effect of high-strength ammonia nitrogen on bio-treatment of landfill leachate using EGSB reactor under mesophilic and atmospheric conditions. *Bioresour Technol*, **113**, 239-43.

Liu, J., Zhong, J., Wang, Y., Liu, Q., Qian, G., Zhong, L., Guo, R., Zhang, P., Xu, Z.P. 2010. Effective bio-treatment of fresh leachate from pretreated municipal solid waste in an expanded granular sludge bed bioreactor. *Bioresour Technol*, **101**(5), 1447-52.

Liu, W., Cai, W., Guo, Z., Wang, L., Yang, C., Varrone, C., Wang, A. 2016b. Microbial electrolysis contribution to anaerobic digestion of waste activated sludge, leading to accelerated methane production. *Renewable Energy*, **91**, 334-339.

Liu, Y., Zhang, J., Cao, X., Sakamaki, T., Li, X. 2023. Performance and mechanism of microbial fuel cell coupled with anaerobic membrane bioreactor system for fouling control. *Bioresource Technology*, **374**, 128760.

Logan, B.E. 2009. Exoelectrogenic bacteria that power microbial fuel cells. *Nature Reviews Microbiology*, **7**(5), 375.

Logan, B.E., Call, D., Cheng, S., Hamelers, H.V.M., Sleutels, T.H.J.A., Jeremiasse, A.W., Rozendal, R.A. 2008. Microbial Electrolysis Cells for High Yield Hydrogen Gas Production from Organic Matter. *Environmental Science & Technology*, **42**(23), 8630-8640.

Logan, B.E., Rabaey, K. 2012. Conversion of wastes into bioelectricity and chemicals by using microbial electrochemical technologies. *Science*, **337**(6095), 686-690.

Logan, B.E., Rossi, R., Saikaly, P.E. 2019. Electroactive microorganisms in bioelectrochemical systems. *Nature Reviews Microbiology*, **17**(5), 307-319.

Lopes, S., Wang, X., Capela, M., Lens, P. 2007. Effect of COD/SO42− ratio and sulfide on thermophilic (55° C) sulfate reduction during the acidification of sucrose at pH 6. *Water Research*, **41**(11), 2379-2392.

Lovley, D.R., Ueki, T., Zhang, T., Malvankar, N.S., Shrestha, P.M., Flanagan, K.A., Aklujkar, M., Butler, J.E., Giloteaux, L., Rotaru, A.-E. 2011. Geobacter: the microbe electric's physiology, ecology, and practical applications. in: *Advances in microbial physiology*, Vol. 59, Elsevier, pp. 1-100.

Lü, F., Hao, L., Zhu, M., Shao, L., He, P. 2012. Initiating methanogenesis of vegetable waste at low inoculum-to-substrate ratio: importance of spatial separation. *Bioresource technology*, **105**, 169-173.

Lu, X., Zhen, G., Chen, M., Kubota, K., Li, Y.-Y. 2015. Biocatalysis conversion of methanol to methane in an upflow anaerobic sludge blanket (UASB) reactor: long-term performance and inherent deficiencies. *Bioresource technology*, **198**, 691-700.

Lu, X., Zhen, G., Ni, J., Hojo, T., Kubota, K., Li, Y.-Y. 2016. Effect of influent COD/SO42− ratios on biodegradation behaviors of starch wastewater in an upflow anaerobic sludge blanket (UASB) reactor. *Bioresource technology*, **214**, 175-183.

Lu, X., Zhen, G., Ni, J., Kubota, K., Li, Y.Y. 2017. Sulfidogenesis process to strengthen re-granulation for biodegradation of methanolic wastewater and microorganisms evolution in an UASB reactor. *Water Res*, **108**, 137-150.

Luis Campos, J., Garrido, J.M., Méndez, R., Lema, J.M. 2001. Effect of two broad-spectrum antibiotics on activity and stability of continuous nitrifying system. *Applied biochemistry and biotechnology*, **95**, 1-10.

Luo, H., Fu, S., Liu, G., Zhang, R., Bai, Y., Luo, X. 2014. Autotrophic biocathode for high efficient

sulfate reduction in microbial electrolysis cells. *Bioresource technology*, **167**, 462-468.

Luo, H., Liu, G., Zhang, R., Jin, S. 2009. Phenol degradation in microbial fuel cells. *Chemical Engineering Journal*, **147**(2-3), 259-264.

Luostarinen, S., Rintala, J. 2007. Anaerobic on-site treatment of kitchen waste in combination with black water in UASB-septic tanks at low temperatures. *Bioresour Technol*, **98**(9), 1734-40.

Luostarinen, S., Sanders, W., Kujawa-Roeleveld, K., Zeeman, G. 2007. Effect of temperature on anaerobic treatment of black water in UASB-septic tank systems. *Bioresour Technol*, **98**(5), 980-6.

Ma, K.-l., Li, X.-k., Wang, K., Meng, L.-w., Liu, G.-g., Zhang, J. 2017. Establishment of thermophilic anaerobic terephthalic acid degradation system through one-step temperature increase startup strategy–Revealed by Illumina Miseq Sequencing. *Chemosphere*, **184**, 951-959.

Mahmoud, M., Parameswaran, P., Torres, C.I., Rittmann, B.E. 2014. Fermentation pre-treatment of landfill leachate for enhanced electron recovery in a microbial electrolysis cell. *Bioresour Technol*, **151**, 151-8.

Maier, R.M., Pepper, I.L. 2015. Bacterial growth. in: *Environmental microbiology*, Elsevier, pp. 37-56.

Majone, M., Aulenta, F., Dionisi, D., D'Addario, E.N., Sbardellati, R., Bolzonella, D., Beccari, M. 2010. High-rate anaerobic treatment of Fischer-Tropsch wastewater in a packed-bed biofilm reactor. *Water Res*, **44**(9), 2745-52.

Mao, C., Feng, Y., Wang, X., Ren, G. 2015. Review on research achievements of biogas from anaerobic digestion. *Renewable and Sustainable Energy Reviews*, **45**, 540-555.

Mara, D., Horan, N.J. 2003. *Handbook of water and wastewater microbiology*. Elsevier.

Marone, A., Carmona-Martinez, A.A., Sire, Y., Meudec, E., Steyer, J.P., Bernet, N., Trably, E. 2016. Bioelectrochemical treatment of table olive brine processing wastewater for biogas production and phenolic compounds removal. *Water Res*, **100**, 316-325.

Maroušek, J., Minofar, B., Marousková, A., Strunecký, O., Gavurová, B. 2023. Environmental and economic advantages of production and application of digestate biochar. *Environmental Technology & Innovation*, **30**, 103109.

Maroušek, J., Strunecký, O., Kolář, L., Vochozka, M., Kopecký, M., Marousková, A., Batt, J., Poliak, M., Šoch, M., Bartoš, P. 2020. Advances in nutrient management make it possible to accelerate biogas production and thus improve the economy of food waste processing. *Energy Sources, Part A: Recovery, Utilization, and Environmental Effects*, 1-10.

Maurer, F., Christl, I., Hoffmann, M., Kretzschmar, R. 2012. Reduction and reoxidation of humic acid: influence on speciation of cadmium and silver. *Environ Sci Technol*, **46**(16), 8808-16.

Maurer, F., Christl, I., Kretzschmar, R. 2010. Reduction and reoxidation of humic acid: influence on spectroscopic properties and proton binding. *Environ Sci Technol*, **44**(15), 5787-92.

McAteer, P.G., Trego, A.C., Thorn, C., Mahony, T., Abram, F., O'Flaherty, V. 2020. Reactor configuration influences microbial community structure during high-rate, low-temperature anaerobic treatment of dairy wastewater. *Bioresource technology*, **307**, 123221.

McCarty, P.L., Bae, J., Kim, J. 2011. Domestic wastewater treatment as a net energy producer–can this be achieved?, ACS Publications.

McDonald, D., Jiang, Y., Balaban, M., Cantrell, K., Zhu, Q., Gonzalez, A., Morton, J.T., Nicolaou, G., Parks, D.H., Karst, S.M. 2023. Greengenes2 unifies microbial data in a single reference tree. *Nature biotechnology*, 1-4.

McDonald, D., Price, M.N., Goodrich, J., Nawrocki, E.P., DeSantis, T.Z., Probst, A., Andersen, G.L., Knight, R., Hugenholtz, P. 2012. An improved Greengenes taxonomy with explicit ranks for ecological and evolutionary analyses of bacteria and archaea. *The ISME journal*, **6**(3), 610.

Metcalf, E., Eddy, M. 2014. Wastewater engineering: treatment and Resource recovery. *Mic Graw-Hill, USA*, 1530-1533.

Mo, Y., Liang, P., Huang, X., Wang, H., Cao, X. 2009. Enhancing the stability of power generation

of single-chamber microbial fuel cells using an anion exchange membrane. *Journal of Chemical Technology & Biotechnology*, **84**(12), 1767-1772.

Moges, M.E., Todt, D., Janka, E., Heistad, A., Bakke, R. 2018. Sludge blanket anaerobic baffled reactor for source-separated blackwater treatment. *Water Science and Technology*.

Mohan, S.V., Pandey, A., Varjani, S. 2018. *Biomass, Biofuels, Biochemicals: Microbial Electrochemical Technology: Sustainable Platform for Fuels, Chemicals and Remediation*. Elsevier.

Moreno, R., San-Martín, M., Escapa, A., Morán, A. 2016. Domestic wastewater treatment in parallel with methane production in a microbial electrolysis cell. *Renewable Energy*, **93**, 442-448.

Müller, B., Sun, L., Schnürer, A. 2013. First insights into the syntrophic acetate-oxidizing bacteria–a genetic study. *MicrobiologyOpen*, **2**(1), 35-53.

Müller, B., Sun, L., Westerholm, M., Schnürer, A. 2016. Bacterial community composition and fhs profiles of low-and high-ammonia biogas digesters reveal novel syntrophic acetate-oxidising bacteria. *Biotechnology for biofuels*, **9**(1), 48.

Mutamim, N.S.A., Noor, Z.Z., Hassan, M.A.A., Olsson, G. 2012. Application of membrane bioreactor technology in treating high strength industrial wastewater: a performance review. *Desalination*, **305**, 1-11.

Muyzer, G., Stams, A.J. 2008. The ecology and biotechnology of sulphate-reducing bacteria. *Nature reviews microbiology*, **6**(6), 441-454.

Nayono, S.E., Winter, J., Gallert, C. 2010. Anaerobic digestion of pressed off leachate from the organic fraction of municipal solid waste. *Waste Manag*, **30**(10), 1828-33.

Niaounakis, M., Halvadakis, C.P. 2004. *Olive-mill waste management: literature review and patent survey*. Dardanos.

Nie, E., He, P., Zhang, H., Hao, L., Shao, L., Lü, F. 2021. How does temperature regulate anaerobic digestion? *Renewable and Sustainable Energy Reviews*, **150**, 111453.

Nielsen, A.H., Hvitved-Jacobsen, T., Vollertsen, J. 2008. Effects of pH and Iron Concentrations

on Sulfide Precipitation in Wastewater Collection Systems. *Water Environment Research*, **80**(4), 380-384.

Nijs, H.H., Jacobs, P.A. 1981. On-Line Single Run Analysis of Effluents from a Fischer-Tropsch Reactor. *Journal of Chromatographic Science*, **19**(1), 40-45.

O'Reilly, C., Colleran, E. 2006. Effect of influent COD/SO42− ratios on mesophilic anaerobic reactor biomass populations: physico-chemical and microbiological properties. *FEMS microbiology ecology*, **56**(1), 141-153.

Oba, Y., Futagami, T., Amachi, S. 2014. Enrichment of a microbial consortium capable of reductive deiodination of 2, 4, 6-triiodophenol. *Journal of bioscience and bioengineering*, **117**(3), 310-317.

Oksanen, J., Blanchet, F.G., Kindt, R., Legendre, P., O'hara, R., Simpson, G.L., Solymos, P., Stevens, M.H.H., Wagner, H. 2010. Vegan: community ecology package. R package version 1.17-4. *URL http://CRAN. R-project. org/package= vegan*.

Oksanen, J., Kindt, R., Legendre, P., O'Hara, B., Stevens, M.H.H., Oksanen, M.J., Suggests, M. 2007. The vegan package. *Community ecology package*, **10**(631-637), 719.

Ozbayram, E., Ince, O., Ince, B., Harms, H., Kleinsteuber, S. 2018. Comparison of rumen and manure microbiomes and implications for the inoculation of anaerobic digesters. *Microorganisms*, **6**(1), 15.

Pal, S., Bhadauria, S.S., Kumar, P. 2021. Electrochemical corrosion behavior of type F304 stainless steel in different temperatures. *Journal of Bio-and Tribo-Corrosion*, **7**(2), 1-7.

Parameswaran, P., Torres, C.I., Lee, H.S., Krajmalnik-Brown, R., Rittmann, B.E. 2009. Syntrophic interactions among anode respiring bacteria (ARB) and Non-ARB in a biofilm anode: electron balances. *Biotechnology and bioengineering*, **103**(3), 513-523.

Parameswaran, P., Zhang, H., Torres, C.I., Rittmann, B.E., Krajmalnik-Brown, R. 2010. Microbial community structure in a biofilm anode fed with a fermentable substrate: the significance of hydrogen scavengers. *Biotechnology and bioengineering*, **105**(1), 69-78.

Paraskeva, P., Diamadopoulos, E. 2006. Technologies for olive mill wastewater (OMW) treatment:

a review. *Journal of Chemical Technology & Biotechnology*, **81**(9), 1475-1485.

Park, J.-G., Kwon, H.-J., Sposob, M., Jun, H.-B. 2020. Effect of a side-stream voltage supplied by sludge recirculation to an anaerobic digestion reactor. *Bioresource Technology*, **300**, 122643.

Park, J.-G., Lee, B., Park, H.-R., Jun, H.-B. 2019. Long-term evaluation of methane production in a bio-electrochemical anaerobic digestion reactor according to the organic loading rate. *Bioresource technology*, **273**, 478-486.

Park, J., Lee, B., Tian, D., Jun, H. 2018. Bioelectrochemical enhancement of methane production from highly concentrated food waste in a combined anaerobic digester and microbial electrolysis cell. *Bioresour Technol*, **247**, 226-233.

Parkin, G., Speece, R., Yang, C., Kocher, W. 1983. Response of methane fermentation systems to industrial toxicants. *Journal (Water Pollution Control Federation)*, 44-53.

Pathe, P., Nandy, T., Kaul, S. 2000. Wastewater management in vegetable oil industries. *INDIAN JOURNAL OF ENVIRONMENTAL PROTECTION*, **20**(7), 481-492.

Peces, M., Astals, S., Mata-Alvarez, J. 2013. Response of a sewage sludge mesophilic anaerobic digester to short and long-term thermophilic temperature fluctuations. *Chemical engineering journal*, **233**, 109-116.

Peng, H., Zhang, Y., Tan, D., Zhao, Z., Zhao, H., Quan, X. 2018. Roles of magnetite and granular activated carbon in improvement of anaerobic sludge digestion. *Bioresource technology*, **249**, 666-672.

Peng, Y., Zhang, S., Zeng, W., Zheng, S., Mino, T., Satoh, H. 2008. Organic removal by denitritation and methanogenesis and nitrogen removal by nitritation from landfill leachate. *Water Res*, **42**(4-5), 883-92.

Pikaar, I., Rozendal, R.A., Yuan, Z., Keller, J., Rabaey, K. 2011. Electrochemical sulfide removal from synthetic and real domestic wastewater at high current densities. *Water Res*, **45**(6), 2281-9.

Qiang, H., Li, Y.-Y., Pei, M.-F. 2018. Effect of COD/SO 4 2-Ratio on Anaerobic Digestion of

Penicillin Bacterial Residues. *Huan jing ke xue= Huanjing kexue*, **39**(7), 3443-3451.

Qu, J., Sun, Y., Awasthi, M.K., Liu, Y., Xu, X., Meng, X., Zhang, H. 2021. Effect of different aerobic hydrolysis time on the anaerobic digestion characteristics and energy consumption analysis. *Bioresource technology*, **320**, 124332.

Quashie, F.K., Fang, A., Wei, L., Kabutey, F.T., Xing, D. 2021. Prediction of biogas production from food waste in a continuous stirred microbial electrolysis cell (CSMEC) with backpropagation artificial neural network. *Biomass Conversion and Biorefinery*, 1-12.

Quast, C., Pruesse, E., Yilmaz, P., Gerken, J., Schweer, T., Yarza, P., Peplies, J., Glöckner, F.O. 2012. The SILVA ribosomal RNA gene database project: improved data processing and web-based tools. *Nucleic acids research*, **41**(D1), D590-D596.

Rabaey, K., Van de Sompel, K., Maignien, L., Boon, N., Aelterman, P., Clauwaert, P., De Schamphelaire, L., Pham, H.T., Vermeulen, J., Verhaege, M., Lens, P., Verstraete, W. 2006. Microbial Fuel Cells for Sulfide Removal†. *Environmental Science & Technology*, **40**(17), 5218-5224.

Rago, L., Ruiz, Y., Baeza, J.A., Guisasola, A., Cortés, P. 2015. Microbial community analysis in a long-term membrane-less microbial electrolysis cell with hydrogen and methane production. *Bioelectrochemistry*, **106**, 359-368.

Rajagopal, R., Massé, D.I., Singh, G. 2013. A critical review on inhibition of anaerobic digestion process by excess ammonia. *Bioresource technology*, **143**, 632-641.

Rajkumar, K., Muthukumar, M., Sivakumar, R. 2010. Novel approach for the treatment and recycle of wastewater from soya edible oil refinery industry—An economic perspective. *Resources Conservation & Recycling*, **54**(10), 752-758.

Ramdin, M., Amplianitis, A., Bazhenov, S., Volkov, A., Volkov, V., Vlugt, T.J., de Loos, T.W. 2014. Solubility of CO2 and CH4 in ionic liquids: ideal CO2/CH4 selectivity. *Industrial & Engineering Chemistry Research*, **53**(40), 15427-15435.

Ramirez-Farias, C., Slezak, K., Fuller, Z., Duncan, A., Holtrop, G., Louis, P. 2008. Effect of inulin on the human gut microbiota: stimulation of Bifidobacterium adolescentis and

Faecalibacterium prausnitzii. *British Journal of Nutrition*, **101**(4), 541-550.

Rashama, C., Ijoma, G., Matambo, T. 2019. Biogas generation from by-products of edible oil processing: a review of opportunities, challenges and strategies. *Biomass Conversion and Biorefinery*, 1-24.

Revelle, W.R. 2017. psych: Procedures for personality and psychological research.

Rincon-Llorente, B., De la Lama-Calvente, D., Fernandez-Rodriguez, M.J., Borja-Padilla, R. 2018. Table Olive Wastewater: Problem, Treatments and Future Strategy. A Review. *Front Microbiol*, **9**, 1641.

Rojas, M.d.P.A., Mateos, R., Sotres, A., Zaiat, M., Gonzalez, E.R., Escapa, A., De Wever, H., Pant, D. 2018. Microbial electrosynthesis (MES) from CO2 is resilient to fluctuations in renewable energy supply. *Energy conversion and management*, **177**, 272-279.

Rose, C., Parker, A., Jefferson, B., Cartmell, E. 2015. The characterization of feces and urine: a review of the literature to inform advanced treatment technology. *Critical reviews in environmental science and technology*, **45**(17), 1827-1879.

Rückert, C. 2016. Sulfate reduction in microorganisms—recent advances and biotechnological applications. *Current opinion in microbiology*, **33**, 140-146.

Sangeetha, T., Guo, Z., Liu, W., Cui, M., Yang, C., Wang, L., Wang, A. 2016. Cathode material as an influencing factor on beer wastewater treatment and methane production in a novel integrated upflow microbial electrolysis cell (Upflow-MEC). *International Journal of Hydrogen Energy*, **41**(4), 2189-2196.

Sankaran, K., Premalatha, M., Vijayasekaran, M., Somasundaram, V. 2014. DEPHY project: distillery wastewater treatment through anaerobic digestion and phycoremediation—a green industrial approach. *Renewable and Sustainable Energy Reviews*, **37**, 634-643.

Sasaki, D., Sasaki, K., Watanabe, A., Morita, M., Matsumoto, N., Igarashi, Y., Ohmura, N. 2013. Operation of a cylindrical bioelectrochemical reactor containing carbon fiber fabric for efficient methane fermentation from thickened sewage sludge. *Bioresour Technol*, **129**, 366-73.

Sasaki, K., Morita, M., Sasaki, D., Hirano, S., Matsumoto, N., Watanabe, A., Ohmura, N., Igarashi, Y. 2011. A bioelectrochemical reactor containing carbon fiber textiles enables efficient methane fermentation from garbage slurry. *Bioresour Technol*, **102**(13), 6837-42.

Sasaki, K., Sasaki, D., Morita, M., Hirano, S., Matsumoto, N., Ohmura, N., Igarashi, Y. 2010. Bioelectrochemical system stabilizes methane fermentation from garbage slurry. *Bioresour Technol*, **101**(10), 3415-22.

Satyawali, Y., Van de Wiele, T., Saveyn, H., Van der Meeren, P., Verstraete, W. 2007. Electrolytic reduction improves treatability of humic acids containing water streams. *Journal of Chemical Technology & Biotechnology*, **82**(8), 730-737.

Savant, D., Ranade, D. 2004. Application of Methanobrevibacter acididurans in anaerobic digestion. *Water Science and Technology*, **50**(6), 109-114.

Sawyer, C.N., McCarty, P.L., Parkin, G.F. 2003. *Chemistry for environmental engineering and science*. McGraw-Hill.

Seelam, J.S., Maesara, S.A., Mohanakrishna, G., Patil, S.A., ter Heijne, A., Pant, D. 2018. Resource recovery from wastes and wastewaters using bioelectrochemical systems. in: *Waste Biorefinery*, Elsevier, pp. 535-570.

Segata, N., Izard, J., Waldron, L., Gevers, D., Miropolsky, L., Garrett, W.S., Huttenhower, C. 2011. Metagenomic biomarker discovery and explanation. *Genome biology*, **12**(6), 1-18.

Shade, A., Peter, H., Allison, S.D., Baho, D.L., Berga, M., Bürgmann, H., Huber, D.H., Langenheder, S., Lennon, J.T., Martiny, J.B. 2012. Fundamentals of microbial community resistance and resilience. *Frontiers in microbiology*, **3**, 417.

Shahriari, H., Warith, M., Hamoda, M., Kennedy, K.J. 2012. Anaerobic digestion of organic fraction of municipal solid waste combining two pretreatment modalities, high temperature microwave and hydrogen peroxide. *Waste Management*, **32**(1), 41-52.

Shi, K., Cheng, W., Cheng, D., Xue, J., Qiao, Y., Gao, Y., Jiang, Q., Wang, J. 2023. Stability improvement and the mechanism of a microbial electrolysis cell biocathode for treating wastewater containing sulfate by quorum sensing. *Chemical Engineering Journal*, **455**,

140597.

Sieber, J.R., Sims, D.R., Han, C., Kim, E., Lykidis, A., Lapidus, A.L., McDonnald, E., Rohlin, L., Culley, D.E., Gunsalus, R. 2010. The genome of Syntrophomonas wolfei: new insights into syntrophic metabolism and biohydrogen production. *Environmental microbiology*, **12**(8), 2289-2301.

Siegert, M., Li, X.-F., Yates, M.D., Logan, B.E. 2015. The presence of hydrogenotrophic methanogens in the inoculum improves methane gas production in microbial electrolysis cells. *Frontiers in microbiology*, **5**, 778.

Singhania, R.R., Patel, A.K., Christophe, G., Fontanille, P., Larroche, C. 2013. Biological upgrading of volatile fatty acids, key intermediates for the valorization of biowaste through dark anaerobic fermentation. *Bioresource technology*, **145**, 166-174.

Sleutels, T.H., Hamelers, H.V., Rozendal, R.A., Buisman, C.J. 2009. Ion transport resistance in microbial electrolysis cells with anion and cation exchange membranes. *International Journal of Hydrogen Energy*, **34**(9), 3612-3620.

Sleutels, T.H., Ter Heijne, A., Buisman, C.J., Hamelers, H.V. 2012. Bioelectrochemical systems: an outlook for practical applications. *ChemSusChem*, **5**(6), 1012-9.

Sleutels, T.H., Ter Heijne, A., Buisman, C.J., Hamelers, H.V. 2013. Steady-state performance and chemical efficiency of Microbial Electrolysis Cells. *international journal of hydrogen energy*, **38**(18), 7201-7208.

Song, L.-J., Zhu, N.-W., Yuan, H.-P., Hong, Y., Ding, J. 2010. Enhancement of waste activated sludge aerobic digestion by electrochemical pre-treatment. *Water research*, **44**(15), 4371-4378.

Song, T.-s., Wu, X.-y., Zhou, C.C. 2014. Effect of different acclimation methods on the performance of microbial fuel cells using phenol as substrate. *Bioprocess and biosystems engineering*, **37**(2), 133-138.

Song, Y.-C., Feng, Q., Ahn, Y. 2016. Performance of the Bio-electrochemical Anaerobic Digestion of Sewage Sludge at Different Hydraulic Retention Times. *Energy & Fuels*, **30**(1), 352-

359.

Spormann, A.M., Widdel, F. 2000. Metabolism of alkylbenzenes, alkanes, and other hydrocarbons in anaerobic bacteria. *Biodegradation*, **11**(2-3), 85-105.

Su, M., Wei, L., Qiu, Z., Wang, G., Shen, J. 2016. Hydrogen production in single chamber microbial electrolysis cells with stainless steel fiber felt cathodes. *Journal of Power Sources*, **301**, 29-34.

Sugnaux, M., Happe, M., Cachelin, C.P., Gasperini, A., Blatter, M., Fischer, F. 2017. Cathode deposits favor methane generation in microbial electrolysis cell. *Chemical Engineering Journal*, **324**, 228-236.

Sun, C., Yu, Q., Zhao, Z., Zhang, Y. 2020. Syntrophic metabolism of phenol in the anodic degradation within a Phenol-Cr (VI) coupled microbial electrolysis cell. *Science of The Total Environment*, **723**, 137990.

Sun, M., Mu, Z.-X., Chen, Y.-P., Sheng, G.-P., Liu, X.-W., Chen, Y.-Z., Zhao, Y., Wang, H.-L., Yu, H.-Q., Wei, L., Ma, F. 2009. Microbe-Assisted Sulfide Oxidation in the Anode of a Microbial Fuel Cell. *Environmental Science & Technology*, **43**(9), 3372-3377.

Sun, R., Zhou, A., Jia, J., Liang, Q., Liu, Q., Xing, D., Ren, N. 2015. Characterization of methane production and microbial community shifts during waste activated sludge degradation in microbial electrolysis cells. *Bioresour Technol*, **175**, 68-74.

Takashima, M., Tanaka, Y. 2014. Acidic thermal post-treatment for enhancing anaerobic digestion of sewage sludge. *Journal of Environmental Chemical Engineering*, **2**(2), 773-779.

Tervahauta, T., Bryant, I., Leal, L., Buisman, C., Zeeman, G. 2014. Improved energy recovery by anaerobic grey water sludge treatment with black water. *Water*, **6**(8), 2436-2448.

Torres, C.I., Krajmalnik-Brown, R., Parameswaran, P., Marcus, A.K., Wanger, G., Gorby, Y.A., Rittmann, B.E. 2009. Selecting anode-respiring bacteria based on anode potential: phylogenetic, electrochemical, and microscopic characterization. *Environmental science & technology*, **43**(24), 9519-9524.

Traversi, D., Capone, C., Villa, S., Valeria, R., Pietrangeli, B., Gilli, G. 2014. Assessing archeal

indicators of performance by RT-qPCR methods during anaerobic co-digestion of organic wastes. *BioEnergy Research*, **7**, 720-727.

Tsigkou, K., Zagklis, D., Parasoglou, M., Zafiri, C., Kornaros, M. 2022. Proposed protocol for rate-limiting step determination during anaerobic digestion of complex substrates. *Bioresource Technology*, **361**, 127660.

van Eerten-Jansen, M.C.A.A., Jansen, N.C., Plugge, C.M., de Wilde, V., Buisman, C.J.N., ter Heijne, A. 2015. Analysis of the mechanisms of bioelectrochemical methane production by mixed cultures. *Journal of Chemical Technology & Biotechnology*, **90**(5), 963-970.

Van Zyl, P.J., Wentzel, M.C., Ekama, G.A., Riedel, K.J. 2008. Design and start-up of a high rate anaerobic membrane bioreactor for the treatment of a low pH, high strength, dissolved organic waste water. *Water Sci Technol*, **57**(2), 291-5.

Vanwonterghem, I., Jensen, P.D., Rabaey, K., Tyson, G.W. 2015. Temperature and solids retention time control microbial population dynamics and volatile fatty acid production in replicated anaerobic digesters. *Scientific reports*, **5**, 8496.

Vergine, P., Salerno, C., Berardi, G., Pollice, A. 2021. Self-Forming Dynamic Membrane BioReactors (SFD MBR) for municipal wastewater treatment: Relevance of solids retention time and biological process stability. *Separation and Purification Technology*, **255**, 117735.

Villano, M., Scardala, S., Aulenta, F., Majone, M. 2013. Carbon and nitrogen removal and enhanced methane production in a microbial electrolysis cell. *Bioresource technology*, **130**, 366-371.

Vu, M.T., Noori, M.T., Min, B. 2020. Conductive magnetite nanoparticles trigger syntrophic methane production in single chamber microbial electrochemical systems. *Bioresource technology*, **296**, 122265.

Wang, A., Liu, W., Cheng, S., Xing, D., Zhou, J., Logan, B.E. 2009. Source of methane and methods to control its formation in single chamber microbial electrolysis cells. *international journal of hydrogen energy*, **34**(9), 3653-3658.

Wang, D., Han, H., Han, Y., Li, K., Zhu, H. 2017a. Enhanced treatment of Fischer-Tropsch (F-T) wastewater using the up-flow anaerobic sludge blanket coupled with bioelectrochemical system: Effect of electric field. *Bioresour Technol*, **232**, 18-26.

Wang, D., Han, Y., Han, H., Li, K., Xu, C. 2017b. Enhanced treatment of Fischer-Tropsch wastewater using up-flow anaerobic sludge blanket system coupled with micro-electrolysis cell: A pilot scale study. *Bioresour Technol*, **238**, 333-342.

Wang, D., Ma, W., Han, H., Li, K., Hao, X. 2017c. Enhanced treatment of Fischer–Tropsch (F-T) wastewater by novel anaerobic biofilm system with scrap zero valent iron (SZVI) assisted. *Biochemical Engineering Journal*, **117**, 66-76.

Wang, D., Ma, W., Han, H., Li, K., Xu, H., Fang, F., Hou, B., Jia, S. 2016. Enhanced anaerobic degradation of Fischer-Tropsch wastewater by integrated UASB system with Fe-C micro-electrolysis assisted. *Chemosphere*, **164**, 14-24.

Wang, G., Li, Q., Li, Y., Xing, Y., Yao, G., Liu, Y., Chen, R., Wang, X.C. 2020. Redox-active biochar facilitates potential electron tranfer between syntrophic partners to enhance anaerobic digestion under high organic loading rate. *Bioresource Technology*, **298**, 122524.

Wang, H., Du, H., Xie, H., Zhu, J., Zeng, S., Igarashi, Y., Luo, F. 2021a. Dual-chamber differs from single-chamber microbial electrosynthesis in biogas production performance under low temperature (15℃). *Bioresource Technology*, **337**, 125377.

Wang, H., Du, H., Zeng, S., Pan, X., Cheng, H., Liu, L., Luo, F. 2021b. Explore the difference between the single-chamber and dual-chamber microbial electrosynthesis for biogas production performance. *Bioelectrochemistry*, **138**, 107726.

Wang, H., Ren, Z.J. 2013. A comprehensive review of microbial electrochemical systems as a platform technology. *Biotechnology advances*, **31**(8), 1796-1807.

Wang, K., Cao, Z., Chang, J., Sheng, Y., Cao, H., Yan, K., Zhang, Y., Xia, Z. 2017d. Promoted bioelectrocatalytic activity of microbial electrolysis cell (MEC) in sulfate removal through the synergy between neutral red and graphite felt. *Chemical Engineering Journal*, **327**, 183-192.

Wang, K., Sheng, Y., Cao, H., Yan, K., Zhang, Y. 2017e. Impact of applied current on sulfate-rich wastewater treatment and microbial biodiversity in the cathode chamber of microbial electrolysis cell (MEC) reactor. *Chemical Engineering Journal*, **307**, 150-158.

Wang, W., Ma, W., Han, H., Li, H., Yuan, M. 2011. Thermophilic anaerobic digestion of Lurgi coal gasification wastewater in a UASB reactor. *Bioresource technology*, **102**(3), 2441-2447.

Wang, X.-T., Zhang, Y.-F., Wang, B., Wang, S., Xing, X., Xu, X.-J., Liu, W.-Z., Ren, N.-Q., Lee, D.-J., Chen, C. 2022. Enhancement of methane production from waste activated sludge using hybrid microbial electrolysis cells-anaerobic digestion (MEC-AD) process–A review. *Bioresource Technology*, **346**, 126641.

Wang, X.-T., Zhao, L., Chen, C., Chen, K.-Y., Yang, H., Xu, X.-J., Zhou, X., Liu, W.-Z., Xing, D.-F., Ren, N.-Q. 2021c. Microbial electrolysis cells (MEC) accelerated methane production from the enhanced hydrolysis and acidogenesis of raw waste activated sludge. *Chemical Engineering Journal*, **413**, 127472.

Wang, Z., Banks, C.J. 2006. Report: anaerobic digestion of a sulphate-rich high-strength landfill leachate: the effect of differential dosing with FeCl3. *Waste Manag Res*, **24**(3), 289-93.

Wendland, C., Deegener, S., Behrendt, J., Toshev, P., Otterpohl, R. 2007. Anaerobic digestion of blackwater from vacuum toilets and kitchen refuse in a continuous stirred tank reactor (CSTR). *Water Science and Technology*, **55**(7), 187-194.

Wilson, E.L., Kim, Y. 2016. The yield and decay coefficients of exoelectrogenic bacteria in bioelectrochemical systems. *Water research*, **94**, 233-239.

Wu, J., Niu, Q., Li, L., Hu, Y., Mribet, C., Hojo, T., Li, Y.-Y. 2018. A gradual change between methanogenesis and sulfidogenesis during a long-term UASB treatment of sulfate-rich chemical wastewater. *Science of the Total Environment*, **636**, 168-176.

Xiao, B., Chen, X., Han, Y., Liu, J., Guo, X. 2018. Bioelectrochemical enhancement of the anaerobic digestion of thermal-alkaline pretreated sludge in microbial electrolysis cells. *Renewable Energy*, **115**, 1177-1183.

Xin, X., Qiu, W. 2021. Linking microbial mechanism with bioelectricity production in sludge matrix-fed microbial fuel cells: Freezing/thawing liquid versus fermentation liquor. *Science of The Total Environment*, **752**, 141907.

Xu, F., Li, Y., Ge, X., Yang, L., Li, Y. 2018a. Anaerobic digestion of food waste - Challenges and opportunities. *Bioresour Technol*, **247**, 1047-1058.

Xu, R., Yang, Z.-H., Wang, Q.-P., Bai, Y., Liu, J.-B., Zheng, Y., Zhang, Y.-R., Xiong, W.-P., Ahmad, K., Fan, C.-Z. 2018b. Rapid startup of thermophilic anaerobic digester to remove tetracycline and sulfonamides resistance genes from sewage sludge. *Science of the Total Environment*, **612**, 788-798.

Xu, R., Yang, Z.-H., Zheng, Y., Liu, J.-B., Xiong, W.-P., Zhang, Y.-R., Lu, Y., Xue, W.-J., Fan, C.-Z. 2018c. Organic loading rate and hydraulic retention time shape distinct ecological networks of anaerobic digestion related microbiome. *Bioresource technology*, **262**, 184-193.

Xu, S., Han, R., Zhang, Y., He, C., Liu, H. 2018d. Differentiated stimulating effects of activated carbon on methanogenic degradation of acetate, propionate and butyrate. *Waste Management*, **76**, 394-403.

Yadav, A.N., Sachan, S.G., Verma, P., Kaushik, R., Saxena, A.K. 2016. Cold active hydrolytic enzymes production by psychrotrophic Bacilli isolated from three sub-glacial lakes of NW Indian Himalayas. *Journal of Basic Microbiology*, **56**(3), 294-307.

Yamaguchi, T., Harada, H., Hisano, T., Yamazaki, S., Tseng, I.-C. 1999. Process behavior of UASB reactor treating a wastewater containing high strength sulfate. *Water Research*, **33**(14), 3182-3190.

Yang, Z., Zhang, L., Nie, C., Hou, Q., Zhang, S., Pei, H. 2019. Multiple anodic chambers sharing an algal raceway pond to establish a photosynthetic microbial fuel cell stack: voltage boosting accompany wastewater treatment. *Water Research*, **164**, 114955.

Ye, J., Mu, Y., Cheng, X., Sun, D. 2011. Treatment of fresh leachate with high-strength organics and calcium from municipal solid waste incineration plant using UASB reactor. *Bioresour*

Technol, **102**(9), 5498-503.

Ye, R., Jin, Q., Bohannan, B., Keller, J.K., Bridgham, S.D. 2014. Homoacetogenesis: A potentially underappreciated carbon pathway in peatlands. *Soil Biology and Biochemistry*, **68**, 385-391.

Yenigün, O., Demirel, B. 2013. Ammonia inhibition in anaerobic digestion: A review. *Process Biochemistry*, **48**(5-6), 901-911.

Yilmaz, P., Parfrey, L.W., Yarza, P., Gerken, J., Pruesse, E., Quast, C., Schweer, T., Peplies, J., Ludwig, W., Glöckner, F.O. 2014. The SILVA and "all-species living tree project (LTP)" taxonomic frameworks. *Nucleic acids research*, **42**(D1), D643-D648.

Yu, D., Wang, X., Fan, X., Ren, H., Hu, S., Wang, L., Shi, Y., Liu, N., Qiao, N. 2018a. Refined soybean oil wastewater treatment and its utilization for lipid production by the oleaginous yeast Trichosporon fermentans. *Biotechnol Biofuels*, **11**, 299.

Yu, N., Xing, D., Li, W., Yang, Y., Li, Z., Li, Y., Ren, N. 2017. Electricity and methane production from soybean edible oil refinery wastewater using microbial electrochemical systems. *International Journal of Hydrogen Energy*, **42**(1), 96-102.

Yu, Z., Leng, X., Zhao, S., Ji, J., Zhou, T., Khan, A., Kakde, A., Liu, P., Li, X. 2018b. A review on the applications of microbial electrolysis cells in anaerobic digestion. *Bioresour Technol*, **255**, 340-348.

Yuan, Y., Cheng, H., Chen, F., Zhang, Y., Xu, X., Huang, C., Chen, C., Liu, W., Ding, C., Li, Z. 2020. Enhanced methane production by alleviating sulfide inhibition with a microbial electrolysis coupled anaerobic digestion reactor. *Environment international*, **136**, 105503.

Yuan, Y., Wang, S., Liu, Y., Li, B., Wang, B., Peng, Y. 2015. Long-term effect of pH on short-chain fatty acids accumulation and microbial community in sludge fermentation systems. *Bioresource Technology*, **197**, 56-63.

Yuan, Y., Zhang, L., Chen, T., Huang, Y., Qian, X., He, J., Li, Z., Ding, C., Wang, A. 2022. Simultaneous recovery of bio-sulfur and bio-methane from sulfate-rich wastewater by a bioelectrocatalysis coupled two-phase anaerobic reactor. *Bioresource Technology*, **363**,

127883.

Zakaria, B.S., Dhar, B.R. 2020. Changes in syntrophic microbial communities, EPS matrix, and gene-expression patterns in biofilm anode in response to silver nanoparticles exposure. *Science of The Total Environment*, **734**, 139395.

Zakaria, B.S., Dhar, B.R. 2021a. Characterization and significance of extracellular polymeric substances, reactive oxygen species, and extracellular electron transfer in methanogenic biocathode. *Scientific Reports*, **11**(1), 1-13.

Zakaria, B.S., Dhar, B.R. 2022. Intermittent energization catalyzes direct interspecies electron transfer in electro-anaerobic digestion of sewage sludge. *Chemical Engineering Journal*, **442**, 136177.

Zakaria, B.S., Dhar, B.R. 2021b. An intermittent power supply scheme to minimize electrical energy input in a microbial electrolysis cell assisted anaerobic digester. *Bioresource Technology*, **319**, 124109.

Zakaria, B.S., Dhar, B.R. 2019. Progress towards catalyzing electro-methanogenesis in anaerobic digestion process: Fundamentals, process optimization, design and scale-up considerations. *Bioresource technology*, 121738.

Zakaria, B.S., Guo, H., Kim, Y., Dhar, B.R. 2022. Molecular biology and modeling analysis reveal functional roles of propionate to acetate ratios on microbial syntrophy and competition in electro-assisted anaerobic digestion. *Water Research*, 118335.

Zakaria, B.S., Lin, L., Chung, T., Dhar, B.R. 2020. An overview of complementary microbial electrochemical technologies for advancing anaerobic digestion. *Advances in Bioenergy*, **5**, 129-167.

Zamalloa, C., Arends, J.B., Boon, N., Verstraete, W. 2013. Performance of a lab-scale bio-electrochemical assisted septic tank for the anaerobic treatment of black water. *N Biotechnol*, **30**(5), 573-80.

Zealand, A.M., Mei, R., Roskilly, A.P., Liu, W., Graham, D.W. 2019. Molecular microbial ecology of stable versus failing rice straw anaerobic digesters. *Microbial biotechnology*, **12**(5),

879-891.

Zeng, D., Yin, Q., Du, Q., Wu, G. 2019. System performance and microbial community in ethanol-fed anaerobic reactors acclimated with different organic carbon to sulfate ratios. *Bioresource technology*, **278**, 34-42.

Zeng, X., Borole, A.P., Pavlostathis, S.G. 2015. Biotransformation of Furanic and Phenolic Compounds with Hydrogen Gas Production in a Microbial Electrolysis Cell. *Environ Sci Technol*, **49**(22), 13667-75.

Zeppilli, M., Lai, A., Villano, M., Majone, M. 2016. Anion vs cation exchange membrane strongly affect mechanisms and yield of CO2 fixation in a microbial electrolysis cell. *Chemical Engineering Journal*, **304**, 10-19.

Zeppilli, M., Villano, M., Aulenta, F., Lampis, S., Vallini, G., Majone, M. 2015. Effect of the anode feeding composition on the performance of a continuous-flow methane-producing microbial electrolysis cell. *Environmental Science and Pollution Research*, **22**(10), 7349-7360.

Zhang, J., Mao, L., Zhang, L., Loh, K.-C., Dai, Y., Tong, Y.W. 2017. Metagenomic insight into the microbial networks and metabolic mechanism in anaerobic digesters for food waste by incorporating activated carbon. *Scientific Reports*, **7**(1), 11293.

Zhang, J., Zhang, Y., Quan, X., Chen, S. 2013a. Effects of ferric iron on the anaerobic treatment and microbial biodiversity in a coupled microbial electrolysis cell (MEC)–anaerobic reactor. *Water Research*, **47**(15), 5719-5728.

Zhang, J., Zhang, Y., Quan, X., Chen, S., Afzal, S. 2013b. Enhanced anaerobic digestion of organic contaminants containing diverse microbial population by combined microbial electrolysis cell (MEC) and anaerobic reactor under Fe(III) reducing conditions. *Bioresour Technol*, **136**, 273-80.

Zhang, L., Guo, B., Mou, A., Li, R., Liu, Y. 2020a. Blackwater biomethane recovery using a thermophilic upflow anaerobic sludge blanket reactor: Impacts of effluent recirculation on reactor performance. *Journal of Environmental Management*, **274**, 111157.

Zhang, L., Jahng, D. 2012. Long-term anaerobic digestion of food waste stabilized by trace elements. *Waste Manag*, **32**(8), 1509-15.

Zhang, L., Loh, K.-C., Zhang, J. 2019. Enhanced biogas production from anaerobic digestion of solid organic wastes: Current status and prospects. *Bioresource Technology Reports*, **5**, 280-296.

Zhang, L., Mou, A., Sun, H., Zhang, Y., Zhou, Y., Liu, Y. 2021a. Calcium phosphate granules formation: Key to high rate of mesophilic UASB treatment of toilet wastewater. *Science of The Total Environment*, **773**, 144972.

Zhang, L., Zhang, Y., Yuan, Y., Mou, A., Park, S., Liu, Y. 2022a. Impacts of granular activated carbon addition on anaerobic granulation in blackwater treatment. *Environmental Research*, **206**, 112406.

Zhang, T., Zhang, P., Liu, C., Zheng, Y., Chen, X. 2022b. Feasibility of hydrogen recovery and optimization of gas production from protein-rich food waste by bio-electrochemical system. *International Journal of Hydrogen Energy*, **47**(73), 31241-31254.

Zhang, Y., Angelidaki, I. 2016. Microbial electrochemical systems and technologies: it is time to report the capital costs, ACS Publications.

Zhang, Y., Angelidaki, I. 2014. Microbial electrolysis cells turning to be versatile technology: recent advances and future challenges. *Water Res*, **56**, 11-25.

Zhang, Y., Guo, B., Zhang, L., Liu, Y. 2020b. Key syntrophic partnerships identified in a granular activated carbon amended UASB treating municipal sewage under low temperature conditions. *Bioresource Technology*, **312**, 123556.

Zhang, Y., Guo, B., Zhang, L., Zhang, H., Liu, Y. 2021b. Microbial community dynamics in granular activated carbon enhanced up-flow anaerobic sludge blanket (UASB) treating municipal sewage under sulfate reducing and psychrophilic conditions. *Chemical Engineering Journal*, **405**, 126957.

Zhang, Y., Zhang, L., Guo, B., Zhou, Y., Gao, M., Sharaf, A., Liu, Y. 2020c. Granular Activated Carbon Stimulated Microbial Physiological Changes for Enhanced Anaerobic Digestion

of Municipal Sewage. *Chemical Engineering Journal*, 125838.

Zhang, Y., Zhang, L., Yu, N., Guo, B., Liu, Y. 2022c. Enhancing the resistance to H2S toxicity during anaerobic digestion of low-strength wastewater through granular activated carbon (GAC) addition. *Journal of Hazardous Materials*, **430**, 128473.

Zhao, F., Heidrich, E.S., Curtis, T.P., Dolfing, J. 2020. Understanding the complexity of wastewater: The combined impacts of carbohydrates and sulphate on the performance of bioelectrochemical systems. *Water Research*, 115737.

Zhao, L., Wang, X.-T., Chen, K.-Y., Wang, Z.-H., Xu, X.-J., Zhou, X., Xing, D.-F., Ren, N.-Q., Lee, D.-J., Chen, C. 2021. The underlying mechanism of enhanced methane production using microbial electrolysis cell assisted anaerobic digestion (MEC-AD) of proteins. *Water Research*, **201**, 117325.

Zhao, W., Su, X., Zhang, Y., Xia, D., Hou, S., Zhou, Y., Fu, H., Wang, L., Yin, X. 2022. Microbial electrolysis enhanced bioconversion of coal to methane compared with anaerobic digestion: Insights into differences in metabolic pathways. *Energy Conversion and Management*, **259**, 115553.

Zhao, Z., Li, Y., Quan, X., Zhang, Y. 2017. Towards engineering application: Potential mechanism for enhancing anaerobic digestion of complex organic waste with different types of conductive materials. *Water research*, **115**, 266-277.

Zhao, Z., Zhang, Y., Chen, S., Quan, X., Yu, Q. 2014. Bioelectrochemical enhancement of anaerobic methanogenesis for high organic load rate wastewater treatment in a up-flow anaerobic sludge blanket (UASB) reactor. *Sci Rep*, **4**, 6658.

Zhao, Z., Zhang, Y., Li, Y., Zhao, H., Quan, X. 2016a. Electrochemical reduction of carbon dioxide to formate with Fe-C electrodes in anaerobic sludge digestion process. *Water Res*, **106**, 339-343.

Zhao, Z., Zhang, Y., Ma, W., Sun, J., Sun, S., Quan, X. 2016b. Enriching functional microbes with electrode to accelerate the decomposition of complex substrates during anaerobic digestion of municipal sludge. *Biochemical Engineering Journal*, **111**, 1-9.

Zhao, Z., Zhang, Y., Quan, X., Zhao, H. 2016c. Evaluation on direct interspecies electron transfer in anaerobic sludge digestion of microbial electrolysis cell. *Bioresour Technol*, **200**, 235-44.

Zhao, Z., Zhang, Y., Yu, Q., Dang, Y., Li, Y., Quan, X. 2016d. Communities stimulated with ethanol to perform direct interspecies electron transfer for syntrophic metabolism of propionate and butyrate. *Water research*, **102**, 475-484.

Zhao, Z., Zhang, Y., Yu, Q., Ma, W., Sun, J., Quan, X. 2016e. Enhanced decomposition of waste activated sludge via anodic oxidation for methane production and bioenergy recovery. *International Biodeterioration & Biodegradation*, **106**, 161-169.

Zhen, G., Kobayashi, T., Lu, X., Xu, K. 2015. Understanding methane bioelectrosynthesis from carbon dioxide in a two-chamber microbial electrolysis cells (MECs) containing a carbon biocathode. *Bioresour Technol*, **186**, 141-148.

Zhen, G., Lu, X., Kato, H., Zhao, Y., Li, Y.-Y. 2017a. Overview of pretreatment strategies for enhancing sewage sludge disintegration and subsequent anaerobic digestion: Current advances, full-scale application and future perspectives. *Renewable and Sustainable Energy Reviews*, **69**, 559-577.

Zhen, G., Lu, X., Kobayashi, T., Su, L., Kumar, G., Bakonyi, P., He, Y., Sivagurunathan, P., Nemestothy, N., Xu, K., Zhao, Y. 2017b. Continuous micro-current stimulation to upgrade methanolic wastewater biodegradation and biomethane recovery in an upflow anaerobic sludge blanket (UASB) reactor. *Chemosphere*, **180**, 229-238.

Zhen, G., Lu, X., Kumar, G., Bakonyi, P., Xu, K., Zhao, Y. 2017c. Microbial electrolysis cell platform for simultaneous waste biorefinery and clean electrofuels generation: Current situation, challenges and future perspectives. *Progress in Energy and Combustion Science*, **63**, 119-145.

Zhen, G., Lu, X., Li, Y.-Y., Zhao, Y. 2014. Combined electrical-alkali pretreatment to increase the anaerobic hydrolysis rate of waste activated sludge during anaerobic digestion. *Applied Energy*, **128**, 93-102.

Zhou, M., Wang, H., Hassett, D.J., Gu, T. 2013. Recent advances in microbial fuel cells (MFCs) and microbial electrolysis cells (MECs) for wastewater treatment, bioenergy and bioproducts. *Journal of Chemical Technology & Biotechnology*, **88**(4), 508-518.

Ziganshin, A.M., Schmidt, T., Lv, Z., Liebetrau, J., Richnow, H.H., Kleinsteuber, S., Nikolausz, M. 2016. Reduction of the hydraulic retention time at constant high organic loading rate to reach the microbial limits of anaerobic digestion in various reactor systems. *Bioresource technology*, **217**, 62-71.

Zou, L., Wang, C., Zhao, X., Wu, K., Liang, C., Yin, F., Yang, B., Liu, J., Yang, H., Zhang, W. 2021. Enhanced anaerobic digestion of swine manure via a coupled microbial electrolysis cell. *Bioresource Technology*, **340**, 125619.

Appendix A. Supplementary Information for Chapter 3

Text A.1 Bacterial structures at phylum level

The bacterial community at the phylum level (see Appendix A Figure A.4) in all samples showed the predominance of Firmicutes (6.4-65.1%), Bacteroidetes (11.9-51.6%), and Proteobacteria (1.4-44.0%). Firmicutes and Bacteroidetes have been frequently detected in anaerobic digesters, which include diverse acid-forming/fermentative bacteria capable of degrading various proteins and carbohydrates (Gao et al., 2018). Members of Firmicutes have been reported as a predominant community at high ammonia levels, which could play a critical role in maintaining process stability (Li et al., 2015a). Bacteroidetes were reported to be predominant in human feces and protein-rich digesters as acidogenic bacteria involved in the proteolytic process, and usually showed high resistance against the changes in pH and substrate types (Gao et al., 2018). Further, most of *Alpha-*, *Beta-*, *Gamma-*, and *Deltaproteobacteria* in phylum Proteobacteria are well-known communities in utilizing glucose and SCVFAs (Ariesyady et al., 2007). However, members of Proteobacteria can be inhibited by excess FA during the digestion processes (Li et al., 2015a). A previous study reported a higher fraction of phylum Proteobacteria in 9 L flushed diluted blackwater than in 1 L flushed concentrated blackwater due to the FA concentration difference (Gao et al., 2018).

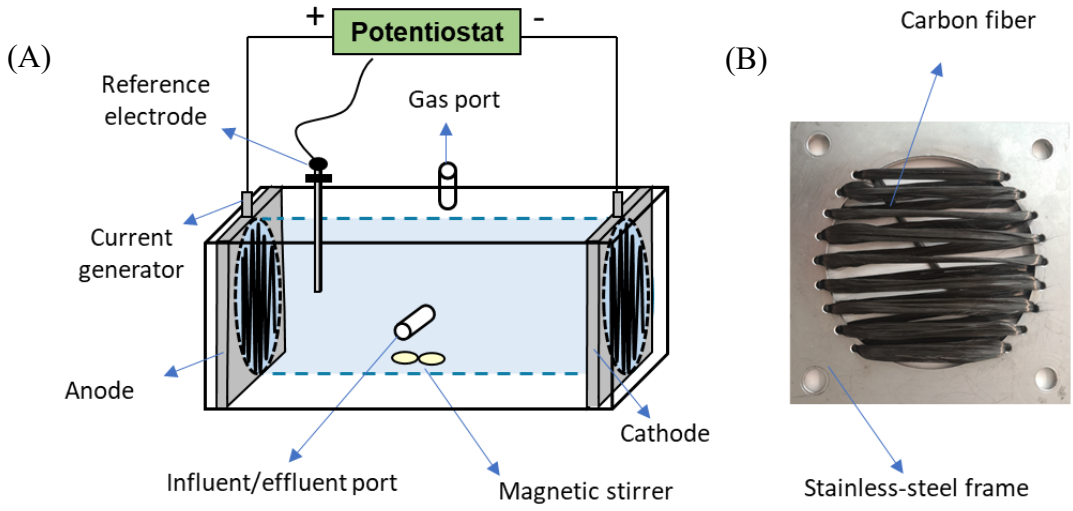

Figure A.1 (A) Configuration of the MEC-AD reactor; (B) Electrode made with stainless-steel frame and carbon fibers.

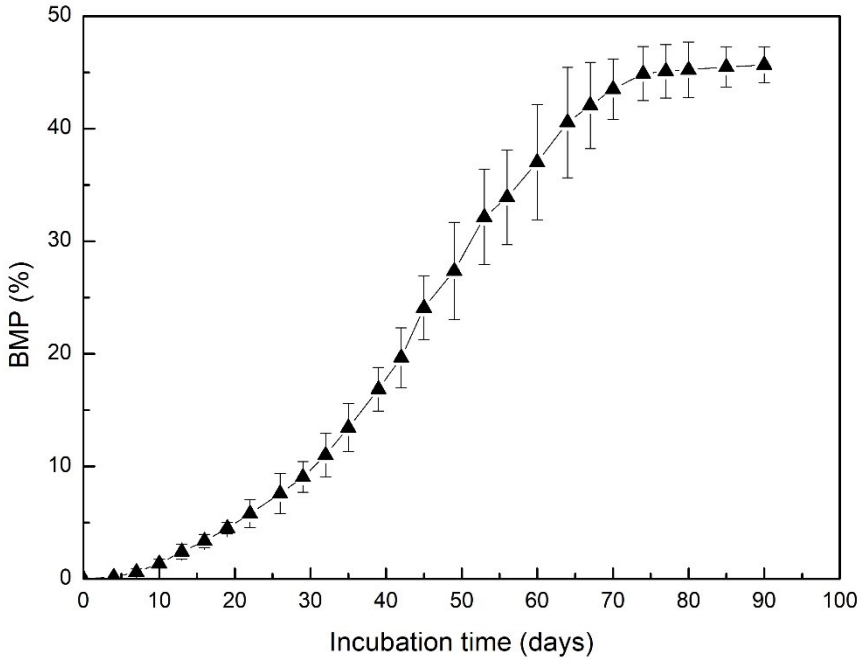

Figure A.2 Biochemical methane potential of blackwater feedstock.

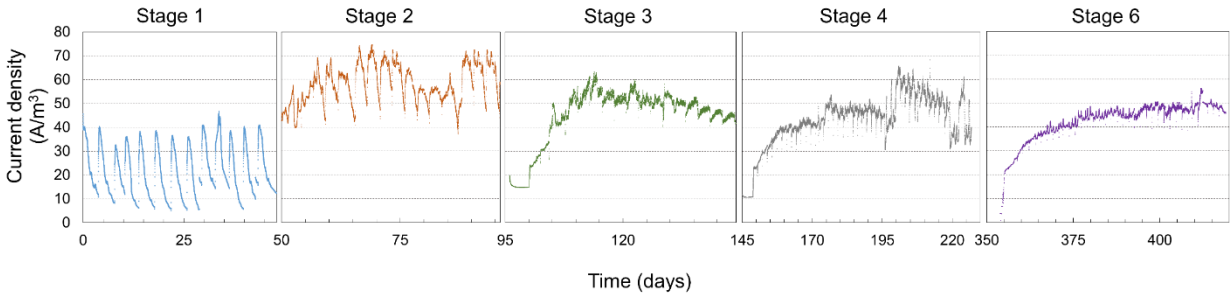

Figure A.3 Current density of different stages.

Figure A.4 Relative abundances of the 3 most abundant bacterial phyla in each sample from reactor sludge.

Table A.1 Topological properties of each node.

Nodes (genus)	Degree centrality	Betweenness centrality	Closeness centrality	Eigenvector centrality
p__Bacteroidetes	6	6.73	0.029	0.52
g__Geobacter	1	0.00	0.022	0.09
g__Petrimonas	3	34.00	0.024	0.12
o__Clostridiales	8	6.41	0.030	0.84
f__Ruminococcaceae	8	0.91	0.026	0.87
o__Clostridiales (1)	5	6.17	0.026	0.23
g__T78	2	0.00	0.021	0.23
o__Bacteroidales	11	23.10	0.033	1.00
f__Christensenellaceae	10	10.79	0.028	0.96
g__HA73	1	0.00	0.013	0.00
g__Syntrophomonas	7	0.77	0.025	0.77
g__Methanosarcina	7	0.55	0.025	0.78
c__Clostridia	5	1.60	0.026	0.34
g__Methanobacterium	3	0.00	0.025	0.26
f__Porphyromonadaceae	9	11.48	0.031	0.95
g__vadinCA02	2	18.00	0.018	0.02
g__Sedimentibacter	6	0.14	0.023	0.66
g__Erysipelothrix	9	19.86	0.031	0.89
g__Methanosaeta	11	77.48	0.036	0.68
g__vadinCA11	2	0.00	0.022	0.12

Table A.2 Parameters for energy efficiency calculation.

	Current (mA)	Applied voltage (V)	Electric energy consumed (J/d)	Methane production (mL/d)	Energy recovery as methane (J/d)	Energy efficiency (%)
Open-circuit Stage 5	-	-	-	90.78	3361.81	-
Closed-circuit Stage 6	15.52	0.90	1206.84	127.413	4718.68	104.5%

Appendix B. Supplementary Information for Chapter 4

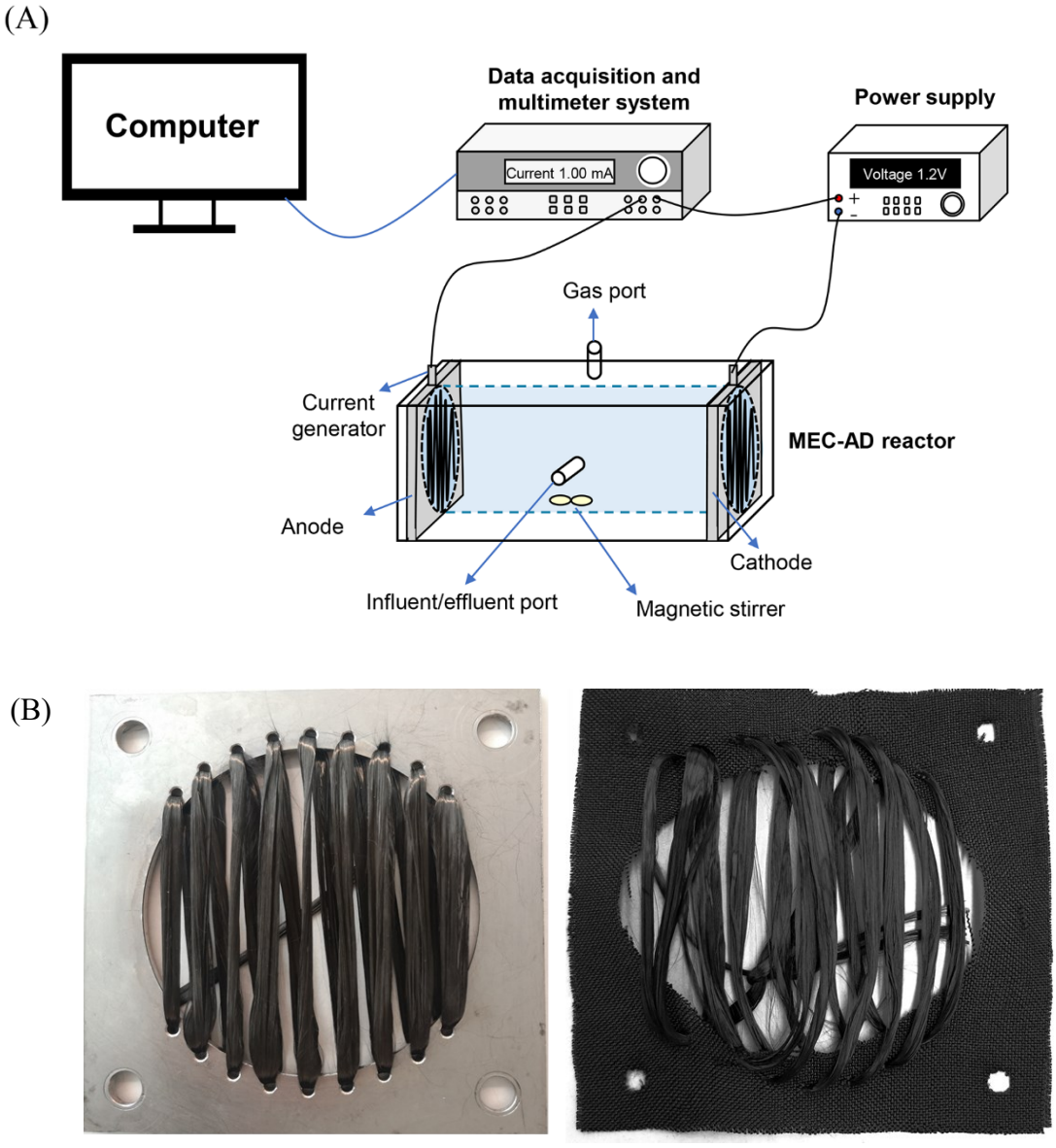

Figure B.1 (A) The schematic diagram of the MEC-AD reactor setup; (B) The electrode equipped with a stainless-steel current collector (left) and the electrode after replacing the stainless-steel with carbon cloth (right).

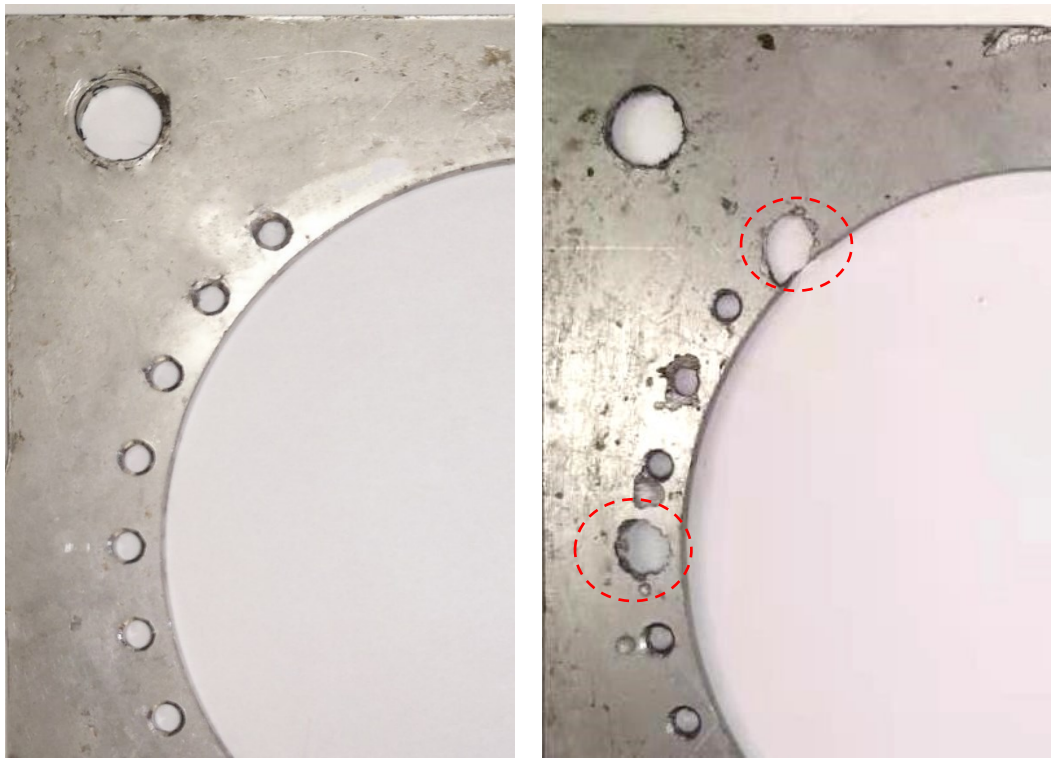

Figure B.2 The stainless-steel current collector before (left) and after (right) corrosion.

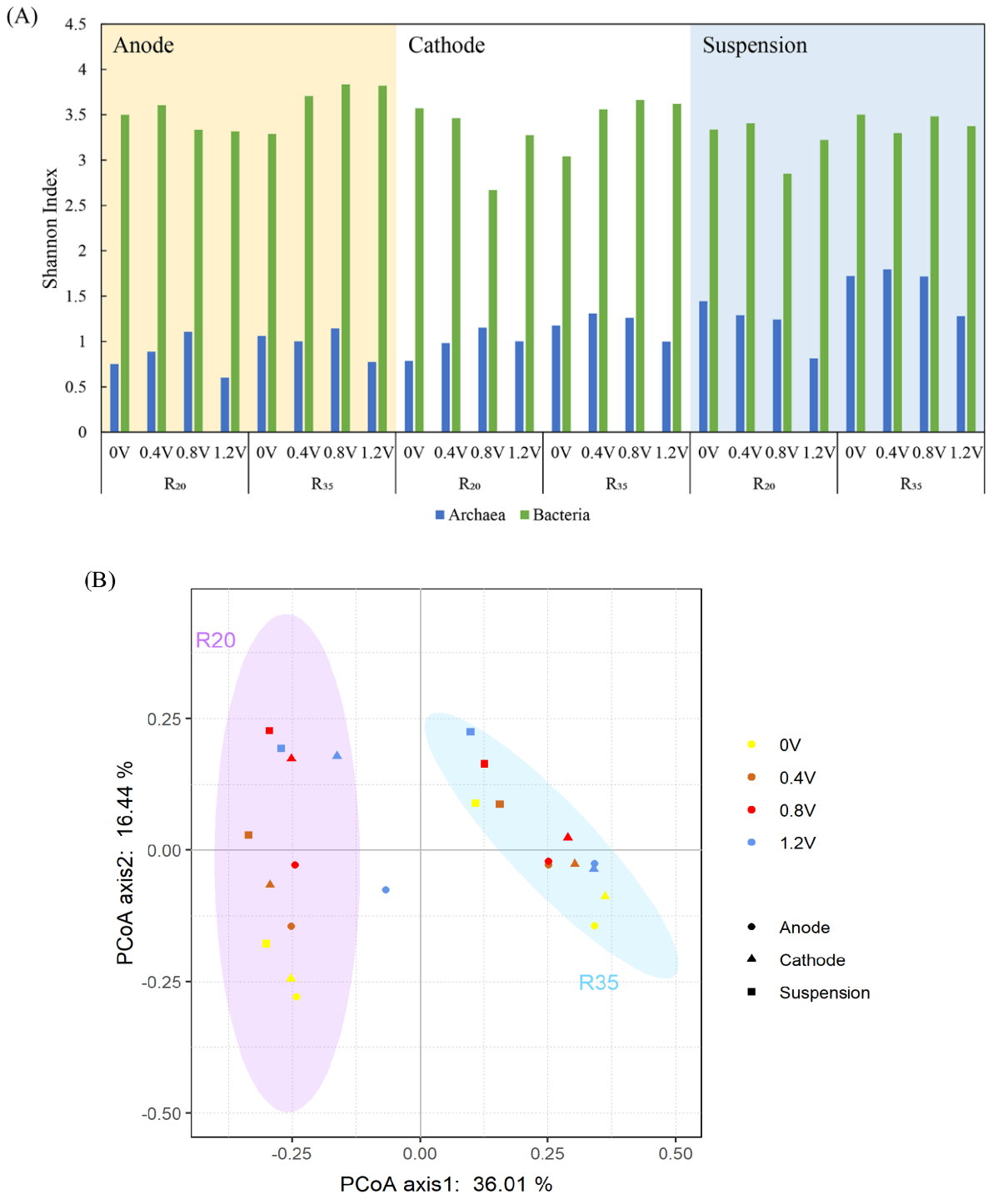

Figure B.3 (A) Shannon index analyzed at the genus level; (B) Principal coordinate analysis (PCoA) of microbial communities computed using Bray-Curtis distance based on genus abundance data (ellipse confidence level = 95%).

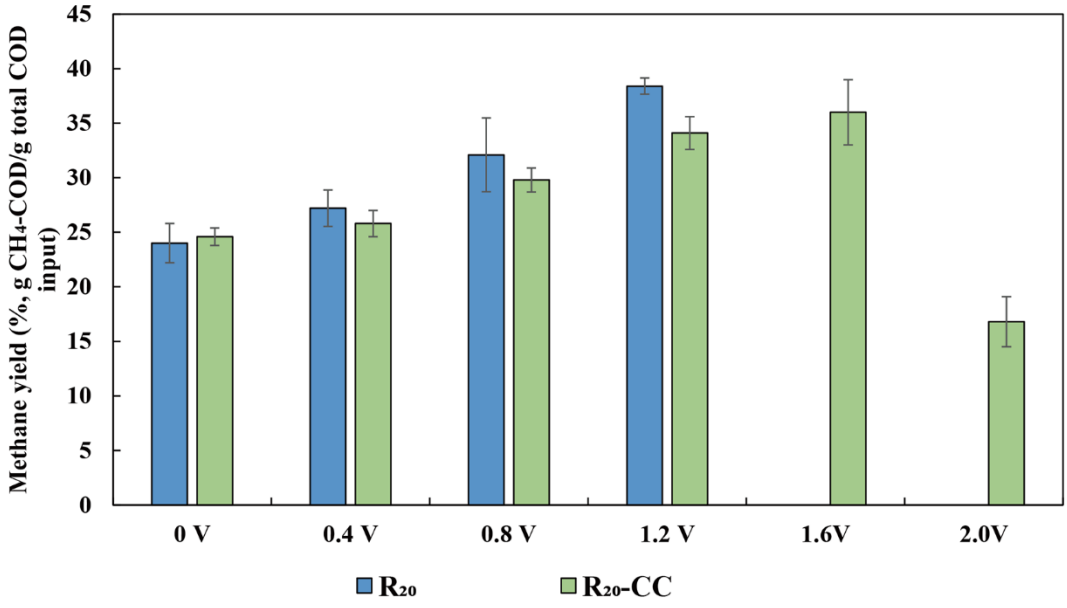

Figure B.4 Methane yield in R_{20} from the main experiment and R_{20}-CC (the carbon cloth amended reactor) from the supplementary test.

Table B.1 Dissolved methane content at different applied voltages in both reactors.

	R_{20}				R_{35}			
	0V	0.4V	0.8V	1.2V	0V	0.4V	0.8V	1.2V
Dissolved methane	72.68	76.93	75.89	78.1	26.76	25.65	26.3	20.61
(mg CH_4-COD/L)	± 1.2	± 0.6	± 0.8	± 0.6	± 1.0	± 0.8	± 1.1	± 0.7
Dissolved methane (%)	2.10	1.97	1.65	1.42	0.37	0.36	0.36	0.31

Appendix C. Supplementary Information for Chapter 5

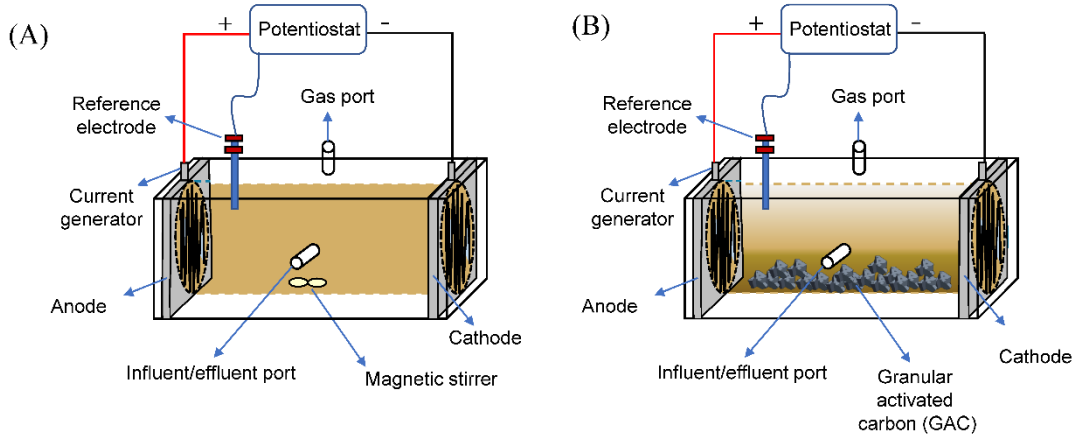

Figure C.1 Schematic diagrams of the MEC-AD reactor setup. (A) The MEC-AD reactor with mixing and without GAC addition; (B) The MEC-AD reactor without mixing and with GAC addition.

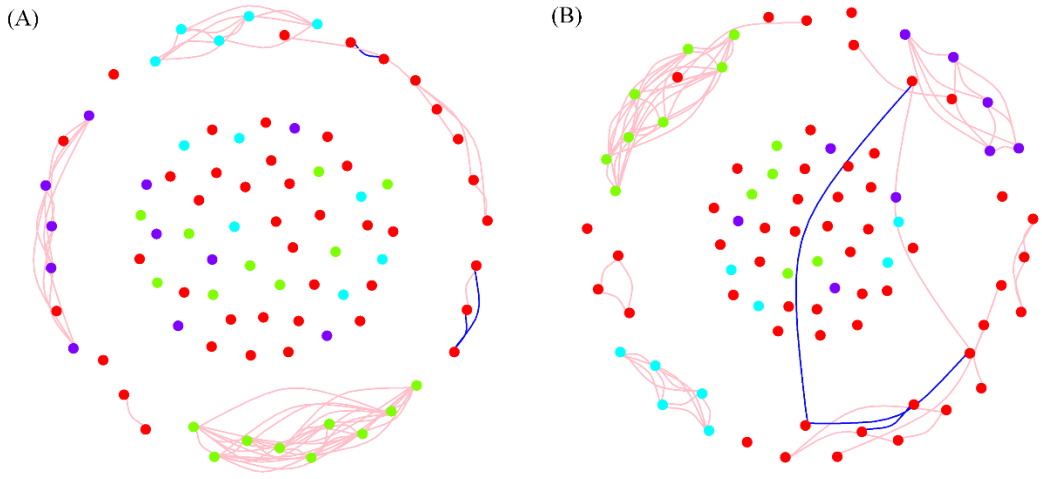

Figure C.2 Network of co-occurring microbial genera in GAC-sludge aggregates based on correlation analysis for GAC biofilm and settled sludge samples. A connection (edge) stands for a strong (Spearman's $\rho>0.6$) and significant ($p < 0.05$) correlation. Pink and blue edges represent positive and negative correlations, respectively. (A) Community in MEC reactor; (B) Community in control reactor.

Table C.1 Key characteristics of co-occurrence networks of GAC-sludge aggregates in the reactors.

	MEC-AD	Control
Clustering coefficient	0.868	0.784
Average path length	1.166	1.272
Positive ratio	0.955	0.953
Average normalized betweenness	0.002	0.003